Università Cattolica del Sacro Cuore
Universität Bielefeld

Essays on Computational and Analytical Macro Modeling

Doctoral Thesis of

Debmallya Chanda

Academic Year: 2025/2026

Committee

Supervisors: Prof. Dr. Domenico Delli Gatti & Prof. Dr. Herbert Dawid

External readers: Dr. Massimo Ferrari Minesso & Dr. Eugenio Caverzasi

This work has received funding from the European Union's Horizon 2020 research and innovation programme under the Marie Sklodowska Curie grant agreement No. 956107, "Economic Policy in Complex Environments (EPOC)"

Acknowledgement

Although my journey with economics began a long time ago, a significant milestone has been completing my PhD in the field. Throughout this journey, I have mostly been a student, and I would like to remain one. The final years of my PhD taught me how to conduct research, ask meaningful questions, and remain patient through moments of failure and uncertainty. I take this opportunity, through writing this acknowledgment, to reflect on the people who have shaped my academic thinking and supported me throughout.

First and foremost, I would like to thank my primary supervisor, Prof. Domenico Delli Gatti. He has been a guiding force in my academic pursuits. His deep understanding of economics, sharp sense of humor, and warm personality made our project discussions both intellectually stimulating and truly enjoyable. I am also deeply grateful to my second supervisor, Prof. Herbert Dawid from Universität Bielefeld. His consistent availability, constructive feedback, and expertise in computational economics helped me make important improvements to my work.

While my supervisors were my main support during the PhD, several other mentors and coauthors made this research journey both productive and fun. I would like to thank Dr. Rafael Gerke of the Deutsche Bundesbank for the incredible opportunity to immerse myself in central banking research. During my internship at the Bundesbank, I worked closely with Mr. Thomas Dengler, from whom I learned how to ask better macroeconomic questions and navigate computational challenges. I am immensely grateful to my master's thesis supervisor, Prof. Bertrand Wigniolle, who first introduced me to macroeconomic research and inspired me to pursue a PhD.

I would also like to thank my coauthor, Dr. Aldo Gliemo, for his generous support in helping me learn Julia and for always being available to discuss research. Many thanks as well to Prof. Maurizio Motolese for his early guidance and feedback during the initial stages of my PhD.

A special note of appreciation goes to Diana and Ulrike, the administrative staff at Universität Bielefeld, whose kindness, responsiveness, and unwavering support helped me navigate the logistics and formalities with ease. I am also very thankful to Eleni at Uni-

versità Cattolica, whose help and availability made the administrative side of academic life far more manageable. Their behind-the-scenes work made my life as a PhD student much smoother and less stressful.

Friends become especially important during a PhD, as we share the highs and lows of academic life together. I am grateful to my fellow PhD colleagues Elisa, Alpe, Zhongli, Matt, Predrag, Tommaso, Rosa, Nurten, Miquel, Dan, Qingchuan, and Martina for making every EPOC event so memorable and enjoyable. Special thanks to Enrico, Filippo, and Franzi for the much-needed coffee breaks, lunch chats, and meaningful conversations about life and economics. I'm also thankful to Antonino, Andrea, Matteo, Mattia, Caterina, Gabriele, and Edoardo for helping me survive the early PhD coursework and for all the aperitivos we shared. Giovanni and Francesco, writing papers and working on projects has become far more enjoyable with you both. I cannot thank you enough for enriching my academic journey and making this experience truly memorable.

To my mom and dad, none of this would have been possible without you. Your countless sacrifices, unwavering love, and constant encouragement made this journey possible. I hope I have done justice to all that you have given me, and I will strive to continue doing so.

Kaku, this is the final outcome of your daily inquiries about my research. Now you can proudly show off your chotobabu's work to your friends. Kakima, thank you for being there for me at every step of this journey. Mimi, Biswa, and Pakum, I am truly fortunate to have you in my life. Your presence has kept me grounded through many lows of academic life.

Finally, I would like to thank my wife, Rupsa, whose unwavering encouragement, insight, and steady presence during crucial moments have shaped not only my academic path but also the person I am today. I am deeply grateful for everything she has brought into my life and for the love we share. I look forward to celebrating life together, now and always.

Contents

"In other words, money isn't a material reality – it is a psychological construct."

— Yuval Noah Harari,
Sapiens: A Brief History of Humankind

Chapter 1

Introduction and Summary

The existence of money or currency has a long and profound history in the modern course of humanity. It is the fuel of the economy, the common denominator of all transactions, typically within a geographical area, yet it has no fundamental value, especially since the end of the gold standard. The value of sovereign currency is primarily drawn from the collective beliefs of its citizens and its acceptance as legal tender.

There are two aspects to the value of currency, often known as tier 1 money. The primary concern of many central banks around the world is centered on the first aspect, i.e., price stability[1]. A stable price level or contained inflation is key to maintaining trust in the central bank. If a central bank cannot deliver on its objective of keeping prices stable, consumers might revise their inflation expectations upward, commonly known as *de-anchoring*. On the other hand, higher trust in central banks helps contain inflationary pressures (Christelisa et al. (2020)).

The second aspect is the role of money as a numeraire. Tier 1 monies are special in this regard, since they are claims on themselves, unlike other forms of money. Therefore, Central Bank Digital Currencies (CBDCs) are a new addition to this category. While they closely resemble reserves, they are intended for retail use and thus made available to the public, similar to cash. In recent decades, the use of cash has steadily declined, currently comprising only about 15% of the M1 supply in many developed economies. Meanwhile, bank money, classified as tier 2 money since it represents claims on central bank money, has taken center stage in the payment system. Central banks therefore have a legitimate reason to be concerned about losing relevance, especially in the digital domain.

When Milton Friedman and Anna J. Schwartz wrote the influential paper *Has Government Any Role In Money?*, they were entering relatively new territory in the world of fiat currencies. However, they were certain about the necessity of government intervention in

[1] For example, the primary objective of the ECB is to maintain price stability according to Article 105 of the Treaty establishing the European Community. (p. 75) `https://eur-lex.europa.eu/legal-content/EN/TXT/PDF/?uri=CELEX:12002E/TXT`

the monetary system:
Of course, recognition that there are 'good reasons' for government to intervene and that, as a matter of historical fact, governments, and especially modern governments, almost invariably have done so, does not mean that the actual interventions have promoted the public welfare or that the modes of intervention have been wisely chosen. A major aim of our monetary history was precisely to investigate this question for the U.S. for the period after the Civil War. - Friedman and Schwartz (1986)
In this pivotal moment in monetary history, many central banks around the world are seeking to maintain their footprint in the digital payments space by issuing digital currencies. According to IMF (2020), this move could reduce the operational cost of cash by approximately 0.5 to 1% of GDP. Many authors, such as Bordo (2021), argue that digital currencies could address the declining demand for central bank-issued payment instruments. Their argument rests on the observation that the use of cash for payments has dropped significantly. For instance, in the euro area, the number of cash payments declined from 79% in 2016 to 52% in 2024, while the volume of cash payments fell from 54% to only 39% over the same period. This decline can be attributed to the increased usage of digital payment methods (e.g., cards, mobile apps), even for small-value transactions (see ECB (2024b)).
However, this optimistic view should be taken with a pinch of salt. A recent survey conducted by the ECB (see Georgarakos et al. (2025)) found that, although awareness of the digital euro program has increased since the last survey, the actual adoption rate may remain low. The study also identified significant habit persistence in consumer payment behavior. As a result, a significant number of consumers responded negatively when asked about adopting the digital euro. The proposal by Hayek (1976), advocating a system of private currency competition, is problematic, as currencies tend to exhibit strong network externalities, as noted by Brunnermeier et al. (2019). These externalities could similarly affect the digital euro, which would need to compete with private payment systems such as debit cards or mobile apps. Moreover, behavioral and cultural factors play a major role in payment choices. For example, in Germany, the preference for cash stems primarily from concerns about losing control. Cash provides a tangible way to visualize and track spending, which is especially valued by debt-averse consumers.
The main theme of this doctoral dissertation is to understand to what extent consumers' preferences in payments and behavior in the deposit market matter for the success of digital currency if introduced by central banks. From the consumer survey conducted by ECB researchers Georgarakos et al. (2025), it is clear that consumer payment behavior will play a major role in determining the amount of digital euros actually used in the economy and the overall demand for such digital instruments. As mentioned in Bindseil

and Senner (2024), both the DSGE models in Chapter 2 and Chapter 3 fail to account for the conservative approach of central banks, especially the ECB, which do not wish to alter the traditional role of commercial banks but do aim to increase their digital footprint in payment infrastructure through the introduction of a central bank-backed digital currency.

Thus, the introduction of CBDCs can be seen more as a reaction to changing public payment behavior than as a proactive disruption of the monetary system. Existing DSGE models such as Burlon et al. (2024a), Ferrari Minesso et al. (2022) typically include CBDCs in households' utility functions, implying non-pecuniary benefits from holding these assets. However, this approach does not fully capture the central bank's actual motivations, as outlined in recent progress reports on the Digital Euro (see ECB (2024a)). That said, the main objective of my DSGE models is not to endogenize the central bank's behavior, but rather to understand the implications for monetary and fiscal policy when a central bank introduces a CBDC, given the existing structure of the deposit market and the behavioral characteristics of consumers in terms of financial savings and liquidity demand.

In Chapter 2, I construct a Dynamic Stochastic General Equilibrium (DSGE) model to explore how the introduction of a CBDC affects the banking sector, monetary transmission, and macroeconomic dynamics, particularly under varying consumer preferences for liquidity. The motivation stems from growing concerns among central banks over disintermediation risks and loss of monetary control, especially as digital payment ecosystems become increasingly dominated by private actors. The model builds on the banking structure of Gerali et al. (2010), introducing monopolistic competition in the deposit market to capture observed stickiness and market power in bank pricing, as emphasized by empirical studies such as Drechsler et al. (2017). It incorporates a two-household framework with heterogeneous liquidity preferences: patient households derive utility from holding both cash and CBDC, while impatient households borrow to smooth consumption and do not hold liquid assets. The CBDC instrument is parameterized to allow varying degrees of substitutability with cash, following the approach of Agur et al. (2019). Storage costs apply to cash but not to CBDC, creating a structural advantage for the latter. The model captures the potential for CBDC to reduce banks' deposit base, increasing funding costs and impacting loan supply. However, the consequences of this substitution depend critically on banks' pricing power and the liquidity needs of households. When households are homogeneous, greater deposit elasticity (i.e., reduced market power of banks) results in contractionary outcomes, as deposit outflows constrain credit provision and dampen aggregate demand. In contrast, with heterogeneous liquidity preferences, these effects are mitigated: High-liquidity households continue to supply deposits despite

lower returns, and the macroeconomy experiences a milder or even expansionary adjustment. This result highlights a key policy insight: CBDC-induced disintermediation is not uniform across demographic or behavioral lines and must be evaluated in the context of underlying heterogeneity in financial preferences. Moreover, the analysis shows that monetary policy transmission is weakened in the presence of CBDC. The availability of a costless, interest-bearing digital asset lowers the sensitivity of household saving behavior to changes in the nominal interest rate. This decoupling can reduce the effectiveness of traditional policy levers, particularly when CBDC and cash are complements rather than substitutes. The model also reveals that design features of CBDC, such as its remuneration and substitutability, have significant implications for investment behavior, with higher substitutability supporting stronger investment responses under technology shocks but exacerbating bank disintermediation under financial shocks.

In Chapter 3, I extend the analysis by addressing an important but often overlooked dimension in the debate on CBDC: the long-term relationships between banks and depositors. While much of the existing literature evaluates the disintermediation risk through the lens of competitive deposit markets, empirical evidence suggests that households often maintain persistent relationships with their banks, shaped by switching costs, bundled financial services, and behavioral inertia. This persistence can significantly cushion the impact of CBDC on bank funding but also introduces new frictions that matter for welfare and policy transmission. To study this, I develop a medium-scale DSGE model with financial frictions à la Gertler and Karadi (2011), augmented with a deep-habits framework in the banking sector based on Airaudo and Olivero (2019) and Aliaga-Díaz and Olivero (2010). The model features a banking sector with endogenous spread dynamics, where deposit rates evolve sluggishly due to habit persistence and relationship-specific frictions. These frictions mimic the hold-up problem in long-term depositor-bank relationships, allowing banks to exert market power and insulate themselves from short-run shocks, including the competitive pressure induced by the introduction of a CBDC. The model is calibrated to match key features of the U.S. banking sector, including the low pass-through of policy rates to retail deposit rates, as observed in data from the Federal Reserve and confirmed in studies such as Drechsler et al. (2017). Simulations show that in the presence of CBDC, the credit intermediation channel of banks becomes more sensitive to monetary shocks, especially when central banks manage retail CBDC instruments less efficiently or without tiered remuneration. While contractionary monetary policy increases funding costs and compresses bank profits, deep-habit dynamics in deposit pricing allow banks to smooth out the adjustment and protect margins. More interestingly, the model reveals that the depositor-bank relationship itself becomes a stabilizing force. In scenarios where banks maintain strong relationships with depositors, CBDC-induced deposit outflows are

significantly muted, limiting the potential for disintermediation. However, when these relationships weaken, due to either policy shocks or declining switching costs, deposit spreads compress, and banks respond by deleveraging or increasing lending spreads, amplifying the macroeconomic impact. Finally, I explore the welfare implications of CBDC introduction in the presence of relationship banking. While CBDC can discipline excessive rent extraction by banks, it also imposes a cost on central banks in managing retail instruments and may reduce the efficiency of credit allocation if disintermediation is not properly mitigated. These results highlight that CBDC is not a neutral policy instrument; it interacts with existing market structures in non-trivial ways. As such, central banks must carefully weigh the competitive and relational aspects of banking when designing CBDC frameworks.

Brunnermeier and Niepelt (2019) provide a useful benchmark for thinking about the macroeconomic consequences of introducing a central bank digital currency. In their general framework, a swap of deposits for CBDC is neutral, leaving equilibrium allocations and prices unchanged, whenever wealth neutrality and liquidity neutrality hold. Wealth neutrality requires that households' net worth be unaffected when they reallocate between deposits and CBDC, while liquidity neutrality requires that this reallocation does not tighten or relax any of the economy's means-of-payment constraints. When these conditions are satisfied, and when the central bank supplies pass-through funding to offset banks' lost deposits, the deposit supply schedule is effectively replicated. In that case, households, firms, and banks face the same feasible sets as before the introduction of CBDC, and the initial allocation remains an equilibrium. The models developed in Chapters 2 and 3 deliberately move away from this neutrality benchmark. First, CBDC and deposits are modeled as imperfect substitutes, implying that changes in their relative composition alter households' liquidity services and thereby violate liquidity neutrality. Second, the deposit market features monopolistic competition, so even with full pass-through funding, banks cannot preserve their pre-CBDC profit margins. These distributional effects break wealth neutrality by shifting seigniorage rents away from banks. Finally, under Gertler and Karadi (2011)-type financial frictions with moral hazard, the composition of bank funding is itself incentive-relevant: household deposits provide discipline that central-bank funding does not. Replacing deposits with CBDC therefore changes banks' moral-hazard constraints and invalidates the equivalence conditions. As a result, in the environments I study, the introduction of CBDC generally induces non-neutral reallocations in the banking sector and the broader economy.

There is another concern for policymakers besides the neutrality of CBDC, namely its effect on banks, especially when they have monopoly power in the deposit market. Andolfatto (2020) shows that the introduction of CBDC can enhance lending, as bankers will

face competition from the CBDC interest rate, thereby reducing their monopoly power. Using an overlapping-generations model, he shows that when CBDC and deposits are perfect substitutes, what matters for private banks is whether the CBDC interest rate is set below the IOR rate set by the central bank. If so, banks face direct competition from the CBDC interest rate. In my DSGE models, there are several differences compared with Andolfatto (2020). First, banks in my model do not have alternative funding options. Therefore, there is a direct impact on the balance sheet of the bank, and a reduction in deposits leads to a decline in overall loans. I model deposits and CBDC in a non-separable money-in-utility framework. By design, an increase in CBDC leads to an increase in the deposit base. Surprisingly, due to the presence of monopoly power in the banking sector, deposit spreads increase as well. Hence, households are willing to hold greater deposits even at a lower return on deposits.

There is little empirical work on CBDC to complement the growing theoretical literature. Despite the lack of data on actual CBDC usage, Li (2023) use the Canadian Financial Monitor Survey and the Methods of Payment Survey to estimate a nested logit model of CBDC demand. They find that if the attributes of CBDC are more similar to cash, demand for CBDC would be around 4 percent of total liquid assets, whereas if CBDC is designed to resemble deposits, demand could be as high as 52 percent. This result is driven by the fact that households tend to store liquid assets in deposits because they are often bundled with other banking services. In another paper, Li et al. (2024) shows that neglecting the financial services provided by deposits can lead to a significant overestimation of CBDC demand. Moreover, if an unremunerated CBDC does not have service locations such as post offices or bank branches, its demand can be very low, capturing only about 0.7 percent of the market. Complementing this demand-based evidence, Whited et al. (2022) estimate a dynamic banking model and find that a one-dollar increase in CBDC holdings replaces roughly eighty cents of bank deposits, although only a fraction of this reduction translates into lower lending because banks substitute toward wholesale funding. They also show that this shift raises banks' interest rate risk and weakens their resilience, particularly for smaller banks that face higher wholesale funding costs.

In Chapter 4, I turn to a methodological contribution motivated by one of the most persistent critiques of agent-based macroeconomic models (ABMs): their calibration. While ABMs offer a powerful framework for capturing heterogeneity, network effects, and bounded rationality, their flexibility comes at a cost. Critics often point out that ABMs feature high-dimensional parameter spaces, and without rigorous empirical grounding, calibration risks becoming ad hoc or even arbitrary. Addressing this challenge is essential if ABMs are to be taken seriously in policy or forecasting contexts, particularly in areas like CBDC, where agent behavior and institutional design interact in complex ways. This

chapter proposes a novel calibration framework for ABMs that leverages recent advances in machine learning and reinforcement learning to efficiently search parameter spaces and improve fit with empirical data. The approach is tested on the well-established ADG model introduced in Assenza et al. (2015), which serves as a representative benchmark for macro-financial ABMs. The calibration procedure is structured in three stages. First, a machine learning-based search algorithm, such as a random forest surrogate, is used to identify promising regions of the parameter space. Second, we run extensive simulations in those regions. Third, a loss function quantifies the fit between simulated outcomes and real-world time series data, allowing us to iteratively refine our search toward optimal parameter sets. This method offers several practical advantages. First, we show that random forest surrogates are particularly effective in navigating the highly irregular and non-convex landscape of ABM loss functions. Second, combining multiple search strategies into a mixed method consistently improves calibration performance across different empirical targets. Most notably, reinforcement learning can be employed to dynamically weight and aggregate these strategies during the search process, achieving better outcomes than any single method alone. The results demonstrate that it is not only feasible to calibrate ABMs to macroeconomic data, but that doing so with modern AI tools can greatly enhance both the speed and robustness of the calibration process. This is particularly important for large-scale policy-oriented ABMs, such as those modeling the transition to digital currencies, where policy parameters interact with agent-level decisions in nonlinear and path-dependent ways. By offering a systematic and data-driven method of calibration, this chapter helps bridge the gap between ABMs and empirical macroeconomics, bringing the flexibility of agent-based approaches closer to the standards of validation required for practical policy analysis.

In Chapter 5, we develop an agent-based macroeconomic (ABM) framework to study the introduction of a CBDC as a novel payment instrument in an economy where both cash and deposit money already coexist. This modeling approach allows us to explicitly incorporate heterogeneous behaviors among consumers and firms, particularly focusing on how payment preferences and technology adoption evolve over time in response to the introduction of CBDC. Unlike representative-agent models, the ABM framework captures the endogenous emergence of frictions in payment coordination due to the decentralized nature of decision-making. The model simulates an economy with multiple consumers and firms interacting on markets for goods, labor, and credit. A key novelty is the explicit treatment of the payment system as a two-sided market: consumers derive utility from using different payment instruments, and firms decide which ones to accept based on their expectations of consumer behavior. The introduction of CBDC shifts the equilibrium in this two-sided market and induces a regime transition that is nontrivial and

temporally uneven. Simulation results suggest that the economy undergoes an initial contraction following the introduction of CBDC. This contraction stems from a mismatch between consumer adoption and merchant acceptance, leading to payment frictions and underutilization of consumption budgets. Uncertainty about CBDC's privacy and security features further delays adoption, creating a coordination failure that suppresses aggregate demand, reduces output, and raises unemployment in the short run. Over time, as consumers and firms gradually update their expectations and adoption spreads, the economy recovers. The long-run effects are positive: payment efficiency increases, and the economy reaches a higher level of output and employment compared to the pre-CBDC equilibrium. However, the magnitude and duration of the transitional effects depend heavily on consumers' feature preferences and the substitutability between CBDC and other forms of money. Simulations under different CES preference parameterizations show that stronger complementarity between payment features significantly delays adoption and deepens the short-run downturn, even if long-run outcomes improve. The agent-based framework also captures path-dependent dynamics that are difficult to model in more traditional setups. For example, the inertia in firm acceptance behavior can generate persistent underutilization of CBDC unless nudged by policy interventions such as public communication, incentives, or standard-setting around CBDC design. Importantly, the model highlights that successful CBDC implementation requires more than just technical availability; it demands alignment between institutional design, user preferences, and network effects in payment behavior. Together, these results contribute to a growing recognition that digital currency adoption is not simply a technological change but a deep institutional shift with complex macroeconomic repercussions. Agent-based modeling, with its granularity and behavioral realism, offers a powerful lens for capturing these dynamics and guiding policy decisions in the design and roll-out of sovereign digital currencies.

Taken together, the chapters of this thesis aim to provide a comprehensive and multi-method exploration of how a Central Bank Digital Currency could reshape the financial landscape. From structural DSGE models capturing institutional frictions and policy trade-offs to agent-based simulations highlighting coordination failures and behavioral dynamics, and finally to methodological advances in calibrating such complex models, this dissertation offers both theoretical insight and practical tools. While the promise of CBDC is often framed in terms of innovation and inclusion, the findings here underscore that its success will ultimately hinge on a deeper understanding of household behavior, banking market structure, and the slow-moving but powerful forces of habit and trust. As central banks navigate this digital frontier, the evidence presented across these chapters makes clear that the design of CBDC cannot be separated from the social and economic systems into which it is introduced.

Chapter 2

A Macroeconomic Model of Central Bank Digital Currency

2.1 Introduction

Central bank digital currency (CBDC) has quickly become a substantial focus of central bank research, and many claim that this is due to central banks around the world experiencing a major fear of missing out. The presence of many cryptocurrencies has led to this belief, and central banks do not want to leave significant control in the hands of private companies when it comes to payments and money. Gorton and Zhang (2022) goes to great lengths discussing why the government should be cautious when considering the coexistence of privately issued digital money, like stablecoins, and fiat currencies, as it could result in the relinquishment of their monopoly on issuing and circulating money. The introduction of CBDC poses several concerns to the monetary authorities of economies. For example, CBDC might substitute conventional private money, i.e., deposits held at banks, leading to a substantial increase in the funding cost of banks; see Carapella and Flemming (2020). Keister and Sanches (2022) have shown that if CBDCs become highly competitive with bank deposits, disintermediation is unavoidable. The impact of CBDCs on bank funding depends on whether they are cash-like or deposit-like. A cash-like CBDC would have no direct effect on bank funding, but a deposit-like CBDC would lead to a reduction in deposits and lending. Despite this, the introduction of a CBDC would increase the aggregate stock of liquid assets, leading to more efficient exchange and improved social welfare. In their work, they model the banking sector as a competitive market using the framework of Lagos and Wright (2005). This outcome has solid ground, as households around the world consider the central bank's liability the safest one, as recently conveyed by the survey of OMFIF (2020).

Although the above claim can be contested, as empirical studies seem to show that banks

have market power. [1] In another work, Chiu et al. (2023) micro-founded a general equilibrium model of the payments and banking market and calibrated it to the U.S., finding an imperfectly competitive banking sector. An interest-bearing CBDC could increase bank intermediation by raising bank lending by 1.57%, as well as deposit and loan rates, but CBDC remuneration must remain within a specific range. Garratt et al. (2022) created a simplified model in which big and small banks compete to illustrate how the introduction of a CBDC could have varying effects. They assumed that big banks offer nonpecuniary benefits to depositors, but this benefit could be mimicked by a bank-distributed CBDC, even if policymakers could independently set the convenience yield. In their scenario, introducing an interest-bearing CBDC reduces the convenience gap between small and large banks, thereby weakening the market power of big banks.

Although banks might see their profits squeezed by the CBDC, the extent of this effect will depend on how easily they can switch to alternative market-based funding, increase lending rates (which could lead to a loss of potential borrowers), or deleverage. Hence, the business strategy of banks, their level of leverage, the size of the bank, and its reputation are all important considerations in understanding the effect of CBDC. Different hypothetical scenarios regarding these dynamics are discussed in detail in Adalid et al. (2022).

The success of the newly introduced payment instrument in the economy (CBDC in this case) hinges on many important factors. Some of these factors include consumer preferences and its similarity to cash. Since a CBDC is a central bank liability and is promoted as a digital alternative to cash, consumers will evaluate its usefulness based on how closely it resembles cash. In this paper, I study two major aspects of digital currency: cash similarity and the heterogeneity of utility that consumers derive from holding liquid payment instruments.

This paper contributes to the important and growing body of work on bank intermediation and lending in the presence of CBDC by developing a Dynamic Stochastic General Equilibrium (DSGE) model featuring bank monopoly and the adoption of a liquid asset, following Gerali et al. (2010). The supply side of the credit market is primarily populated by private banks. Monopolistic competition, along with market power, is one of the key characteristics of these banks. Banks often exploit lock-in effects, i.e., long-term relationships with customers—as the latter find it costly to switch banks frequently. These long-term relationships often give rise to asymmetric information in the contracts between borrowers and lenders (see Diamond (1984), Sharpe (1990)). Many empirical studies have confirmed that interest rate spreads and bank profitability are strongly influenced by the

[1] In their study, Drechsler et al. (2017) provided evidence of the market power that U.S. banks hold in deposit markets. Their findings indicated that when the federal funds rate increases, the policy rates and deposit rates exhibit a wider spread, ultimately leading to a decrease in the total volume of deposits.

degree of competition among banks (for more detailed studies, see Berger et al. (2004), Degryse and Ongena (2008)). This monopoly power might attenuate the crowding-out effect on deposits, as Andolfatto (2020) shows that banks may leverage this power to counteract the impact of CBDC. Moreover, monopolistic competition in the banking sector might lead to an increase in lending activity, as banks may raise deposit rates and subsequently lower lending rates, resulting in higher volumes of credit supplied to firms due to increased demand. Andolfatto (2020) developed an overlapping generations model to study these effects, whereas this paper employs a DSGE modeling approach, allowing for the analysis of general equilibrium effects and policy rules.

The paper follows Gerali et al. (2010) to develop the DSGE model and incorporates CBDC into the economy. Among the two types of households, patient households derive utility from holding cash and CBDC, whereas impatient households are net borrowers in the economy and do not hold any liquid assets. Cash entails a quadratic storage cost that increases with the level of cash holding, following Burlon et al. (2024a), whereas CBDC is free from such costs, thereby offering a potential advantage over cash. The central bank can adjust the degree to which CBDC behaves like cash or deposits by modifying its elasticity of substitution and a scaling parameter, following Agur et al. (2019). Impatient households smooth their consumption by borrowing from banks, with housing used as collateral, as in Iacoviello (2005). Entrepreneurial firms produce wholesale goods by borrowing from banks to finance capital purchases. They face a borrowing constraint, with the present value of capital serving as collateral, following Kiyotaki and Moore (1997). The banking sector is divided into two components: the retail sector and the wholesale sector. The wholesale sector determines the spread between the deposit rate and the policy rate. In the retail sector, banks decide the interest rates to charge households and firms. Banks' market power is captured through the interest rate elasticity of deposit and loan demand. Additionally, banks face quadratic adjustment costs when changing interest rates.

The introduction of CBDC reduces the typical responses of output, consumption, etc., when the economy is faced with a total factor productivity shock. On the other hand, the response of investment is the opposite; investment is higher in the model with CBDC. Although banks experience an outflow of deposits, they reduce the interest rate charged on firm loans, which helps them recover some of the lost profit margins. Monetary policy transmission is weakened under the CBDC model. Since households have an alternative savings instrument without a storage cost, an increase in the interest rate does not raise the opportunity cost of holding sovereign currency, as it does in the absence of CBDC. To understand the implications of CBDC design choices, I conducted simulations with scenarios where CBDC and cash are either substitutes or complements. When the economy

faces a bank capital quality shock, the banking sector is worse off in the case where cash and CBDC are complements. In this case, the increase in deposit holdings is smaller than in the substitution scenario. As households increase their savings in central bank-backed assets, the overall outflow of deposits becomes higher. When households are heterogeneous in terms of liquidity preference, changes in banks' market power in the deposit market have varying consequences. In the homogeneous case, an increase in deposit elasticity, i.e., a reduction in banks' market power, is contractionary. As banks face larger deposit outflows, they become less able to supply loans to firms and households. As a result, investment declines, along with output and consumption. Since households have less income, they save less in both CBDC and cash, leading to a decline in the holdings of both. In contrast, when liquidity preference is heterogeneous, a decrease in banks' market power has an expansionary effect on the economy. A significant portion of the population has a higher demand for liquidity services, so banks still receive deposits from households even when their market power is reduced. The same applies to cash and CBDC holdings. Policymakers designing digital currencies need to account for heterogeneity in liquidity preferences across the population when drawing conclusions about the crowding-out effect of CBDC on bank deposits.
The rest of the paper is structured as follows: Section 3.3 describes the model and its features; Section 3.4 explains the calibration and estimation of the model; Section 3.5 presents the results; and finally, Section 3.7 concludes the paper.

2.2 Model

My model is constructed upon the closed-economy DSGE framework by Gerali et al. (2010), in which the economy consists of households, firms, capital-good producers, entrepreneurs, retailers, one representative bank, and a central bank.
Households are of two types: impatient and patient. They differ in how they discount the future, or in other words, how impatient they are. By construction, the discount factor of patient households (β_P) is greater than that of impatient households (β_I). Households work, accumulate housing services, and use financial instruments for consumption smoothing. Entrepreneurs, on the other hand, hire labor from both types of households, purchase capital goods, produce intermediate goods, and sell them to retailers.
Workers supply labor in a frictionless, competitive framework to entrepreneurs, and their wages are determined to match firm demand. Capital goods producers transform retail goods and depreciated capital into new capital, which is used in the production of intermediate goods. Retailers buy intermediate goods from entrepreneurs in a competitive market and repackage them in a differentiated monopolistic market, subject to nominal

price rigidity following Rotemberg (1982).
In the financial sector, there is a representative bank that provides loans to impatient households using housing services as collateral. It also lends to entrepreneurs using inflation-adjusted capital as collateral. Banks are subject to regulations in the form of costly deviations from the optimal bank capital-to-asset ratio. Patient households hold deposits at the bank and earn interest rates set under monopolistic competition. The central bank must make two policy decisions: set the policy interest rate or the supply of cash, and set either the supply or interest rate of the CBDC. Patient households hold both cash and CBDC, which are supplied by the central bank.

2.2.1 Patient Household

The infinitely lived patient household maximizes their following utility function by choosing a level of consumption, how much to work, and a financial portfolio for saving.

$$\mathbb{E}_0 \sum_{t=0}^{\infty} \beta_P^t \left[(1-a^P)\epsilon_t^Z \log(C_t^P(i) - a^P C_{t-1}^P) + \epsilon_t^h \log\ H_t^P(i) - \frac{L_t^P(i)^{1+\phi}}{1+\phi} + \chi_{z,t}\ \log\ Z_t \right] \tag{2.1}$$

where the z_t represents the consumption of liquidity services provided by deposits, cash, and CBDC, as in Burlon et al. (2024a). z_t is a CES aggregate bundle of the liquid asset and has the following expression:

$$Z_t = \left[M_t^{\frac{\eta_{z,t-1}}{\eta_{z,t}}} + \vartheta_t\, DC_t^{\frac{\eta_{z,t-1}}{\eta_{z,t}}} + \omega_d\, D_t^{\frac{\eta_{z,t-1}}{\eta_{z,t}}} \right]^{\frac{\eta_{z,t}}{\eta_{z,t-1}}} \tag{2.2}$$

Household consumption C_t^P is affected by the external and group-specific consumption habits of the last period C_{t-1}^P. The steady-state impact of habits is offset by the factor of $1 - a^P$. They supply L_t^P units of labor and are paid an hourly wage of W_t^P. The labor disutility is parameterized by the inverse Frisch elasticity parameter ϕ. The patient household opts for H_t^P units of housing services, which are subject to housing demand shock ϵ_t^h.

$$\begin{aligned} &C_t^P(i) + Q_t^P \Delta H_t^P(i) + D_t^P(i) + M_t^P(i) + DC_t^P(i) + f(M_t^P(i)) \leq \\ &W_t^P L_t^P(i) + (1+R_{t-1}^d)\frac{D_{t-1}^P(i)}{\Pi_t} + (1+R_{t-1}^{DC})\frac{DC_{t-1}^P(i)}{\Pi_t} + \frac{M_{t-1}^P(i)}{\Pi_t} + T_t^P(i) \end{aligned} \tag{2.3}$$

The cash is subject to storage cost in the form of $f(M_t) = \frac{\psi_M}{2} M_t^2$ with $\psi_M > 0$ following Burlon et al. (2024a). Deposit holding is remunerated by the net rate R_t^D from the bank,

and CBDC holding is remunerated by the net rate R_t^{DC} from the central bank. Π_t is the gross inflation rate and T_t^P is the lump-sum transfer that includes dividends from firms and banks.

Effective lower bound The first-order condition of cash can be rewritten as

$$\begin{aligned}\Lambda_t^P &= \beta_P \mathbb{E}_t \frac{\Lambda_{t+1}^P}{\Pi_{t+1}} - \Lambda_t^P \psi_M M_t + \left(\frac{\chi_t^Z}{Z_t}\right)\left(\frac{Z_t}{M_t}\right)^{\frac{1}{\eta_t^Z}} \\ &= \beta_P \mathbb{E}_t \frac{\Lambda_{t+1}^P}{\Pi_{t+1}} \left[1 - \frac{\Lambda_t^P \psi_M M_t \mathbb{E}_t \Pi_{t+1}}{\beta_P \mathbb{E}_t \Lambda_{t+1}^P}\right] + \left(\frac{\chi_t^Z}{Z_t}\right)\left(\frac{Z_t}{M_t}\right)^{\frac{1}{\eta_t^Z}}\end{aligned}$$

Thus, we can think of $\left[1 - \frac{\Lambda_t^P \psi_M M_t \mathbb{E}_t \Pi_{t+1}}{\beta_P \mathbb{E}_t \Lambda_{t+1}^P}\right]$ the gross return on cash by drawing a similarity with other assets. The marginal cost of storage of cash is $\psi_M M_t$. Thus the term $\frac{\Lambda_t^P \psi_p M_t \mathbb{E}_t \Pi_{t+1}}{\beta_P \mathbb{E}_t \Lambda_{t+1}^P}$ represents the next period's value of the marginal cost of storing 1 unit of real cash balance today. The return on cash is therefore negative as typically $\psi_M > 0$. The return on cash decreases with (1) a higher level of cash balance and (2) a higher level of inflation. A consumer who only holds cash will be interested in holding another asset if its return is slightly higher than the negative return on cash, even if the return on that asset is itself negative. Therefore, the *effective lower bound* of the economy is given by

$$-\frac{\Lambda_t^P \psi_M M_t \mathbb{E}_t \Pi_{t+1}}{\beta_P \mathbb{E}_t \Lambda_{t+1}}$$

In a zero-inflation steady state, the lower bound simplifies to $-\psi_M M/\beta_P$ which corresponds to the marginal storage cost of cash in the steady state.

2.2.2 Impatient Household

Impatient households are net borrowers of the economy and maximize the following utility function by choosing the level of consumption C_t^I, number of hours to work, L_t^I and housing services H_t^I.

$$\max_{C_t^I, H_t^I, L_t^I, B_t^I} \mathbb{E}_0 \sum_{t=0}^{\infty} \beta_I^t \left[(1-a^I)\epsilon_t^Z \log(C_t^I(i) - a^I C_{t-1}^I) + \epsilon_t^h \log H_t^I(i) - \frac{L_t^I(i)^{1+\phi}}{1+\phi}\right]$$

subject to the budget constraint

$$C_t^I(i) + Q_t^h \Delta H_t^I(i) + (1 + R_{t-1}^{bH}) \frac{B_{t-1}^I(i)}{\Pi_t} \leq W_t^I L_t^I(i) + B_t^I(i) + T_t^I(i) \tag{2.4}$$

In order to smooth their consumption, impatient households borrow B_t^I units of loan against the housing service as collateral, thus subject to eq 2.5

$$(1 + R_t^{bH})B_t^I(i) \leq m_t^I \mathbb{E}_t[Q_{t+1}^h H_t^I(i)\Pi_{t+1}] \tag{2.5}$$

where m_t^I stands for the loan-to-value ratio for the credit that the bank lends to the impatient household. The m_t^I has been considered exogenous and subject to shocks, representing the fact that during the bad or good times, banks might face different levels of risk and thus change the percentage of capital required as collateral.

2.2.3 Entrepreneurs

The entrepreneurs maximize the following utility function

$$\mathbb{E}_0 \sum_{t=0}^{\infty} \beta_E^t \log(C_t^E(i) - a^E C_{t-1}^E)$$

by choosing their consumption C_t^E, level of utilization of physical capital U_t , level of physical capital K_{t+1}. Their optimization problem is subject to two constraints, namely the budget constraint and the borrowing constraint. The budget constraint for the entrepreneurs is as follows:

$$C_t^E(i) + W_t^P L_t^{E,P}(i) \; + \; W_t^I L_t^{E,I}(i) \; + \; (1 + R_{t-1}^{bE})\frac{B_{t-1}^E(i)}{\Pi_t} \; + \; Q_t^k K_t^E(i) \; + \; \psi(U_t(i))K_{t-1}^E(i) = \frac{Y_t^E(i)}{X_t} \; + \; B_t^E(i) \; + \; Q_t^k(1-\delta)K_{t-1}^E(i) \tag{2.6}$$

Entrepreneurs produce intermediate goods according to Eq. 2.7. They hire labor from patient and impatient households and pay them hourly wages W_t^P and W_t^I respectively. Total labor employed is L_t^E and it is aggregated using a Cobb-Douglas function, $L_t^E = [L_t^{E,P}]^{\mu}[L_t^{E,I}]^{1-\mu}$ where μ is the labor income share of the patient household (Iacoviello and Neri (2010)). Physical capital is priced at, Q_t^k and its utilization comes at a cost of $\psi(U_t(i))$. X_t is the relative price of wholesale goods to retail goods and is defined as $\frac{P_t^W}{P_t} = \frac{1}{X_t}$.

$$Y_t^E(i) = A_t^E[K_{t-1}^E(i)U_t(i)]^{\alpha} L_t^E(i)^{1-\alpha} \tag{2.7}$$

In order to meet their funding gap, entrepreneurs borrow B_t^E units of loans from the bank at the net interest rate R_t^{bE} per unit. Banks ask for physical capital as collateral. Therefore, the borrowing constraint becomes the discounted value of next period's stock of physical capital. Like in the case of impatient households, the borrowing constraint of

the entrepreneurs is also subject to a loan-to-Value ratio M_t^E.

$$(1 + R_t^{bE})B_t^E(i) \leq m_t^E \mathbb{E}_t[Q_{t+1}^k(1-\delta)K_t^E(i)\Pi_{t+1}] \tag{2.8}$$

2.2.4 Loan and Deposit Demand

Banks are subject to monopolistic competition in the deposit and loan market. Each financial product is differentiated, and its demand is inversely proportional to the return/cost of the product. Therefore, demand for two types of loans to bank j is given by

$$B_t^I(j) = \left(\frac{R_t^{bH}(j)}{R_t^{bH}}\right)^{-\epsilon_t^{bH}} B_t^I \qquad B_t^E(j) = \left(\frac{R_t^{bE}(j)}{R_t^{bE}}\right)^{-\epsilon_t^{bE}} B_t^E \tag{2.9}$$

with

$$R_t^{bH} = \left[\int_0^1 R_t^{bH}(j)^{\epsilon^{bH}-1} dj\right]^{\frac{1}{\epsilon^{bH}-1}} \quad \text{and} \quad R_t^{bE} = \left[\int_0^1 R_t^{bH}(j)^{\epsilon^{bE}-1} dj\right]^{\frac{1}{\epsilon^{bE}-1}}$$

Similarly, aggregate deposit demand for patient household j is given by

$$D_t^P(j) = \left(\frac{R_t^d(j)}{R_t^d}\right)^{-\epsilon_t^d} D_t^P \tag{2.10}$$

and the interest on the deposit is given by

$$R_t^d = \left[\int_0^1 R_t^{bH}(j)^{1-\epsilon^d} dj\right]^{\frac{1}{1-\epsilon^d}}$$

Here, steady-state elasticities of the financial products have values $\epsilon^{bH}, \epsilon^{bE} > 1$ for the loans and $\epsilon^d < -1$ for the deposit. These elasticities are considered to be stochastic to allow for the unexpected changes in different bank rate spreads. For more details, see Gerali et al. (2010).

2.2.5 Banking sector

The banking sector model developed in Gerali et al. (2010) provides a solid foundation for analyzing the effects of disintermediation if a central bank were to introduce a CBDC. In this model, banks gain market power through the differentiation of financial products and the gradual accumulation of capital via retained earnings. These features make it a natural choice for studying how banking markets might respond to disintermediation pressures and economic shocks.

Each representative bank of this type j has two branches, namely a *wholesale branch* and

a *retail branch*. The *wholesale branch* is responsible for managing bank capital, wholesale loans, and wholesale deposits. This branch of the bank can be typically thought to be with the other financial institutions, taking part in the open market operation of the Federal Reserve in the US, etc. This branch accumulates bank capital K_t^B according to the following rule:

$$\pi_t K_t^b = (1-\delta^b)K_{t-1}^b + j_{t-1}^b \tag{2.11}$$

where j_{t-1}^b is the retained bank profit from the last period. Banks target for an exogenous leverage ratio, and any deviation from that target would be costly for the bank, implying poor portfolio management, bad economic conditions, etc. We also assume that the bank is able to maintain the exogenous leverage ratio in steady-state, thus removing the cost of deviation from this ratio in the steady-state. Bank capital is also subject to exogenous shocks i.e. *Bank capital shock* to simulate the phenomenon of exogenous changes in banks valuation or equity in the face of financial turmoil.

Wholesale branch of the bank maximize their profit by choosing wholesale loans B_t and wholesale deposit D_t, thus maximizing the following,

$$\max_{B_t,D_t} \mathbb{E}_o \sum_{t=0}^{\infty} \Lambda_{0,t}^P \Big[\left(1+R_t^b\right) B_t - B_{t+1}\pi_{t+1}\, x + D_{t+1}\pi_{t+1} - (1+R_t^{d,w})D_t \\ + K_{t+1}^b\pi_{t+1} - K_t^b - \frac{\kappa_{KB}}{2}\left(\frac{K_t^b}{B_t} - \nu^b\right)^2 \Big]$$

subject to the balance sheet constrain,

$$B_t = D_t + K_t^b \tag{2.12}$$

First order condition of the above optimization problem gives us the wholesale loan rate as,

$$R_t^b = R_t^{d,w} - \kappa_{KB}\left(\frac{K_t^b}{B_t} - \nu^b\right)\left(\frac{K_t^b}{B_t}\right)^2 \tag{2.13}$$

If the wholesale deposit rate $R_t^{d,w}$ (net rate) is the same as the net policy rate of the central bank R_t^{CB}[2], then the spread between the wholesale loan rate and the policy rate is driven by the costs that banks incur when they deviate from the optimal leverage ratio. A decrease in a bank's leverage ratio implies that the bank faces more favorable financial conditions in the market. Therefore, the greater the cost of deviation, the lower the spread between the wholesale interest rate and the policy rate, and banks cannot bid the interest

[2] In open market operations, many central banks, e.g., the Federal Reserve, use the window on the overnight repurchase agreement, creating a ceiling and floor for borrowing and lending. Banks in the interbank markets might use one of these rates, making this assumption viable.

rate higher than what the central bank requires.
The *retail branch* of the bank borrows wholesale loans from the wholesale branch of the bank at the net rate R_t^b and differentiates the loans to offer them to impatient households and entrepreneurs. They apply a markup over the wholesale rate R_t^b and face quadratic costs when changing the interest rates they charge for retail loans. These effects are captured by parameters κ_{bE} and κ_{bH}. Therefore, banks optimize profits by maximizing the following expression by choosing the retail net interest rates, namely R_t^{bH}, R_t^{bE} for loans to impatient households and entrepreneurs, respectively:

$$\max_{R_t^{bH}(j),R_t^{bE}(j)} \mathbb{E}_o \sum_{t=0}^{\infty} \Lambda_{0,t}^P \Bigg[R_t^{bH}(j)B_t^I(j) + R_t^{bE}(j)B_t^E(j) - R_t^b B_t(j) \\ -\frac{\kappa_{bH}}{2}\left(\frac{R_t^{bH}(j)}{R_{t-1}^{bH}(j)} - 1\right)^2 R_t^{bH} B_t^I - \frac{\kappa_{bE}}{2}\left(\frac{R_t^{bE}(j)}{R_{t-1}^{bE}(j)} - 1\right)^2 R_t^{bE} B_t^E \Bigg]$$

subject to the loan-specific demands obtained in section 2.2.4 as

$$B_t^I(j) = \left(\frac{R_t^{bH}(j)}{R_t^{bH}}\right)^{-\epsilon_t^{bH}} B_t^I \quad ; \quad B_t^E(j) = \left(\frac{R_t^{bE}(j)}{R_t^{bE}}\right)^{-\epsilon_t^{bE}} B_t^E \tag{2.14}$$

and the supply of wholesale loan constraint,

$$B_t(j) = B_t^I(j) + B_t^E(j) \tag{2.15}$$

The *retail branch* collects deposits from patient households, pays them R_t^d for their deposit holding, and passes the collection on to the *wholesale branch*, gaining remuneration at the central bank's policy rate R_t^{CB}. Similar to the case of retail loans, the bank faces adjustment costs parameterized by κ_d changing the net deposit interest rate R_t^d. The optimization problem faced by deposit collection is to maximize the profits of deposit funding by choosing R_t^d as

$$\max_{R_t^d(j)} \mathbb{E}_o \sum_{t=0}^{\infty} \Lambda_{0,t}^P \left[R_t D_t(j) - R_t^d(j) D_t^P(j) - \frac{\kappa_d}{2}\left(\frac{R_t^d(j)}{R_{t-1}^d(j)} - 1\right)^2 R_t^d D_t \right]$$

subject to demand for deposits from patient households as described in 2.2.4

$$D_t^P(j) = \left(\frac{R_t^d(j)}{R_t^d}\right)^{-\epsilon_t^d} D_t \tag{2.16}$$

and the wholesale deposit supply constraint,

$$D_t(j) = D_t^P(j) \tag{2.17}$$

The overall bank profit coming from these two branches of the bank is given by

$$J_t^b = R_t^{bH} B_t^H + R_t^{bE} B_t^E - R_t^d D_t - \frac{\kappa_{KB}}{2}\left(\frac{K_t^b}{B_t} - \nu^b\right)^2 K_t^b - \text{Adj}_t^B \tag{2.18}$$

where Adj_t^B is the sum of all adjustment costs incurred during the adjustment of the retail loan and deposit rates.

2.2.6 Capital Producers

Capital producers buy depreciated physical capital $(1-\delta)K_{t-1}$ from the entrepreneurs at a price Q_t^k and final goods from the retailers at a price P_t in a perfectly competitive market. Using these as input, they increase the stock of new physical capital and sell it to the entrepreneurs at price Q_t^k. Hence their optimization problem is given by,

$$\max_{\overline{X}_t, I_t} \mathbb{E}_0 \sum_{t=0}^{\infty} \Lambda_{0,t}^E \left[Q_t^k \Delta \overline{X}_t - I_t \right]$$

subject to

$$\overline{X}_t = \overline{X}_{t-1} + \left[1 - \frac{\kappa_i}{2}\left(\frac{I_t \epsilon_t^{qk}}{I_{t-1}} - 1\right)^2\right] I_t \tag{2.19}$$

where $\Delta \overline{X}_t = K_t - (1-\delta)K_{t-1}$ and $Q_t^k = \frac{Q_t^k}{P_t}$ is the real price of capital.

2.2.7 Retailers

A representative retailer produces in a monopolistically competitive market where prices are sticky, and it follows a pricing using Rotemberg (1982). They maximize the following by choosing an optimal $P_t(j)$ as

$$\max_{P_t(j)} \mathbb{E}_0 \sum_{t=0}^{\infty} \Lambda_{0,t}^P \left[P_t(j) Y_t(j) - P_t^W Y_t(j) - \frac{\kappa_p}{2}\left(\frac{P_t(j)}{P_{t-1}(j)} - \pi_{t-1}^{\iota_p} \pi^{1-\iota_p}\right)^2 P_t Y_t \right]$$

subject to the demand of the specific good j obtained from utilization maximization of a household,

$$Y_t(j) = \left(\frac{P_t(j)}{P_t}\right)^{-\epsilon_t^y} Y_t$$

2.2.8 Central bank

The central bank has two monetary policy tools in this economy. It sets the policy interest rate following

$$R_t^{CB} = (R^{CB})^{1-\phi_R}(R_{t-1}^{CB})^{\phi_R}\left[\left(\frac{\Pi_t}{\pi}\right)^{\phi_\pi}\left(\frac{Y_t}{Y_{t-1}}\right)^{\phi_y}\right]^{1-\phi_R}(1+\epsilon_t^r) \tag{2.20}$$

It also sets the remuneration rate on the CBDC as

$$R_t^{DC} = \phi_{dc,r} R_t^{CB} \tag{2.21}$$

where $\phi_{dc,r}$ is the parameter governing the markdown applied to the net policy rate set by the central bank. Therefore, $\phi_{dc,r} = 0$ is the unremunerated CDBC case as often discussed by relevant policy makers (see ECB (2024a))

2.2.9 Aggregation

The total consumption for the economy is the weighted sum of the group consumption of patient and impatient households and entrepreneurs.

$$C_t = \gamma_P C_t^P + \gamma_I C_t^I + \gamma_E C_t^E \tag{2.22}$$

The supply of the housing services in the economy is considered fixed in the economy to an exogenous level of $\overline{H}$. Thus, the market-clearing condition in the housing market is

$$\overline{H} = \gamma_P H_t^P + \gamma_I H_t^I \tag{2.23}$$

The aggregate output of the economy is the following:

$$\begin{aligned} Y_t = {} & C_t + Q_t^k\left(K_t - (1-\delta_k)K_{t-1}\right) + \delta_{Kb}K_{t-1}^b + f(M_t) + \psi(U_t) + Y_t\frac{\kappa_p}{2}\left(\Pi_t - \pi_{t-1}^{\iota_p}\pi^{1-\iota_p}\right)^2 \\ & + D_t^b R_t^b \frac{\kappa_d}{2}\left(\frac{R_t^d}{R_{t-1}^d} - 1\right)^2 + B_t^H R_t^{bH}\frac{\kappa_d}{2}\left(\frac{R_t^{bH}}{R_{t-1}^{bH}} - 1\right)^2 + B_t^E R_t^{bE}\frac{\kappa_{bE}}{2}\left(\frac{R_t^{bE}}{R_{t-1}^{bE}} - 1\right)^2 \end{aligned} \tag{2.24}$$

2.3 Calibration

I have mostly followed Gerali et al. (2010) and Burlon et al. (2024a) to calibrate my DSGE model. The discount factor for patient households (β_p) is set to 0.9943, matching the annualized deposit interest rate typically observed for the Euro Area. The discount factors

for impatient households (β_i) and entrepreneurs (β_e) are both set to 0.975, reflecting their higher preference for present consumption. Bankers share the same discount factor as patient households, with (β_b) also set at 0.9943. Preferences are calibrated following Gerali et al. (2010): The weight of housing in the utility function (j_h) is 0.2, and the inverse Frisch elasticity of labor supply (ϕ) is set to 1. The loan-to-value ratios are set at 0.7 for impatient households (m_{iss}) and 0.35 for entrepreneurs (m_{ess}). The production function assumes a capital share (α) of 0.25. Physical capital depreciates at a quarterly rate of 2.5% ($\delta_k = 0.025$). The labor income share for patient households (ni) is set at 0.8. Banking parameters are largely adopted from Gerali et al. (2010). The elasticity of substitution between different types of deposits (ε_d) is calibrated at –1.46025. Therefore, the steady-state spread between policy and deposit rates ($R - R^d$) is found to be 0.2650, while the spread between lending rates and CBDC rates ($R - R^{DC}$) depends on the CBDC remuneration policy set by the central bank as a markdown on the policy rate. For loans, the elasticity of substitution between loans to households (ε_{bh}) and loans to firms (ε_{be}) is set at 2.932806 for both categories. The bank capital-to-loans ratio (vi) is set at 0.09. Additional financial frictions include habit formation, which is only active for impatient households ($a_i = 0.867$), while entrepreneurs (a_e) and patient households (a_p) have no habit persistence.

Cash management costs are introduced via a small parameter ($\psi_m = 0.02$) based on Burlon et al. (2024a), and the utility derived from holding liquid instruments (χ_z^{ss}) is set at 0.018. This value of χ_z^{ss} is calibrated to make sure that the cash-to-output ratio is 0.3443 (see Burlon et al. (2024b)). Monetary policy follows a Taylor rule specification: the coefficient on inflation (ϕ_π) is 2.00384, and the coefficient on output (ϕ_y) is 0.30324. Steady-state inflation (π^{ss}) is normalized to 1, and the housing supply (h) is kept constant at 1.

Wherever possible, parameter choices are guided by standard references, notably Gerali et al. (2010) and Burlon et al. (2024a), to maintain consistency with established DSGE modeling practices.

2.4 Results

2.4.1 Steady-State Comparison Across Policy Regimes

This section examines how the steady state of the economy changes once a CBDC is introduced. The analysis highlights how different CBDC policy designs influence the long-run allocation of liquidity between the private banking sector and the central bank. Because the model incorporates a liquidity bundle in the household utility function, there is no analytical closed-form solution for the steady state. Therefore, the steady state is computed

numerically. In all policy cases, the preference parameter χ_z, which governs households' valuation of liquidity services, is calibrated to 0.018. Given this calibration, the numerical solver determines the steady-state values of four endogenous variables jointly: the deposit interest rate, labor of the patient household, cash, and CBDC holdings or interest rate on CBDC.

Two types of CBDC policy rules are considered. Under the *interest rate rule*, the CBDC rate is linked to the policy rate according to:

$$r_{dc} = \phi_{dc,r}\, r_{ib} \tag{2.25}$$

where $\phi_{dc,r} \in \{0, 0.01, 0.1\}$ determines the degree of pass-through from the policy rate to the CBDC rate. Under the *quantity rule*, the central bank fixes the supply of CBDC as a constant share of steady-state output:

$$dc_t = \phi_{dc} y_e \tag{2.26}$$

where ϕ_{dc} takes values $\{0.3443, 0.6886\}$. These regimes are compared with a benchmark economy in which no CBDC is issued, that is, $\phi_{dc} = 0$.

In the benchmark steady state without CBDC, households hold deposits and cash as the only liquid assets. The deposit-to-output ratio equals 2.69, while the cash-to-output ratio is 0.53, which is a bit higher than with evidence from advanced economies, where cash holdings typically represent 20 to 40% of GDP. The total liquidity-to-output ratio equals 2.76, showing that deposits dominate liquidity provision. The steady-state CBDC interest rate is negative at -0.24, and the spread relative to the policy rate is around 97.6 annualized percentage points. As holding CBDC becomes extremely costly, households choose to hold only cash and deposits for liquidity purposes.

Introducing a CBDC under the interest rate rule changes the composition of liquidity in household portfolios. When the CBDC is non-interest-bearing (that is, $\phi_{dc,r} = 0$), the equilibrium CBDC-to-output ratio reaches 0.58, while the cash-to-output ratio declines to 0.34. Total liquidity increases to 3.63, reflecting an increase in the overall liquidity demand driven by CBDC. As CBDC is introduced, households allocate a larger share of liquidity to digital balances, substituting away from deposits while maintaining overall liquidity close to its baseline level.

As the degree of interest rate pass-through rises, the role of CBDC becomes more prominent. When $\phi_{dc,r} = 0.01$, the CBDC-to-output ratio increases to 0.59, and when $\phi_{dc,r} = 0.1$, it rises further to 0.73. These changes correspond to total liquidity-to-output ratios of 3.70 and 3.81, respectively. The higher CBDC return makes it a more attractive store of value, inducing substitution from deposits to CBDC and a small decline in cash holdings.

The CBDC share of total liquidity rises from 0.16 for $\phi_{dc,r} = 0$ to 0.19 for $\phi_{dc,r} = 0.1$. Despite these compositional changes, aggregate variables such as consumption, investment, and real interest rates remain virtually unchanged, suggesting that the macroeconomic impact is confined to balance-sheet reallocation rather than changes in overall activity.

Under the quantity rule, the steady-state outcomes depend on the target share ϕ_{dc}. For the lower target, $\phi_{dc} = 0.3443$, the CBDC-to-output ratio equals 0.34, roughly matching cash holdings in the baseline economy. The total liquidity-to-output ratio rises to 3.34, with a small decline in deposits. For the higher target, $\phi_{dc} = 0.6886$ which is roughly double the cash-to-output ratio, the spread of CBDC interest rate decreases to 1.9337 annualized percentage points, indicating a higher pass-through of the policy rate. This makes CBDC a more attractive savings instrument with respect to cash. The cash-to-output ratio falls slightly to 0.321, confirming that CBDC mainly substitutes for deposits but also marginally reduces cash usage. Across both cases, the preference parameter χ_z remains fixed at 0.018, implying that households' valuation of liquidity services is stable while the composition of liquidity adjusts endogenously to the CBDC policy stance.

The steady-state results also reveal clear evidence of crowding-out effects on both cash and deposit holdings as the role of CBDC expands. Under the interest rate rule, increasing the CBDC return relative to the policy rate leads to a gradual substitution away from traditional liquid assets. When the CBDC rate increases from 0 to $0.01r$, the cash-to-output ratio declines by approximately 0.70%, and the deposit-to-output ratio falls by about 0.06%. A further increase in the CBDC rate from $0.01r$ to $0.1r$ amplifies these effects, with cash holdings decreasing by an additional 7.00% and deposits falling by roughly 0.59%. These results indicate that households primarily substitute CBDC for cash, while the impact on deposits remains modest.

A similar pattern is observed under the quantity rule, where higher CBDC issuance targets generate stronger crowding-out effects. When the CBDC-to-output target rises from 0 to 0.3443, the cash-to-output ratio drops by around 25.73%, and the deposit-to-output ratio decreases by 3.22%. Further increasing the target from 0.3443 to 0.6886 causes cash holdings to fall by another 17.92% and deposits by 1.77%. These results suggest that an expansion of CBDC supply substantially reduces the demand for both cash and deposits, with the effect being much more pronounced for cash. Overall, the findings confirm that CBDC acts as a close substitute for other liquid assets, particularly currency in circulation, leading to a rebalancing of the household liquidity portfolio as digital balances become more prominent in equilibrium.

A marginal policy experiment helps to highlight the different ways in which the two CBDC regimes affect traditional forms of liquidity, whose results are reported in table 2.1. Under the interest rate rule, a 1% increase in the policy parameter $\phi_{dc,r}$ leads to only minor

adjustments in household portfolios: the cash-to-output ratio falls by around 0.007%, and the deposit-to-output ratio declines by roughly 0.0006%. By contrast, when the CBDC supply parameter ϕ_{dc} rises by 1% under the quantity rule, cash holdings drop by about 0.217% and deposits by 0.0207%. This comparison shows that the quantity-based CBDC policy exerts a much stronger crowding-out effect on cash and deposits than the interest rate rule. The reason is that an expansion in the quantity of CBDC directly replaces existing liquid assets in household portfolios, while an increase in the CBDC rate mainly affects portfolio allocation through relative returns rather than through the total stock of liquidity.

The effects of CBDC policy on the long-run allocation of liquidity are contractionary in our calibration and operate primarily through portfolio rebalancing and bank disintermediation. Figure 2.1a varies the CBDC quantity target ϕ_{dc} and shows that a larger CBDC share leads households to substitute away from cash and deposits toward CBDC balances. Accordingly, the cash-to-output ratio declines monotonically, the deposit-to-output ratio falls, and the CBDC-to-output ratio rises. On the price side, the policy rate r^{ib} and loan rates r^{bh} and r^{be} increase with ϕ_{dc}, while the spread between the policy rate and the CBDC rate, $r^{ib} - r^{DC}$, collapses from very high values toward near-zero as CBDC becomes more prevalent and closer in remuneration to other liquid assets. At the same time, the interbank deposit spread $r^{ib} - r^{d}$ widens, consistent with weaker deposit demand and lower deposit remuneration in equilibrium. These balance-sheet and price adjustments reduce the scale of bank intermediation: bank capital K_b contracts and household and firm bond positions (B^H and B^E) edge down, and the stock of bank credit D shrinks. With less external finance available to firms and a higher user cost of capital, investment falls and aggregate output and consumption decline. Although the direction of changes for values for the variables in steady state do not change much, there is a clear effect of decreasing deposit elasticity on the magnitude of values. As deposits become more elastic, i.e., for higher values of ϵ_d, the level of output, consumption, and loans are higher. This implies that although reducing the monopoly power of the bank does not change the behavior of the model as found in Andolfatto (2020), higher CBDC levels are found to have a lower impact on the level of values of output, consumption, and investment. Figure 2.1b varies the pass-through parameter $\phi_{dc,r}$ in the interest-rate rule for CBDC. Raising $\phi_{dc,r}$ increases the return on CBDC relative to deposits, reinforcing its attractiveness as a near-deposit substitute. As a result, CBDC balances rise, while both cash and deposits fall, and bank capital and total lending decline. Loan and policy rates move up with $\phi_{dc,r}$, the interbank–deposit spread $r^{ib} - r^{d}$ widens, and—importantly—the interbank–CBDC spread $r^{ib} - r^{DC}$ narrows as CBDC remuneration more closely tracks the policy rate. The macroeconomic consequences are again contractionary but quantitatively more muted

Table 2.1: Marginal policy exercise: 1% increase in the CBDC policy parameter and steady-state effects on cash and deposits

	Cash-to-output			Deposit-to-output		
Policy change	Baseline	+1%	%Δ	Baseline	+1%	%Δ
Interest rate rule: increase $\phi_{dc,r}$ by 1%	0.33849383	0.33846969	−0.007131	2.56664293	2.56662754	−0.0006
Quantity rule: increase ϕ_{dc} by 1%	0.39113214	0.39028144	−0.2175	2.60007991	2.59954063	−0.02074

Notes: The baseline case for interest rate policy is $\phi_{dc,r} = 0.01$ and for quantity rule is $\phi_{dc} = 0.3443$

Table 2.2: Steady-state solution across CBDC policy regimes (levels)

Policy regime	r_{dss}	I_{pss}	mss	$dcss$	r_{dcss}
Interest rate rule: $r_{dc} = 0$	0.003050	0.762206	0.452082	0.765831	—
Interest rate rule: $r_{dc} = 0.01r$	0.003057	0.762166	0.448875	0.782643	—
Interest rate rule: $r_{dc} = 0.1r$	0.003132	0.761736	0.417108	0.961044	—
No CBDC: $\phi_{dc} = 0$	0.002515	0.764004	0.701564	—	−0.239819
Quantity rule: $\phi_{dc} = 0.3443$	0.002898	0.762945	0.519525	—	−0.001291
Quantity rule: $\phi_{dc} = 2 \times 0.3443$	0.003112	0.761853	0.425352	—	0.000410

Notes: mss denotes steady-state cash, $dcss$ denotes steady-state CBDC balances when the CBDC quantity is endogenous (interest rate rule), and r_{dcss} is the CBDC interest rate when quantity is set exogenously (no-CBDC counterfactual and quantity rules). Dashes indicate not applicable.

than under the quantity rule: investment, consumption, and output drift down as funding conditions tighten, yet the changes remain small because the size of the CBDC balance sheet is not forced to expand; only its relative return improves. Overall, both figures make clear that the long-run impact of CBDC works mainly through a reallocation of liquidity away from deposits and cash, with adverse effects on bank intermediation and real activity; the quantity-based design generates the stronger crowding-out and the larger steady-state output loss.

Overall, the steady-state results show that introducing a CBDC mainly redistributes liquidity across instruments rather than altering macroeconomic aggregates. The CBDC acts as a substitute for deposits, modestly increasing the size of the central bank's balance sheet while leaving real activity and prices broadly unaffected. The equilibrium CBDC-to-output ratio varies between 0.3 and 0.7 across policy regimes, comparable to empirical magnitudes of cash holdings in advanced economies. The limited macroeconomic effect reflects an offsetting mechanism: while CBDC issuance reduces deposit funding for banks, the expansion of the central bank's balance sheet enhances the supply of overall liquidity. These steady-state results provide the foundation for understanding the transition dynamics discussed later, as the economy moves between long-run equilibria characterized by different liquidity compositions but similar macroeconomic fundamentals.

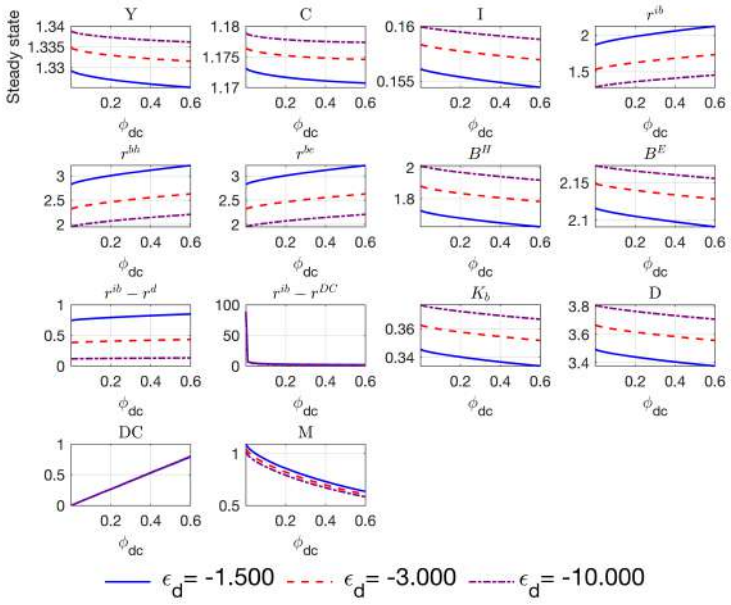

(a) Steady state values of few selected variables and interest rate spreads (expressed as annual percentage points) as a function of ϕ_{dc} i.e. CBDC-to-output ratio

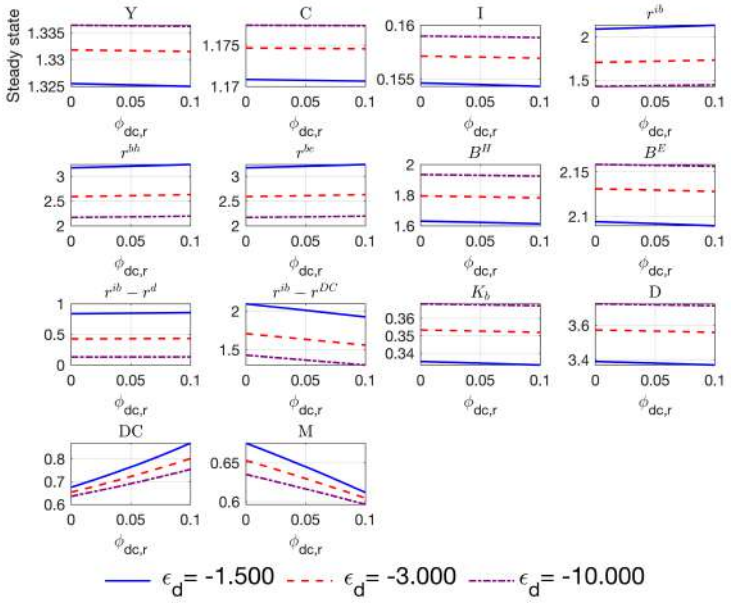

(b) Steady state values of few selected variables and interest rate spreads (expressed as annual percentage points) as a function of $\phi_{dc,r}$ i.e. CBDC interest rate as a markdown to policy rate

Figure 2.1: Increasing CBDC supply either with interest rate policy or quantity policy has a contractionary effect on the economy for varying degrees of deposit elasticity.

Table 2.3: Computed steady-state ratios across CBDC policy regimes

Ratio / Variable	**Interest rate rule:** $r_{dc} = 0$	**Interest rate rule:** $r_{dc} = 0.01r$	**Interest rate rule:** $r_{dc} = 0.1r$	**No CBDC:** $\phi_{dc} = 0$	**Quantity rule:** $\phi_{dc} = 0.3443$	**Quantity rule:** $\phi_{dc} = 2 \times 0.3443$
$(R^e - R) \times 400$	1.0634	1.0660	1.0920	0.8770	1.0104	1.0852
$(R - R_{DC}) \times 400$	2.0554	2.0398	1.8996	97.6228	2.4692	1.9337
$(R - R_d) \times 400$	0.8354	0.8375	0.8579	0.6890	0.7938	0.8526
C_P/Y	0.6885	0.6886	0.6894	0.6853	0.6872	0.6892
C_I/Y	0.1153	0.1153	0.1152	0.1163	0.1156	0.1152
DC/Y	0.5775	0.5902	0.7253	0.0000	0.3443	0.6886
M/Y	0.3409	0.3385	0.3148	0.5266	0.3911	0.3210
D/Y	2.5682	2.5666	2.5515	2.6865	2.6001	2.5554
Z/Y	3.6348	3.6502	3.8111	2.7577	3.3419	3.7678
I/Y	0.1168	0.1168	0.1166	0.1180	0.1171	0.1166

Notes: All interest rate spreads are in annualized percentage points. Ratios are expressed relative to steady-state output Y. Values are obtained from the model's numerical steady state and rounded to four decimals. The table reports liquidity and consumption ratios across alternative CBDC policy configurations.

2.4.2 Effect of introducing CBDC

This section presents the dynamic responses of the economy to various structural shocks under two regimes: one with a CBDC and one without. The solid blue lines represent the CBDC regime with zero remuneration, while the dashed red lines depict the no-CBDC, i.e., $\phi_{dc} = 0$

A positive technology shock raises productivity, which leads to expansions in output, consumption, and investment in both regimes. However, these responses are not very pronounced in the absence of CBDC, as shown in Figure 2.2. In the no-CBDC regime, output peaks at around 0.5% above the steady state in both cases. Similarly, investment rises by over 0.4% with CBDC and without it. There are small differences in the response of the banking variables due to the difference of the deposit spread. We see that in the case of no CBDC, the deposit spread is a little lower than the CBDC case at the peak response, allowing banks to provide more loans and lower interest rates. This causes firms to produce little more in the absence of CBDC. As deposits rise in both cases, cash and CBDC demand increase as well since the CES aggregate function makes the demand for these two non-separable. Despite that, a clear substitution effect can be seen between cash and CBDC; the cash demand is lower by about 2.5 percentage points at peak when there is CBDC in contrast to when there is none. Although the CBDC earns a zero interest rate as cash, the storage cost of cash causes the lower demand of cash whenever there is CBDC.

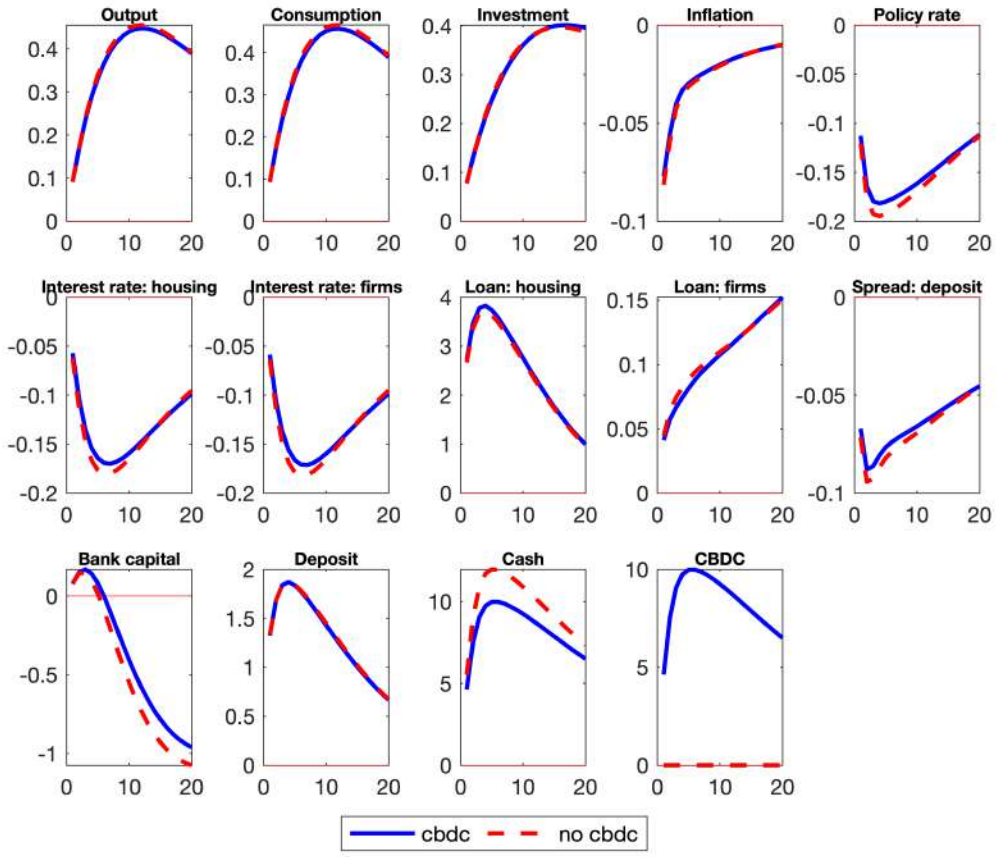

Figure 2.2: Response of various liquidity instruments and macroeconomic variables to TFP shock under two economies: (1) economy without CBDC (red lines) i.e $\phi_{dc} = 0$ and (2) economy with CBDC (blue lines) but no remuneration, i.e. $R_t^{DC} = 0$. Impulse response functions are percentage deviations from steady state.

Since rising asset values ease borrowing constraints, a positive TFP shock typically activates the collateral channel in models with financial frictions Gerali et al. (2010). However, when a CBDC is present, part of the bank-based credit expansion is crowded out, weakening the strength of the collateral channel. Additionally, the debt-deflation channel, which normally hinders expansion by increasing the real burden of debt during deflationary periods, is slightly less pronounced because the nominal response is smoother under the CBDC regime. Importantly, by reducing bank profits and narrowing spreads, CBDC also limits bank capital accumulation. This, in turn, lowers future credit availability and further reinforces financial disintermediation dynamics.

A contractionary monetary policy shock, i.e., a surprise increase in the nominal policy rate by roughly 50 basis points, generates the expected declines in output, investment, and consumption. In the no-CBDC regime, output falls by around 0.25%, while in the CBDC regime, the decline is marginally higher. Investment contracts are up over 3% in both cases, but recovery is slower in the case of CBDC, taking about 4 quarters, as

illustrated in Figure 2.3.

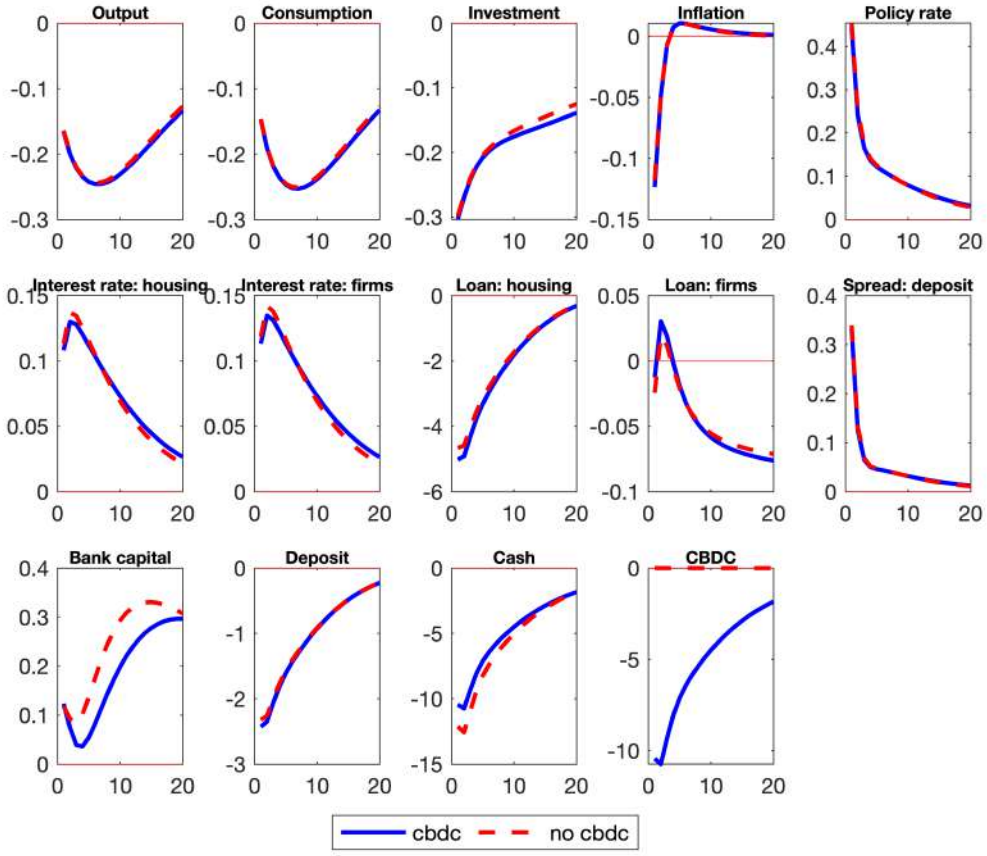

Figure 2.3: Response of various liquidity instruments and macroeconomic variables to contractionary monetary policy shock under two economies: (1) economy without CBDC (red lines) i.e $\phi_{dc} = 0$ and (2) economy with CBDC (blue lines) but no remuneration, i.e. $R_t^{DC} = 0$. Impulse response functions are percentage deviation from steady state.

The introduction of a CBDC modifies the functioning of the traditional bank lending channel, following the framework developed in Gerali et al. (2010). In their model, an increase in the policy rate causes lending rates to rise, asset and collateral values to fall, and the volume of loans to contract. However, with a CBDC in place, households and firms have access to an alternative source of liquidity, making them more sensitive to increases in deposit rates. As Gerali et al. (2010) also demonstrates, this initially leads to a rise in intermediation spreads and an increase in bank profits. Over time, however, as both loan demand and deposit volumes decrease, banks accumulate less capital. This dynamic gradually strains bank balance sheets, weakens the transmission of monetary policy through interest rate changes, and ultimately helps to moderate the severity of the real economic contraction.

A positive shock to deposit elasticity, essentially a reduction in the deposit market power

of retail banks, leads to a more severe drop in deposits for banks (about 0.55%) in the presence of CBDC than in the absence of it (in the absence of CBDC deposit declines about 0.45%). Hence, the bank's capital is contracted even more under the CBDC case. Banks increase their lending rates to make up for the loss of deposits in order to maintain similar profit margins. The real sector cannot afford such an increase in interest rates. This causes a sharper decline in mortgage loans (by about 1.2%, whereas in a no-CBDC world, declines in mortgage loans are smaller).

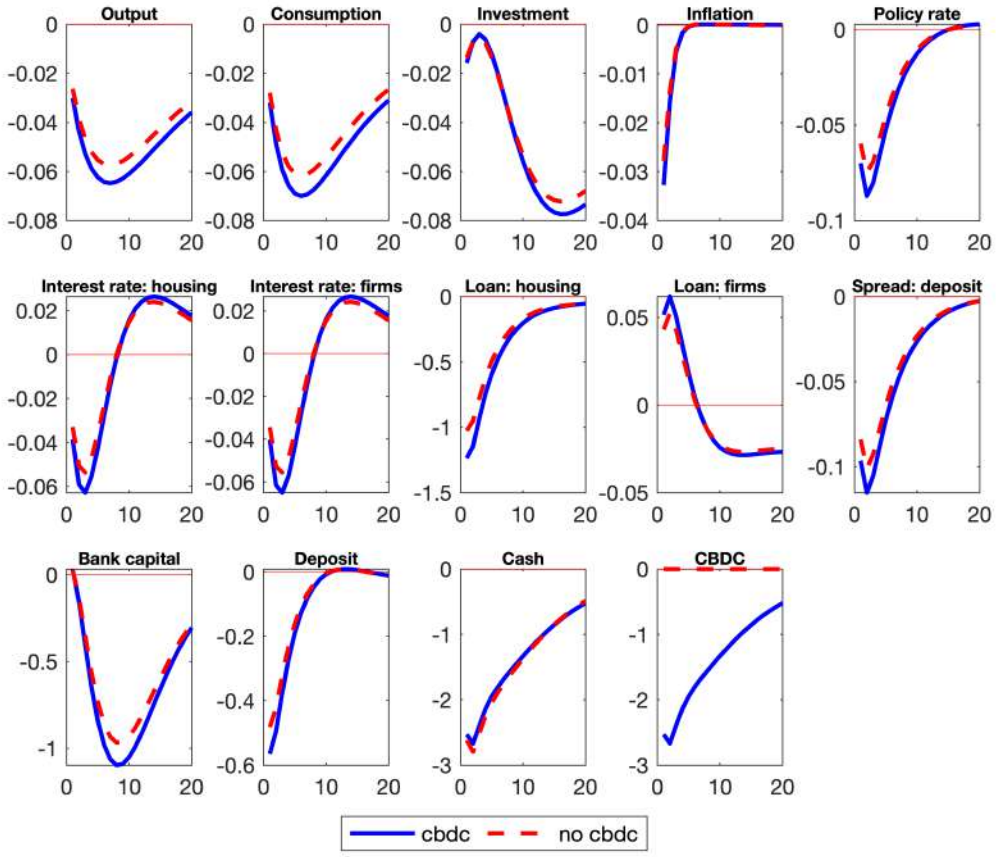

Figure 2.4: Response of various liquidity instruments and macroeconomic variables to deposit elasticity shock under two economies: (1) economy without CBDC (red lines) i.e $\phi_{dc} = 0$ and (2) economy with CBDC (blue lines) but no remuneration, i.e. $R_t^{DC} = 0$. Impulse response functions are percentage deviations from steady state.

Therefore, the introduction of CBDC reduces the net interest margins of the banks even more during a crucial time when they are at a loss of market power. Therefore, the timing of CBDC introduction could be a deciding factor of financial stability. If the central bank decides to introduce CBDC during a period when the financial market is fragile, this might cause failures of banks and increase the risk of a recession. Thus, when a household has an additional payment instrument directly competing with bank deposits,

it makes the transmission mechanism mentioned in Drechsler et al. (2017) much stronger. The spreads of private intermediation are effectively capped by the presence of a public digital currency, introducing a new friction in the transmission of money.

An increase in the elasticity of substitution between intermediate goods reduces firm-level market power, which in turn lowers both prices and marginal costs. As a consequence, output experiences a temporary rise, and aggregate supply expands and inflation declines—a textbook cost-push shock. As shown in Figure 2.5, the responses of output, consumption, inflation, and the policy rate are essentially the same with or without CBDC. Any differences that do appear are extremely small and not persistent.

.

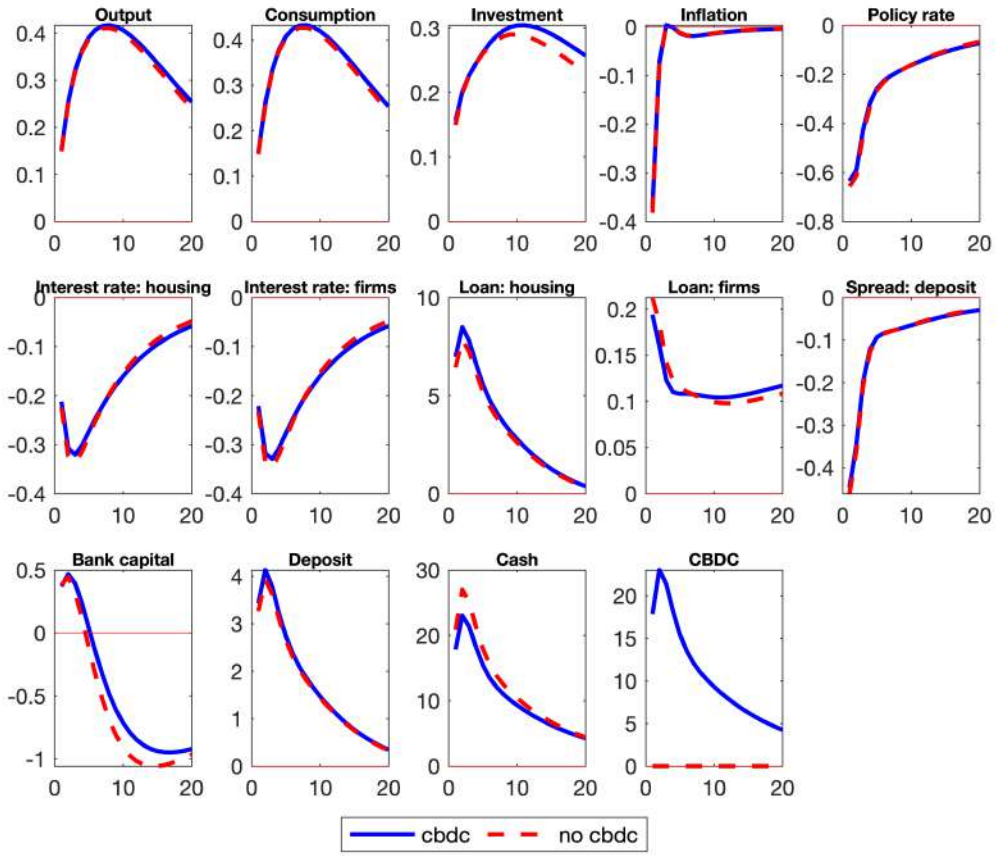

Figure 2.5: Response of various liquidity instruments and macroeconomic variables to intermediate goods elasticity shock under two economies: (1) economy without CBDC (red lines) i.e $\phi_{dc} = 0$ and (2) economy with CBDC (blue lines) but no remuneration, i.e. $R_t^{DC} = 0$. Impulse response functions are percentage deviations from steady state.

Where CBDC does still matter is in balance sheet composition. Deposits and cash shift somewhat more in the CBDC economy, with a modest partial substitution toward CBDC holdings. However, this portfolio reshuffling remains largely on the financial side; it does not propagate into materially different real activity, price dynamics, or lending

rates after a cost-push disturbance. Under a cost-push shock of this type, CBDC does not materially change the macro transmission mechanism of the shock. The economy with CBDC converges back to steady state on almost the exact same path as the economy without CBDC.

By providing a risk-free and seamless alternative to bank deposits, CBDC improves liquidity management for both households and firms; however, this enhancement comes with trade-offs, including a reduction in bank intermediation and, in some cases, lower levels of credit creation. The mechanism behind the portfolio reshuffling is directly linked to the CES liquidity aggregator in Eq (2.2): because deposits, cash, and CBDC jointly provide liquidity services, households optimally adjust all three assets in the same direction whenever aggregate liquidity demand changes. The relative magnitude of these adjustments reflects their cost structure. Although CBDC and cash both earn zero nominal returns, cash is costly to store, whereas CBDC is not. Consequently, CBDC becomes the intensive margin instrument within the liquidity bundle, absorbing most of the marginal adjustment, while deposits and cash move in parallel but to a smaller extent. In this sense, CBDC reshapes the composition of household liquid portfolios without mechanically altering the sign of movements in aggregate liquidity variables. While this brings certain stabilizing advantages, these benefits must still be weighed against the potential risks of weakening the resilience of the financial sector and undermining traditional monetary transmission channels.

2.4.3 CBDC remuneration policies

In this policy exercise, I aim to understand how different remuneration schemes for CBDC impact the economy. Recent updates from the digital euro team indicate that the ECB does not intend to remunerate CBDC. This decision is driven by a desire to prevent CBDC from becoming a store of value, which would otherwise lead to large interest payment obligations. Nevertheless, it remains interesting to explore how macroeconomic variables respond under two different scenarios: one where CBDC is not remunerated and another where it is remunerated. In this analysis, I consider 3 cases for a remuneration plan for CBDC i.e. $\phi_{dc,r} = \{0, 0.05, 0.1\}$. When the CBDC carries a zero interest rate, the opportunity cost of holding it with respect to deposit becomes comparable to cash. While cash in the economy is also not remunerated, its physical storage cost makes it less attractive than CBDC, which has no such cost[3]. As a central bank reduces the markdown, i.e, higher value of $\phi_{dc,r}$, CBDC becomes similar to a deposit. Thus in the face of a contractionary monetary policy shock, the income effect kicks in and the patient house-

[3] Storage cost may arise due to several risks associated with holding cash. For more details, see Burlon et al. (2024a)

hold reduces its demand for liquidity as illustrated in figure 2.6 The qualitative behavior

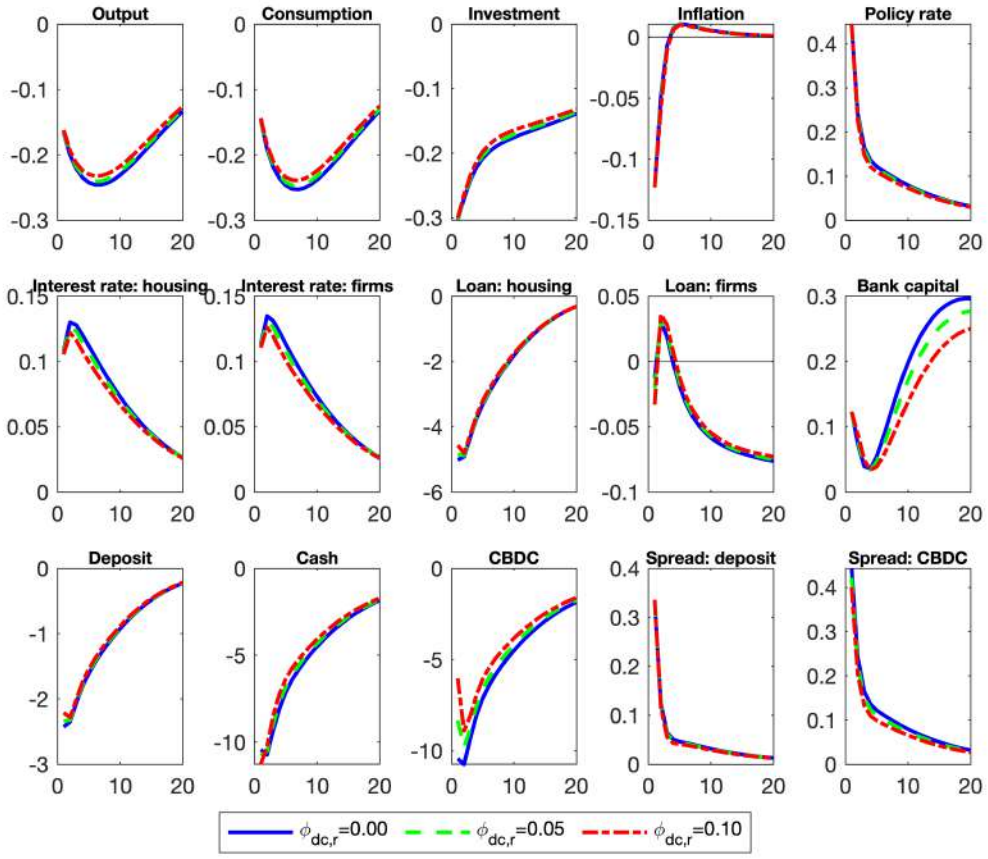

Figure 2.6: Response of various liquidity instruments and macroeconomic variables to a contractionary monetary policy shock under 3 cases for a remuneration plan for CBDC i.e. $\phi_{dc,r} = \{0, 0.05, 0.1\}$. Impulse response functions are percentage deviations from steady state.

of these responses mirrors the mechanisms discussed in Gerali et al. (2010), but the introduction of CBDC changes the quantitative outcomes. As the CBDC spread increases most when it is unremunerated, the opportunity cost of holding CBDC increases significantly. The initial drop in demand for CBDC is almost similar to that of cash. When the interest rate markdown for CBDC decreases, policy rate pass-through increases. Therefore, households lower their demand for CBDC by a lesser amount. As a result, the effect on the output is lower when the CBDC is remunerated. When the central bank is increasing the policy rate to lower the inflation, the effect on output is lower in the presence of CBDC and the central bank faces a lower output-inflation trade-off. Since in our model the representative bank holds monopoly power over the deposit market, we can transparently study how different CBDC remuneration regimes erode (or accelerate the erosion of) this monopoly position. Because the strength of the transmission mechanism

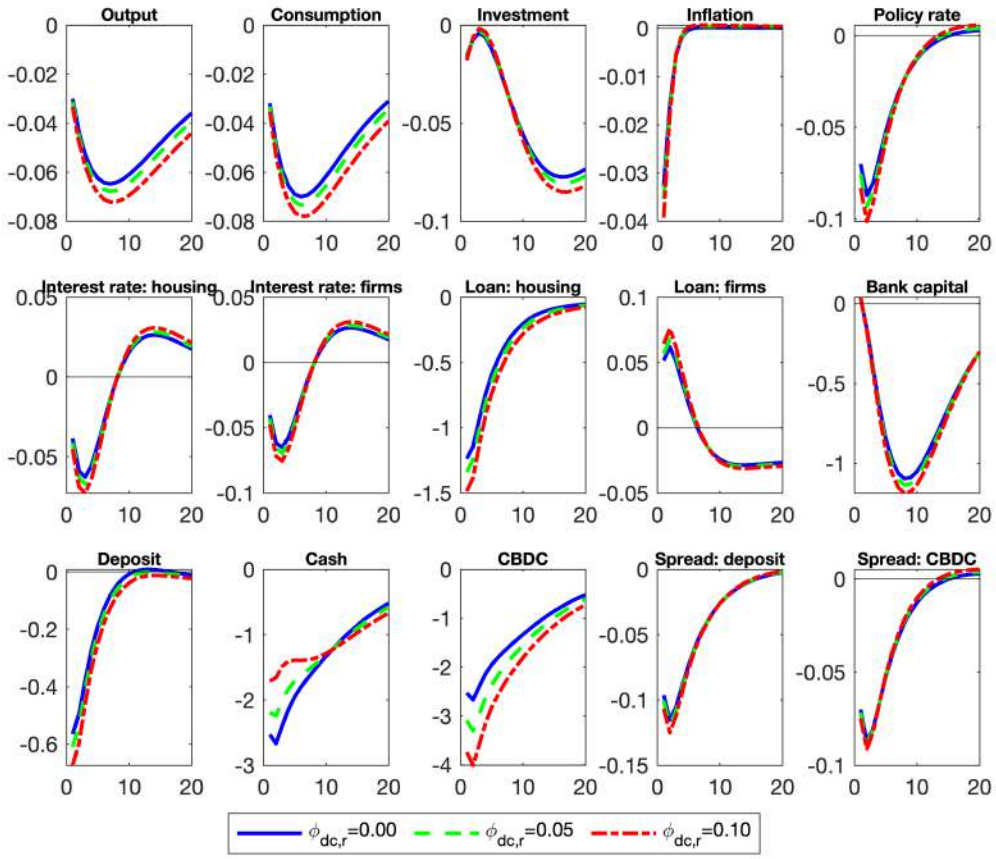

Figure 2.7: Response of various liquidity instruments and macroeconomic variables to a deposit elasticity shock under 3 cases for a remuneration plan for CBDC i.e. $\phi_{dc,r} = \{0, 0.05, 0.1\}$. Impulse response functions are percentage deviations from steady state.

inside the financial system crucially depends on this bank market power, it is therefore economically meaningful to ask whether CBDC mechanically alters this channel itself, beyond pure substitution of balance sheet instruments.

In Figure 2.7 we plot the general equilibrium responses of the relevant liquidity instruments and macroeconomic aggregates to a positive shock to deposit elasticity under three separate CBDC remuneration regimes, $\phi_{dc,r} = \{0, 0.05, 0.1\}$. Higher deposit elasticity here is interpreted as a gradual loss of monopoly power of the bank (this can be thought of as increasing contestability or increasing ease of substitution on the household side across liquidity technologies).

As deposit elasticity rises, deposits flow out of the bank in materially large volume. This reduction in deposits decreases the bank's internal liquidity demand. Consequently, both cash holdings and deposits decline. When the CBDC interest rate is zero, households do not view CBDC as a return-bearing asset; therefore, the quantitative response of CBDC in equilibrium is extremely close to the response of cash. In contrast, when the CBDC

pays interest, the CBDC spread barely declines, while the deposit spread compresses noticeably more. Because of this wedge, the household optimally reduces CBDC holdings more aggressively relative to both cash and deposits.
This produces a very clear crowding-out channel: deposits contract substantially more in states of the world where CBDC is remunerated. Output and consumption also decline much more strongly in the positive interest CBDC regime (e.g., visually: the red paths) than in the zero remuneration case. The mortgage/housing loan channel makes this even more transparent: mortgage credit falls about 1.5% when CBDC earns interest, versus roughly 1.2% when CBDC is non-remunerated. Firm loan credit increases somewhat, but this increase is mechanically insufficient to offset the decline in housing credit. As a result, there is an unambiguous contraction of the bank's overall loan portfolio, and the contraction is strictly worse at the peak when CBDC is remunerated.

2.4.4 CBDC Implementation Strategies: Interest Rate vs. Quantity Rule

This section evaluates the macroeconomic and financial responses to various structural shocks under two distinct CBDC implementation regimes: one in which the central bank sets the interest rate on the CBDC (interest rate rule), and another in which it pegs the quantity of CBDC (quantity rule) as a constant share of output. When implementing an interest rate rule, the central bank marks down its policy rate as follows:

$$R_t^{DC} = \phi_{dc,r} R_t \tag{2.27}$$

where $\phi_{dc,r}$ is the policy parameter that controls the markdown to the policy rate. The supply rule of the CBDC is as follows:

$$DC_t = \phi_{dc} Y_t \tag{2.28}$$

Therefore, the supply of CBDC is pro-cyclical. I consider it $\phi_{dc,r}$ to be 0.1 and ϕ_{dc} to be equal to cash-to-output ratio, i.e., 0.3443, following Burlon et al. (2024b)
A positive TFP shock (Figure 2.8), under both rules, produces the expected expansions in output, consumption, and investment. However, the quantity rule amplifies the real responses significantly more. Output rises by over 0.45% compared to 0.4% under the interest rate rule, and investment increases by nearly 0.5% versus 0.4%. This stronger expansion is fueled by the pro-cyclical quantity of CBDC, which leads to a larger fall in its opportunity cost, stimulating spending and credit. As the effect of a positive TFP shock is more direct on CBDC and increases its supply, the overall consumption of all

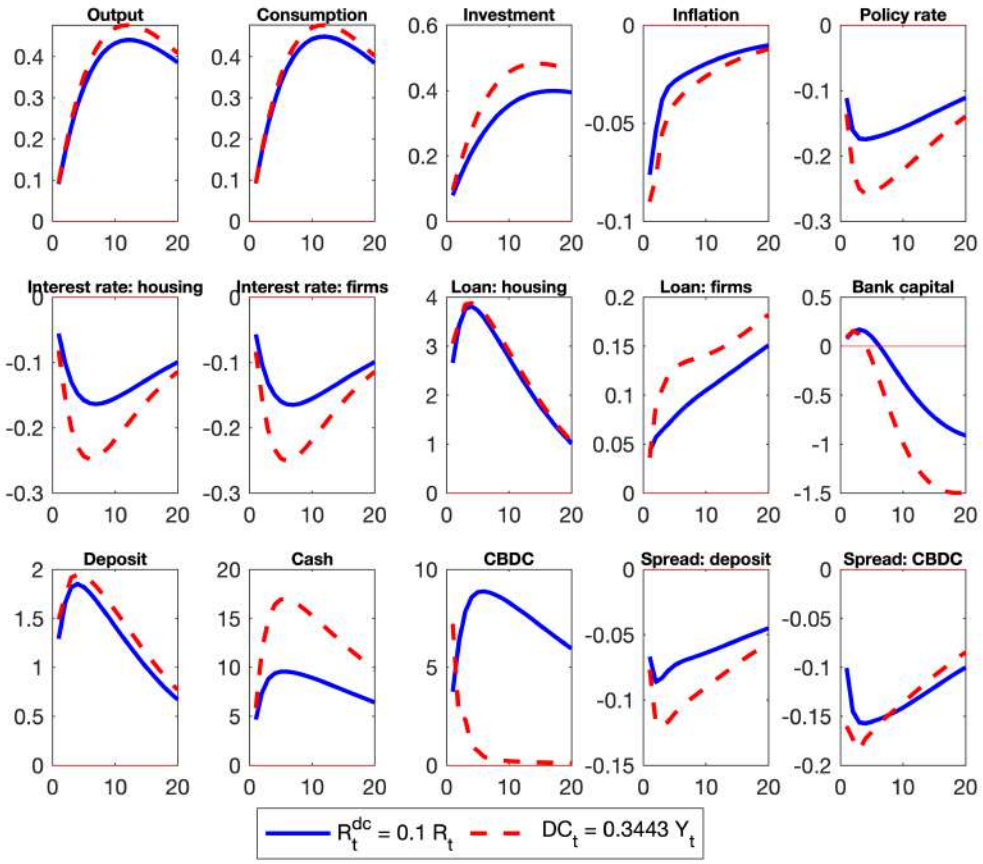

Figure 2.8: Response of various liquidity instruments and macroeconomic variables to shock to TFP under two different CBDC policy rules, i.e., (1) CBDC supply rule (red lines) and (2) CBDC interest rate (blue lines). Impulse response functions are percentage deviations from steady state.

payment instruments increases. This causes even the deposit to increase; the bank has more funding available to lend to firms and households. Thus, a quantity rule is more favorable for banks than an interest rate rule. One interesting factor to note here is that the response of cash and CBDC is similar under the interest rate since the opportunity cost of holding both becomes negative as the policy rate declines. Under the CBDC quantity rule, a lower interest rate on CBDC is needed to discourage patient households from holding a higher than the ϕ_{dc} share. Thus the CBDC response quickly reverts back to the steady-state value in about 8 quarters.

A positive deposit elasticity shock, implying a decline in market power in the deposit market, leads to an overall recessionary effect in the economy, although the decline in output and consumption is much larger under an interest rate rule than a quantity rule. When the deposit market becomes more elastic, households become more sensitive to changes in the deposit interest rate, as seen in Figure 2.9.

Under the interest rate rule, the decline in the CBDC on the impact of the shock is almost double that of the cash. This is due to the response of the policy rate. As the policy rate declines more, the return of the CBDC is affected more, making it a less attractive savings instrument. Under the quantity rule of the CBDC, the decline in deposit is smaller, making it easier for banks to supply loans to firms. Hence, the quantity rule is less contractionary when banks lose their monopoly power over the deposit market and deposits are crowded out by other liquidity instruments.

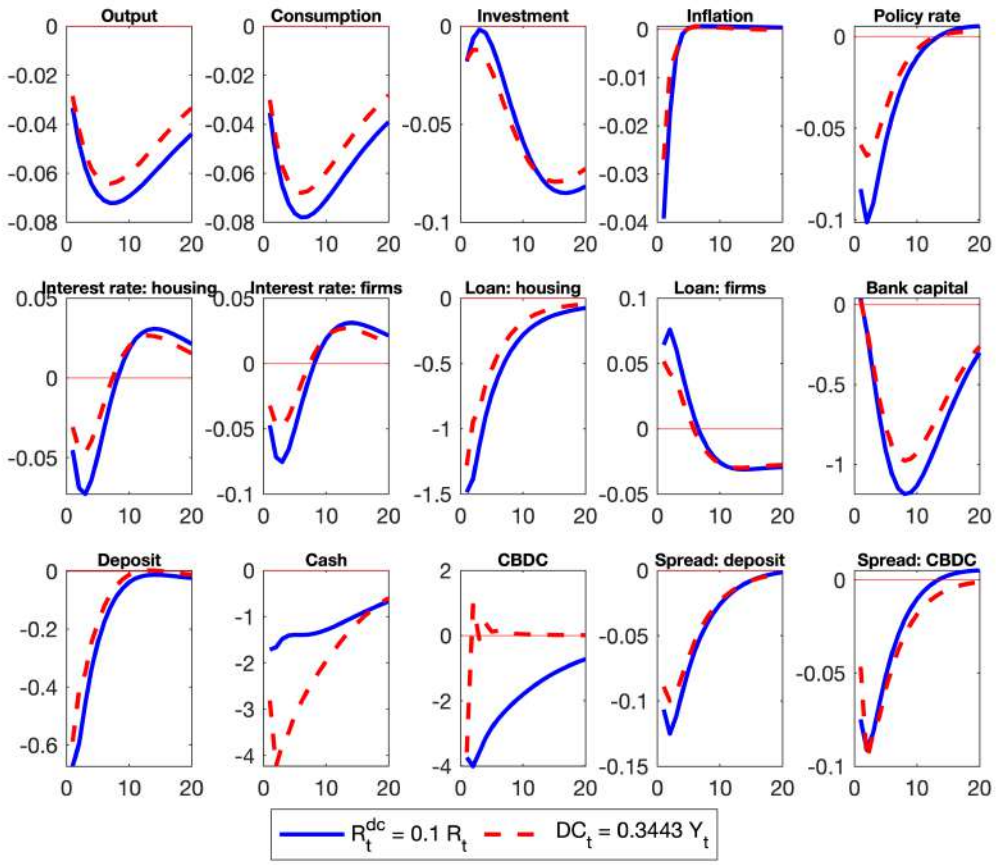

Figure 2.9: Response of various liquidity instruments and macroeconomic variables to deposit elasticity shock for two different CBDC policy rules, i.e., (1) CBDC supply rule (red lines) and (2) CBDC interest rate (blue lines). Impulse response functions are percentage deviations from steady state.

A contractionary monetary policy shock (Figure 2.10) leads to the expected slowdown in real activity under both CBDC implementation strategies, but the size and timing of the responses differ clearly across the two regimes. When the central bank follows an interest rate rule, output declines by around 0.23% on impact. Under the quantity rule, the drop is slightly larger, close to 0.28%, as procyclical CBDC supply makes the contraction more pronounced. Consumption and investment follow a similar pattern: consumption falls

by roughly 0.22% in the interest rate regime and 0.26% under the quantity rule, while investment contracts by about 0.20% and 0.30%, respectively. Although inflation falls by around 0.12 percentage points in both cases, the responses in credit markets show much larger differences. Loan rates rise more strongly under the quantity rule (up to 18 basis points) compared to the interest rate rule (15 basis points), and firm credit contracts by about 6% instead of 4%. Housing loans also shrink more under the quantity rule, by roughly 5% versus 3%. Because CBDC supply increases less in downturns under the quantity rule, households reduce their CBDC holdings more sharply, leading to a decline of about 12%, compared with an 8% reduction under the interest rate rule. Deposits fall by 2.4% in the quantity regime and by 1.8% under the interest rate rule, which places additional pressure on banks' balance sheets and reinforces the contraction in lending. Bank capital also reacts more strongly under the quantity rule, showing a pronounced hump that peaks around 0.55%, whereas the interest rate rule generates only a small and brief decline. These results indicate that the quantity rule significantly strengthens the real and financial effects of monetary tightening by amplifying liquidity fluctuations and deepening the transmission of policy shocks through household balance sheets and bank credit channels.

A positive shock to the elasticity of substitution across intermediate goods (Figure 2.11) increases price flexibility and reduces firms' markups, which boosts real activity in the short run, but the size of the expansion varies across the two CBDC regimes. Output and consumption rise under both rules, peaking at roughly 0.33% and 0.34% under the interest rate rule and about 0.38% and 0.40% under the quantity rule, respectively, while investment expands more moderately in 10 quarters by 0.28% under the interest rate rule, yet reaches nearly 0.38% under the quantity rule as the pro-cyclical CBDC supply provides additional liquidity. Inflation falls sharply on impact, by about 0.4 percentage points, prompting a policy rate decline of around 0.70%, and loan rates also drop, with the quantity rule generating a larger reduction of nearly 50 basis points compared to roughly 30 basis points under the interest rate rule. These monetary and credit conditions translate into stronger lending responses in the quantity regime, where housing loans rise by close to 8% in cases for both rules and firm loans by about 0.3% under the quantity rule and 0.20% under the interest rate rule. The behavior of bank capital, however, diverges sharply: it rises slightly under the interest rate rule before easing but falls more than 1.5% under the quantity rule, reflecting the greater balance-sheet pressure created when CBDC supply expands with output. The magnitude of responses of monetary aggregates are also higher in the quantity regime, with deposits increasing by about 3.5% relative to 3% under the interest rate rule, and cash holdings rising by 32% against 28%. CBDC balances show the most notable difference, jumping roughly 20% under the interest rate

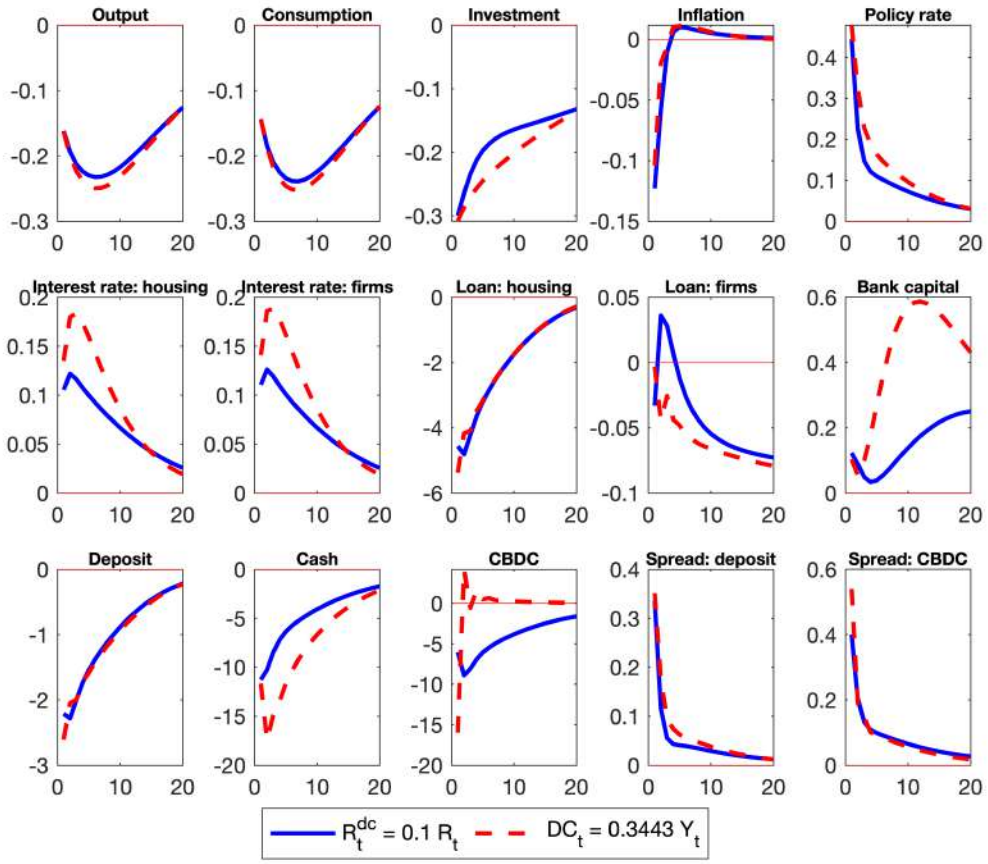

Figure 2.10: Response of various liquidity instruments and macroeconomic variables to a contractionary monetary policy shock under two different CBDC policy rules, i.e., (1) CBDC supply rule (red lines) and (2) CBDC interest rate (blue lines). Impulse response functions are percentage deviations from steady state.

rule but only about 10% under the quantity rule, since the pro-cyclical supply rule mitigates the movement in CBDC demand. The intermediate goods elasticity shock produces a stronger real and financial expansion under the CBDC supply rule, as the resulting liquidity channel amplifies the impact of lower markups on credit, household balance sheets, and investment.

2.5 Conclusion

This paper highlights the significant macro-financial implications of introducing a CBDC within a standard DSGE framework augmented for banking frictions. The quantitative analysis reveals that CBDC issuance alters the transmission of traditional structural shocks, particularly by crowding out bank deposits, compressing intermediation spreads, and weakening the collateral channel of credit expansion. Notably, across a range of

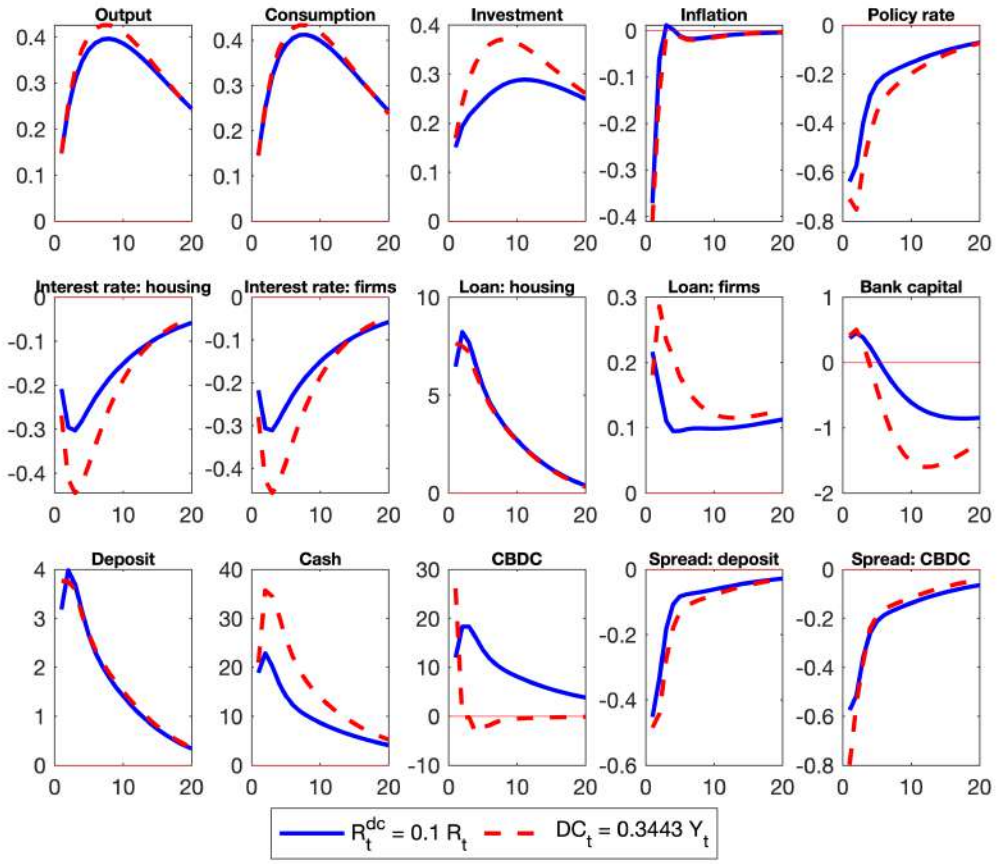

Figure 2.11: Response of various liquidity instruments and macroeconomic variables to shock to intermediate goods elasticity under two different CBDC policy rules, i.e., (1) CBDC supply rule (red lines) and (2) CBDC interest rate (blue lines). Impulse response functions are percentage deviations from steady state.

shocks, macroeconomic volatility is generally reduced when CBDC is properly remunerated, but the resilience of the banking sector deteriorates. For instance, under positive technology shocks, the peak output gain was 0.2 percentage points lower in the CBDC regime, while monetary tightening caused output to fall 0.1 percentage points less when CBDC was present, reflecting muted financial amplification. Further, the design choice between remunerated and non-remunerated CBDC matters critically: a zero-rate CBDC exacerbates downturns by accelerating deposit outflows and eroding bank capital, whereas a positively remunerated CBDC cushions monetary contractions by retaining liquidity within the system.

Policy-wise, the findings underscore that CBDC introduction must be accompanied by careful calibration of remuneration mechanisms. The simulation evidence shows that remunerated CBDC mitigates macro-financial instability by preserving the traditional monetary policy transmission channels and alleviating the erosion of banks' deposit bases.

Moreover, the timing of CBDC deployment emerges as crucial. Introducing CBDC during periods of banking sector fragility—such as heightened deposit competition or weakened capital positions—could amplify financial vulnerabilities and risk systemic crises. The analysis of CBDC design choices (cash similarity, quantity vs. interest rate rules) suggests that allowing greater flexibility through interest rate targeting provides superior macroeconomic stabilization compared to a rigid quantity rule, especially under monetary shocks.

The role of household heterogeneity in liquidity preference, explored through a two-type model extension, further reveals that the degree of CBDC uptake and its macroeconomic consequences can vary substantially across populations [4]. When a large fraction of households highly value liquidity, CBDC usage rises sharply, compressing deposit demand and bank profitability, a dynamic not captured by representative agent models. Thus, incorporating realistic household portfolio behavior into CBDC policy assessments is indispensable.

These results invite several promising avenues for future research. First, future models could integrate endogenous banking crises and default risk, allowing for a richer characterization of financial stability trade-offs. Second, extending the framework to open economy settings would help evaluate how CBDC affects cross-border capital flows and exchange rate dynamics. We leave them to be explored in our future research projects.

Overall, while CBDC offers potential gains in monetary control and price stability, policymakers must recognize the trade-offs with banking sector health and design dynamic implementation strategies that safeguard financial intermediation and systemic stability.

[4] See appendix 2.E for the detailed explanation of the phenomenon

Appendices

2.A Calibrated Parameters

Table 2.4: Relevant model parameters

Parameter	Value	Description
β_p	0.9943	Discount factor, patient households Gerali et al. (2010)
β_i	0.975	Discount factor, impatient households Gerali et al. (2010)
β_b	0.9943	Discount factor, bankers Gerali et al. (2010)
β_e	0.975	Discount factor, entrepreneurs Gerali et al. (2010)
j_h	0.2	Weight of housing in utility Gerali et al. (2010)
ϕ	1.0	Inverse Frisch elasticity of labor Gerali et al. (2010)
m_{iss}	0.7	Loan-to-value ratio, impatient households Gerali et al. (2010)
m_{ess}	0.35	Loan-to-value ratio, entrepreneurs Gerali et al. (2010)
α	0.25	Capital share in production Gerali et al. (2010)
ϵ_d	-1.46025	Elasticity of substitution of deposits Gerali et al. (2010)
ϵ_{bh}	2.932806	Elasticity of substitution, loans to households Gerali et al. (2010)
ϵ_{be}	2.932806	Elasticity of substitution, loans to firms Gerali et al. (2010)
ϵ_{yss}	6	Output elasticity Gerali et al. (2010)
ϵ_{lss}	5	Labor elasticity Gerali et al. (2010)
ni	0.8	Wage share of patient households Gerali et al. (2010)
δ_k	0.025	Depreciation rate of physical capital Gerali et al. (2010)
π^{ss}	1	Steady-state inflation
h	1	Housing supply
vi	0.09	Banking capital ratio over loans Gerali et al. (2010)
a_i	0.867	Habit formation, impatient households Gerali et al. (2010)
a_e	0.0	Habit formation, entrepreneurs
a_p	0.0	Habit formation, patient households
ω_d	0.9	Deposit weight in liquid instrument bundle

Continued on next page

Parameter	**Value**	**Description**
ψ_m	0.02	Cash storage cost parameter Burlon et al. (2024a)
χ_z^{ss}	0.018	Liquid instrument utility parameter Burlon et al. (2024a)
η_z^{ss}	3.58	Elasticity of substitution of cash, CBDC, and deposit Burlon et al. (2024a)
ϕ_π	2.00384	Coefficient of inflation in Taylor rule Gerali et al. (2010)
ϕ_y	0.30324	Coefficient of output in Taylor rule Gerali et al. (2010)

Table 2.5: Relevant parameters for shock processes. All values are set following Gerali et al. (2010)

Parameter	Value	Description
ρ_{ee_z}	0.386	Persistence of entrepreneur productivity shock
ρ_{A_e}	0.938	Persistence of entrepreneur productivity
ρ_{ee_j}	0.922	Persistence of investment-specific technology
ρ_{me}	0.901	Persistence of mortgage rate shock (entrepreneurs)
ρ_{mi}	0.922	Persistence of mortgage rate shock (impatient households)
ρ_{mk_d}	0.893	Persistence of deposit markup
$\rho_{mk_{bh}}$	0.851	Persistence of household loan markup
$\rho_{mk_{be}}$	0.874	Persistence of firm loan markup
$\rho_{ee_q k}$	0.572	Persistence of investment adjustment shock
ρ_{ε_y}	0.294	Persistence of output shock
ρ_{ε_l}	0.596	Persistence of labor shock
$\rho_{\varepsilon_{Kb}}$	0.813	Persistence of bank capital shock
κ_p	33.771	Price adjustment cost
κ_w	107.352	Wage adjustment cost
κ_i	10.031	Investment adjustment cost
κ_d	2.775	Deposit adjustment cost
κ_{be}	7.980	Loan adjustment cost (firms)
κ_{bh}	9.044	Loan adjustment cost (households)
κ_{kb}	8.915	Bank capital adjustment cost
ϕ_π	2.004	Taylor rule inflation response
ρ_{ib}	0.750	Interest rate smoothing
ι_p	0.158	Price indexation
ι_w	0.300	Wage indexation

2.B Full model equations

Patient household:

$$\frac{(1-a^P)\epsilon_t^z}{C_t^P - a^P C_{t-1}^P} = \Lambda_t^P \tag{2.29}$$

$$\frac{j\epsilon_t^h}{H_t^P} + \beta_P \Lambda_{t+1}^P Q_{t+1}^h = \Lambda_t^P Q_t^h \tag{2.30}$$

$$\Lambda_t^P = \omega_d \frac{\chi_{z,t}}{Z_t} \left(\frac{Z_t}{D_t} \right)^{\frac{1}{\eta_{z,t}}} + \beta_P \, \mathbb{E}_t \frac{\left(\Lambda^P{}_{t+1} \right) \left(1 + R_t^d \right)}{(\Pi_{t+1})} \tag{2.31}$$

$$\Lambda_t^P = \vartheta_t \frac{\chi_{z,t}}{Z_t} \left(\frac{Z_t}{DC_t} \right)^{\frac{1}{\eta_{z,t}}} + \beta_P \, \mathbb{E}_t \frac{\left(\Lambda^P{}_{t+1} \right) \left(1 + R_t^{DC} \right)}{(\Pi_{t+1})} \tag{2.32}$$

$$\Lambda_t^P (1 + \psi_m M_t) = \frac{\chi_{z,t}}{Z_t} \left(\frac{Z_t}{M_t} \right)^{\frac{1}{\eta_{z,t}}} + \beta_P \, \mathbb{E}_t \frac{\left(\Lambda^P{}_{t+1} \right)}{(\Pi_{t+1})} \tag{2.33}$$

$$Z_t = \left[M_t^{\frac{\eta_{z,t-1}}{\eta_{z,t}}} + \vartheta_t DC_t^{\frac{\eta_{z,t-1}}{\eta_{z,t}}} + \omega_d D_t^{\frac{\eta_{z,t-1}}{\eta_{z,t}}} \right]^{\frac{\eta_{z,t}}{\eta_{z,t-1}}} \tag{2.34}$$

$$(1-\epsilon_t^l) L_t^P + \frac{\epsilon_t^l}{\Lambda_t^P} \frac{\left(L_t^P \right)^{1+\phi}}{W_t^P} - \Pi_t^{w^P} \kappa_w \left(\Pi_t^{w^P} - \Pi_{t-1}^{\iota_w} \Pi^{1-\iota_w} \right) + \kappa_w \beta_P \mathbb{E}_t \frac{\Lambda_{t+1}^P}{\Lambda_t^P} \left(\Pi_{t+1}^{w^P} - \Pi_t^{\iota_w} \Pi^{1-\iota_w} \right) \frac{\left(\Pi_{t+1}^{w^P} \right)^2}{\Pi_{t+1}} = 0 \tag{2.35}$$

$$\Pi_t^{w^P} = \Pi_t \frac{W_t^P}{W_{t-1}^P} \tag{2.36}$$

$$\begin{aligned} C_t^P + Q_t^P \Delta H_t^P + D_t^P + M_t^P + DC_t^P + f(M_t^P) = \\ W_t^P L_t^P + (1 + R_{t-1}^d) \frac{D_{t-1}^P}{\Pi_t} + (1 + R_{t-1}^{DC}) \frac{DC_{t-1}^P}{\Pi_t} + \frac{M_{t-1}^P}{\Pi_t} + T_t^P \end{aligned} \tag{2.37}$$

Impatient household:

$$\frac{(1 - a^I)\epsilon_t^z}{C_t^I - a^I C_{t-1}^I} = \Lambda_t^I \tag{2.38}$$

$$\frac{j\epsilon_t^h}{H_t^I} + \beta_I \mathbb{E}_t \Lambda_{t+1}^I Q_{t+1}^h + s_t^I m_t^I \mathbb{E}_t \Pi_{t+1} Q_{t+1}^h = \Lambda_t^I Q_t^h \tag{2.39}$$

$$\Lambda_t^I = \beta_I \mathbb{E}_t \frac{\Lambda_{t+1}^I (1 + R_t^{bH})}{\Pi_{t+1}} + s_t^I (1 + R_t^{bH}) \tag{2.40}$$

$$\Lambda_t^I W_t^I = (L_t^I)^\phi \tag{2.41}$$

$$C_t^I + Q_t^h \Delta H_t^I + (1 + R_{t-1}^{bH}) \frac{B_{t-1}^I(i)}{\Pi_t} = W_t^I L_t^I + B_t^I + T_t^I \tag{2.42}$$

$$(1 + R_t^{bH}) B_t^I = m_t^I \mathbb{E}_t \Pi_{t+1} Q_{t+1}^h H_t^I \tag{2.43}$$

Capital Producer:

$$K_t = (1 - \delta_k) K_{t-1} + \left[1 - \frac{\kappa_i}{2} \left(\frac{I_t \epsilon_t^{qk}}{I_{t-1}} - 1 \right)^2 \right] I_t \tag{2.44}$$

$$\begin{aligned} 1 = Q_t^k \left[1 - \frac{\kappa_i}{2} \left(\frac{I_t \epsilon_t^{qk}}{I_{t-1}} - 1 \right)^2 - \epsilon_t^{qk} \frac{I_t}{I_{t-1}} \kappa_i \left(\frac{I_t \epsilon_t^{qk}}{I_{t-1}} - 1 \right) \right] \\ + \kappa_i \beta_E \mathbb{E}_t \epsilon_{t+1}^{qk} \frac{\Lambda_{t+1}^E}{\Lambda_t^E} Q_{t+1}^k \left(\frac{I_{t+1} \epsilon_t^{qk}}{I_t} - 1 \right) \left(\frac{I_{t+1}}{I_t} \right)^2 \end{aligned} \tag{2.45}$$

Entrepreneur:

$$\frac{(1 - a^E) \epsilon_t^z}{C_t^E - a^E C_{t-1}^E} = \Lambda_t^E \tag{2.46}$$

$$(1 - \delta_k) \Pi_{t+1} Q_{t+1}^k s_t^E m_t^E + \beta_E \Lambda_{t+1}^E \left[(1 - \delta_k) Q_{t+1}^k + R_{t+1}^k U_{t+1} - \psi(U_{t+1}) \right] = Q_t^k \Lambda_t^E \tag{2.47}$$

$$W_t^P = \frac{\mu(1 - \alpha)}{L_t^{E,P}} \frac{Y_t^E}{X_t} \tag{2.48}$$

$$W_t^I = \frac{(1 - \mu)(1 - \alpha)}{L_t^{E,I}} \frac{Y_t^E}{X_t} \tag{2.49}$$

$$\Lambda_t^E = \beta_E \mathbb{E}_t \frac{\Lambda_{t+1}^I (1 + R_t^{bE})}{\Pi_{t+1}} + s_t^E (1 + R_t^{bE}) \tag{2.50}$$

$$R_t^k = \psi_1 + \psi_2 (U_t - 1) \tag{2.51}$$

$$C_t^E + W_t^P L_t^{E,P} + W_t^I L_t^{E,I} + (1 + R_{t-1}^{bE})\frac{B_{t-1}^E}{\Pi_t} + Q_t^k K_t^E + \psi(U_t)K_{t-1}^E = \frac{Y_t^E}{X_t} + B_t^E + Q_t^k(1-\delta)K_{t-1}^E$$

$$Y_t^E = A_t^E \left[K_{t-1}^E U_t\right]^\alpha \left(L_t^E\right)^{1-\alpha} \tag{2.52}$$

$$(1 + R_t^{bE})B_t^E = (1-\delta_k)K_t^E m_t^E \mathbb{E}_t \Pi_{t+1} Q_{t+1}^k \tag{2.53}$$

$$R_t^k = \left([L_t^{E,P}]^\mu [L_t^{E,I}]^{1-\mu}\right)^{1-\alpha} \alpha A_t^E U_t^{\alpha-1} (K_{t-1}^E)^{\alpha-1}/X_t \tag{2.54}$$

Bank:

$$R_t^B = R_t - \kappa_{Kb}\left(\frac{K_t^B}{B_t} - \nu_i\right)\left(\frac{K_t^B}{B_t}\right)^2 \tag{2.55}$$

$$\Pi_t K_t^B = (1-\delta_{Kb})K_{t-1}^B + J_{t-1}^B \tag{2.56}$$

$$B_t^E + B_t^H = K_t^B + D_t^B \tag{2.57}$$

$$1-\epsilon_t^{bH}+\epsilon_t^{bH}\frac{R_t^B}{R_t^{bH}}-\kappa_{bH}\left(\frac{R_t^{bH}}{R_{t-1}^{bH}}-1\right)\frac{R_t^{bH}}{R_{t-1}^{bH}}+\beta_P\mathbb{E}_t\left[\frac{\Lambda_{t+1}^P}{\Lambda_t^P}\kappa_{bH}\left(\frac{R_{t+1}^{bH}}{R_t^{bH}}-1\right)\left(\frac{R_{t+1}^{bH}}{R_t^{bH}}\right)^2\frac{B_{t+1}^H}{B_t^H}\right]=0 \tag{2.58}$$

$$1-\epsilon_t^{bE}+\epsilon_t^{bE}\frac{R_t^B}{R_t^{bE}}-\kappa_{bE}\left(\frac{R_t^{bE}}{R_{t-1}^{bE}}-1\right)\frac{R_t^{bE}}{R_{t-1}^{bE}}+\beta_P\mathbb{E}_t\left[\frac{\Lambda_{t+1}^P}{\Lambda_t^P}\kappa_{bE}\left(\frac{R_{t+1}^{bE}}{R_t^{bE}}-1\right)\left(\frac{R_{t+1}^{bE}}{R_t^{bE}}\right)^2\frac{B_{t+1}^E}{B_t^E}\right]=0 \tag{2.59}$$

$$-1+\epsilon_t^{D}-\epsilon_t^{D}\frac{R_t}{R_t^{D}}-\kappa_{D}\left(\frac{R_t^{D}}{R_{t-1}^{D}}-1\right)\frac{R_t^{D}}{R_{t-1}^{D}}+\beta_P\mathbb{E}_t\left[\frac{\Lambda_{t+1}^P}{\Lambda_t^P}\kappa_{D}\left(\frac{R_{t+1}^{D}}{R_t^{D}}-1\right)\left(\frac{R_{t+1}^{D}}{R_t^{D}}\right)^2\frac{D_{t+1}}{D_t}\right]=0 \tag{2.60}$$

$$J_t^B = R_t^{bH} B_t^I + R_t^{bE} B_t^E - R_t^D D_t^B - D_t^B R_t^B \frac{\kappa_D}{2}\left(\frac{R_t^D}{R_{t-1}^D} - 1\right)^2 - B_t^H R_t^{bH} \frac{\kappa_D}{2}\left(\frac{R_t^{bH}}{R_{t-1}^{bH}} - 1\right)^2 - B_t^E R_t^{bE} \frac{\kappa_{bE}}{2}\left(\frac{R_t^{bE}}{R_{t-1}^{bE}} - 1\right)^2 - K_t^B \frac{\kappa_{Kb}}{2}\left(\frac{K_t^B}{K_{t-1}^B} - \nu_i\right)^2 \tag{2.61}$$

Retailer:

$$J_t^R = Y_t\left[1 - \frac{1}{X_t} - \frac{\kappa_p}{2}\left(\Pi_t - \Pi_{t-1}^{\iota_p}\Pi^{1-\iota_p}\right)^2\right] \tag{2.62}$$

$$1 - \epsilon_t^Y + \frac{\epsilon_t^Y}{X_t} - \Pi_t\kappa_p\left(\Pi_t - \Pi_{t-1}^{\iota_p}\Pi^{1-\iota_p}\right) + \beta_P\kappa_p\mathbb{E}_t\frac{\Lambda_{t+1}^P}{\Lambda_t^P}\left(\Pi_{t+1} - \Pi_t^{\iota_p}\Pi^{1-\iota_p}\right)\Pi_{t+1}^2\frac{Y_{t+1}}{Y_t} = 0 \tag{2.63}$$

Aggregate/ Market Clearance:

$$C_t = \gamma_P C_t^P + \gamma_I C_t^I + \gamma_E C_t^E \tag{2.64}$$

$$B_t^E + B_t^H = B_t \tag{2.65}$$

$$\overline{H} = \gamma_P H_t^P + \gamma_I H_t^I \tag{2.66}$$

$$Y_t = C_t + Q_t^K\left(K_t - (1-\delta_k)K_{t-1}\right) + \delta_{Kb}K_{t-1}^B + f(M_t) + \psi(U_t) + Y_t\frac{\kappa_p}{2}\left(\Pi_t - \Pi_{t-1}^{\iota_p}\Pi^{1-\iota_p}\right)^2 + D_t^B R_t^B\frac{\kappa_d}{2}\left(\frac{R_t^D}{R_{t-1}^D} - 1\right)^2 + B_t^H R_t^{bH}\frac{\kappa_d}{2}\left(\frac{R_t^{bH}}{R_{t-1}^{bH}} - 1\right)^2 + B_t^E R_t^{bE}\frac{\kappa_{bE}}{2}\left(\frac{R_t^{bE}}{R_{t-1}^{bE}} - 1\right)^2 \tag{2.67}$$

Central bank :

$$R_t^{DC} = \phi_{dc,r} R_t \tag{2.68}$$

$$1 + R_t = (1+R)^{1-\phi_R}(1+R_{t-1})^{\phi_R}\left[\left(\frac{\Pi_t}{\Pi}\right)^{\phi_\pi}\left(\frac{Y_t}{Y_{t-1}}\right)^{\phi_y}\right]^{1-\phi_R}(1+\epsilon_t^r) \tag{2.69}$$

Shocks

$$\text{Consumption preference shock:} \quad \epsilon_t^z = \rho_z \epsilon_{t-1}^z + \varepsilon_t^z \tag{2.70}$$

$$\text{TFP shock:} \quad a_t^E = \rho_z a_{t-1}^E + \varepsilon_t^a \tag{2.71}$$

$$\text{Housing preference shock:} \quad \epsilon_t^h = \rho_z \epsilon_{t-1}^h + \varepsilon_t^h \tag{2.72}$$

$$\text{LTV ratio shock households:} \quad m_{t-1}^I = \rho_{m^I} m_{t-1}^I + \varepsilon_t^{m^I} \tag{2.73}$$

$$\text{LTV ratio shock entrepreneurs:} \quad m_t^E = \rho_{m^E} m_{t-1}^E + \varepsilon_t^{m^E} \tag{2.74}$$

$$\text{deposit markup shock:} \quad \epsilon_t^d = \rho_d \epsilon_{t-1}^d + \varepsilon_t^d \tag{2.75}$$

$$\text{loan markup (entrepreneurs):} \quad \epsilon_t^{bE} = \rho_z \epsilon_{t-1}^{bE} + \varepsilon_t^{bE} \tag{2.76}$$

$$\text{loan markup (households):} \quad \epsilon_t^{bH} = \rho_z \epsilon_{t-1}^{bH} + \varepsilon_t^{bH} \tag{2.77}$$

$$\text{Monetary policy shock:} \quad \epsilon_t^r = \rho_d \epsilon_{t-1}^r + \varepsilon_t^r \tag{2.78}$$

2.B.1 Log-linearization derivations

Patient Households:

$$\frac{(1-a^P)\epsilon_t^z}{c_t^P - a^P c_{t-1}^P} = \lambda_t^P$$

Taking log of both sides we get,

$$\log(1-a^P) - \log(c_t^P - a^P c_{t-1}^P) = \log\lambda_t^P$$

Doing Taylor expansion around the steady states we get,

$$\log(1-a^P) - \log(c^P - a^P c^P) - \frac{1}{c^P(1-a^P)}\{c^P \hat{c}_t^P - a^P c^P \hat{c}_{t-1}^P\} = \log\lambda^P + \hat{\lambda}_t^P$$

Using steady state version of eq(2.B.1) and canceling appropriate terms, we get,

$$\boxed{(1-a^P)\hat{\lambda}_t^P = a^P \hat{c}_{t-1}^P - \hat{c}_t^P} \tag{2.79}$$

$$\frac{\epsilon_t^h}{h_t^P} + \beta^P \lambda_{t+1}^P q_{t+1}^h = \lambda_t^P q_t^h$$

Taking 2nd term on LHS to RHS and taking log, we get,

$$\log\epsilon_t^h - \log h_t^P = \log\left(\lambda_t^P q_t^h - \beta^P \lambda_{t+1}^P q_{t+1}^h\right)$$

Doing Taylor expansion around the steady states we get,

$$\log\left(\lambda^P q^h - \beta^P \lambda^P q^h\right) + \frac{1}{\lambda^P q^h - \beta^P \lambda^P q^h}\{\lambda^P q^h(\hat{\lambda}_t^P + \hat{q}_t^h) - \beta^P \lambda^P q^h(\hat{\lambda}_{t+1}^P + \hat{q}_{t+1}^h)\}$$
$$= \log\epsilon^h - \log h^P + \hat{\epsilon}_t^h - \hat{h}_t^P$$

Hence finally we get,

$$\boxed{(\hat{\lambda}_t^P + \hat{q}_t^h) - \beta^P(\hat{\lambda}_{t+1}^P + \hat{q}_{t+1}^h) = \hat{\epsilon}_t^h - \hat{h}_t^P} \tag{2.80}$$

Labor supply of the patient household becomes,

$$\boxed{\hat{\lambda}_t^P + \hat{w}_t^P = \phi \hat{l}_t^P} \tag{2.81}$$

Now lets go back to the first order conditions of payment instruments.

$$\Lambda_t^P = \omega_d \frac{\chi_{z,t}}{Z_t}\left(\frac{Z_t}{D_t}\right)^{\frac{1}{\eta_{z,t}}} + \beta_P\, \mathbb{E}_t \frac{\left(\Lambda^P{}_{t+1}\right)\,\left(1 + R_t^d\right)}{(\Pi_{t+1})}$$

taking log of the both sides we get

$$\begin{aligned}
& \log \Lambda_t^P = \log\left[\omega_d \frac{\chi_{z,t}}{Z_t}\left(\frac{Z_t}{D_t}\right)^{\frac{1}{\eta_{z,t}}} + \beta_P\, \mathbb{E}_t \frac{\left(\Lambda^P{}_{t+1}\right)\,\left(1 + R_t^d\right)}{(\Pi_{t+1})}\right] \\
\Leftrightarrow \quad & \log \Lambda^P + \hat{\lambda}_t^P = \log\left[\omega_d \frac{\chi_z}{Z}\left(\frac{Z}{D}\right)^{\frac{1}{\eta_z}} + \beta_P \Lambda^P (1 + R^d)\right] + \text{taylor expansion of RHS} \\
\Leftrightarrow \quad & \hat{\lambda}_t^P = \frac{1}{\Lambda^P}\left\{\omega_d \frac{\chi_z}{Z}\left(\frac{Z}{D}\right)^{\frac{1}{\eta_z}}\left[\hat{\chi}_{z,t} + \left(\frac{1}{\eta_z} - 1\right)\hat{z}_t - \frac{1}{\eta_z}\hat{d}_t - \log\left(\frac{Z}{\eta_z D}\right)\hat{\eta}_{z,t}\right]\right. \\
& \left. + \beta_P \Lambda^P (1 + R^d)\left[\hat{\lambda}_{t+1}^P - \hat{\pi}_{t+1} + \left(\frac{R^d}{1 + R^d}\right)\hat{r}_t^d\right]\right\}
\end{aligned} \tag{2.82}$$

Notice that from the steady state, we have

$$\omega_d \frac{\chi_z}{Z}\left(\frac{Z}{D}\right)^{\frac{1}{\eta_z}} = \Lambda^P[1 - \beta_P(1 + R^d)]$$

Using the above identity in the first term of the RHS, we get,

$$\begin{aligned}
\Leftrightarrow \qquad \hat{\lambda}_t^P &= \frac{1}{\Lambda^P}\left\{\Lambda^P[1-\beta_P(1+R^d)]\left[\hat{\chi}_{z,t}+\left(\frac{1}{\eta_z}-1\right)\hat{z}_t-\frac{1}{\eta_z}\hat{d}_t-\log\left(\frac{Z}{\eta_z D}\right)\hat{\eta}_{z,t}\right]\right. \\
&\quad \left.+\beta_P\Lambda^P(1+R^d)\left[\hat{\lambda}_{t+1}^P-\hat{\pi}_{t+1}+\left(\frac{R^d}{1+R^d}\right)\hat{r}_t^d\right]\right\} \\
\Leftrightarrow \qquad \hat{\lambda}_t^P &= [1-\beta_P(1+R^d)]\left[\hat{\chi}_{z,t}+\left(\frac{1}{\eta_z}-1\right)\hat{z}_t-\frac{1}{\eta_z}\hat{d}_t-\log\left(\frac{Z}{\eta_z D}\right)\hat{\eta}_{z,t}\right] \\
&\quad +\beta_P(1+R^d)\left[\hat{\lambda}_{t+1}^P-\hat{\pi}_{t+1}+\left(\frac{R^d}{1+R^d}\right)\hat{r}_t^d\right]
\end{aligned} \tag{2.83}$$

Similarly for CBDC, we have

$$\begin{aligned}
\Leftrightarrow \qquad \hat{\lambda}_t^P &= [1-\beta_P(1+R^{DC})]\left[\hat{\chi}_{z,t}+\left(\frac{1}{\eta_z}-1\right)\hat{z}_t-\frac{1}{\eta_z}\hat{dc}_t-\log\left(\frac{Z}{\eta_z DC}\right)\hat{\eta}_{z,t}\right] \\
&\quad +\beta_P(1+R^{DC})\left[\hat{\lambda}_{t+1}^P-\hat{\pi}_{t+1}+\left(\frac{R^{dc}}{1+R^{dc}}\right)\hat{r}_t^d\right]
\end{aligned} \tag{2.84}$$

Similarly for cash, we have

$$\begin{aligned}
\hat{\lambda}_t^P+\left(\frac{\psi_M M}{1+\psi_M M}\right)\hat{m}_t = & \\
&+\left(1-\frac{\beta_P}{1+\psi_M M}\right)\left[\hat{\chi}_{z,t}+\left(\frac{1}{\eta_z}-1\right)\hat{z}_t-\frac{1}{\eta_z}\hat{m}_t-\log\left(\frac{Z}{\eta_z M}\right)\hat{\eta}_{z,t}\right] \\
&+\left(\frac{\beta_P}{1+\psi_M M}\right)\left[\hat{\lambda}_{t+1}^P-\hat{\pi}_{t+1}\right]
\end{aligned} \tag{2.85}$$

For the CES aggregator of payment instruments, we have

$$\hat{z}_t = Z_M\hat{m}_t + Z_{DC}\hat{dc}_t + Z_D\hat{d}_t + Z_\nu\hat{\nu}_t + Z_{\eta_z}\hat{\eta}_{z,t} \tag{2.86}$$

where,

$$Z_M = \left(\frac{M}{Z}\right)^{\left(1-\frac{1}{\eta_z}\right)} \tag{2.87}$$

$$Z_{DC} = \nu \left(\frac{DC}{Z}\right)^{\left(1-\frac{1}{\eta_z}\right)} \tag{2.88}$$

$$Z_D = \omega_d \left(\frac{D}{Z}\right)^{\left(1-\frac{1}{\eta_z}\right)} \tag{2.89}$$

$$Z_\nu = \frac{\nu}{\left(1-\frac{1}{\eta_z}\right)} \left(\frac{DC}{Z}\right)^{\left(1-\frac{1}{\eta_z}\right)} \tag{2.90}$$

$$Z_{\eta_z} = Z_M \log M + Z_D \log D + Z_{DC} \log DC \tag{2.91}$$

$$\frac{\epsilon_t^h}{h_t^I} + \beta^I \mathbb{E}_t(\lambda_{t+1}^I q_{t+1}^h + s_t^I m_t^I \pi_{t+1} q_{t+1}^h) = \lambda_t^I q_t^h$$

Taking log doing some side changes we obtain,

$$\log \epsilon_t^h - \log h_t^I = \log(\lambda_t^I q_t^h - \beta^I \mathbb{E}_t(\lambda_{t+1}^I q_{t+1}^h + s_t^I m_t^I \pi_{t+1} q_{t+1}^h))$$

Doing Taylor expansion we get,

$$\begin{aligned}\frac{1}{\lambda^I q^h - \beta^I \lambda^I q^h - \beta^I s^I m^I \pi q^h} \Big\{ & \lambda^I q^h (\hat{\lambda}_t^I + \hat{q}_t^h) \\ & -\beta^I \lambda^I q^h (\hat{\lambda}_{t+1}^I + \hat{q}_{t+1}^h) - \beta^I s^I m^I q^h \pi (\hat{s}_t^I + \hat{m}_t^I + \hat{q}_{t+1}^h + \hat{\pi}_{t+1}) \Big\} \\ & = \hat{\epsilon}_t^h - \hat{h}_t^I\end{aligned}$$

Finally,

$$\boxed{\lambda^I q^h \{(\hat{\lambda}_t^I + \hat{q}_t^h) - \beta^I (\hat{\lambda}_{t+1}^I + \hat{q}_{t+1}^h)\} - \beta^I s^I m^I q^h \pi (\hat{s}_t^I + \hat{m}_t^I + \hat{q}_{t+1}^h + \hat{\pi}_{t+1}) = \frac{\epsilon^h}{h^I} (\hat{\epsilon}_t^h - \hat{h}_t^I)} \tag{2.92}$$

$$\lambda_t^I = \beta^I \, \mathbb{E}_t \frac{\left(\lambda^I{}_{t+1}\right) \, \left(1 + r_t^{bH}\right)}{(\pi_{t+1})} + s_t^I (1 + r_t^{bH}) \tag{2.93}$$

Taking log doing some side changes we obtain,

$$\log \left(\lambda_t^I - \beta^I \, \mathbb{E}_t \frac{\left(\lambda^I{}_{t+1}\right) \, \left(1 + r_t^{bH}\right)}{(\pi_{t+1})} \right) = \log\Big(s_t^I (1 + r_t^{bH})\Big)$$

Doing Taylor expansion we get,

$$\boxed{\lambda^I \hat{\lambda}_t^I - \frac{\beta^I \lambda^I R^{bH}}{\pi}(\hat{\lambda}_{t+1}^I + \hat{R}_t^{bH} - \hat{\pi}_{t+1}) = s^I R^{bH}(\hat{s}_t^I + \hat{R}_t^{bH})} \tag{2.94}$$

$$(1 + r_t^{bH}) b_t^I = h_t^I m_t^I \mathbb{E}_t \pi_{t+1} q_{t+1}^h \tag{2.95}$$

Taking log on both sides we get,

$$\log(1 + r_t^{bH}) + \log b_t^I = \log h_t^I + \log m_t^I + \log \pi_{t+1} + \log q_{t+1}^h$$

Doing Taylor expansion we get,

$$\boxed{\hat{R}_t^{bH} + \hat{b}_t^I = \hat{h}_t^I + \hat{m}_t^I + \hat{\pi}_{t+1} + \hat{q}_{t+1}^h} \tag{2.96}$$

Labor supply of the impatient household becomes,

$$\boxed{\hat{\lambda}_t^I + \hat{w}_t^I = \phi \hat{l}_t^I} \tag{2.97}$$

Entrepreneurs:

$$\boxed{(1 - a^E)\hat{\lambda}_t^E = a^E \hat{c}_{t-1}^E - \hat{c}_t^E} \tag{2.98}$$

$$\begin{aligned} \lambda^E q^k (\hat{\lambda}_t^E + \hat{q}_t^k) - \beta^E \lambda^E \Big[(1 - \delta^k) q^k + r^k\Big] \hat{\lambda}_{t+1}^E \\ - \beta^E \lambda^E \Big[(1 - \delta^k) q^k\Big] \hat{q}_{t+1}^k - \beta^E \lambda^E r^k (\hat{r}_{t+1}^k + \hat{u}_{t+1}) \\ = s^E m^E q^k \pi (1 - \delta^k)(\hat{s}_t^E + \hat{m}_t^E + \hat{q}_{t+1}^k + \hat{\pi}_{t+1}) \end{aligned} \tag{2.99}$$

$$\boxed{\lambda^E \hat{\lambda}_t^E - \frac{\beta^E \lambda^E R^{bE}}{\pi}\Big(\hat{\lambda}_{t+1}^E + \hat{R}_t^{bE} - \hat{\pi}_{t+1}\Big) = s^E R^{bE}\Big(\hat{s}_t^E + \hat{R}_t^{bE}\Big)} \tag{2.100}$$

$$\boxed{\hat{R}_t^{bE} + \hat{b}_t^E = \hat{h}_t^E + \hat{m}_t^E + \hat{\pi}_{t+1} + \hat{q}_{t+1}^k} \tag{2.101}$$

$$\boxed{\hat{y}_t^E = \hat{a}_t^E + \alpha\Big(\hat{u}_t + \hat{k}_{t-1}^E\Big) + (1 - \alpha)\Big\{\mu \hat{l}_t^P + (1 - \mu)\hat{l}_t^I\Big\}} \tag{2.102}$$

$$\boxed{\hat{w}_t^P = \hat{y}_t^E - \hat{l}_t^P - \hat{x}_t} \tag{2.103}$$

$$\boxed{\hat{w}_t^E = \hat{y}_t^E - \hat{l}_t^I - \hat{x}_t} \tag{2.104}$$

$$\boxed{\hat{r}_t^k = \hat{a}_t^E + (\alpha - 1)\Big(\hat{u}_t + \hat{k}_{t-1}^E\Big) + (1-\alpha)\Big\{\mu \hat{l}_t^P + (1-\mu)\hat{l}_t^I\Big\} - \hat{x}_t} \tag{2.105}$$

$$\boxed{\hat{r}_t^k = \frac{\psi_2}{\psi_1}\hat{u}_t} \tag{2.106}$$

Capital producers

$$K_t = (1-\delta^k)K_{t-1} + \left[1 - \frac{\kappa_i}{2}\left(\frac{i_t \epsilon_t^{qk}}{i_{t-1}} - 1\right)^2\right] i_t$$

Taking log after bringing 1st term on RHS to LHS, we get

$$\log\Big(K_t - (1-\delta^k)K_{t-1}\Big) = \log\left[1 - \frac{\kappa_i}{2}\left(\frac{i_t \epsilon_t^{qk}}{i_{t-1}} - 1\right)^2\right] + \log i_t$$

Doing Taylor expansion we get,

$$\log\Big(K - (1-\delta^k)K\Big) + \frac{1}{K - (1-\delta^k)K}\Big\{K\hat{k}_t - (1-\delta^k)K\hat{k}_{t-1}\Big\} = \log i + \hat{i}_t$$

Finally,

$$\boxed{\hat{k}_t - (1-\delta^k)\hat{k}_{t-1} = \delta^k\ \hat{i}_t} \tag{2.107}$$

$$\begin{aligned} 1 = q_t^k \left[1 - \frac{\kappa_i}{2}\left(\frac{i_t \epsilon_t^{qk}}{i_{t-1}} - 1\right)^2 - \epsilon_t^{qk}\frac{i_t}{i_{t-1}}\kappa_i\left(\frac{i_t \epsilon_t^{qk}}{i_{t-1}} - 1\right)\right] \\ + \kappa_i \beta^E \mathbb{E}_t \epsilon_{t+1}^{qk} \frac{\lambda_{t+1}^E}{\lambda_t^E} q_{t+1}^k \left(\frac{i_{t+1}\epsilon_{t+1}^{qk}}{i_t} - 1\right)\left(\frac{i_{t+1}}{i_t}\right)^2 \end{aligned}$$

Taking log of both sides we get,

$$\begin{aligned} 0 = \log\Bigg(q_t^k \left[1 - \frac{\kappa_i}{2}\left(\frac{i_t \epsilon_t^{qk}}{i_{t-1}} - 1\right)^2 - \epsilon_t^{qk}\frac{i_t}{i_{t-1}}\kappa_i\left(\frac{i_t \epsilon_t^{qk}}{i_{t-1}} - 1\right)\right] \\ + \kappa_i \beta^E \mathbb{E}_t \epsilon_{t+1}^{qk} \frac{\lambda_{t+1}^E}{\lambda_t^E} q_{t+1}^k \left(\frac{i_{t+1}\epsilon_{t+1}^{qk}}{i_t} - 1\right)\left(\frac{i_{t+1}}{i_t}\right)^2\Bigg) \end{aligned}$$

Taylor expansion gives us,

$$0 = \hat{q}_t^k - \kappa_i(\hat{i}_t + \hat{\epsilon}_t^{qk} - \hat{i}_{t-1}) + \kappa_i\beta^E(\hat{i}_{t+1} + \hat{\epsilon}_{t+1}^{qk} - \hat{i}_t)$$

or more compact form,

$$\boxed{\hat{q}_t^k = \kappa_i(\hat{i}_t + \hat{\epsilon}_t^{qk} - \hat{i}_{t-1}) - \kappa_i\beta^E(\hat{i}_{t+1} + \hat{\epsilon}_{t+1}^{qk} - \hat{i}_t)} \tag{2.108}$$

Retailer:

$$\boxed{\hat{J}_t^R = \hat{y}_t + \frac{1}{x-1}\hat{x}_t} \tag{2.109}$$

$$1 - \epsilon_t^y + \frac{\epsilon_t^y}{x_t} - \pi_t\kappa_p\Big(\pi_t - \pi_{t-1}^{\iota_p}\pi^{1-\iota_p}\Big) + \beta^P\kappa_p\mathbb{E}_t\frac{\lambda_{t+1}^P}{\lambda_t^P}\Big(\pi_{t+1} - \pi_t^{\iota_p}\pi^{1-\iota_p}\Big)\pi_{t+1}\frac{Y_{t+1}}{Y_t} = 0$$

or,

$$1 = \epsilon_t^y - \frac{\epsilon_t^y}{x_t} + \pi_t\kappa_p\Big(\pi_t - \pi_{t-1}^{\iota_p}\pi^{1-\iota_p}\Big) - \beta^P\kappa_p\mathbb{E}_t\frac{\lambda_{t+1}^P}{\lambda_t^P}\Big(\pi_{t+1} - \pi_t^{\iota_p}\pi^{1-\iota_p}\Big)\pi_{t+1}\frac{Y_{t+1}}{Y_t}$$

In steady state, we get,

$$1 = \epsilon^y - \frac{\epsilon^y}{x} \qquad \Rightarrow x = \frac{\epsilon^y}{\epsilon^y - 1}$$

Taking log of the actual equation we get,

$$0 = \log\left(\epsilon^y - \frac{\epsilon^y}{x}\right) + \left\{\epsilon^y\hat{\epsilon}_t^y - \frac{\epsilon^y}{x}\hat{\epsilon}_t^y + \frac{\epsilon^y}{x}\hat{x}_t - \pi^2\kappa_p\Big(\hat{\pi}_t - \iota_p\hat{\pi}_{t-1}\Big) + \beta^P\pi^2\kappa_p\Big(\hat{\pi}_{t+1} - \iota_p\hat{\pi}_t\Big)\right\}$$

or more compact form,

$$\boxed{\hat{\epsilon}_t^y + (\epsilon^y - 1)\hat{x}_t = \pi^2\kappa_p\Big(\hat{\pi}_t - \iota_p\hat{\pi}_{t-1}\Big) - \beta^P\pi^2\kappa_p\Big(\hat{\pi}_{t+1} - \iota_p\hat{\pi}_t\Big)} \tag{2.110}$$

Bank:

$$R_t^b = r_t + -\kappa_{Kb}\left(\frac{K_t^b}{B_t} - \nu_i\right)\left(\frac{K_t^b}{B_t}\right)^2$$

Taking log we get,

$$\log R_t^b = \log\left(r_t + -\kappa_{Kb}\left(\frac{K_t^b}{B_t} - \nu_i\right)\left(\frac{K_t^b}{B_t}\right)^2\right)$$

Considering that in steady state, $K^b/B = \nu_i$ (which implies $R^b = r^{CB}$ i.e. steady state

policy rate is same as wholesale loan rate) we get,

$$\hat{R}_t^b = \frac{1}{r^{CB}}\left\{ r^{CB}\hat{r}_t^{CB} - \kappa_{Kb}\left(\frac{K^b}{B}\right)^2 (\hat{K_t^b} - \hat{B}_t) \right\}$$

Finally,

$$\boxed{\hat{R}_t^b = \hat{r}_t^{CB} - \frac{\kappa_{Kb}}{r^{CB}} v_i^2 (\hat{K_t^b} - \hat{B}_t)}$$

$$\pi_t K_t^b = (1-\delta^b)K_{t-1}^b + j_{t-1}^b \tag{2.111}$$

Taking Taylor expansion, we get

$$\hat{\pi}_t + \hat{K}_t^b = \frac{1}{K^b}\left\{ (1-\delta^b)K^b\hat{K}_{t-1}^b + j^b\hat{j}_{t-1}^b \right\}$$

Now from steady state, we obtain $j^b = \delta^b K^b$. Substituting this in the above,

$$\boxed{\hat{\pi}_t + \hat{K}_t^b = (1-\delta^b)\hat{K}_{t-1}^b + \delta^b\hat{j}_{t-1}^b} \tag{2.112}$$

$$B_t = K_t^b + D_t^b$$

In steady state, we get $B = K^b + d^b$. Dividing this by B, we have $1 = \frac{K^b}{B} + \frac{D}{B}$. Thus we get $\frac{D}{B} = 1 - \nu_i$. Hence the Taylor expansion of the balance sheet constrain gives us,

$$\boxed{\hat{B}_t = \nu_i\hat{K}_t^b + (1-\nu_i)\hat{D}_t} \tag{2.113}$$

Similarly for the total loan, we have

$$\boxed{\hat{B}_t = \frac{b^I}{B}\hat{b}_t^I + \frac{b^E}{B}\hat{b}_t^E} \tag{2.114}$$

$$1 = \epsilon_t^{bH} - \epsilon_t^{bH}\frac{R_t^b}{r_t^{bH}} + \kappa_{bH}\left(\frac{r_t^{bH}}{r_{t-1}^{bH}} - 1\right)\frac{r_t^{bH}}{r_{t-1}^{bH}} - \beta^P\mathbb{E}_t\left[\frac{\lambda_{t+1}^P}{\lambda_t^P}\kappa_{bH}\left(\frac{r_{t+1}^{bH}}{r_t^{bH}} - 1\right)\left(\frac{r_{t+1}^{bH}}{r_t^{bH}}\right)^2\frac{b_{t+1}^I}{b_t^I}\right]$$

Taking log and doing Taylor expansion we get,

$$\epsilon^{bH}\hat{\epsilon}_t^{bH} - \epsilon^{bH}\frac{R^b}{r^{bH}}(\hat{\epsilon}_t^{bH} + \hat{R}_t^b - \hat{r}_t^{bH}) + \kappa_{bH}(\hat{r}_t^{bH} - \hat{r}_{t-1}^{bH}) - \beta^p\kappa_{bH}(\hat{r}_{t+1}^{bH} - \hat{r}_t^{bH}) = 0$$

or,

$$\hat{\epsilon}_t^{bH} - (\epsilon^{bH} - 1)\hat{R}_t^b + (\epsilon^{bH} - 1)\hat{r}_t^{bH} + \kappa_{bH}(1 + \beta^p)\hat{r}_t^{bH} - \kappa_{bH}\hat{r}_{t-1}^{bH} - \beta^p\kappa_{bH}\hat{r}_{t+1}^{bH} = 0$$

Finally,

$$\begin{aligned}\hat{r}_t^{bH} = &\left(\frac{\epsilon^{bH} - 1}{\epsilon^{bH} - 1 + \kappa_{bH}(1 + \beta^p)}\right)\hat{R}_t^b + \left(\frac{\beta^p\kappa_{bH}}{\epsilon^{bH} - 1 + \kappa_{bH}(1 + \beta^p)}\right)\hat{r}_{t+1}^{bH} \\ &+ \left(\frac{\kappa_{bH}}{\epsilon^{bH} - 1 + \kappa_{bH}(1 + \beta^p)}\right)\hat{r}_{t-1}^{bH} - \left(\frac{1}{\epsilon^{bH} - 1 + \kappa_{bH}(1 + \beta^p)}\right)\hat{\epsilon}_t^{bH}\end{aligned} \tag{2.115}$$

$$\begin{aligned}\hat{r}_t^{bE} = &\left(\frac{\epsilon^{bE} - 1}{\epsilon^{bE} - 1 + \kappa_{bE}(1 + \beta^p)}\right)\hat{R}_t^b + \left(\frac{\beta^p\kappa_{bE}}{\epsilon^{bE} - 1 + \kappa_{bE}(1 + \beta^p)}\right)\hat{r}_{t+1}^{bE} \\ &+ \left(\frac{\kappa_{bE}}{\epsilon^{bE} - 1 + \kappa_{bE}(1 + \beta^p)}\right)\hat{r}_{t-1}^{bE} - \left(\frac{1}{\epsilon^{bE} - 1 + \kappa_{bE}(1 + \beta^p)}\right)\hat{\epsilon}_t^{bE}\end{aligned} \tag{2.116}$$

$$\begin{aligned}\hat{r}_t^{d} = &\left(\frac{\epsilon^{d} - 1}{\epsilon^{d} - 1 - \kappa_{d}(1 + \beta^p)}\right)\hat{r}_t^{CB} + \left(\frac{\beta^p\kappa_{d}}{\epsilon^{d} - 1 - \kappa_{d}(1 + \beta^p)}\right)\hat{r}_{t+1}^{d} \\ &+ \left(\frac{\kappa_{d}}{\epsilon^{d} - 1 - \kappa_{d}(1 + \beta^p)}\right)\hat{r}_{t-1}^{d} - \left(\frac{1}{\epsilon^{d} - 1 - \kappa_{d}(1 + \beta^p)}\right)\hat{\epsilon}_t^{d}\end{aligned} \tag{2.117}$$

$$\boxed{j^b\hat{j}_t^b = r^{bH}b^I(\hat{r}_t^{bH} + \hat{b}_t^I) + r^{bE}b^E(\hat{r}_t^{bE} + \hat{b}_t^E) - r^d d^b(\hat{r}_t^d + \hat{d}_t^b)} \tag{2.118}$$

Central Bank:

$$\boxed{\hat{R}_t^{CB} = \phi_R\hat{R}_{t-1}^{CB} + \phi_\pi(1 - \phi_R)\hat{\pi}_t + \phi_y(1 - \phi_R)(\hat{Y}_t - \hat{Y}_{t-1}) + \hat{\epsilon}_t^r} \tag{2.119}$$

Aggregate:

$$\boxed{\hat{Y}_t = \left(1 - \delta^k\frac{K}{Y}\right)\hat{C}_t + \frac{K}{Y}\hat{K}_t - (1 - \delta^k)\frac{K}{Y}\hat{K}_{t-1}} \tag{2.120}$$

2.C Steady-state calculation

The most straightforward ones are below,

$$\pi = 1 \tag{2.121}$$

$$\pi^w = \pi \tag{2.122}$$

$$X = \frac{\epsilon^y}{\epsilon^y - 1} \tag{2.123}$$

$$Q^k = 1 \tag{2.124}$$

Interest rates
From the FOC of deposits for patient households, we get

$$R^d = \frac{1}{\beta^p} - 1 \tag{2.125}$$

Bank's FOC for retail deposits gives policy rate in SS

$$R = \left(\frac{\epsilon^d - 1}{\epsilon^d}\right) R^d \tag{2.126}$$

FOC of wholesale bank gives us wholesale loan rate is SS,

$$R^b = R \tag{2.127}$$

From the FOCs of retail loans we get,

$$R^{bE} = \left(\frac{\epsilon^{bE}}{\epsilon^{bE} - 1}\right) R^b \tag{2.128}$$

$$R^{bH} = \left(\frac{\epsilon^{bH}}{\epsilon^{bH} - 1}\right) R^b \tag{2.129}$$

Borrowing constraint LMs From the foc of mortgage loand and firm loans, we derive Lagrange multipliers per unit of consumption Langrage multipliers as,

$$\frac{s^I}{\lambda^I} = \frac{1 - \beta^I(1 + R^{bH})}{1 + R^{bH}} \tag{2.130}$$

$$\frac{s^E}{\lambda^E} = \frac{1 - \beta^E(1 + R^{bE})}{1 + R^{bE}} \tag{2.131}$$

We can derive R^k in SS from the FOC of capital for firms as

$$R^k = \frac{1}{\beta^E}\left[1 - \frac{s^E}{\lambda^E} m^E (1 - \delta)\right] - (1 - \delta) \tag{2.132}$$

Housing-consumption ratios FOC of housing for households,

$$H^p Q^h = oo_1 C^p \tag{2.133}$$

$$H^I Q^h = oo_2 C^I \tag{2.134}$$

where,

$$oo_1 = \frac{j}{1-\beta^p} \tag{2.135}$$

$$oo_2 = \frac{j}{1-\beta^I - \frac{s^I}{\lambda^I} m^I} \tag{2.136}$$

Now the trick will be to express consumptions as wage-labor ratios. To do it, first we need expression for loans and deposit to be substituted in the budget constraints. Capital-Asset ratio is calibrated at the ν^b i.e.

$$\frac{K^b}{B} = \nu^b \tag{2.137}$$

Since $B = K^b + D$, we have $D = (1-\nu^b)B$. Now from the constraints,

$$b^I = \left(\frac{m^I}{1+R^{bH}}\right) Q^h H^I \tag{2.138}$$

$$b^E = \left(\frac{m^E}{1+R^{bE}}\right) (1-\delta) K^E \tag{2.139}$$

Therefore,

$$D = (1-\nu^b)\left[\left(\frac{m^I}{1+R^{bH}}\right) Q^h H^I + \left(\frac{m^E}{1+R^{bE}}\right)(1-\delta)K^E\right] \tag{2.140}$$

From the budget constraint of the patient household,

$$C^p = W^p L^p + R^d D + t^p$$

In SS, $t^p = Y^E(1-\frac{1}{X}) + \Pi^b$ where Π^b is bank's profit and in SS takes value $\Pi^b = R^{bH} b^I + R^{bE} b^E - R^d D$. I will define a parameter to set $t^p = 0$ say τ_p, τ_b. If $\tau_p = 0$, the transfer from the firm does not enter the budget constraint of the patient household (for now we would consider $\tau_p = 1, \tau_b = 1$). So $t^p = \tau_p Y^E(1-\frac{1}{X}) + \tau_b \Pi^b$. Now lets turn to

budget constraint of impatient household.

$$\begin{aligned} C^I &= W^I L^I - R^{bH} b^I \\ &= W^I L^I - R^{bH} \left(\frac{m^I}{1+R^{bH}} \right) Q^h H^I \\ &= W^I L^I - R^{bH} \left(\frac{m^I}{1+R^{bH}} \right) oo_2 C^I \qquad using \;\; Q^h H^I = oo_2 C^I \end{aligned}$$

Therefore,

$$C^I = oo_3 W^I L^I \tag{2.141}$$

where

$$oo_3 = \frac{1}{1 + \left(\frac{m^I R^{bH}}{1+R^{bH}} \right) oo_2} \tag{2.142}$$

So C^p becomes

$$\begin{aligned} C^p &= W^p L^p + R^d D + t^p \\ &= W^p L^p + R^d D + \tau_p Y^E \left(1 - \frac{1}{X} \right) + \tau_b \Pi^b \\ &= W^p L^p + R^d D + \tau_p Y^E \left(1 - \frac{1}{X} \right) + \tau_b \Pi^b \\ &= W^p L^p + R^d D + \tau_p Y^E \left(1 - \frac{1}{X} \right) + \tau_b (R^{bH} b^I + R^{bE} b^E - R^d D) \\ &= W^p L^p + \tau_p Y^E \left(1 - \frac{1}{X} \right) + (1-\tau_b) R^d D + \tau_b R^{bH} b^I + \tau_b R^{bE} b^E \\ &= W^p L^p + \tau_p Y^E \left(1 - \frac{1}{X} \right) + (1-\tau_b)(1-\nu^b) R^d (b^I + b^E) + \tau_b R^{bH} b^I + \tau_b R^{bE} b^E \\ &= W^p L^p + \tau_p Y^E \left(1 - \frac{1}{X} \right) + [(1-\tau_b)(1-\nu^b) R^d + \tau_b R^{bH}] b^I + [(1-\tau_b)(1-\nu^b) R^d + \tau_b R^{bE}] b^E \end{aligned}$$

Notice that if $\tau_b = 1$, the R^d terms disappear from the expression. Replacing all these in budget constraint of patient household, we get

$$\begin{aligned} C^p = {} & W^p L^p + \tau_p Y^E \left(1 - \frac{1}{X} \right) \\ & + [(1-\tau_b)(1-\nu^b) R^d + \tau_b R^{bH}] \left(\frac{m^I}{1+R^{bH}} \right) Q^h H^I \\ & + [(1-\tau_b)(1-\nu^b) R^d + \tau_b R^{bE}] \left(\frac{m^E}{1+R^{bE}} \right) (1-\delta) K^E \end{aligned}$$

Now replacing $Q^h H^I = oo_2 C^I = oo_2 oo_3 W^I L^I$ and $K^E = \frac{\alpha Y^E}{R^K X}$ (from definition of R^k) above we get,

$$\begin{aligned} C^p = W^p L^p + \tau_p Y^E \left(1 - \frac{1}{X}\right) \\ + [(1-\tau_b)(1-\nu^b)R^d + \tau_b R^{bH}] \left(\frac{m^I}{1+R^{bH}}\right) oo_2 oo_3 W^I L^I \\ + [(1-\tau_b)(1-\nu^b)R^d + \tau_b R^{bE}] \left(\frac{m^E}{1+R^{bE}}\right) (1-\delta)\frac{\alpha Y^E}{R^K X} \end{aligned}$$

Now from FOC of wage of firms we have,

$$W^p L^p = \mu(1-\alpha)\frac{Y^E}{X}$$

or,

$$Y^E = \frac{X}{\mu(1-\alpha)} W^p L^p$$

Using all these above in C^p finally we have,

$$C^p = oo_4 W^I L^I + oo_5 W^p L^p \tag{2.143}$$

where,

$$oo_4 = [(1-\tau_b)(1-\nu^b)R^d + \tau_b R^{bH}] \left(\frac{m^I}{1+R^{bH}}\right) oo_2 oo_3 \tag{2.144}$$

$$oo_5 = 1 + \tau_p \frac{X}{\mu(1-\alpha)} \left(1 - \frac{1}{X}\right) \tag{2.145}$$

$$+ [(1-\tau_b)(1-\nu^b)R^d + \tau_b R^{bE}] \left(\frac{m^E}{1+R^{bE}}\right) \frac{\alpha(1-\delta)}{R^K \mu(1-\alpha)} \tag{2.146}$$

Solving for labor

From FOC of labor unions,

$$W^s \lambda^s = \left(\frac{\epsilon^L}{\epsilon^L - 1}\right) (L^s)^\phi \qquad s \in \{p, I\}$$

Using the expression above and $\lambda = \frac{1}{C}$, we obtain wage-consumption ratio as following

$$\frac{W^p}{C^p} = \left(\frac{\epsilon^L}{\epsilon^L - 1}\right)(L^p)^\phi$$
$$\frac{W^I}{C^I} = \left(\frac{\epsilon^L}{\epsilon^L - 1}\right)(L^I)^\phi$$

Now the trick is to express consumption as function of corresponding wage-labor factor so that wage gets cancelled both from denominator and numerator. Taking the ratio of firm FOC of labor demand,

$$\frac{W^p L^p}{W^I L^I} = \frac{\mu}{1-\mu} \tag{2.147}$$

Replacing $W^I L^I$ in eq (2.143), we obtain

$$\begin{aligned} C^p &= oo_4 \left(\frac{1-\mu}{\mu}\right) W^p L^p + oo_5 W^p L^p \\ &= oo_6 W^p L^p \end{aligned}$$

where

$$oo_6 = oo_4 \left(\frac{1-\mu}{\mu}\right) + oo_5 \tag{2.148}$$

Thus solving for L^p,

$$\frac{W^p}{C^p} = \left(\frac{\epsilon^L}{\epsilon^L - 1}\right)(L^p)^\phi$$
$$\text{or,} \quad \frac{W^p}{oo_6 W^p L^p} = \left(\frac{\epsilon^L}{\epsilon^L - 1}\right)(L^p)^\phi$$
$$\text{or,} \quad \frac{1}{oo_6} = \left(\frac{\epsilon^L}{\epsilon^L - 1}\right)(L^p)^{1+\phi}$$

Finally,

$$L^p = \left[\frac{1}{oo_6}\left(\frac{\epsilon^L - 1}{\epsilon^L}\right)\right]^{\frac{1}{1+\phi}} \tag{2.149}$$

Similarly using eq (2.141) and wage-consumption ratio,

$$L^I = \left[\frac{1}{oo_3}\left(\frac{\epsilon^L - 1}{\epsilon^L}\right)\right]^{\frac{1}{1+\phi}} \tag{2.150}$$

Solving for housing

To solve for housing we need consumption-output ratios.

$$C^p = oo_6 W^p L^p \qquad\qquad C^I = oo_3 W^I L^I$$
$$= oo_6 \mu(1-\alpha)\frac{Y^E}{X} \qquad\qquad = oo_3(1-\mu)(1-\alpha)\frac{Y^E}{X}$$
$$\text{or,} \quad \frac{C^p}{Y^E} = oo_6\mu(1-\alpha)\frac{1}{X} \qquad\qquad \text{or,} \quad \frac{C^I}{Y^E} = oo_3(1-\mu)(1-\alpha)\frac{1}{X}$$

Now first solve for C^E/Y^E (although not needed now). Using the budget constraint of the entreprenurs,

$$C^E + W^p L^p + W^I L^I + R^{bE} b^E + \delta K^E = \frac{Y^E}{X}$$
$$C^E + (1-\alpha)\frac{Y^E}{X} + R^{bE} b^E + \delta K^E = \frac{Y^E}{X}$$
$$C^E = \frac{\alpha Y^E}{X} - R^{bE} b^E - \delta K^E$$
$$= \alpha\frac{Y^E}{X} - R^{bE}\left(\frac{m^E}{1+R^{bE}}\right)(1-\delta)K^E - \delta K^E$$
$$= \frac{\alpha Y^E}{X} - \left[R^{bE}\left(\frac{m^E}{1+R^{bE}}\right)(1-\delta)+\delta\right]K^E$$
$$= \frac{\alpha Y^E}{X} - \left[R^{bE}\left(\frac{m^E}{1+R^{bE}}\right)(1-\delta)+\delta\right]\frac{\alpha Y^E}{XR^k}$$
$$\frac{C^E}{Y^E} = \frac{\alpha}{X} - \left[R^{bE}\left(\frac{m^E}{1+R^{bE}}\right)(1-\delta)+\delta\right]\frac{\alpha}{XR^k}$$

Now lets turn back to housing. The housing consumption ratios can be expressed as a function of consumption-output ratios as

$$Q^h H^p = oo_1(C^p/Y^E)Y^E \qquad\qquad Q^h H^I = oo_2(C^I/Y^E)Y^E$$

Therefore taking the ratio of the two above, we get,

$$\frac{H^p}{H^I} = \frac{oo_1(C^p/Y^E)}{oo_2(C^I/Y^E)}$$

Since $H^p + H^I = 1$, we can find each as

$$H^I = \frac{1}{1+(H^p/H^I)} \tag{2.151}$$

and $H^p = 1 - H^I$

To find out output, lets use definition of output,

$$\begin{aligned} Y^E &= (K^E)^\alpha [(L^p)^\mu (L^I)^{1-\mu}]^{1-\alpha} \\ &= \left(\frac{\alpha Y^E}{R^k X}\right)^\alpha [(L^p)^\mu (L^I)^{1-\mu}]^{1-\alpha} \\ (Y^E)^{1-\alpha} &= \left(\frac{\alpha}{R^k X}\right)^\alpha [(L^p)^\mu (L^I)^{1-\mu}]^{1-\alpha} \end{aligned}$$

Finally,

$$Y^E = \left[\frac{\alpha}{R^k X}\right]^{\frac{\alpha}{1-\alpha}} (L^p)^\mu (L^I)^{1-\mu} \tag{2.152}$$

- Hence, we can now find C^p, C^E, C^I in SS using Y^E and output-consumption ratios.
- $\lambda^p, \lambda^I, \lambda^E$ are inverses of respective consumptions.
- W^p, W^I can be found using foc of labor demand by firms.
- K^E can be found from $K^E = \frac{\alpha Y^E}{R^k X}$
- Investment is $I = \delta K^E$
- Housing price Q^h is given by $Q^h = oo_1 C^p / H^p$
- Bank loans B^I, B^E are found using eqs (2.138)
- Given bank loans we have $K^E = \nu^b B,\ D = (1 - \nu^b)B$

2.D Cash similarity

Another widely discussed feature of CBDC is how closely it will replicate the features of cash[5]. To study the effect of similarities between cash and CBDC, I consider the following liquidity bundle Z_t used by patient households,

$$Z_t = \left[\left\{ M_t^{\frac{\eta_{z,t}-1}{\eta_{z,t}}} + \vartheta_t DC_t^{\frac{\eta_{z,t}-1}{\eta_{z,t}}} \right\}^{\frac{\sigma_{z,t}}{\eta_{z,t}}} + \omega_d D_t^{\frac{\eta_{z,t}-1}{\eta_{z,t}}} \right]^{\frac{\eta_{z,t}}{\eta_{z,t}-1}} \tag{2.153}$$

[5] The main idea of CBDC is to allow households to have a direct claim to the central bank's balance sheet, just like in the case of cash. In today's payment system, a new form of payment could only be useful if it were different from the existing ones, as the existing ones are quite efficient. Thus, a CBDC having features like cash can be useful and incentivize households to hold it. For more details, see Ferrari Minesso et al. (2022), Bordo and Levin (2017)

where the variable $\sigma_{z,t}$ controls the degree of similarity between CBDC and cash. If $\sigma_{z,t} = \eta_{z,t}$, we return to the previous form of the liquidity bundle. On the other hand, if $\sigma_{z,t} > \eta_{z,t}$, then cash and CBDC become substitutes, and for $\sigma_{z,t} < \eta_{z,t}$, they are complements. The parameter $\sigma_{z,t}$ allows us to control the degree of similarity only between cash and CBDC so that we can conduct experiments regarding the technical design of CBDC. The first-order conditions with respect to cash and CBDC become,

$$\Lambda_t^P = \vartheta_t \frac{\chi_{z,t}}{Z_t} \left(\frac{Z_t}{DC_t} \right)^{\frac{1}{\eta_{z,t}}} \left(\frac{\sigma_{z,t}}{\eta_{z,t}} \right) CB_t^{1-\frac{\eta_{z,t}}{\sigma_{z,t}}} + \beta_P \, \mathbb{E}_t \frac{\left(\Lambda^P{}_{t+1}\right) \left(1 + R_t^{DC}\right)}{(\Pi_{t+1})} \tag{2.154}$$

$$\Lambda_t^P (1 + \psi_m M_t) = \frac{\chi_{z,t}}{Z_t} \left(\frac{Z_t}{M_t} \right)^{\frac{1}{\eta_{z,t}}} \left(\frac{\sigma_{z,t}}{\eta_{z,t}} \right) CB_t^{1-\frac{\eta_{z,t}}{\sigma_{z,t}}} + \beta_P \, \mathbb{E}_t \frac{\left(\Lambda^P{}_{t+1}\right)}{(\Pi_{t+1})} \tag{2.155}$$

where I have defined

$$CB_t = \left\{ M_t^{\frac{\eta_{z,t}-1}{\eta_{z,t}}} + \vartheta_t DC_t^{\frac{\eta_{z,t}-1}{\eta_{z,t}}} \right\}^{\frac{\sigma_{z,t}}{\eta_{z,t}}} \tag{2.156}$$

which represents a cash-CBDC bundle.

Figure 2.12 presents the responses of the important macroeconomic variables to a positive TFP shock. The more complementary cash and CBDC are (i.e., the lower the σ_z), the larger the increase in consumption, output, and investment. For , output peaks near 0.35% for lower values of σ_z, whereas it reaches only around 0.3% for higher values of σ_z. The greater substitutability flattens the response of CBDC holdings, as households easily shift between the two, reducing the expansionary impulse.

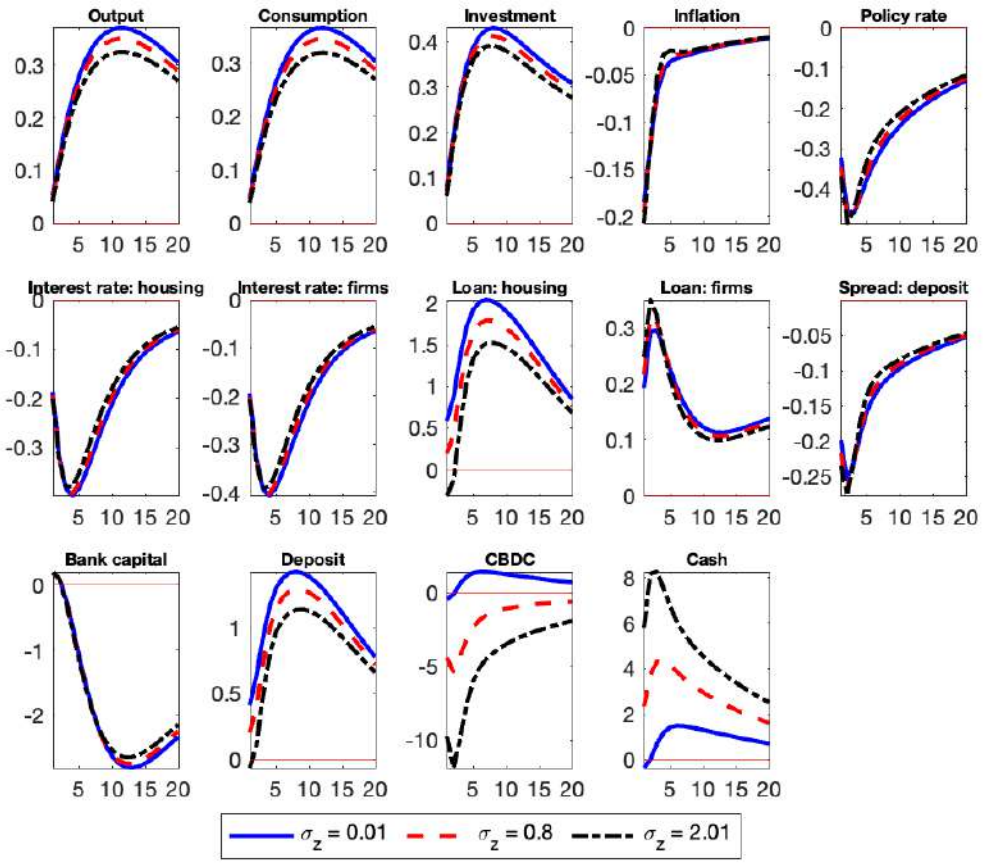

Figure 2.12: Response of various liquidity instruments and macroeconomic variables to a TFP shock for varying degrees of substitution of cash and CBDC. Impulse response functions are percentage deviations from steady state.

Under a bank capital shock (Figure 2.13), output and investment decline in all three cases, but the contraction is softened as increases. When CBDC complements cash, the rise in CBDC demand substitutes away from bank deposits, alleviating financial stress. Bank capital falls by over 3% for all values of σ_z Following a deposit elasticity shock (Figure 2.14), which captures higher competitiveness in the deposit market, the responses of all other variables are quite similar. In this case, the IRFs of CBDC and cash are worth noting. Although the changing σ_z is supposed to make CBDC and cash have varying substitution, the effect on the deposit market is much stronger. Therefore, both cash and CBDC behave as if they are complements due to the overall decline in the liquidity bundle. The contractionary monetary policy shock (Figure 2.15) IRFs reveal that design choice in terms of substitution or complements of CBDC and cash does affect the transmission of policy shocks of the central bank. Thus the economy might respond differently; the response to a monetary policy shock does not necessarily get altered, and policymakers can expect more traditional responses. For the elasticity of substitution in intermediate

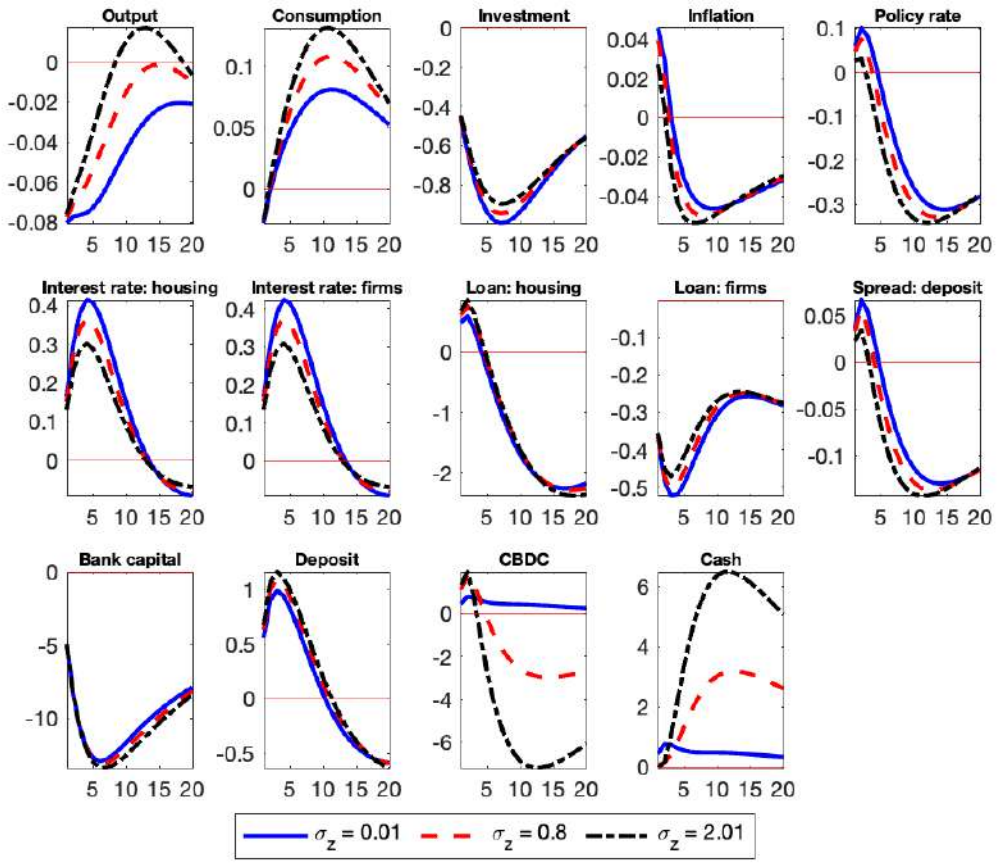

Figure 2.13: Response of various liquidity instruments and macroeconomic variables to a shock to the value of bank capital for varying degrees of substitution of cash and CBDC. Impulse response functions are percentage deviations from steady state.

goods (Figure 2.16), macro responses vary little across values. This result suggests that substitutability or complementarity in the cash-CBDC bundle has a limited effect on price-markup shocks but larger effects when financial variables or liquidity preferences are directly involved.

2.E Heterogeneity in liquidity preference

The success of the digital euro project hinges on many factors. The ECB acknowledges that for the digital euro to be widely adopted, it must address the diverse needs of its users. To explore this, I extend my model to incorporate heterogeneity in the parameter $\chi_{z,t}$ across patient households. For tractability, I introduce two distinct types of patient households: those with a high value and those with a low value of $\chi_{z,t}$, which represents the weight assigned to the liquid instrument bundle in their utility function. Specifically, I assume that a fraction γ_χ of patient households have a high preference for liquidity,

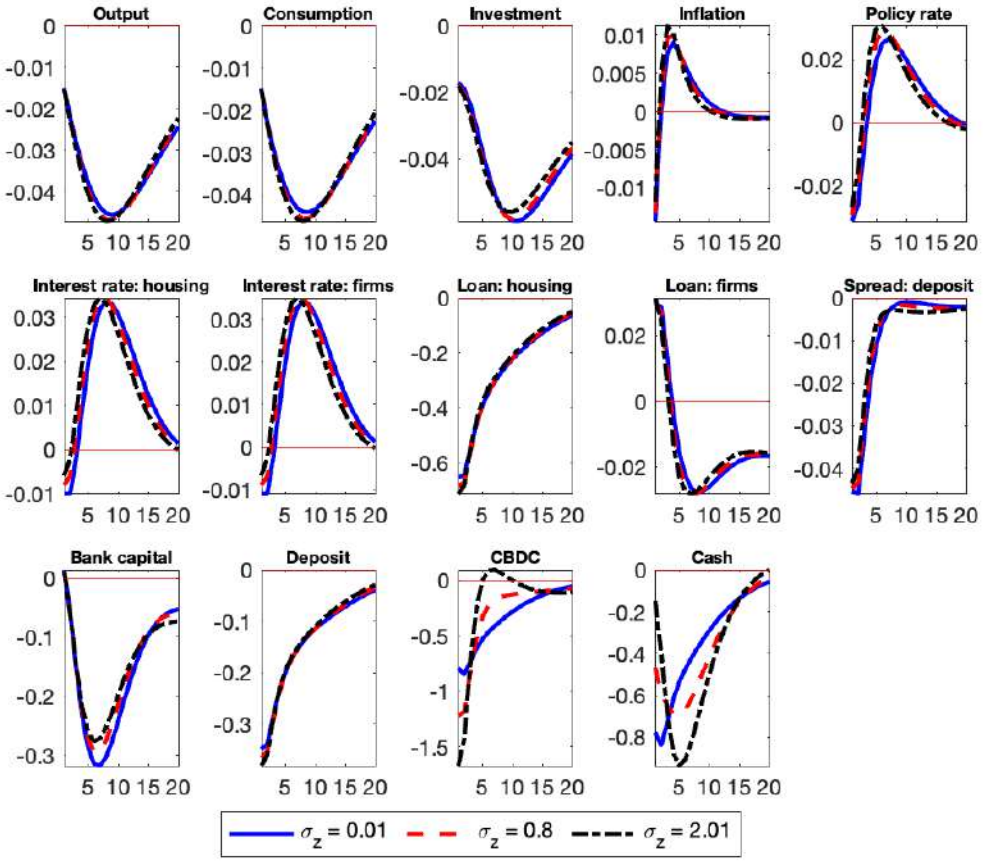

Figure 2.14: Response of various liquidity instruments and macroeconomic variables to a deposit elasticity shock for varying degrees of substitution of cash and CBDC. Impulse response functions are percentage deviations from steady state.

denoted by $\chi_{z,t}^{\text{high}}$, while the remaining fraction, $1-\gamma_\chi$, have a lower preference, $\chi_{z,t}^{\text{low}}$. The variation in $\chi_{z,t}$ can stem from several factors. For instance, lower-income households may have a greater need for liquidity due to tighter financial constraints, or frequent shoppers might derive more utility from holding readily available payment instruments. Rather than modeling the exact source of this heterogeneity, my focus is on examining its implications for CBDC usage and the resulting effects on the financial conditions of the banking sector. Each type of patient household maximizes the following lifetime utility function:

$$\mathbb{E}_0 \sum_{t=0}^{\infty} \beta_P^t \left[(1-a^P)\epsilon_t^Z \log\left(C_t^{P(i)} - a^P C_{t-1}^{P(i)}\right) + \epsilon_t^h \log H_t^{P(i)} - \frac{\left(L_t^{P(i)}\right)^{1+\phi}}{1+\phi} + \chi_{z,t}^{(i)} \log Z_t^{(i)} \right] \tag{2.157}$$

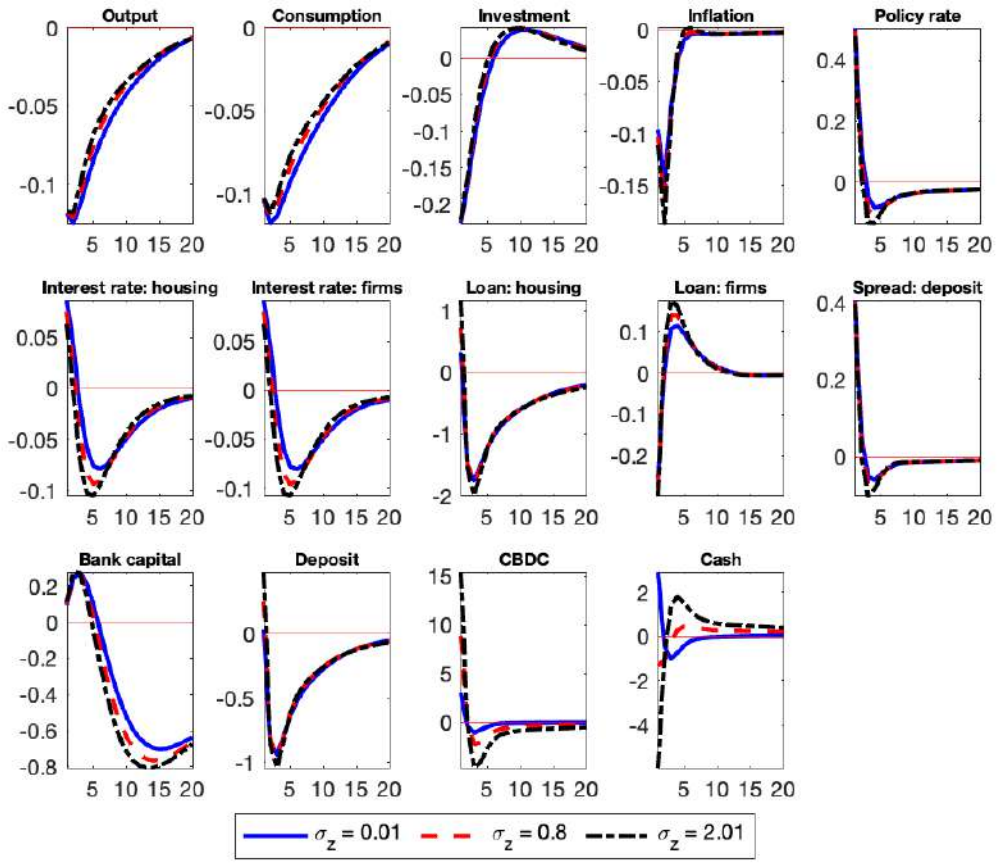

Figure 2.15: Response of various liquidity instruments and macroeconomic variables to a contractionary monetary policy shock for varying degrees of substitution of cash and CBDC. Impulse response functions are percentage deviations from steady state.

The term $Z_t^{(i)}$ represents the consumption of liquidity services and is defined as a CES aggregator over cash, CBDC, and bank deposits:

$$Z_t^{(i)} = \left[\left(M_t^{(i)} \right)^{\frac{\eta_{z,t}-1}{\eta_{z,t}}} + \vartheta_t \left(DC_t^{(i)} \right)^{\frac{\eta_{z,t}-1}{\eta_{z,t}}} + \omega_d \left(D_t^{(i)} \right)^{\frac{\eta_{z,t}-1}{\eta_{z,t}}} \right]^{\frac{\eta_{z,t}}{\eta_{z,t}-1}} \tag{2.158}$$

Each household chooses consumption $C_t^{P(i)}$, labor $L_t^{P(i)}$, housing services $H_t^{P(i)}$, and asset holdings $M_t^{(i)}$ (cash), $DC_t^{(i)}$ (CBDC), and $D_t^{(i)}$ (deposits), subject to the following budget constraint:

$$\begin{aligned} &C_t^{P(i)} + Q_t^P \Delta H_t^{P(i)} + D_t^{(i)} + M_t^{(i)} + DC_t^{(i)} + f(M_t^{(i)}) \\ &\quad \leq W_t^P L_t^{P(i)} + (1 + R_{t-1}^d) \frac{D_{t-1}^{(i)}}{\Pi_t} + (1 + R_{t-1}^{DC}) \frac{DC_{t-1}^{(i)}}{\Pi_t} + \frac{M_{t-1}^{(i)}}{\Pi_t} + T_t^{(i)} \end{aligned} \tag{2.159}$$

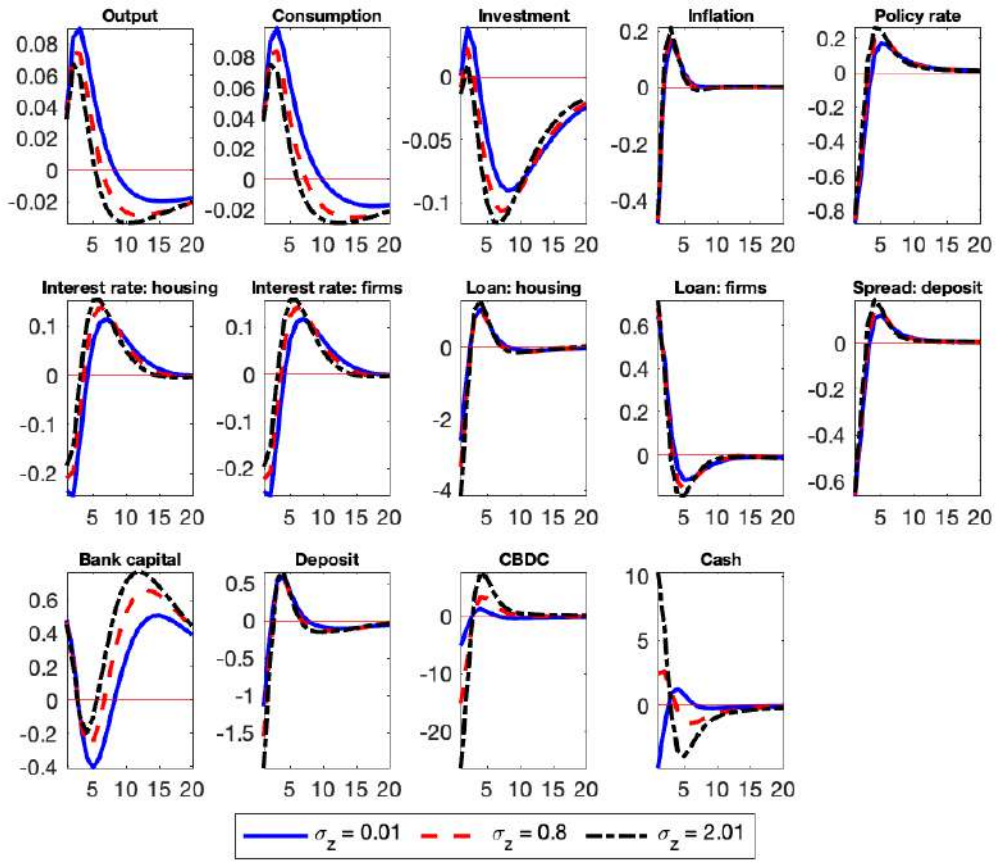

Figure 2.16: Response of various liquidity instruments and macroeconomic variables to a shock to intermediate goods elasticity for varying degrees of substitution of cash and CBDC. Impulse response functions are percentage deviations from steady state.

As in the baseline model, cash incurs a quadratic storage cost:

$$f(M_t^{(i)}) = \frac{\psi_M}{2}\left(M_t^{(i)}\right)^2, \quad \psi_M > 0 \tag{2.160}$$

Aggregate variables are constructed as weighted averages of each type:

$$C_t^P = \gamma_\chi\, C_t^{P(\text{high})} + (1-\gamma_\chi)\, C_t^{P(\text{low})} \tag{2.161}$$

$$D_t = \gamma_\chi\, D_t^{(\text{high})} + (1-\gamma_\chi)\, D_t^{(\text{low})} \tag{2.162}$$

$$DC_t = \gamma_\chi\, DC_t^{(\text{high})} + (1-\gamma_\chi)\, DC_t^{(\text{low})} \tag{2.163}$$

$$M_t = \gamma_\chi\, M_t^{(\text{high})} + (1-\gamma_\chi)\, M_t^{(\text{low})} \tag{2.164}$$

$$L_t^P = \gamma_\chi\, L_t^{P(\text{high})} + (1-\gamma_\chi)\, L_t^{P(\text{low})} \tag{2.165}$$

$$H_t^P = \gamma_\chi\, H_t^{P(\text{high})} + (1-\gamma_\chi)\, H_t^{P(\text{low})} \tag{2.166}$$

In response to a contractionary monetary policy shock (Figure 2.17), where the policy rate increases by 50 basis points, both models exhibit the expected contraction: output falls by around 0.12%, consumption and investment decline, and real lending rates increase. The heterogeneous specification displays a slightly smaller fall in output and consumption—approximately 0.1 percentage points less than the homogeneous case—reflecting the liquidity-smoothing role of CBDC for high-χ_z households. At the same time, the fall in deposits is sharper and the increase in CBDC use is more pronounced (peaking around 0.4%) in the heterogeneous case, indicating a stronger portfolio shift. Bank profits briefly rise due to wider spreads but decline faster, resulting in a more persistent drop in bank capital by up to 1.3%, consistent with the mechanism in Gerali et al. (2010) and the cost-channel effects described in Piazzesi et al. (2022)

Following a positive TFP shock (Figure 2.18), output and consumption rise, peak-

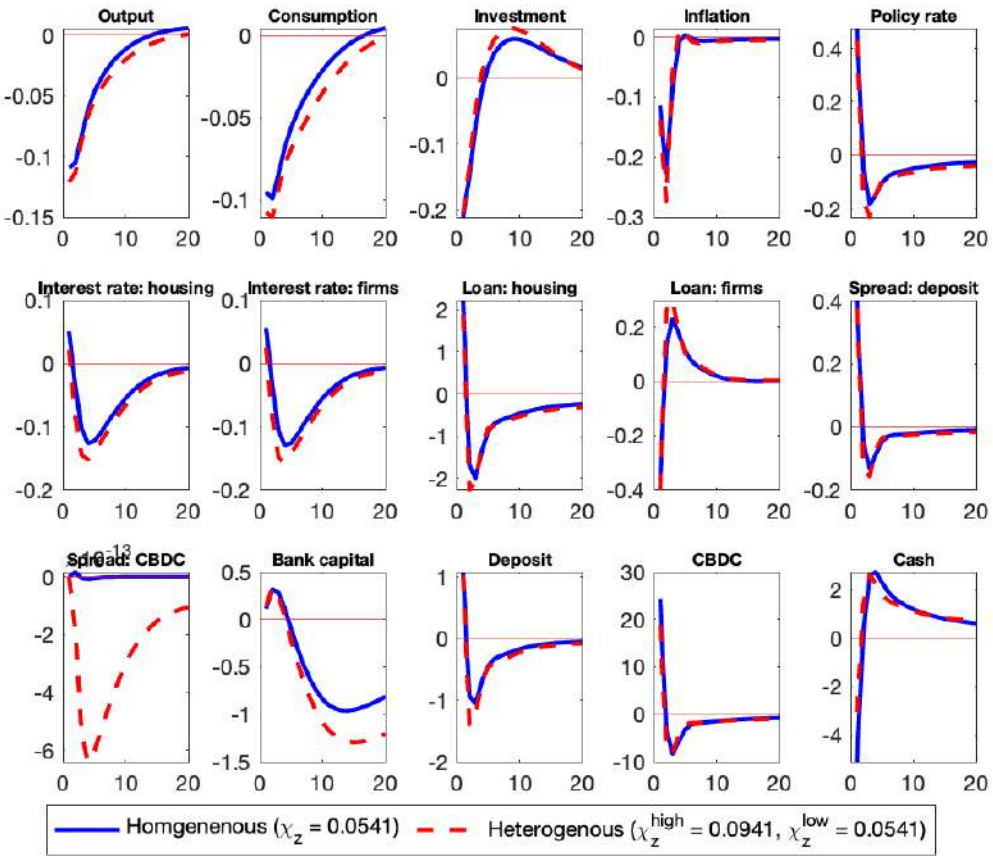

Figure 2.17: Response of various liquidity instruments and macroeconomic variables to a contractionary monetary policy shock under two scenarios, i.e., (1) the liquidity utility parameter is heterogeneous across patient households (red lines) and (2) the liquidity utility parameter is homogeneous across patient households (blue lines). Impulse response functions are percentage deviations from steady state.

ing around 0.3% and 0.3%, respectively, in both models. However, investment rises

more slowly in the heterogeneous model—about 0.3% versus 0.4% in the homogeneous case—due to differences in household saving responses. The CES liquidity aggregator induces highχ_z types to substitute away from deposits less aggressively than the average household in the baseline model. As a result, the expansion in bank capital is modestly weaker under heterogeneity, reflecting a smaller financial multiplier through the collateral and intermediation channels. CBDC usage increases less under this shock (about 13% in the heterogeneous case vs. 18% in the homogeneous case), in line with a lower marginal convenience yield during expansions. A positive deposit elasticity shock (Figure 2.19)—interpreted as a reduction in banks' deposit markup—results in a 0.4% decline in deposits under homogeneity but only about a 0.09% increase in the heterogeneous model. Investment and output decline as well under the homogeneous χ_z but increase under the heterogeneous. Moreover, the magnitude differs: investment increases by 0.35% in the homogeneous case and about 0.15% with heterogeneous preferences, reflecting weaker

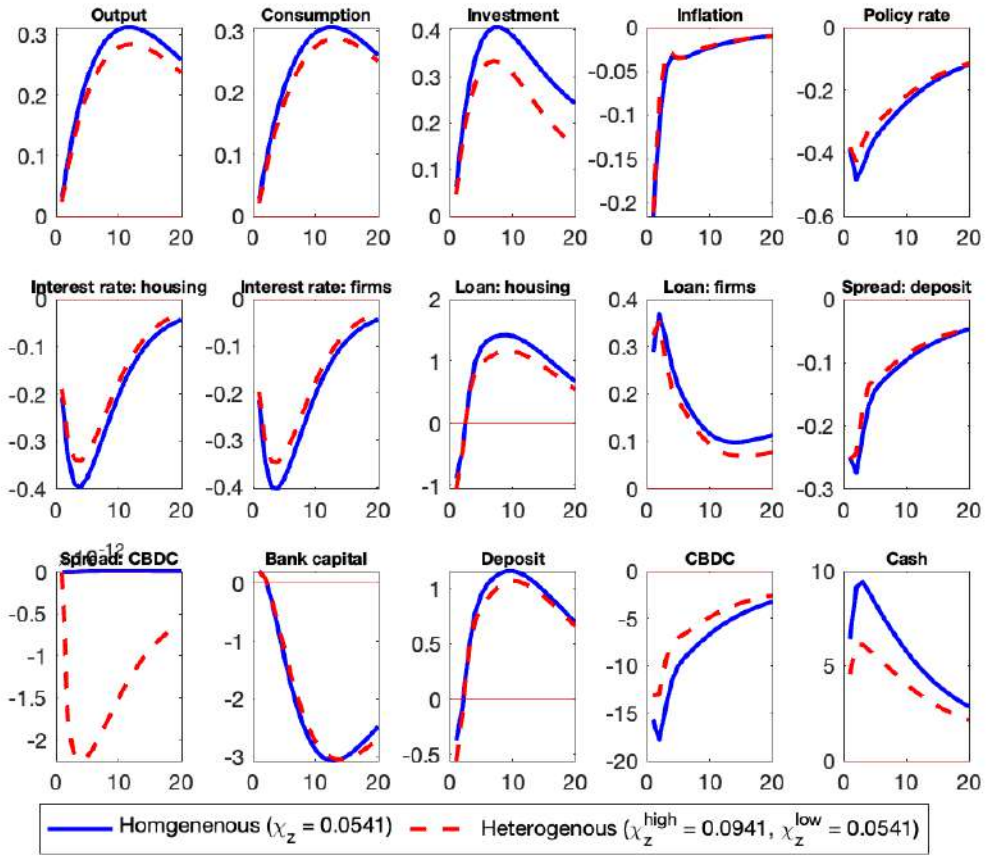

Figure 2.18: Response of various liquidity instruments and macroeconomic variables to a TFP shock under two scenarios, i.e., (1) the liquidity utility parameter is heterogeneous across patient households (red lines) and (2) the liquidity utility parameter is homogeneous across patient households (blue lines). Impulse response functions are percentage deviations from steady state.

deposit growth. This is consistent with the model's deposit FOC, where the marginal utility of liquidity services plays a central role; high-χ_z households benefit more from the improved deposit return, but low-χ_z households are relatively unresponsive, which dampens the overall negative effect of intermediation loss. The response change sign shows large asymmetry when the competitiveness of the deposit market increases. As seen before, when the benefit obtained from liquidity services is homogenous, the financial intermediation is disrupted under this shock. As a result, the output and consumption decline (about 0.05% in this case). An interesting phenomenon occurs when the benefit obtained from liquidity services is heterogeneous in an economy. The presence of high χ_z household drive-up demand of deposit to the extent that it becomes positive offsets the negative effect of the decline in deposit market power of the bank. A tightening in firm

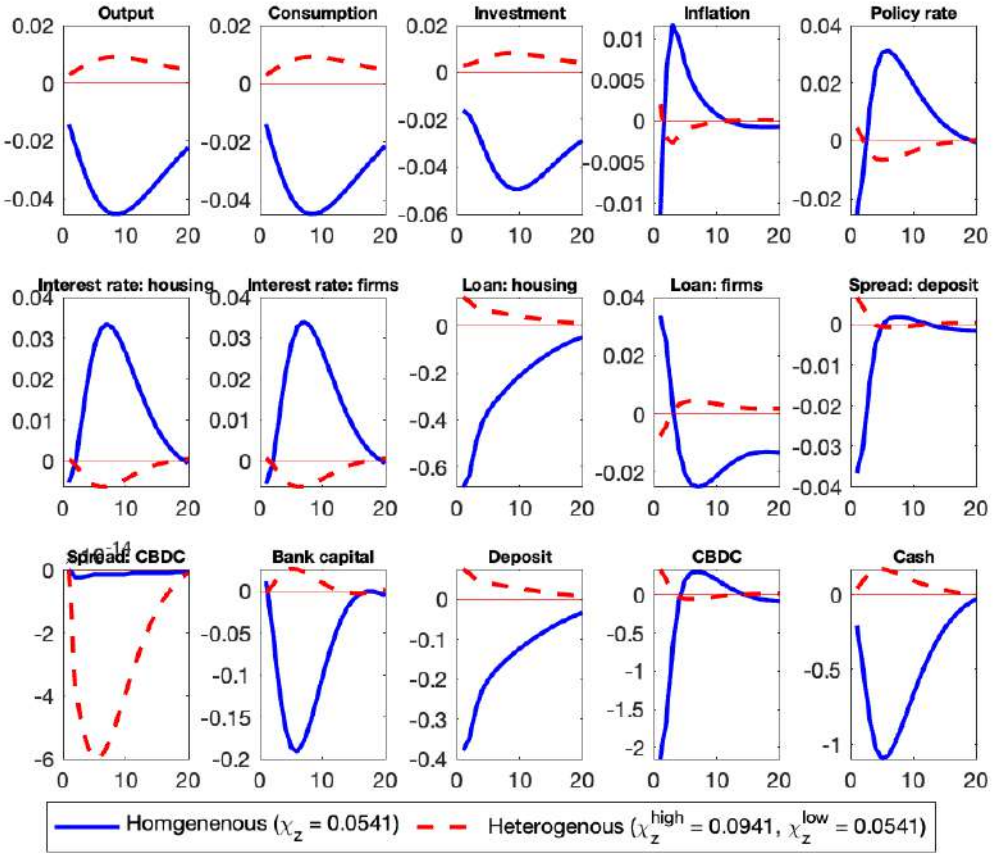

Figure 2.19: Response of various liquidity instruments and macroeconomic variables to a deposit elasticity shock under two scenarios, i.e., (1) the liquidity utility parameter is heterogeneous across patient households (red lines) and (2) the liquidity utility parameter is homogeneous across patient households (blue lines). Impulse response functions are percentage deviations from steady state.

borrowing constraints (Figure 2.20)—modeled as an increase in the firm loan-to-value ratio—triggers an increase in output of roughly 0.035% in the homogeneous case versus

0.027% in the heterogeneous setup. Loans to firms expand more severely in the former, despite the marginally smaller fall in output, due to stronger disintermediation among high-χ_z households. CBDC usage declines by over 3.5% under homogeneity compared to 2.5% in the heterogeneous case. Deposits increase more despite having a similar trend in deposit spread (dropping about 0.05% in both cases). The divergence between firm credit and aggregate output highlights the importance of financial segmentation: real effects can appear significant even when financial stress is less pronounced when the heterogeneity is taken into account. Next, a negative bank capital shock (Figure 2.21) generates a contrac-

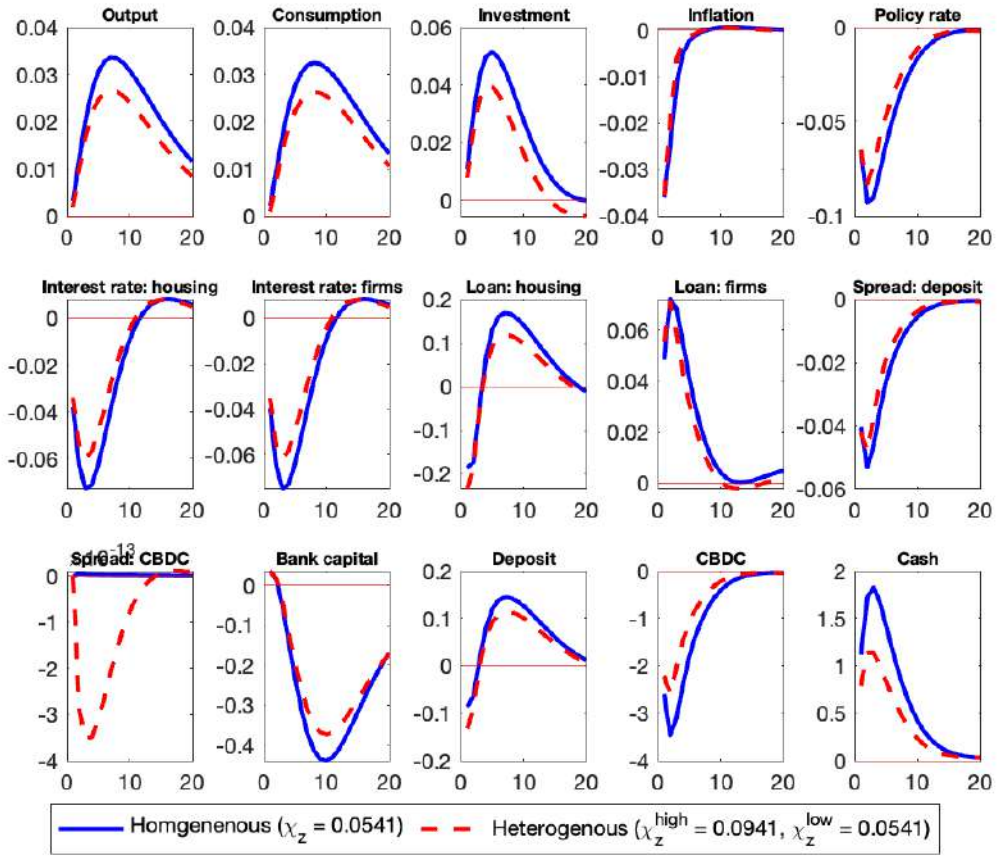

Figure 2.20: Response of various liquidity instruments and macroeconomic variables to a shock to loan-to-value ratio of firm loans under two scenarios i.e., (1) the liquidity utility parameter is heterogeneous across patient households (red lines), and (2) the liquidity utility parameter is homogeneous across patient households (blue lines). Impulse response functions are percentage deviations from steady state.

tion in lending that reduces output by nearly 0.1% across both models, but bank capital deteriorates more rapidly in the heterogeneous case, with a peak decline of 15% versus 13% in the homogeneous case. Deposits fall further in the heterogeneous model, and CBDC rises by roughly 5%, reflecting flight-to-liquidity behavior among high-χ_z agents. The sharper disintermediation feeds back into reduced bank profitability and slower re-

covery, consistent with the bank capital transmission channel emphasized in Gerali et al. (2010).

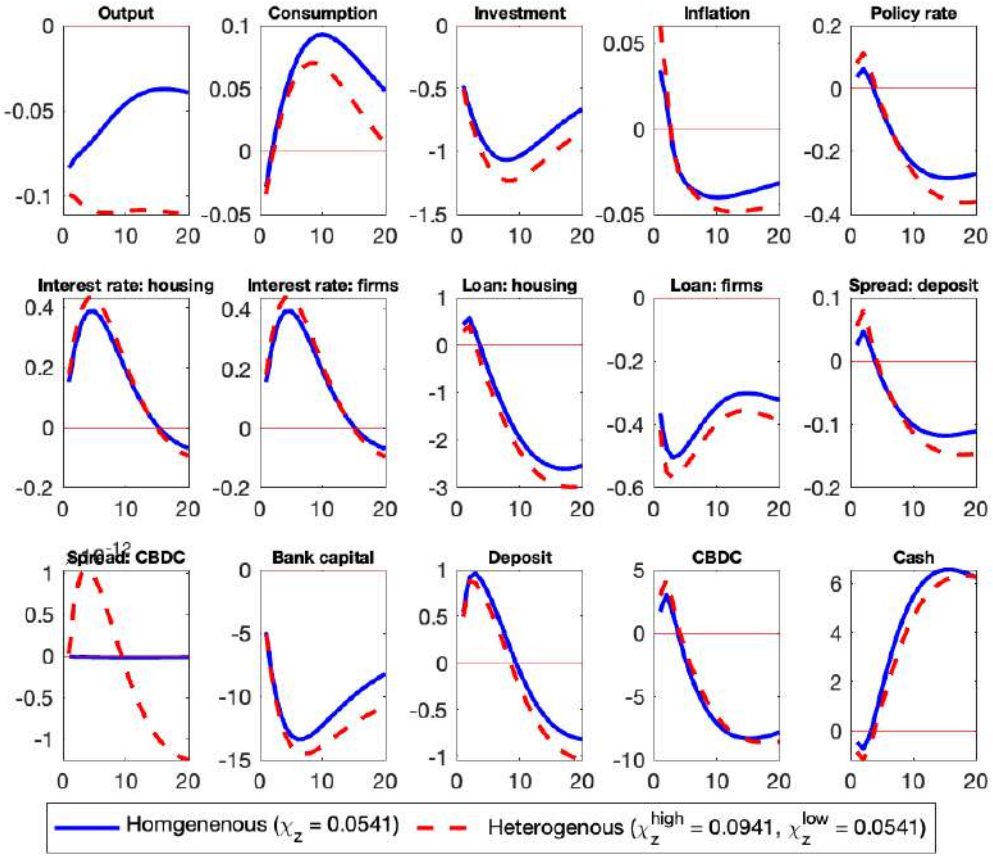

Figure 2.21: Response of various liquidity instruments and macroeconomic variables to a shock to the value of bank capital under two scenarios, i.e., (1) the liquidity utility parameter is heterogeneous across patient households (red lines) and (2) the liquidity utility parameter is homogeneous across patient households (blue lines). Impulse response functions are percentage deviations from steady state.

Figures 2.22b and 2.22a illustrate the steady-state outcomes under two alternative CBDC policy regimes, each reflecting a different choice by the central bank: either targeting the interest rate on CBDC or fixing the supply of CBDC as a share of output. In both cases, we explore how outcomes vary with the share of liquidity-preference households (γ_χ), which governs the degree of heterogeneity in portfolio demand across patient households.

In Figure 2.22b, the central bank sets the interest rate on CBDC (R^{dc}), and the quantity of CBDC is determined endogenously in equilibrium. The surface plots the steady-state ratio of CBDC to output (DC/Y) as a function of γ_χ and the spread between the deposit rate and the CBDC rate ($R - R^{dc}$). The results are intuitive and highly nonlinear: for a given interest rate spread, CBDC demand is much higher when a larger share of house-

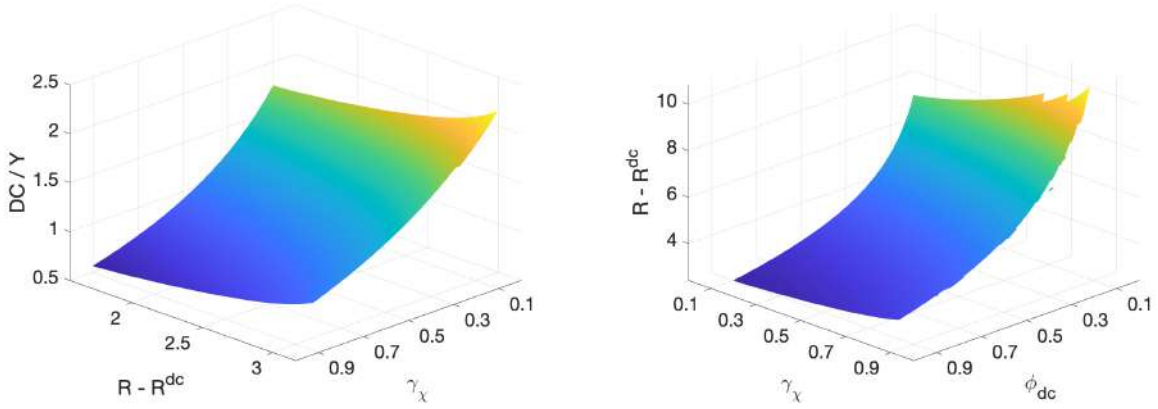

(a) CBDC holdings as a function of $R - R^{dc}$ and γ_χ

(b) Interest rate spread $R - R^{dc}$ as a function of ϕ_{dc} and γ_χ

Figure 2.22: Partial equilibrium effects of heterogeneity of liquidity utility parameter and CBDC policy parameters under different policy regimes

holds highly value liquidity. When $\gamma_\chi = 0.1$, CBDC usage stays below 1% of output across all interest rate spreads. But when $\gamma_\chi = 0.9$, CBDC holdings rise steeply with the spread, surpassing 2.5% of output when the deposit-CBDC spread reaches 3.2 percentage points. This illustrates the sensitivity of portfolio allocation to both preference composition and relative returns. As more households strongly prefer liquidity services, they shift away from deposits and toward CBDC more aggressively in response to favorable pricing.

Figure 2.22a reverses the policy lever: here, the central bank fixes CBDC supply according to a simple rule $DC = \phi_{dc} Y$, and the interest rate on CBDC adjusts endogenously to equilibrate household portfolios. The plot shows how the resulting interest rate spread $(R - R^{dc})$ depends jointly on ϕ_{dc} and γ_χ. As expected, larger CBDC allocations (higher ϕ_{dc}) and a higher mass of liquidity-seeking households both put downward pressure on the CBDC rate, requiring a larger spread to clear the market. For instance, when $\phi_{dc} = 0.9$ and $\gamma_\chi = 0.9$, the required spread exceeds 10 percentage points—highlighting a severe interest rate distortion necessary to absorb a large CBDC quantity. By contrast, when CBDC supply is modest ($\phi_{dc} = 0.1$) or the population has fewer high-χ_z households, the spread remains close to 2–3 percentage points.

Together, these figures underscore a key trade-off in CBDC policy design. Targeting the interest rate gives the central bank direct control over relative asset returns but leaves it exposed to potentially large and uneven take-up depending on household preferences. Fixing the CBDC quantity, on the other hand, introduces market-clearing volatility in interest rates, especially when preference heterogeneity is high. In both regimes, the interaction between household-level liquidity preferences and CBDC policy choices plays a critical role in shaping steady-state portfolio allocations and bank intermediation.

Chapter 3

Depositor-banker Relationship and CBDC

3.1 Introduction

The possibility of a Central Bank Digital Currency (CBDC) has swiftly captured significant attention within central bank research circles, with many attributing this phenomenon to a prevalent fear of missing out among central banks worldwide. The proliferation of various cryptocurrencies has amplified this apprehension, compelling central banks to assert control over payment systems and currency issuance, wary of ceding significant authority to private entities in monetary matters. Gorton and Zhang (2022) extensively elaborate on the importance of government vigilance concerning the concurrent existence of privately issued digital currencies, such as stablecoins, alongside fiat currencies. They caution against the potential ramifications, emphasizing the risk of central banks relinquishing their monopoly on money issuance and circulation.

The introduction of CBDC poses several concerns for monetary authorities. For example, CBDC might substitute conventional private money, i.e., deposits held at banks, leading to a substantial increase in bank funding costs (see Carapella and Flemming (2020)). Keister and Sanches (2022) shows that if CBDCs become highly competitive with bank deposits, disintermediation is unavoidable. The impact of CBDCs on bank funding depends on whether the CBDC is cash-like or deposit-like. A cash-like CBDC would have no direct effect on bank funding, whereas a deposit-like CBDC could reduce deposits and lending. Despite this, introducing a CBDC could increase the aggregate stock of liquid assets, enhancing exchange efficiency and social welfare. Their findings, modeled using the framework of Lagos and Wright (2005), are supported by global sentiment, evidenced by a recent survey from OMFIF (2020), which indicates that households worldwide view central bank liabilities as the safest form of money. Bindseil (2020) shows how

a tiered-remuneration system might mitigate the risks banks face from CBDC adoption. Brunnermeier and Niepelt (2019) establishes the conditions for equilibrium and welfare outcomes under a dual funding model using public and private money. Meanwhile, disintermediation might compel banks to retain more capital or turn to alternative, more volatile funding sources. Piazzesi and Schneider (2020) point to another function of banks, providing credit lines to depositors for payments, and argue that if CBDC lacks a credit component, it might be welfare-reducing.

AVERAGE DEPOSIT INTEREST RATE IN USA

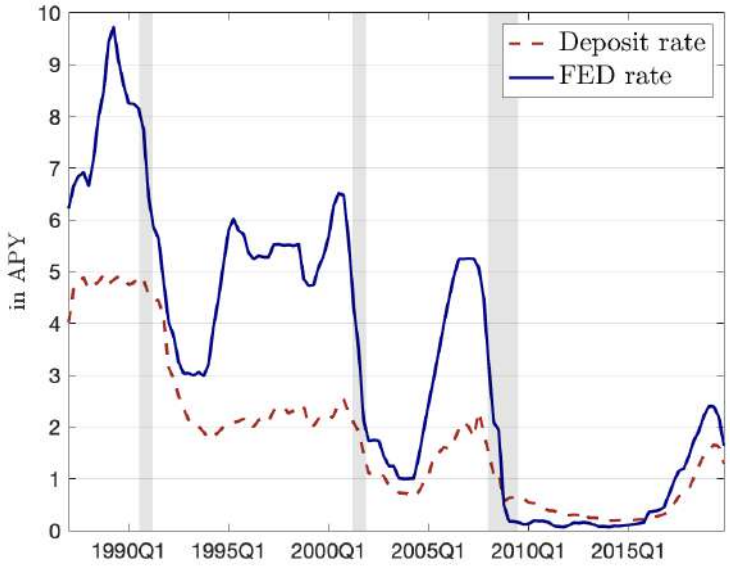

Figure 3.1: This figure plots the average deposit interest rate of chartered banks in the USA from 1987Q1–2019Q4. The deposit interest rate refers to transaction deposits and related interest expenses, reported by banks in the FDIC Call Report items RCON3485 and RIAD4508. The policy rate is the federal funds rate (FEDFUNDS) from the St. Louis Fed. Shaded areas represent NBER recession dates. (Data references: Drechsler et al. (2017) and McCracken and Ng (2021))

The validity of the aforementioned claims is open to debate, as empirical studies suggest the presence of significant market power among banks. As a result, the disintermediation effect of CBDC may be less pronounced. Drechsler et al. (2017) provide evidence of such market power in U.S. deposit markets. They find that when the federal funds rate rises, the spread between policy and deposit rates widens, leading to a reduction in total deposits. This market power enables banks to maintain low interest sensitivity on the expense side, mirroring the low interest sensitivity on the income side from credit issuance. Thus, maturity mismatches in their portfolios are offset by the ability to align interest sensitivities on both sides of the balance sheet, as highlighted by Drechsler et al. (2021).

Figure 3.1 shows that deposit rates on liquid accounts do not move one-for-one with the policy rate, thereby weakening monetary policy transmission. When the policy rate approaches the zero lower bound (ZLB), deposit rates tend to remain above it, as zero returns on deposits might lead savers to switch to cash. Similar trends are observed in the Euro Area and Canada. Figures 3.3 and 3.4 reveal particularly poor policy transmission in Canada. Despite policy rate liftoffs from ZLB, deposit rates remained low. The large deposit base and customer reluctance to switch banks are cited as reasons for the low interest rate sensitivity offered by Canadian banks.

Chiu et al. (2023) develop a micro-founded general equilibrium model of the payments and banking market calibrated to the U.S., revealing an imperfectly competitive banking sector. An interest-bearing CBDC could enhance bank intermediation by raising bank lending by 1.57%, as well as deposit and loan rates, provided CBDC remuneration stays within a specific range. Garratt et al. (2022) present a simplified model of competition between big and small banks, showing that a bank-distributed CBDC could erode the nonpecuniary benefits large banks offer depositors, especially if policymakers can set the convenience yield. Hence, bank strategy, leverage, size, and reputation all influence the CBDC's effect. These dynamics are explored in Adalid et al. (2022). Niepelt (2022) notes that CBDC could discipline 'too-big-to-fail' banks when other market power remedies are too costly. Chen et al. (2024) finds that CBDC rates directly affect household liquidity costs and indirectly influence deposit rates via bank competition, while reserve rates affect deposit rates directly. Their effectiveness, however, depends on market concentration. Cirelli and Nyffenegger (2023) argue that whether spread movements are driven by monopoly or leverage constraints determines the extent of disintermediation. Similarly, Andolfatto (2020) shows that monopolistic competition might actually increase lending activity, as banks raise deposit rates and lower lending rates to remain competitive, thereby expanding credit volume.

This paper contributes to this growing literature on the disintermediation effects of CBDC in the presence of bank market power and long-term banking relationships. These relationships affect both households and firms. Using Anacredit data, Lamas and Martinez Miera (2021) shows that households hold a significant share of bank equity, especially domestic banks—and often act as liquidity providers during small-scale crises. Their behavior is shaped by long-term relationships with banks. As a result, households often hold equity in their own banks and others. The duration of such relationships is influenced by switching costs. Using Italian household survey data, Brunetti et al. (2016) find that the probability of switching banks is inversely related to the number of services offered and positively related to the number of banks used by a depositor. Banks exploit economies of scale by bundling more services, thereby raising switching costs. Stenbacka and Takalo (2019)

emphasize switching costs as a proxy for both financial stability and a robust banking system.

However, a research gap remains: existing CBDC literature does not explore the role of hold-up effects from long-term depositor–banker relationships. This paper seeks to fill that gap using a medium-scale Dynamic Stochastic General Equilibrium (DSGE) model incorporating the financial frictions of Gertler and Karadi (2011) and deep habits in banking, as modeled by Airaudo and Olivero (2019), Aliaga-Díaz and Olivero (2010). Numerous empirical studies confirm that bank profitability and interest rate spreads are heavily influenced by the degree of banking sector competition (see Berger et al. (2004), Degryse and Ongena (2008)).

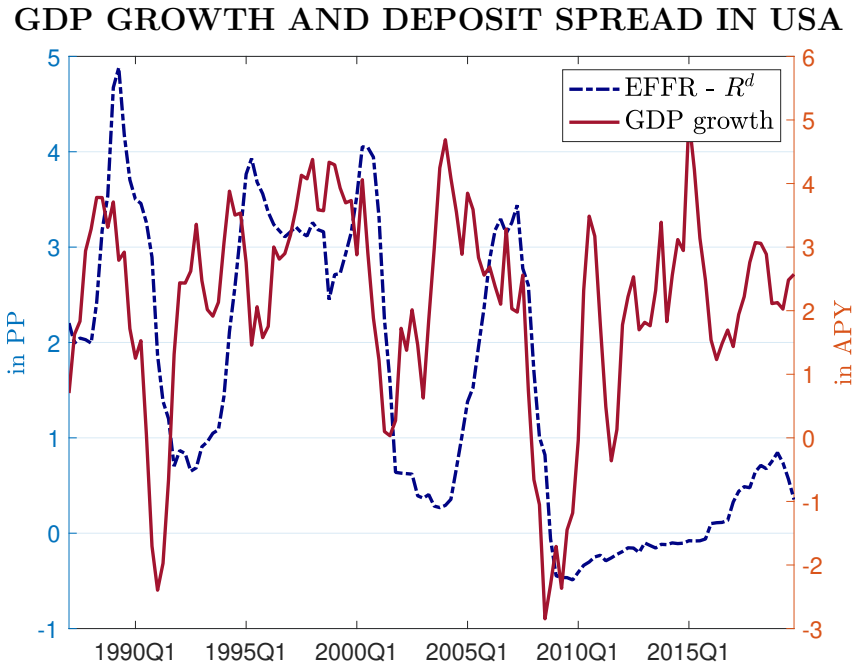

Figure 3.2: Deposit spread is defined as the difference between the FEDFUNDS rate and the average deposit rate shown in Figure 3.1. GDP growth is the log difference of quarterly GDP (data: Drechsler et al. (2017), McCracken and Ng (2021)).

The rest of the paper is structured as follows: Section 3.3 describes the model and its features, Section 3.4 outlines the calibration and estimation procedures, Section 3.5 presents the results, and Section 3.7 concludes.

3.2 Simple Model to Explore Long-Term Relationships

Let us consider a two-period economy with households and banks. The household receives an endowment y in period 1 and decides on consumption c and deposits d to hold at a

AVERAGE DEPOSIT INTEREST RATE IN EU

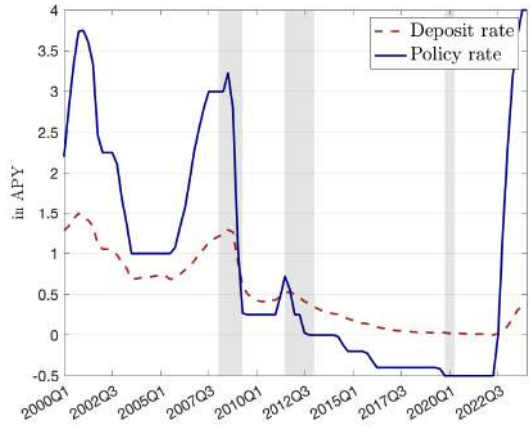

Figure 3.3: Deposit interest rate: overnight household deposits in the Euro Area (MIR.M.U2.B.L21.A.R.A.2250.EUR.N); policy rate: ECB deposit facility rate (ECBDFR). Source: ECB and FRED.

AVERAGE DEPOSIT INTEREST RATE IN CANADA

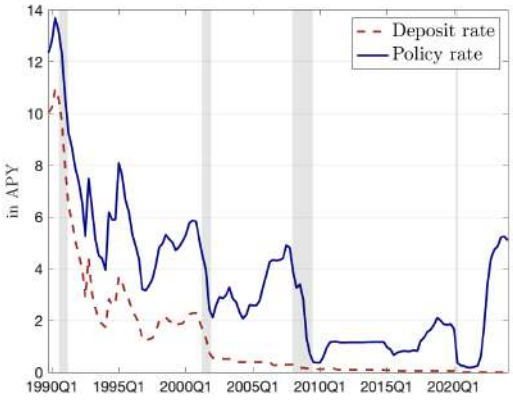

Figure 3.4: Deposit rate: average paid on transaction deposits in six major Canadian banks. Policy rate: 3-month interbank rate. Source: Bank of Canada.

representative bank in the economy. In each period, households search for a bank to hold deposits and may form a long-term relationship. The importance of this long-term relationship lies in the fact that the household will not search for other banks in the next period and will continue to hold its deposits with the previously chosen bank.

This long-term relationship is exogenously destroyed with some probability λ, in which case the household must search for a new bank. An increase in λ implies a weaker depositor–bank relationship in the economy. Whenever a household is forced to find a new bank, it incurs a fixed cost ϕ, representing search and matching frictions. We denote households with an existing bank connection as c_O and those forming new connections as c_N. The budget constraints of households in period 1 are:

$$C_O + d_O \leq y \qquad C_N + d_N + \phi \leq y \tag{3.1}$$

In the second period, households receive interest on deposits and profits from the bank. Their budget constraints in period 2 are

$$C'_O \leq R^d d_O + \pi \qquad C'_N \leq R^d d_N + \pi \tag{3.2}$$

Assume all households are matched with a bank and each holds deposits with only one bank. The household utility function is given by:

$$U(C) = \frac{C^{1-\gamma}}{1-\gamma} \tag{3.3}$$

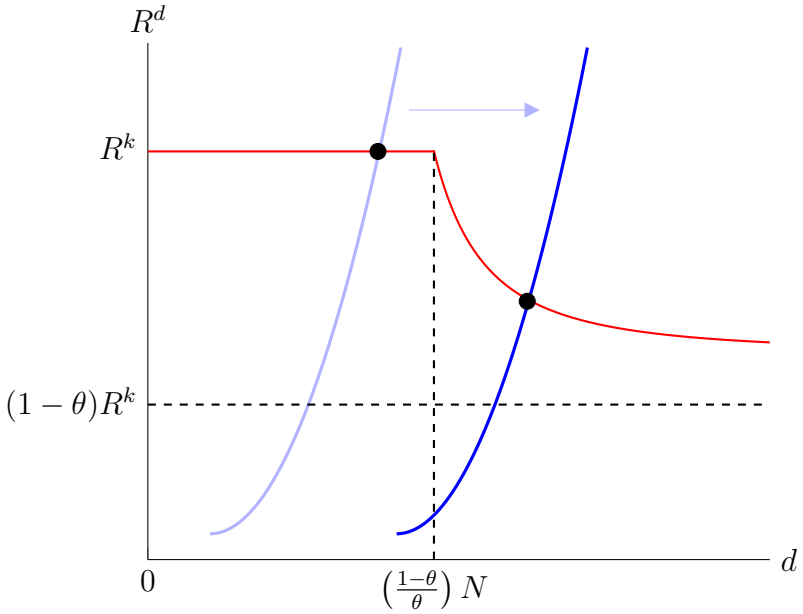

Figure 3.5: Equilibrium shifts from first-best to inefficient as depositor–banker relationships intensify (i.e., λ decreases).

Each household type solves the following optimization problem:

$$\max_{C_i, C_i', d_i} \; U(C_i) + \beta U(C_i') \qquad i \in \{O, N\} \tag{3.4}$$

subject to equations 3.1 and 3.2. The solutions for deposit demand by each household type are:

$$d_O = \frac{y(\beta R^d)^{\frac{1}{\gamma}} - NR^k}{R^k + (\beta R^d)^{\frac{1}{\gamma}}}, \qquad d_N = \frac{y(\beta R^d)^{\frac{1}{\gamma}} - NR^k - \phi(R^k + (\beta R^d)^{\frac{1}{\gamma}})}{R^k + (\beta R^d)^{\frac{1}{\gamma}}} \tag{3.5}$$

Total deposit demand is:

$$\begin{aligned} d &= \lambda d_N + (1-\lambda) d_O \\ &= d_O - \lambda\phi \end{aligned} \tag{3.6}$$

The banking sector follows a two-period version of the Gertler and Karadi (2011) model with financial frictions. Banks may abscond with a fraction θ of assets, and households receive no deposit insurance. A bank is indifferent between staying in business or running away when its return in both cases is equal. The bank's problem is:

$$\begin{aligned} \max_{d} \quad & R^k(N+d) - R^d d \\ \text{subject to} \quad & R^k(N+d) - R^d d \geq \theta R^k(N+d) \end{aligned}$$

The deposit interest rate R^d clears the market and is determined by the household Euler equation. Depending on the value of R^d, different equilibrium outcomes arise. The first-best occurs when $R^k = R^d$, i.e., in the absence of financial frictions. In that case, the bank is indifferent to any level of d for $0 \leq d \leq \left(\frac{1-\theta}{\theta}\right) N$. In the case where $(1-\theta)R^k \leq R^d \leq R^k$, the equilibrium is no longer first-best, and the bank demands the maximum d allowed by the constraint. The level of deposit in this case is:

$$d = \frac{R^k N(1-\theta)}{R^d - (1-\theta)R^k} \tag{3.7}$$

Notably, for a sufficiently large decrease in λ i.e., when the probability of forming a new bank-depositor link falls, the deposit market may shift to an inefficient equilibrium. Stronger depositor–banker relationships (implied by a lower λ) thus increase bank market power, potentially resulting in an inefficient allocation in the economy.

3.3 Full Model

The model in this paper is a DSGE framework featuring financial frictions and *deep habits* in the deposit market. Figure 3.6 illustrates the interactions among the different agents in the economy.

Representative households hold deposits at banks, supply labor, and maintain a liquidity portfolio from which they derive utility (see Burlon et al. (2024b), Ferrari Minesso et al. (2022), Schiller and Gross (2021)). Changing the nominal level of cash involves a quadratic cost, interpreted as the cost of frequent ATM visits or exceeding the bank-provided limit.

The banking sector is divided into retail and wholesale segments. The retail banking sector collects deposits from households, offering a bank-specific deposit interest rate, and bundles these deposits to create wholesale deposits. These are then placed with the wholesale bank, earning the central bank's policy rate. Long-term depositor–bank relationships are modeled following Airaudo and Olivero (2019), who adopt the *deep habits* approach of Ravn et al. (2006) to explain counter-cyclical credit spreads in the U.S. economy.

The wholesale branch of the bank purchases equity from firms and funds credit lines using wholesale deposits. These wholesale banks function as financial intermediaries and are not subject to stringent central bank regulations, thereby acting more like shadow banks.[1] Financial frictions in the banking sector are modeled in the spirit of Gertler and Karadi (2011). The production side of the economy follows a standard New Keynesian structure,

[1] For more on shadow banking, see Jiang et al. (2020), Moreira and Savov (2017).

consistent with much of the existing literature.

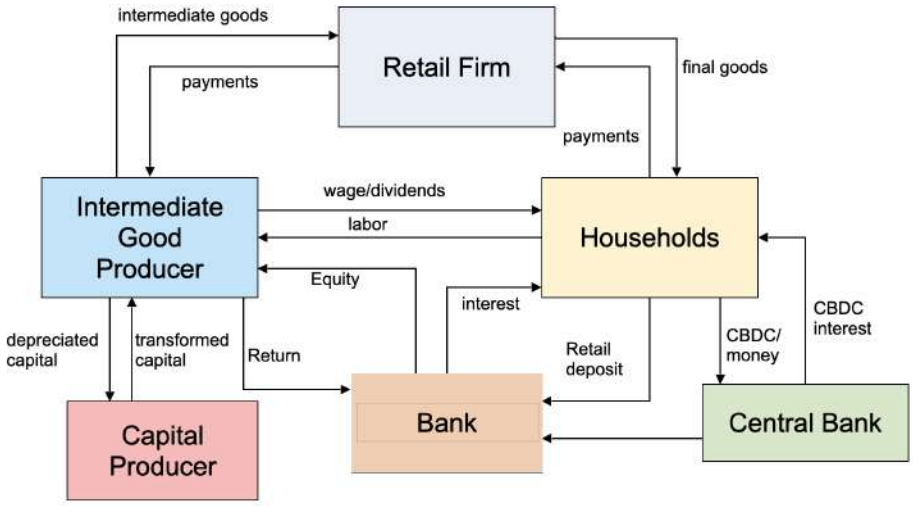

Figure 3.6: Flowchart showing the cash flows between different agents in the model.

3.3.1 Households

There is a unit mass of identical households that supply labor to firms, derive utility from liquidity services, and consume optimally each period. Liquidity services, denoted by LB_t and measured in consumption units, are modeled as a CES aggregate of deposit composite, cash, and CBDC, each with distinct weights.

The deposit composite $X^d_{i,t}$ consists of current deposits and the habit stock of past deposits held at individual banks. It is defined as

$$X^d_{i,t} = \left[\int_0^1 (D_{i,j,t} - \theta^d S_{j,t-1})^{\frac{\epsilon^d_t - 1}{\epsilon^d_t}} dj \right]^{\frac{\epsilon^d_t}{\epsilon^d_t - 1}} \tag{3.8}$$

Here, it $D_{i,j,t}$ represents household i's deposit with bank j, and households are assumed to deposit across all banks in the economy. The term $\theta^d S_{j,t-1}$ captures the *hold-up effect* in the depositor–bank relationship, where it θ^d quantifies its intensity. [2] The variable $S_{j,t-1}$ is the average stock of accumulated deposits at the bank j at the beginning of period t:

$$S_{j,t-1} = \int_0^1 S_{ij,t-1}\, di \tag{3.9}$$

The evolution of the deposit stock is governed by:

[2] This corresponds to the *deep habits* formulation in Airaudo and Olivero (2019), Ravn et al. (2006).

$$S_{j,t-1} = \rho_s S_{j,t-2} + (1-\rho_s) D_{j,t-1} \tag{3.10}$$

where $D_{j,t-1}$ is the total deposits held at the bank j by all households. Since it $S_{j,t-1}$ is an average, households treat it as exogenous. Hence, the habit is modeled as *external*. When $\rho_s = 0$, the stock becomes equivalent to the previous period's total deposits.

Each household i chooses $\{C_{i,t}, X^d_{i,t}, D_{i,j,t}, M_{i,t}, DC_{i,t}\}$ to maximize:

$$\mathbb{E}_0 \sum_{t=0}^{\infty} \left\{ \log(C_{i,t} - hC_{i,t-1}) - \frac{\chi}{1+\varphi} L_{i,t}^{1+\varphi} + \chi_{z,t} \log LB_{i,t} \right\}$$

subject to the budget constraint:

$$C_{i,t} + X^d_{i,t} + M_{i,t} + f(M_{i,t}) + DC_{i,t} = W_t L_{i,t} + \frac{R^{DC}_{t-1}}{\Pi_t} DC_{i,t-1} + \frac{M_{i,t-1}}{\Pi_t} + \int_0^1 \frac{R^d_{j,t-1}}{\Pi_t} D_{i,j,t-1} dj$$

where the deposit composite is

$$X^d_{i,t} = \left[\int_0^1 (D_{i,j,t} - \theta^d S_{j,t-1})^{\frac{\epsilon^d_t - 1}{\epsilon^d_t}} dj \right]^{\frac{\epsilon^d_t}{\epsilon^d_t - 1}} \tag{3.11}$$

and the liquidity services bundle is

$$LB_{i,t} = \left[M_{i,t}^{\frac{\eta_{z,t}-1}{\eta_{z,t}}} + \vartheta_t DC_{i,t}^{\frac{\eta_{z,t}-1}{\eta_{z,t}}} + \omega_d X_{i,t}^{\frac{\eta_{z,t}-1}{\eta_{z,t}}} \right]^{\frac{\eta_{z,t}}{\eta_{z,t}-1}} \tag{3.12}$$

The main distinction between the liquidity services considered in Burlon et al. (2024a) and those in this model is that households here derive utility from the entire deposit composite $X^d_{i,t}$, rather than from individual deposit holdings $D_{j,t}$.

Households first determine the optimal relative demand for deposits from each bank j by maximizing the total interest income from deposits, $\int_0^1 R^d_{j,t} D_{ij,t} dj$, subject to a fixed deposit composite $X^d_{i,t}$. The solution to this problem yields the representative household's optimal demand for deposits at bank j:

$$D_{ij,t} = \left(\frac{R^d_{j,t}}{R^d_t} \right)^{-\epsilon^d_t} X^d_{i,t} + \theta^d S_{j,t-1} \tag{3.13}$$

Here,

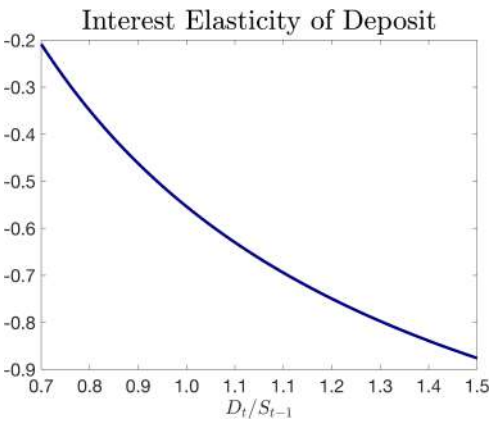

(a) Interest rate elasticity of deposit demand

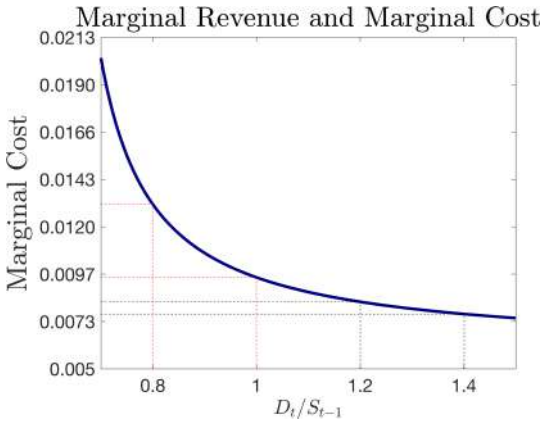

(b) Non-linear marginal cost of retail banks vs. deposit level

Figure 3.7: Non-linear transmission of deposit rates driven by time-varying elasticity and depositor relationships.

$$R_t^d = \left[\int_0^1 (R_{j,t}^d)^{1-\epsilon_t^d} dj\right]^{\frac{1}{1-\epsilon_t^d}} \tag{3.14}$$

is the aggregate deposit interest rate index. The effective deposit savings is given by the composite $X_{i,t}^d$, not simply the sum of deposits across all banks. Furthermore, because deposits are imperfect substitutes, each bank offers a differentiated deposit product.

In the limiting case of perfect substitutability (i.e., $\epsilon_t^d \to -\infty$) and no deep habits ($\theta^d = 0$), the deposit composite reduces to the simple sum of deposits across all banks, i.e., $X_{i,t}^d = \int_0^1 D_{ij,t} dj$.

Equation (3.13) shows that deposit demand from bank j increases if the bank offers a higher relative deposit rate or if the household has a stronger existing relationship with the bank (i.e., higher θ^d and $S_{j,t-1}$). This formulation introduces non-linearity in household responses to deposit rate changes.

The interest elasticity of deposit demand is given by:

$$-\frac{\partial D_{ij,t}}{\partial R_{j,t}^d} \cdot \frac{R_{j,t}^d}{D_{ij,t}} = \epsilon_t^d \left(1 - \frac{\theta^d}{\gamma_{ij,t}}\right) \tag{3.15}$$

where there $\gamma_{ij,t} = \frac{D_{ij,t}}{S_{j,t-1}}$ is a measure of deposit growth at the bank j relative to the deposit stock from the previous period.

Unlike in Gerali et al. (2010) or Drechsler et al. (2017), the deposit interest elasticity here depends not only on interest rates but also on the relative deposit holdings, making it endogenously time-varying.

Figure 3.7a shows how interest rate elasticity of deposit demand varies with the level of deposit held by a household at a bank (i.e., D_t relative to S_{t-1}). Specifically, the plot

displays the right-hand side of equation (3.15) using steady-state values.[3] As households increase their deposit levels at a bank, the elasticity of deposit demand rises, making them more sensitive to interest rate changes. This, in turn, increases competition in the deposit market and limits the ability of banks to suppress deposit rates. Since elasticity is deposit-level dependent, the marginal cost for retail banks becomes nonlinear. Figure 3.7b illustrates this: when deposits are high, marginal costs respond less to changes in deposit levels, while at lower deposit levels or stronger depositor relationships, marginal costs increase more rapidly. This implies that when banks face higher switching costs (low $\gamma_{ij,t}$), they adjust deposit rates less in response to funding shocks. Lower deposit elasticity allows banks to retain more market power and lose fewer customers despite limited rate pass-through. Conversely, when deposits are large or depositor–banker relationships are weak, banks pass through more of the policy rate to attract funding. Note that deposit interest revenue can be simplified as follows:

$$\int_0^1 R^d_{j,t-1} D_{ij,t-1} dj = R^d_{t-1} X^d_{i,t-1} + \Delta^d_{i,t-1}$$

so the household budget constraint becomes:

$$C_{i,t} + X^d_{i,t} + M_{i,t} + f(M_{i,t}) + DC_{i,t} = W_t L_{i,t} + \frac{R^{DC}_{t-1} DC_{i,t-1}}{\Pi_t} + \frac{M_{i,t-1}}{\Pi_t} + \frac{R^d_{t-1}}{\Pi_t} X^d_{i,t-1} + \Delta^d_{i,t-1}$$

where it $\Delta^d_{i,t-1} = \theta^d \int_0^1 R^d_{j,t-1} S_{j,t-2} dj$ captures the pecuniary benefit from a long-term relationship with banks. This term reflects that households with longstanding relationships benefit from more favorable deposit terms. Sharpe (1997), Carbo-Valverde et al. (2011), and Hannan and Adams (2011) provide empirical support showing that banks tend to offer higher deposit rates in markets with weaker customer relationships or a larger share of new clients. Thus, Δ^d_{t-1} quantifies the financial gains from banking loyalty. Finally, I assume that adjusting nominal cash holdings is costly. The cost function is

$$f(\cdot) = \frac{\psi_m}{2} M_t^2 \tag{3.16}$$

this cost represents the inconvenience associated with adjusting nominal cash balances or physical inconveniences of carrying cash, insurance, and security. To model the cost of cash holding, I follow the specification in Burlon et al. (2024b)

[3] In this plot, I use $\epsilon^d = -1.46$ and $\theta^d = 0.62$, consistent with the baseline model.

3.3.2 Bank

From the household's demand for deposit optimization, we get, by summing all deposit demands from households, $i \in [0, 1]$

$$\begin{aligned} D_{j,t} &= \int_0^1 \left[\left(\frac{R_{j,t}}{R_t} \right)^{-\epsilon_t^d} X_{j,t}^d + \theta^d S_{j,t-1} \right] di \\ &= \left(\frac{R_{j,t}^d}{R_t^d} \right)^{-\epsilon_t^d} X_{j,t}^d + \theta^d S_{j,t-1} \end{aligned}$$

Each bank consists of two operating arms, one retail and one wholesale. The wholesale branch is responsible for buying firm equities and managing wholesale deposits. The retail branch is in charge of taking retail deposits $D_{j,t}$ from households by remunerating them $R_{j,t}^d$ and bundling them into wholesale deposits D_t and earning the risk-free government bond rate R_t. Thus, the retail branch of the bank solves the following problem by choosing its demand for wholesale deposit and interest rate paid on retail deposit to households as follows:

$$\max_{D_{j,t}, R_{j,t}^d} \mathbb{E}_0 \sum_{t=0}^{\infty} \lambda_{0,t} \left[R_t D_t - R_{j,t}^d D_{j,t} \right]$$

subject to,

$$D_t = D_{j,t} \tag{3.17}$$

$$D_{j,t} = \left(\frac{R_{j,t}^d}{R_t^d} \right)^{-\epsilon_t^d} X_t^d + \theta^d S_{j,t-1} \tag{3.18}$$

The Lagrangian corresponding to the profit maximization of the jth bank is formulated as:

$$\mathcal{L} = \mathbb{E}_0 \sum_{t=0}^{\infty} \lambda_{0,t} \left[(R_t - R_{j,t}^d) D_{j,t} + \vartheta_{j,t} \left\{ \left(\frac{R_{j,t}^d}{R_t^d} \right)^{-\epsilon_t^d} X_t^d + \theta^d S_{j,t-1} - D_{j,t} \right\} \right] \tag{3.19}$$

Taking the FOC w.r.t $D_{j,t}$ and $R_{j,t}^d$, I get:

$$\vartheta_{j,t} = (R_t - R_{j,t}^d) + \theta^d (1 - \rho_s) \beta \mathbb{E}_t \lambda_{t,t+1} \vartheta_{j,t+1} \tag{3.20}$$

$$D_{j,t} + \epsilon_t^d \vartheta_{j,t} \frac{X_t^d}{R_t^d} \left(\frac{R_{j,t}^d}{R_t^d} \right)^{-(1+\epsilon_t^d)} = 0 \tag{3.21}$$

Let's focus on Eq (3.20). This variable represents the value of the continuation of the business of retail banking. It is clear that in the case of $\rho_s = 1$, the future value of a retail bank, it becomes irrelevant for the present value, and it becomes static. Also, the solution for the deposit stock S^d_{t-1} becomes zero, and deposit-holdup effects become absent from the model. In contrast, the stronger hold-up effect implied by higher θ^d leads to higher accounting of the value of future profits for retail banks on the present value of profits.
From eq (3.18) and eq (3.21) I have the expression for $\vartheta_{j,t}$. I can use the expression for $\vartheta_{j,t}$ in eq (3.20) and obtain the following after simple algebra:

$$R_t - R^d_{j,t} = \frac{R^d_{j,t}}{\epsilon^d_t}\left(\frac{\gamma_{j,t}}{\theta^d - \gamma_{j,t}}\right) - \theta^d(1-\rho_s)\beta\mathbb{E}_t\lambda_{t,t+1}\vartheta_{j,t+1} \tag{3.22}$$

where $\gamma_{j,t} = D_{j,t}/S_{j,t-1}$. Without the loss of generality, I am assuming a symmetric equilibrium for the whole economy so that all firms, banks, and households behave exactly the same as a class. Thus, all retail banks will set exactly the same deposit interest rate, i.e., $R^d_{j,t} = R^d_t$. Moreover, market clearing in the deposit market requires $D_{j,t} = D_t$, $S_{j,t} = S_t$, and $X_{j,t} = X_t$. Therefore, under symmetric equilibrium, I get the following expression for the deposit spread:

$$R_t - R^d_t = \frac{R^d_t}{\epsilon^d_t}\left(\frac{\gamma_t}{\theta^d - \gamma_t}\right) - \theta^d(1-\rho_s)\beta\mathbb{E}_t\lambda_{t,t+1}\frac{R^d_{t+1}}{\epsilon^d_t}\left(\frac{\gamma_{t+1}}{\theta^d - \gamma_{t+1}}\right) \tag{3.23}$$

If we define the markdown on the policy rate as μ^d_t, where $\mu^d_t = r^d_t/r_t$, the log-linearized equation is given by Equation 3.C.[4] This equation is central to understanding the behavior of the deposit spread in the model. The demand condition for deposits is reflected in the term γ_t. An increase in deposit demand or a weakening of the depositor–banker relationship (i.e., an increase in γ_t) raises the first term on the right-hand side (RHS), leading to a decline in the deposit spread. In response, the bank increases its pass-through of the policy rate to depositors in order to retain them and strengthen the relationship.
Conversely, an expected increase in γ_t in the future raises today's deposit spread. Anticipating a deterioration in depositor–banker relationships, banks preemptively reduce pass-through today to widen profit margins—this acts as a precautionary hedge against future losses.
Another important determinant of depositor–banker relationships is θ^d, which has a more nuanced effect. An increase θ^d (implying a stronger relationship) lowers the first term on the RHS, which by itself suggests a reduction in the deposit spread. However, it θ^d also influences the second term, which captures the impact of future profits on the current spread. Holding all else constant, this second term increases with θ^d. Therefore, the net

[4] See Appendix 3.C.

effect of an increase in θ^d the deposit spread is ambiguous: while the first term lowers the spread, the second term raises it.
In summary, while it γ_t has a relatively clear effect on the deposit spread—tightening relationships reduces spreads and loosening relationships increases them—the effect θ^d depends on the relative magnitudes of its influence on present versus future profit expectations.

3.3.3 Wholesale bank

There is a continuum of wholesale banks $j \in [0, 1]$ that are modeled after Gertler and Karadi (2011). They are engaged in buying equities from the non-financial firms and funding their investments through wholesale deposits obtained from the retail branch of the bank. The bank has to decide $S_{j,t}$ financial claims to buy that are priced at Q_t and $D^w_{j,t}$ wholesale deposits to hold at the retail branch. The return on the equity investment R^k_t and wholesale deposit costs R_t per unit. If the net worth of the wholesale bank is $N_{j,t}$ then the balance sheet of the bank is given by

$$N_{j,t} + D^w_{j,t} = Q_t S_{j,t} \tag{3.24}$$

and the net worth evolves as,

$$N_{j,t+1} = R^k_{t+1} Q_t S_{j,t} - R_t D^w_{j,t} \tag{3.25}$$

The bank will not operate unless the discounted return on equities is greater than the discounted cost of maintaining a deposit contract with the retail branch. Therefore at every period τ, the condition for the bank operation is

$$\beta^\tau \mathbb{E}_t \Lambda_{t,t+1} (R^k_{t+1+\tau} - R_{t+\tau}) \geq 0 \quad \text{for all } \tau > 0 \tag{3.26}$$

The stochastic discount factor $\Lambda_{t,t+1}$ is the same as the one for households since all banks are owned by households. If the above condition holds, the bank operates in a period by maximizing expected wealth at exit as follows:

$$V_{j,t} = \max \mathbb{E}_t (1-\theta) \theta^\tau \beta^{\tau+1} \Lambda_{t,t+1+\tau} N_{j,t+1+\tau} \tag{3.27}$$

By defining the gross growth rate of assets $\mathcal{X}_{t,t+\tau} \equiv \frac{Q_{t+\tau} S_{j,t+\tau}}{Q_t S_{j,t}}$ and gross growth rate of net worth as $Z_{t,t+\tau} \equiv \frac{N_{j,t+\tau}}{N_{j,t}}$, it is possible to express the $V_{j,t}$ as

$$V_{j,t} = \nu_t Q_t S_{j,t} + \eta_t N_{j,t} \tag{3.28}$$

where,

$$\eta_t = \beta \mathbb{E}_t \Lambda_{t,t+1}[(1-\theta)R_t + \theta Z_{t+1}\eta_{t+1}] \tag{3.29}$$

$$\nu_t = (1-\theta)\beta \mathbb{E}_t \Lambda_{t,t+1}(R^k_{t+1} - R_t) + \theta\beta \mathbb{E}_t \lambda_{t,t+1} \mathcal{X}_{t+1}\nu_{t+1} \tag{3.30}$$

At each period, the wholesale banker can divert λ a fraction of the funds to the owner household. This will lead to the bankruptcy of the bank since all depositors (retail bank in this case) will run and will recover the $1-\lambda$ fraction of the assets. Hence the incentive constraint for the wholesale banking operation is

$$V_{j,t} \geq \lambda Q_t S_{j,t} \tag{3.31}$$

From eq (3.18) and eq (3.31), I can write,

$$Q_t S_{j,t} = \phi_t N_{j,t} \tag{3.32}$$

where

$$\phi_t = \frac{\eta_t}{\lambda - \nu_t} \tag{3.33}$$

Therefore, variation in the net worth of the wholesale bank will drive the demand for equities from the bank, creating a channel through which the financial sector will be affecting the real sector of the economy.
At each period, $1-\theta$ a fraction of the bankers leave with their net worth, and the aggregate net worth of the remaining bankers is given by

$$N_{e,t} = \theta[(R^k_t - R_{t-1})\phi_{t-1} + R_{t-1}]N_{t-1} \tag{3.34}$$

Households transfer a $\frac{\omega}{1-\theta}$ fraction of the aggregate net worth of the exiting bankers to the new bankers. Since the net worth of the exiting bankers is $(1-\theta)Q_t S_{t-1}$, the net worth of the new bankers are,

$$N_{n,t} = \omega Q_t S_{t-1} \tag{3.35}$$

Therefore, the aggregate net worth of the banking sector is,

$$N_t = \theta[(R^k_t - R_{t-1})\phi_{t-1} + R_{t-1}]N_{t-1} + \omega Q_t S_{t-1} \tag{3.36}$$

3.3.4 Capital producing firms

Capital producers purchase depreciated capital from the intermediate goods producers and create new capital. Both renovated capital and new capital to the intermediate

goods producers. The market for capital is perfectly competitive. The new capital is priced at Q_t. The capital producers face investment adjustment costs associated with the production of new capital. If depreciated capital is renovated at unit cost, the total investment is simply the sum of new investment and renovated capital. In mathematical terms,

$$I_t = I_t^n + \delta(U_t)\xi_t K_t \tag{3.37}$$

Notice that the depreciation of capital depends on the level of utilization of capital, i.e., wear and tear of capital. The functional form of the capital depreciation is given by,

$$\delta(U_t) = \bar{\delta} - \frac{\tilde{\delta}}{1+\zeta} + \frac{\tilde{\delta}}{1+\zeta} U_t^{1+\zeta} \tag{3.38}$$

where, $\bar{\delta}$ is the depreciation in the steady state. Note that the parameter $\tilde{\delta}$ will be endogenously determined in the model.
The capital producer solves the following profit-maximizing problem:

$$\max_{I_t^n} \quad \mathbb{E}_t \sum_{j=0}^{\infty} \beta^j \Lambda_{t,t+j} \left[Q_{t+j} I_{t+j}^n - I_{t+j}^n - \frac{\eta^i}{2} \left(\frac{I_{t+j}^n + I^n}{I_{t+j-1}^n + I^n} - 1 \right)^2 (I_{t+j}^n + I^n) \right] \tag{3.39}$$

Taking derivative with respect to net investment gives the price equation of the capital as follows:

$$\begin{aligned} Q_t^k = 1 + \frac{\eta^i}{2} \left(\frac{I_t^n + I^n}{I_{t-1}^n + I^n} - 1 \right)^2 + \eta^i \left(\frac{I_t^n + I^n}{I_{t-1}^n + I^n} - 1 \right) \left(\frac{I_t^n + I^n}{I_{t-1}^n + I^n} \right) \\ - \beta \mathbb{E}_t \Lambda_{t,t+1} \eta^i \left(\frac{I_{t+1}^n + I^n}{I_t^n + I^n} - 1 \right) \left(\frac{I_{t+1}^n + I^n}{I_t^n + I^n} \right)^2 \end{aligned} \tag{3.40}$$

3.3.5 Intermediate goods producers

In a perfectly competitive market, each m intermediate goods producer produces $Y_{m,t}$ using labor from the household and capital, K_{t-1} which it buys using the funds raised by equity. It sells the produce to the retailers at price P_t^m. In other words, each intermediate goods producer issues a stock S_t priced at the price of capital and sells these stocks to wholesale banks to buy capital. Therefore value of the financial asset satisfies,

$$Q_t S_t = Q_t K_{t-1} \tag{3.41}$$

Please note that since the firm can buy the capital one period before the production and sell it to the capital producers as soon as the production is over, there is no capital accumulation on the firm's side. The production function of the firm is Cobb-Douglas

with following specification,

$$Y_t^m = A_t \Big[U_t \xi_t K_{t-1} \Big]^{\alpha} L_t^{1-\alpha} \tag{3.42}$$

The firm solves the following profit-maximizing problem by optimally choosing L_t and U_t,

$$\max \quad P_t^m Y_t^m + (Q_t - \delta(U_t))\xi_t K_{t-1} - W_t L_t \tag{3.43}$$

subject to the production function in eq (3.42). Taking first order with respect to L_t, U_t, I obtain the following optimality conditions,

$$(1-\alpha) P_t^m \frac{Y_t^m}{L_t} = W_t \tag{3.44}$$

$$\alpha P_t^m \frac{Y_t^m}{U_t} = \delta'(U_t)\xi_t K_{t-1} \tag{3.45}$$

The return on equity investment or capital can be interpreted in this way: since the intermediary earns zero profit in every period, the total return on capital is exactly the same as the capital share of revenue and the depreciated capital itself. Thus the realised return on capital can be expressed as,

$$R_t^k = \frac{\left[\alpha P_t^m \frac{Y_t^m}{\xi_t K_{t-1}} + (Q_t^k - \delta_t) \right] \xi_t}{Q_{t-1}^k} \tag{3.46}$$

3.3.6 Retail producers

The retail producers, a.k.a. final goods producers, buy intermediate goods Y_t^m from the intermediate goods producers at a price P_t^m and bundle them into single final goods Y_t in a monopolistically competitive market. So we have,

$$Y_t = \left(\int_0^1 (Y_t^f)^{\frac{\epsilon-1}{\epsilon}} df \right)^{\frac{\epsilon}{\epsilon-1}} \tag{3.47}$$

Each firm can re-optimize their price occasionally[5] with probability $1-\gamma$. Firms that do not optimize the price, index their price using inflation and parameter μ. Therefore a retail firm optimizes the following problem,

$$\max_{P_t^f} \sum_{i=0}^{\infty} \gamma^i \beta^i \Lambda_{t,t+i} \left(\prod_{\tau=1}^{i} \Pi_{t+\tau-1}^{\mu} \frac{P_t^f}{P_{t+i}} - P_{t+i}^m \right) Y_{t+i}^f \tag{3.48}$$

[5] this is referred to as Calvo pricing in the literature following Calvo (1983)

subject to the demand

$$Y_{t+i}^{f} = \left(\prod_{\tau=1}^{i} \Pi_{t+\tau-1}^{\mu} \frac{P_t^f}{P_{t+i}} \right)^{-\epsilon} Y_{t+i} \tag{3.49}$$

where the aggregate price index is given by

$$P_t = \left(\int_0^1 (P_t^f)^{1-\epsilon} \right)^{\frac{1}{1-\epsilon}} \tag{3.50}$$

Also note that the price dispersion evolves as,

$$\varsigma_t = (1-\gamma) \left(\frac{P_t^*}{P_t} \right)^{-\epsilon} + \gamma \left(\Pi_{t-1}^{\mu} \frac{P_{t-1}}{P_t} \right)^{-\epsilon} \varsigma_{t-1} \tag{3.51}$$

and the intermediate goods and final goods are related by price dispersion as

$$Y_t^m = \varsigma Y_t \tag{3.52}$$

3.3.7 Government

I assume that government funds bond payments through taxes on the household and profit received from the central bank and issuing new bonds. The balance sheet of the government is following

$$\frac{R_{t-1}^g B_{t-1}}{\pi_t} + G_t = T_t + B_t + \Omega_{CB,t} \tag{3.53}$$

where government bonds are purchased by both households and central banks i.e. $B_t = B_t^{CB} + B_t^h$. I also assume that the government gives a subsidy to the household so that the flexible price equilibrium coincides with efficient equilibrium in the steady state. The tax policy followed by the government is as follows:

$$T_t = \nu_\tau B_{t-1} \tag{3.54}$$

3.3.8 Central Bank

The central bank in this economy issues physical currency and digital currency and pays the remunerations if applicable. The profit of the central bank evolves as follows:

$$\Omega_{CB,t} = M_t + DC_t + \frac{R_{t-1}^g B_{t-1}^{CB}}{\pi_t} - \frac{R_{t-1}^{dc} DC_{t-1}}{\pi_t} - \frac{M_{t-1}}{\pi_t} - B_t^{CB} \tag{3.55}$$

Due to the presence of two public assets, the central bank now has to set two policies, i.e., (1) the nominal interest rate on government bonds and (2) either the supply or remuneration of CBDC. The nominal interest rate is set according to a Taylor rule,

$$\frac{R_t^n}{R} = \left(\frac{R_{t-1}^n}{R}\right)^{\rho_R} \left[\Pi_t^{\kappa_\pi} \left(\frac{MU_t}{\frac{\varepsilon}{\varepsilon-1}}\right)^{\kappa_Y}\right]^{1-\rho_R} \exp\left(\varepsilon_t^R\right) \tag{3.56}$$

where MU_t is the markup of the intermediary firms and R_t^n is the nominal interest rate. Notice that nominal and real bond interest rates are connected using the Fisher relation:

$$\frac{R_t^n}{\mathbb{E}_t \Pi_{t+1}} = R_{t+1} \tag{3.57}$$

For the baseline model, I consider that the CBDC is unremunerated. Hence,

$$R_t^{dc} = 1 \tag{3.58}$$

On the other hand, if the central bank follows a quantity-based rule, the interest rate on CBDC will be endogenously determined and the policy will be

$$DC_t = \phi_{DC} Y_t \exp(\xi_t^{dc}) \tag{3.59}$$

where ξ_t^{dc} is the CBDC supply shock is defined as an AR(1) time series. Later on I will consider other policy specifications for different scenario analyses.

3.3.9 Market clearing

The total available resource is given by

$$Y_t = C_t + G_t + I_t + \frac{\eta^i}{2}\left(\frac{I_t^n + I^n}{I_{t-1}^n + I^n} - 1\right)^2 (I_t^n + I^n) + f(M_t) \tag{3.60}$$

where government expenditure G_t is $\bar{g}\bar{Y}$ for simplicity.

3.3.10 Aggregate shocks

The model contains several aggregate exogenous shocks, each following an AR(1) process. Besides the standard shocks to technology, capital quality, and government spending,

$$A_t = \rho_A A_{t-1} + \varepsilon_t^A, \tag{3.61}$$

$$\xi_t = \rho_\xi \xi_{t-1} + \varepsilon_t^\xi, \tag{3.62}$$

$$\mu_t = \rho_\mu \mu_{t-1} + \varepsilon_t^\mu, \tag{3.63}$$

the extended framework includes additional shocks that affect the CBDC sector, liquidity preferences, and retail banking. A CBDC supply shock,

$$\xi_t^{dc} = \rho_{dc}\, \xi_{t-1}^{dc} + \varepsilon_t^{dc}, \tag{3.64}$$

captures unexpected changes in the quantity of CBDC when the supply rule is active. The processes

$$\chi_{z,t} = (1-\rho_\chi)\chi_z + \rho_\chi \chi_{z,t-1} + \varepsilon_t^\chi, \tag{3.65}$$

$$\eta_{z,t} = (1-\rho_\eta)\eta_z + \rho_\eta \eta_{z,t-1} + \varepsilon_t^\eta, \tag{3.66}$$

$$v_t = (1-\rho_v) + \rho_v v_{t-1} + \varepsilon_t^v, \tag{3.67}$$

introduce time variation in liquidity preferences and in the parameters that govern households' relative demand for CBDC, deposits, and cash. Retail banking conditions are subject to a further shock,

$$\epsilon_t^d = \rho_{ed} \epsilon_{t-1}^d + \varepsilon_t^d, \tag{3.68}$$

which moves the elasticity of deposit demand and therefore affects deposit spreads. The monetary policy disturbance ε_t^R remains purely exogenous, and the model also retains shocks to investment efficiency and net worth as in the baseline specification.

3.4 Calibration

Table 3.1: Parameter Values

Parameter	Value	Description
β	0.990	Discount rate
σ	1.000	Consumption EIS

Table 3.1 – Continued

Parameter	Value	Description
h	0.815	Habit formation
φ	0.276	Inverse Frisch elasticity
ζ	7.200	Elasticity of marginal depreciation wrt the utilization rate
θ	0.972	Survival prob. of bankers
α	0.330	Capital share
η^i	1.728	Elasticity of investment adjustment cost
ϵ^p	4.167	goods elasticity
γ	0.779	Calvo param
κ^Π	3	Taylor rule: Inflation coefficient
κ^Y	-0.125	Taylor rule: Output gap
κ	10.000	Credit policy coefficient
δ^{ss}	0.025	SS depreciation
ψ_m	0.020	Cash storage cost Burlon et al. (2024a)
θ^d	0.62	Intensity of bank-deposit relationship
ρ_s	0.4	deposit stock parameter
ν	1	CBDC liquidity preference
ω_d	0.71	Deposit weight in liquid instrument bundle Burlon et al. (2024a)
χ_z^{ss}	0.0269	Liquid instrument utility parameter Burlon et al. (2024a)
η_z^{ss}	3.58	Elasticity of substitution of cash, CBDC, and deposit Burlon et al. (2024a)

The standard parameters and bank-specific parameters are taken from Gertler and Karadi (2011) and Burlon et al. (2024a). Model-specific parameters are the intensity of bank deposit θ^d, deposit stock parameter ρ_s. These parameters are suggestive, and they can take values from 0 to 1. In the baseline model I considered 0.62 for the θ^d and 0.4 for ρ_s. In a later section, I do sensitivity analysis on these parameters. I calibrate the elasticity parameter for liquid assets ι using the steady-state ratio of cash and deposit composition in M1 measure of money for the USA. I calibrate deposit markdown in the USA to 0.85 following Jamilov and Monacelli (2023). This markdown value is consistent with the average deposit spread in the USA of about 60 basis points. The values of the deep habit parameter θ^d and stock parameter ρ_s together are important to have non-negative profit for retail banks. Therefore, the model does not have a solution when the parameters are beyond certain values since the retail bankers cease to participate in the

deposit intermediation and banks lose deposit funding.

$$\frac{1}{\epsilon^d}\left(\frac{1}{\theta^d-1}\right)\left[1-\theta^d(1-\rho_s)\beta\right]\geq 0 \tag{3.69}$$

Notice that for our given calibration of deposit elasticity parameter and discount factor of households, the above condition is satisfied.

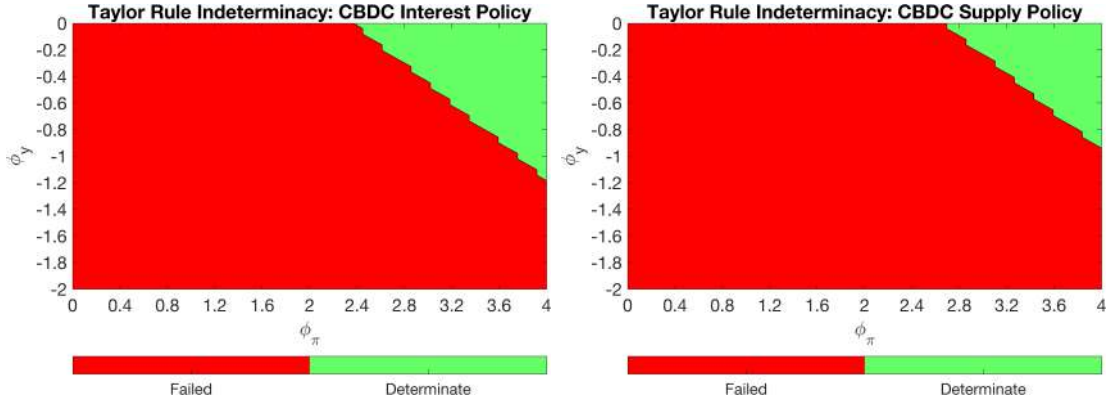

(a) Indeterminate regions for different Taylor rule parameters when the central bank sets an interest rate rule for CBDC

(b) Indeterminate regions for different Taylor rule parameters when the central bank sets a supply rule for CBDC

Figure 3.8: Indeterminacy regions different Taylor rule configurations under 2 different CBDC policies

Figure 3.8 illustrates how the region of indeterminacy changes depending on whether the central bank follows an interest rate rule or a supply rule for CBDC. First, note that the introduction of CBDC into an otherwise standard New Keynesian model increases the required Taylor coefficient on inflation. In standard models, determinacy requires this coefficient to exceed one, a condition known as the *Taylor principle* (see Galí (2015)). However, when CBDC is introduced, the indeterminacy region shifts to the right. This implies that the central bank must respond to inflation more aggressively, by more than 2.5 times the change in inflation, in order to maintain determinacy. Furthermore, the nature of the CBDC policy significantly affects this outcome. If the central bank adopts a CBDC supply rule, the indeterminacy region becomes smaller compared to the case with an interest rate rule on CBDC. This means that under a CBDC supply policy, the central bank must respond even more strongly to both inflation and the output gap to ensure a unique equilibrium.

3.5 Results

3.5.1 Steady-state effects

To understand the implications of CBDC introduction and its steady-state effects, I consider 2 policy scenarios for CBDC, where a central bank either fixes the interest rate and allows the quantity of CBDC to vary endogenously or it fixes the level of CBDC in the economy and lets the interest rate on CBDC vary endogenously. All values are reported in table 3.3

When the CBDC rate is set to zero, CBDC holdings remain modest in steady state. Households hold CBDC equal to about 0.42 of output, while cash amounts to roughly 0.34 of output, and the deposit-to-output ratio is close to 4.83. The liquidity services index is about 2.80. In this environment the central bank holds approximately 0.64 of government bonds, and households hold about 3.73, bringing the total stock of government bonds to about 4.36. Central bank profits are small but positive, and tax revenues adjust to 0.204 to support the consolidated fiscal position. Raising the CBDC rate to one percent of the policy rate increases CBDC demand moderately. CBDC holdings rise to about 0.43 of output, while cash falls slightly to about 0.34. Deposits remain essentially unchanged, at about 4.83 times output. The liquidity index moves up to about 2.81. On the asset side of the public sector balance sheet, total government bonds rise only marginally to about 4.41. The central bank absorbs a slightly larger fraction of these bonds, about 0.64, while households hold approximately 3.77. The increase in CBDC remuneration also lifts central bank profits slightly and leads to a small decline in the tax rate required to support government spending. When the CBDC rate is raised significantly, to one-tenth of the policy rate, the reallocation within the liquidity portfolio becomes more pronounced. CBDC holdings increase to about 0.57 of output, while cash falls to about 0.31. At the same time the deposit ratio declines modestly to about 4.79. These adjustments lift the liquidity services index to about 2.96. The effects on the stock of public debt are more visible in this case. Total government bonds rise to roughly 4.98, reflecting the need to expand central bank assets in order to back a larger CBDC liability. Central bank bond holdings increase to about 0.73, and household bond holdings rise to about 4.26. Central bank profits also increase relative to the previous cases, while the required tax rate falls to about 0.21.

The no-CBDC scenario is constructed assuming a policy rule where the quantity of CBDC supplied is zero. In the economy without CBDC, liquidity is provided almost entirely through cash and deposits. Cash amounts to roughly 0.54 of output, while deposits stand at about 5.04 times output. The liquidity services index is about 2.21, reflecting the overall efficiency of the liquidity bundle. With no CBDC liabilities on the central bank

balance sheet, the total stock of government bonds in steady state is about 3.14, of which the central bank holds roughly 0.46 and households about 2.68. Central bank profits are small, and the required tax rate is around 0.198. Introducing a moderate CBDC quantity rule that $CBDC/Y = 0.3443$ generates noticeable changes in the structure of liquidity. Cash falls substantially, to approximately 0.37 of output, and deposits decline to about 4.85 times output. These adjustments increase the liquidity services indicator to about 2.71, indicating that CBDC provides a meaningful contribution to the liquidity aggregate. On the fiscal side, the total stock of government bonds rises to about 4.07. The central bank's bond holdings increase to about 0.59, while household bond holdings rise to about 3.47. The expansion of public debt reflects the fact that the central bank must acquire additional government bonds to back the higher level of CBDC liabilities. Central bank profits increase marginally, and the required tax rate rises slightly to about 0.202. Under the more aggressive quantity rule, where it $CBDC/Y$ is doubled, CBDC becomes a larger component of the liquidity bundle, equal to about 0.69 of output. Cash falls further, to about 0.28, and the deposit-to-output ratio declines modestly to about 4.75. These rebalancing effects raise the liquidity services index to approximately 3.08. The public sector balance sheet expands further in this case. Total government bonds reach roughly 5.50, central bank bond holdings increase to about 0.80, and households hold approximately 4.69. These values imply that the introduction of a large CBDC liability requires a sizeable expansion of the central bank's asset holdings, while at the same time households shift a greater share of their portfolio toward safe government securities. Central bank profits rise relative to the moderate rule, and the tax rate settles at about 0.214.
These results show that both the interest rate and quantity-based approaches to CBDC issuance lead to economically meaningful shifts in the liquidity structure and in the size of the public sector balance sheet. Higher CBDC remuneration or larger CBDC quantities reduce the use of cash, increase reliance on CBDC, and generate modest declines in deposits, while improving the liquidity index. At the same time, both policies require a substantial expansion in government bond holdings, as the central bank and households rebalance toward safe assets in response to the new composition of liquid claims.

3.5.2 Monetary policy shock

Figure 3.9 shows the response of selected variables to a one-standard-deviation temporary contractionary monetary policy shock. As the policy rate increases, so does the wholesale interest rate, making funding more expensive for the wholesale branches of banks. This results in a contraction in the net worth of banks. Given that asset holdings are modeled as a fraction of bank net worth, capital assets decline accordingly, leading to reduced production.

In the model with deep habits and CBDC (indicated by the brown square line), the declines in output and consumption are the most pronounced. Inflation also drops the most in this specification, indicating that monetary policy transmission is strongest when both CBDC and deep habits in deposit behavior are present.

On the retail side, deposit interest rates rise by less than the risk-free interest rate, causing the deposit spread to widen, by approximately 25%. Notably, while the credit spread is pro-cyclical in this setting, the deposit spread behaves counter-cyclically. This behavior reflects banks' market power: despite reduced investment revenue from firms, banks can still increase the deposit spread due to the presence of deep habits. Indeed, deposit spreads increase by about 15% in models without deep habits, but up to 25% in models with deep habits, allowing banks to preserve profit margins even during downturns.

Retail banks can also delay profit shrinkage by holding deposit rates low, taking advantage of households' switching costs. These switching costs rise by about 6% on impact due to higher deposit rates, but decline gradually as both deposit holdings and deposit rates fall. This makes it cheaper for households to switch to alternative deposit products, particularly as they continue to enjoy higher returns due to *deep habits*.

CBDC and cash respond sharply to the monetary policy shock. CBDC holdings drop by around 800% in both the deep-habit and no-deep-habit models. Since CBDC is not remunerated in the model, the opportunity cost of holding it rises dramatically as nominal interest rates increase. Cash, on the other hand, behaves differently. In the absence of deep habits, cash holdings fall by about 300%. In the presence of deep habits, the decline in cash is more modest—approximately 100%—because the higher deposit spread reduces the relative opportunity cost of holding cash.

Although central bank profits remain unchanged, this sharp drop in CBDC and cash implies a $234 billion reduction in the central bank's balance sheet, assuming current levels of currency in circulation. This suggests that the central bank could substitute CBDC for cash without requiring additional asset purchases (or sell-offs), thereby avoiding potential distortions to the long end of the yield curve.

In contrast to Airaudo and Olivero (2019), where the credit spread enters the New Keynesian Phillips Curve (NKPC) via supply-side effects—due to working capital constraints making loan rates part of marginal costs—this model introduces deep habits in the deposit market, which affect the demand side through the aggregate demand equation.

3.5.3 Capital quality shock

When the quality of capital suddenly declines, it has an overall contractionary effect on the economy. However, the banking sector exhibits a distinct response in this case. As shown in Figure 3.10, capital decreases by approximately 5% on impact following the

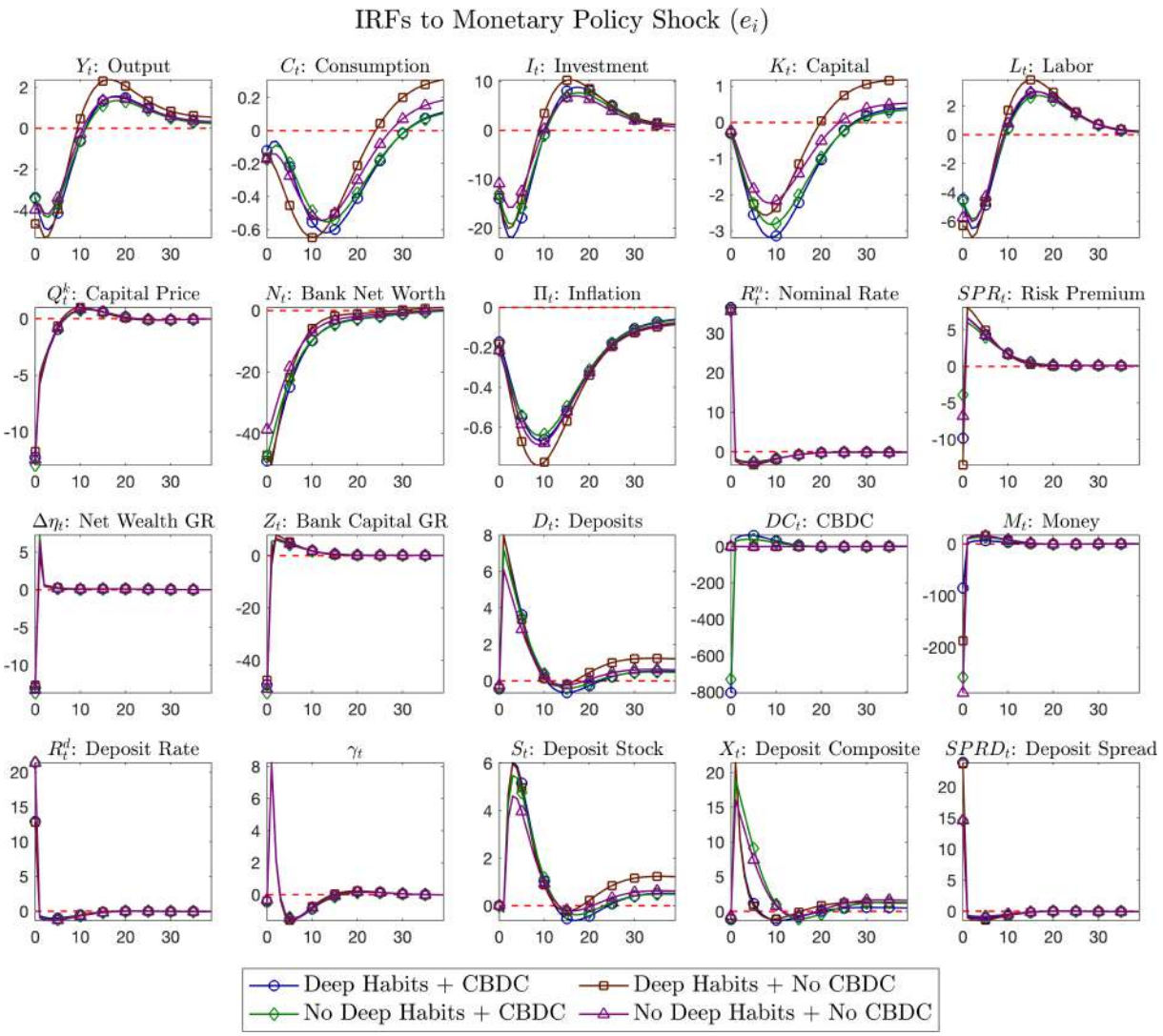

Figure 3.9: Impulse response function of some selected variables of the model to 1 s.d. contractionary and temporary monetary policy shock. Deviations are measured in percentage

capital quality shock.

Notably, the response of capital varies across the four different model specifications. In particular, the presence of deep habits in the deposit market amplifies the decline in capital, even though the response of the capital price remains relatively similar across models. The price of capital assets initially drops by about 15%, but it gradually recovers, returning to its steady-state level within approximately five years. In contrast, the quantity of capital reaches its lowest point around the two-year mark before beginning to recover. This divergence highlights the role of deep habits in shaping the dynamics of capital accumulation and asset pricing in the aftermath of shocks to capital quality.

The return on capital increases immediately following the capital quality shock. This is driven by both the gradual decline in the capital stock and the simultaneous rise in cap-

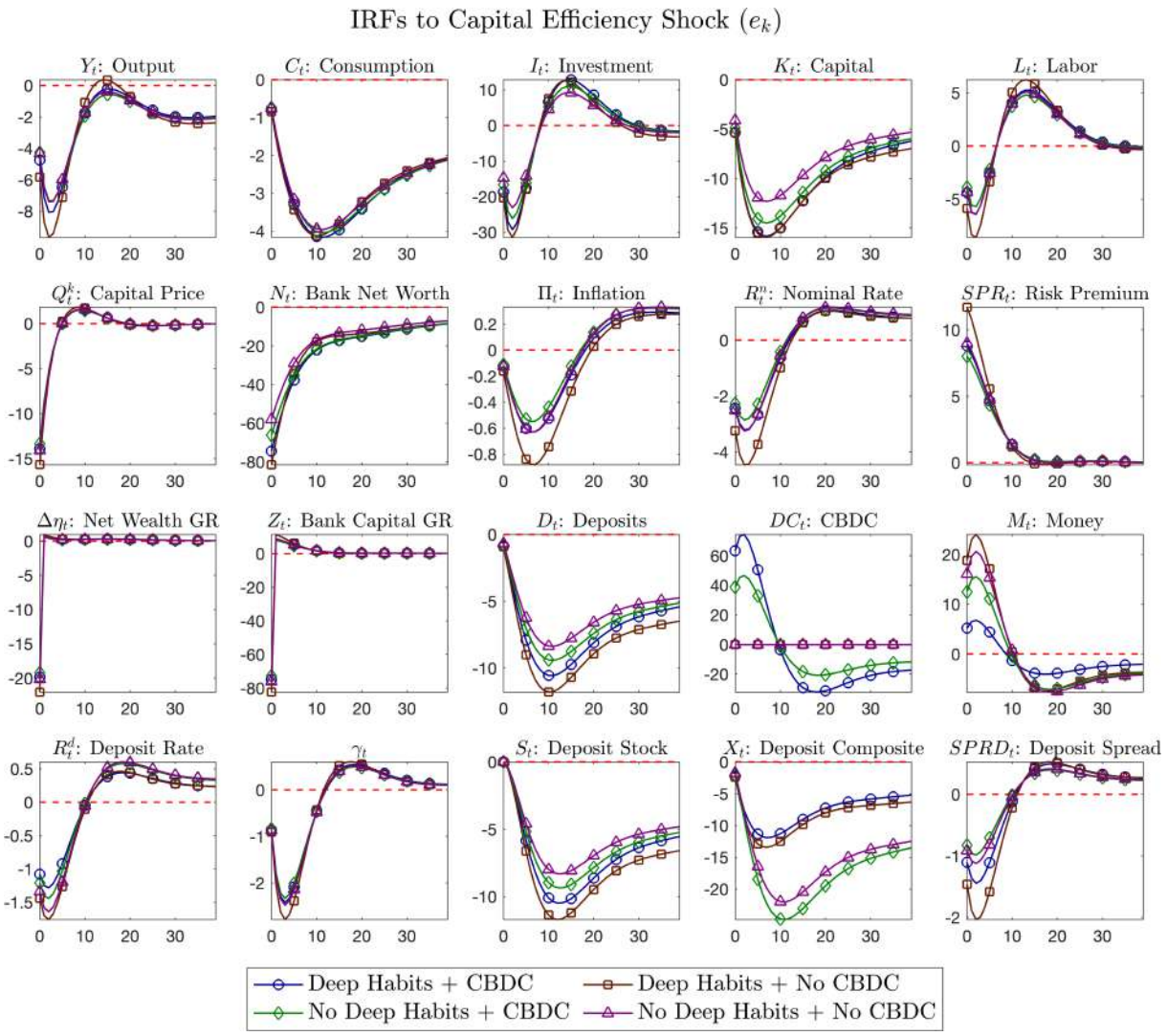

Figure 3.10: Impulse response function of some selected variables of the model to 1 s.d. negative capital quality shock. Deviations are measured in percentage

ital prices, which together push up the marginal return on capital. A stronger depositor-banker relationship enhances the banking sector's risk-taking capacity, resulting in a more pronounced increase in the credit spread. Specifically, the credit spread increases by approximately 15% on impact in the model with strong deep habits, while in the other model variants the response is more muted. This counter-cyclical behavior of the credit spread is consistent with empirical evidence (see, for example, Gertler and Karadi (2015)). The retail banking sector responds differently in this scenario compared to a monetary policy shock. In this case, the demand for deposits declines due to the fall in bank net worth. A roughly 5% drop in aggregate capital leads to an immediate reduction of around 1% in deposits. This downward trend continues for approximately 2.5 years, eventually reaching a decline of about 8% from its steady-state level in the baseline model without CBDC and deep habits. In contrast, under stronger depositor-banker relationships (i.e., deep

habits), the drop in deposits is steeper, nearing 15%. Similarly, bank net worth suffers a much greater contraction, declining by as much as 80% on impact.
As deposits decline, the deposit spread also narrows. According to equation 3.22, a decrease in deposit demand reduces the spread. Therefore, unlike in the monetary policy shock case, where the deposit spread was counter-cyclical ,here it becomes pro-cyclical, falling in line with output and consumption. As deposit interest rates fall, the opportunity cost of holding cash and CBDC also decreases. This is reflected in their respective dynamics: CBDC holdings rise by about 60% on impact in the deep-habit model, whereas cash increases more modestly, by about 5%.
Interestingly, the presence of CBDC helps cushion the decline in deposits, and the increase in the credit spread is mitigated relative to models without CBDC. Furthermore, although total deposits decline, the variable γ_t, which captures the ratio of current deposit holdings to deposit stock, begins to recover within a year. This early rebound is attributable to the persistent strength of the depositor-banker relationship embedded in the model.

3.5.4 Liquidity-related responses

Next, we consider shocks related to liquidity in the model. Figure 3.11 shows the responses of key variables to a 1 standard deviation (s.d.) positive shock to the deposit elasticity. This shock implies that households become more sensitive to changes in the deposit interest rate. The introduction of CBDC amplifies the macroeconomic response: deposit levels rise significantly, reaching a peak increase of around 6% in approximately five years. As banks lose market power due to higher deposit elasticity, they are unable to maintain low pass-through of the policy rate. Consequently, deposit interest rates rise immediately by about 1.7 annual percentage points (APP), and the deposit spread declines sharply by approximately 4 APP.
This decline in the deposit spread increases the opportunity cost of holding other forms of liquidity, namely cash and CBDC. As a result, CBDC holdings decline dramatically, by 60% to 80%, while cash holdings drop by about 12% to 25%. Interestingly, in models with deep habits in the deposit market, the deposit response is more pronounced. The increased elasticity enhances the substitution effect between liquidity instruments: in models without deep habits, CBDC usage drops more than in models *with* deep habits, where existing depositor-banker relationships mitigate the substitution.
The shock leads to economic expansion via the banking channel. Although banks lose some market power, their net worth increases by approximately 5% on impact due to the higher deposit inflow. This reflects a holding effect: increased savings in the form of deposits make the banking sector more robust and better funded. With more capital and labor available, firms expand production. Output rises by about 1% on impact and peaks

around 4% after 10 quarters. On the other hand, consumption declines, as deposit-based saving becomes more attractive in the wake of increased deposit rates.
We also study the response to a 1 s.d. positive shock to liquidity preference in the utility function (also shown in Figure 3.11). This shock, like the deposit elasticity shock, has an expansionary effect on the economy, though the magnitude of the response varies across models. The model with deep habits but no CBDC shows the strongest responses. As liquidity becomes more valuable to households, they increase their holdings of all liquidity instruments: deposits, cash, and CBDC.
However, when CBDC is available, it crowds out bank deposits, as households shift their liquidity portfolios. As a result, the rise in deposits is only about half of what is observed in the model without CBDC. This crowding-out lowers the risk-taking capacity of banks, leading to reduced net worth and a smaller increase in the risk premium. This dynamic illustrates how CBDC, by altering the structure of liquidity demand, can indirectly influence bank funding conditions and financial stability.

3.5.5 Importance of depositor-banker relationship

Now let us focus on the effect of different degrees of hold-up effect or deep habits in the deposit market. Figure (3.13) shows the impulse response of variables to a 1 s.d. positive shock to liquidity preference of the household. As mentioned in the previous section, the shock has an expansionary effect on the economy as savings instruments become more sought after. Deposits, being one of the savings instruments, see increased demand along with CBDC and cash. It is interesting to note that as hold-up effects become stronger (i.e., implied by increasing value of θ^d), the expansionary effects become stronger as well. This is due to the fact that banks have more funding available to them in comparison to lower values of θ^d. As a result, banks can now invest more in capital, allowing firms to increase their production. The increase in output in the case where the hold-up effect is highest reaches a maximum of 2% in about 10 quarters' time. A similar effect of hold-up occurs when the economy is hit by a 1 s.d. positive shock to deposit elasticity, as shown in Figure (3.14). Unlike the previous shock, in this case, the higher the hold-up effect, the less expansionary the shock becomes. This is due to the fact that although an increase in deposit elasticity increases competition in the deposit market, the hold-up effect increases market power. Hence, there is a trade-off in terms of market power. The increase in deposit holding is significantly lower (rising to about 0.5% in 15 quarters' time), whereas for lower values of deep habits, the deposit level increases by about 0.2% from the steady-state level, forcing banks to cut back on investment in firms. Hence, the output increases much less in the case where the hold-up effect is highest. Therefore, in the presence of a stronger hold-up effect, the economy is less deflationary relative to other levels. The

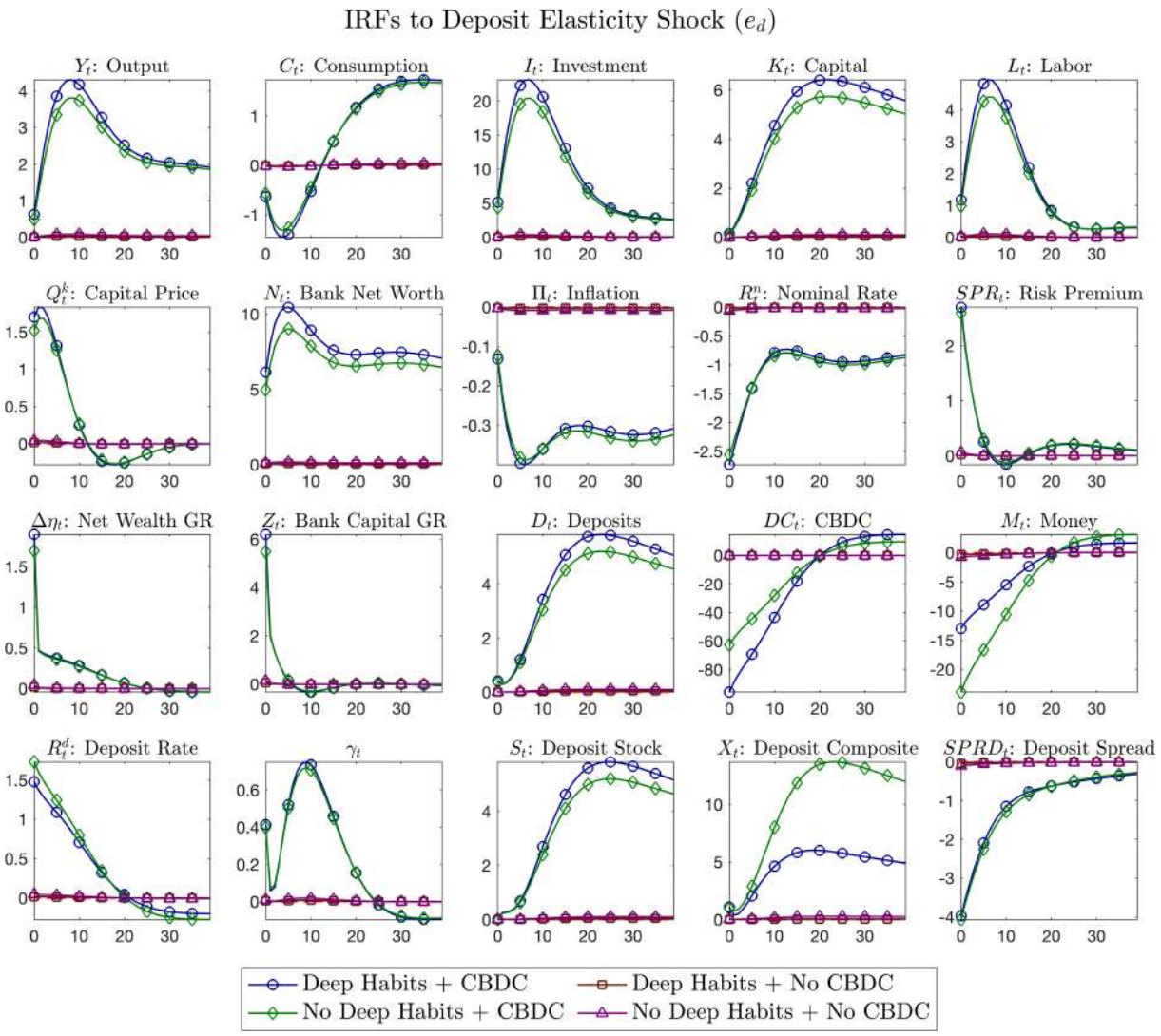

Figure 3.11: Impulse response function of some selected variables of the model to 1 s.d. deposit elasticity shock. Deviations are measured in percentage

decline in CBDC usage is about 1%, whereas cash levels remain almost unchanged.

The changes in the elasticity of substitution of different savings instruments have implications contrary to the previous shocks. In Figure (3.15), I have shown the response of the variables to a 1 s.d. shock to the elasticity of substitution among different liquidity instruments, namely cash, CBDC, and bank deposits. When the deposit-banker relationship is weak in the economy, the shock has an expansionary effect. As cash is expensive to hold, higher elasticity of substitution between liquidity instruments allows households to switch to other instruments. As a result, cash declines by about 8% on impact, whereas deposit holdings increase by 0.1%. The moderate increase in the deposit base is due to a decline in the deposit rate. This increase in available funding allows banks to take up more investment projects, making funds for capital available to firms. Consequently, output and investment increase.

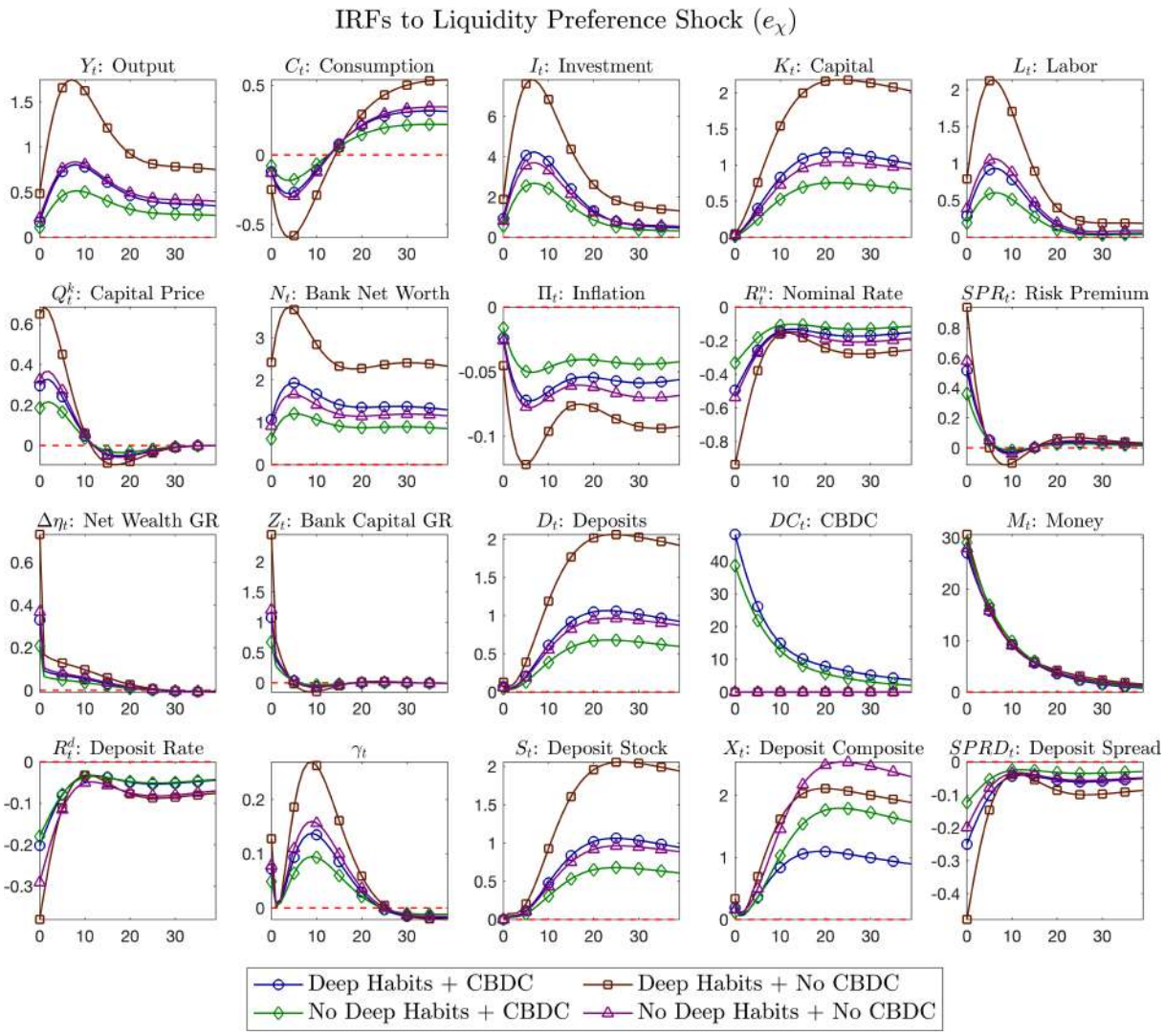

Figure 3.12: Impulse response function of some selected variables of the model to 1 s.d. positive preference shock to liquidity bundle in utility. Deviations are measured in percentage

Now, as the hold-up effect in the deposit market increases, the deposit spread increases. For example, when $\theta^d = 0.9$, the deposit interest rate spread increases by 0.15 APP on impact. Since the elasticity of substitution among liquidity instruments has increased, households can switch to CBDC. This explains the increase in CBDC demand of about 12% on impact. Banks increase the interest rate paid on deposits to retain outgoing depositors, shrinking the profit margin of the bank. This is reflected in the decline in the growth of net wealth and bank capital. Banks reduce the size of their investments, causing a decline in capital. Capital declines by 0.6% in about 5 years' time. This leads to a decline in output for $\theta^d = 0.9$.

As shown in Figure (3.16), the monetary policy transmission is not largely affected by an increase in the hold-up effect in the deposit market. If anything, the transmission of

the monetary policy shock improves with increasing θ^d, indicating that a banking sector with a strong depositor-banker relationship actually works in favor of monetary policy transmission.

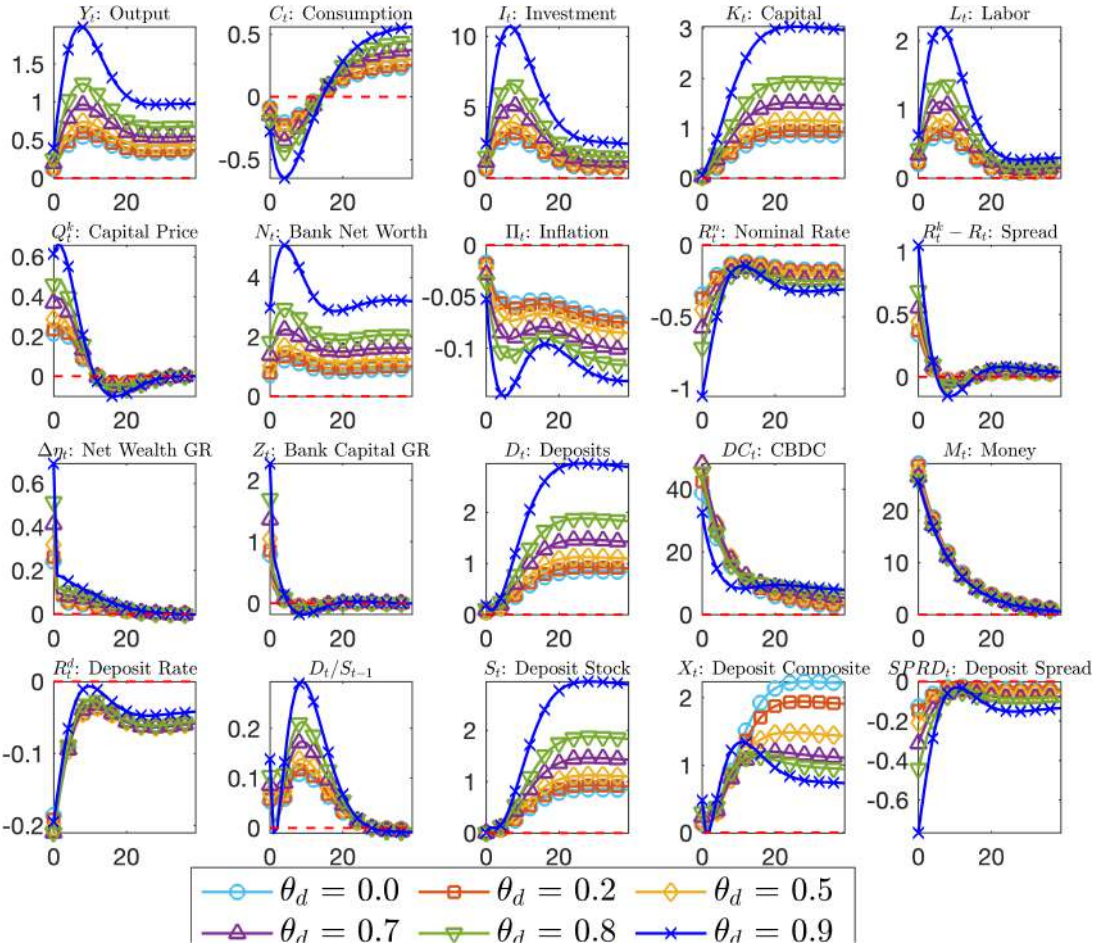

Figure 3.13: Impulse response function of some selected variables of the model to 1 s.d. positive shock to the liquidity bundle weight in the utility function of household for different values of θ^d. Deviations are measured in percentage

3.5.6 Welfare implications

To perform the welfare analysis, I use the following definition of welfare in the recursive form:

$$\text{WELFARE}_t = \log\left(C_t - hC_{t-1}\right) - \frac{\chi}{1+\varphi} L_t^{1+\varphi} + \chi_{z,t} \log Z_t + \beta \mathbb{E}_t \text{WELFARE}_{t+1} \quad (3.70)$$

following Faia and Monacelli (2007), where Z_t is defined in Eq (3.12). In the first experiment, I tried to quantify the welfare improvement due to the introduction of CBDC. Figure 3.17a shows the consumption-equivalent welfare improvements in percentage, where

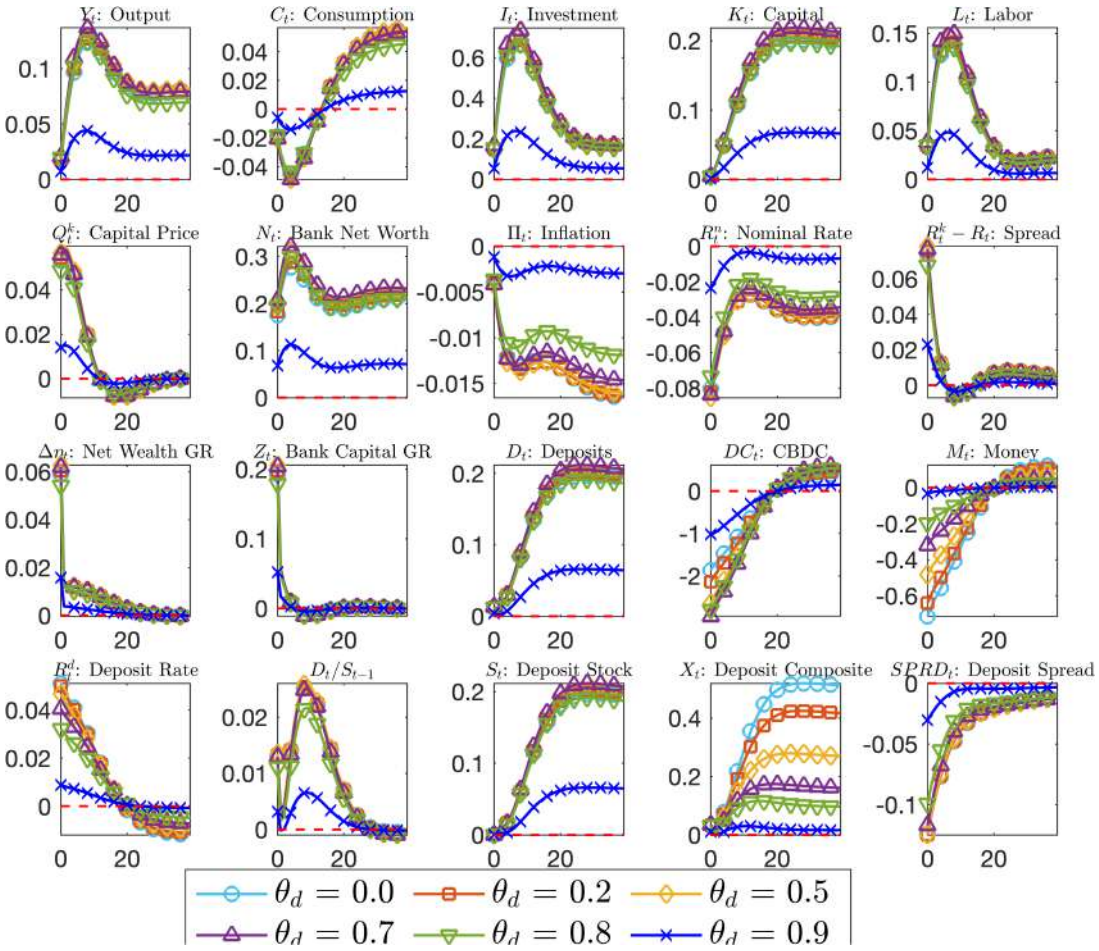

Figure 3.14: Impulse response function of some selected variables of the model to 1 s.d. positive shock to deposit elasticity for different values of θ^d. Deviations are measured in percentage

the baseline model is the economy without any CBDC [6]. Let us consider the case when $\rho_s = 0$. In this case, the deep habit that enters the deposit composite of the household is last period's aggregate deposit (see Eq (3.10)). For lower levels of depositor-banker relationship, the welfare gain remains constant but positive. For stronger depositor-banker relationships, the welfare effect increases significantly and reaches about 2%. Therefore, if the central bank introduces CBDC in an economy where depositors have a higher level of habits in deposit demand, it will significantly increase welfare. Alternatively, when the stock of habits depends more on last period's stock rather than last period's aggregate deposit, the welfare gains from introducing CBDC decrease (they significantly decrease when $\rho_s = 0.6$ and reach a low of about -5% for higher levels of deposit habits). Interestingly, the welfare gain starts to increase after a threshold habit intensity. The gain reaches up to 4%. The welfare effect of CBDC issuance becomes negative for larger val-

[6] The model in this exercise has been solved using second-order perturbation with pruning. See Kim et al. (2008) for more details.

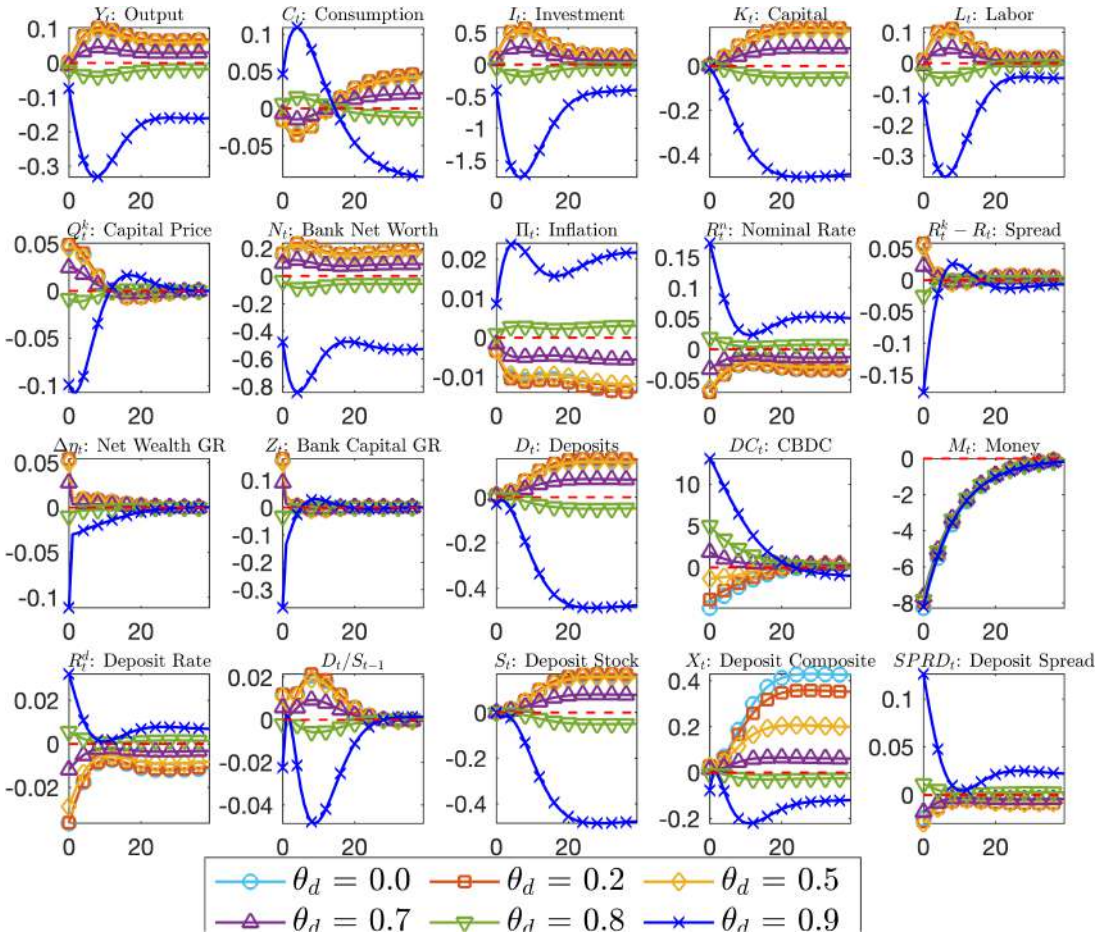

Figure 3.15: Impulse response function of some selected variables of the model to 1 s.d. positive shock to the elasticity of the liquidity bundle for different values of θ^d. Deviations are measured in percentage

ues of θ^d and ρ_s due to two effects, namely the indirect and direct crowding-out effect on bank deposits. A high value of ρ_s implies a higher dependence on past stocks of average deposits in the bank. To see this, realize that $S_{t-1} \simeq (1-\rho_s)\sum_{\tau=1}^{\infty}\rho_s^{\tau} D_{t-\tau}$. As the central bank introduces CBDC in an economy with a higher level of ρ_s, the persistence of the crowding-out effect, it dominates, and the welfare effect becomes negative. In my model, the direct effect of the deposit stock on the welfare seems to be negligible for lower values, ρ_s as the crowding-out effect is only restricted to last period's deposit stock. The welfare of introducing CBDC is primarily driven by the dynamics of the interest spread of CBDC and deposit. Notice that for lower values of ρ_s, the CBDC interest rate is decreasing in θ^d where as for higher values of ρ_s, it is first increasing and then decreasing θ^d (see figure (3.18)). Therefore, introducing CBDC when the spread is higher or increasing is welfare-reducing, as CBDC crowds out deposits without giving much benefit as a savings instrument. Whereas, a lower CBDC interest spread increases the welfare as CBDC provides a store of value despite crowding-out deposits. Therefore, if deposit habit levels in

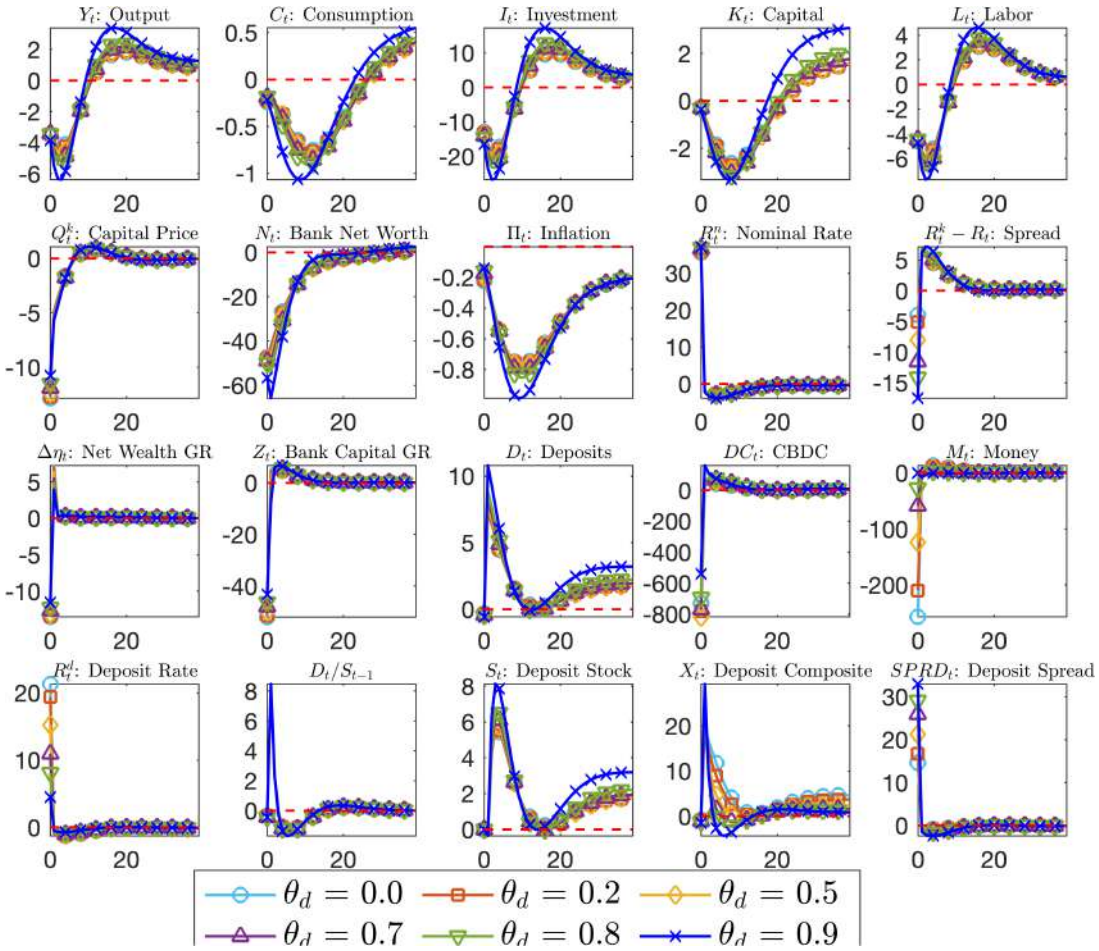

Figure 3.16: Impulse response function of some selected variables of the model to 1 s.d. temporary contractionary monetary policy shock for different values of θ^d. Deviations are measured in percentage

the economy are moderate, introducing CBDC becomes welfare-reducing when the habit is less driven by aggregate deposit. As the deposit stock becomes less and less dependent on aggregate deposit, retail bankers become less forward-looking and care less about future profits. Thus, having a strong deposit base allows banks to pass through the policy rate more, making it a welfare-increasing scenario for policymakers.

Figure 3.19 reports the consumption-equivalent welfare effects associated with varying the steady-state ratio of CBDC to output. The results indicate that the introduction of CBDC is unambiguously welfare-reducing for all admissible values of ϕ_{dc}. Moreover, the magnitude of the welfare loss is monotonically increasing in the size of CBDC issuance. This pattern reflects neither a negative output-gap coefficient in the monetary policy rule, recall that the Taylor rule is expressed in terms of markups, nor an artifact of the welfare metric itself. Instead, the welfare deterioration is a direct consequence of the interaction between CBDC issuance and the underlying depositor–banker relationship. As the stock of CBDC expands, deposits become increasingly crowded out, lowering the deposit base

that intermediaries rely on for funding and reducing the value households derive from the liquidity services embedded in bank deposits. Because the marginal liquidity benefit of CBDC does not offset the erosion of bank-provided liquidity services, higher levels of CBDC issuance translate into progressively larger welfare losses. Consequently, in this environment, any positive level of CBDC supply diminishes household welfare, and the adverse effect intensifies with the extent of CBDC adoption.

In the second experiment, I introduced a quadratic cost of CBDC for the government in the form of $\frac{\psi_{dc}}{2} DC_t^2$. Retail payments are often associated with social costs, and their presence can determine the implications of introducing CBDC[7]. Schmiedel et al. (2012) documents that the social cost associated with cash payments is about 1% of GDP in European countries. Moreover, banks partner with payment intermediaries to access their network of payments. This may allow them to be in an advantageous position, as they may have more data on consumer behavior related to payments. A central bank moving into the payment market may face large costs due to lack of information.

The modified cash-flow equation for central bank becomes:

$$\Omega_t = M_t + DC_t - \chi_{dc}\frac{DC_t^2}{2} + \frac{R_{t-1}B_{t-1}^g}{\Pi_t} - \frac{R_{t-1}^{dc}DC_{t-1}}{\Pi_t} - \frac{M_{t-1}}{\Pi_t} - B_t^{CB} \tag{3.71}$$

and the total resource in the economy is given by

$$Y_t = C_t + G_t + I_t + \frac{\eta^i}{2}\left(\frac{I_t^n + I^n}{I_{t-1}^n + I^n} - 1\right)^2 (I_t^n + I^n) + \frac{\psi_{dc}}{2} DC_t^2 + f(M_t) \tag{3.72}$$

Introducing the maintenance cost of CBDC has implications for the steady state of the model. I have reported the steady-state values in Table 3.2. Most of the macroeconomic variables of concern, such as output, consumption, capital, etc., decrease in the steady state when there is a significant cost of introducing CBDC (the cost parameter considered in this exercise is $\psi_{DC} = 0.02$). In the banking sector, CBDC introduction cost has an opposite effect. The discounted marginal value of bank capital increases by about 0.62%, and the discounted marginal value of the bank's net worth increases by about 0.63%. The deposit spread increases by about 2.88 annualized basis points, but the aggregate level of deposits decreases by 0.57%. The reduced usage of deposits can be attributed to the reduction in the overall liquidity bundle consumption in the steady state. Although the banking sector loses its most stable and cheaper funding base, it can afford to pass through less of the policy rate to depositors due to a more robust banking sector when there is a significant cost to introducing CBDC.

[7] The ECB has estimated the rollout cost of the CBDC project to be about 432 million euros. See https://www.ecb.europa.eu/press/inter/date/2025/html/ecb.in250324~ff1c69da91.en.html

The baseline model in this experiment is the economy where introducing CBDC is cost-free and there is no depositor hold-up effect (i.e., $\theta_d = 0$ and $\psi_{dc} = 0$). In Figure 3.17b, I show the consumption-equivalent welfare heat map for different values of the CBDC introduction cost ψ_{dc} and the depositor hold-up effect θ_t^d. The welfare gains are positive when there is no cost for central banks to manage or maintain CBDC, and the gains increase with higher values of the deposit hold-up effect. Therefore, it is welfare-improving if the depositor-banker relationship is stronger, conditional on no cost of managing CBDC. From the heatmap, it is clear that for a given level of habits in the deposit market, the welfare loss in terms of consumption equivalence is increasing in the cost of CBDC management.

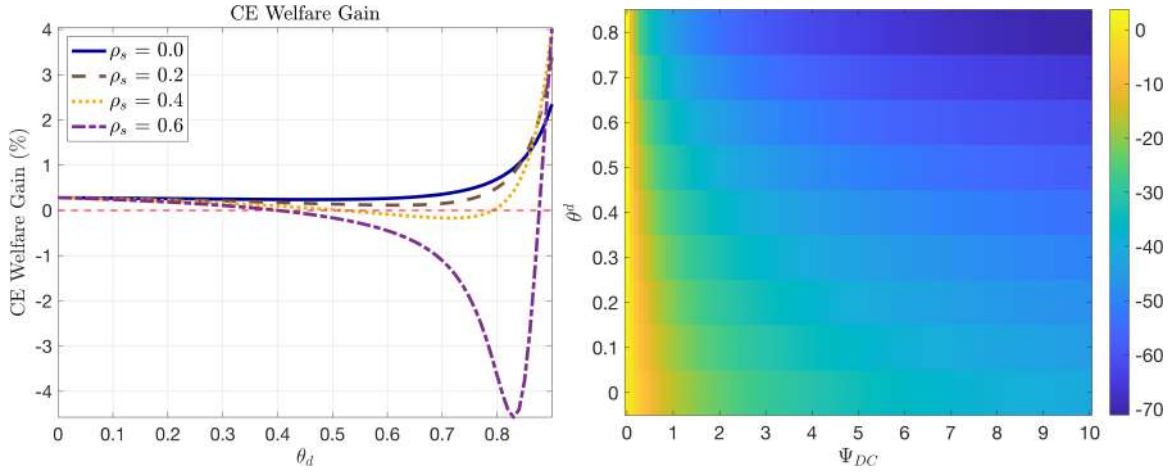

(a) Changes to welfare in comparison to the economy without CBDC and varying degree of hold-up effect and different values of deposit stock share. Welfare values are expressed as consumption equivalent values in percentage.

(b) Welfare differences in case in comparison to model with no hold-up effects and no cost of introducing CBDC. Welfare values are expressed as consumption equivalent values in percentage

3.6 Robustness: Fixed asset of Central Bank

In this exercise, I fix the asset side of the central bank's balance sheet. Therefore, B_t^{CB} is held constant at its steady-state value. Any change in the level of CBDC must therefore be offset by an opposite change in the level of cash in the economy. The purpose of this robustness check is to confirm the results in a setting where the central bank does not want to expand its balance sheet. In this case, central bank profits are driven by the interest rate paid on CBDC and the interest earned on government bond holdings.
Figure 3.21 shows the impulse responses to a contractionary monetary policy shock for two versions of the model. The red lines represent the model in which CBDC issuance is

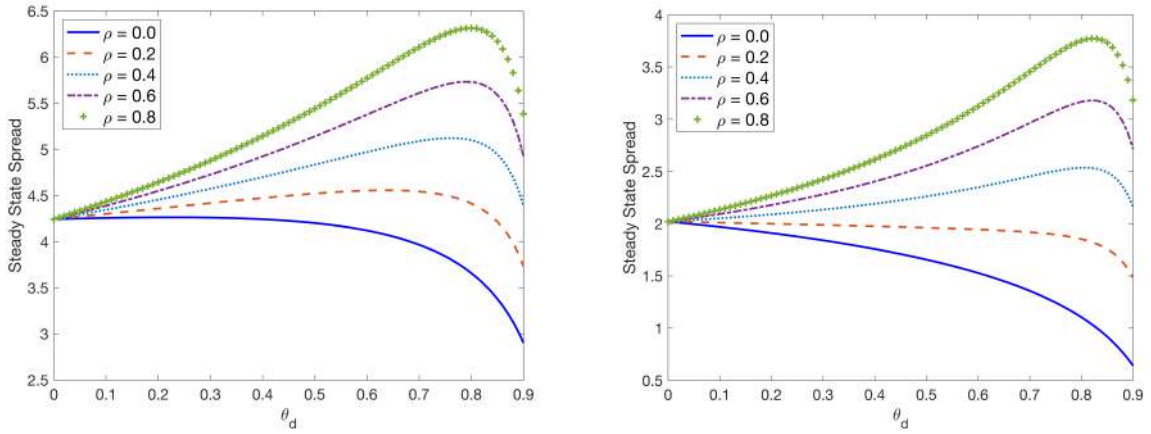

(a) Interest rate spread $R_t - R_t^{dc}$ for CBDC for different values of ρ_s and θ^d. The spread is expressed as an annualized percentage.

(b) Interest rate spread $R_t - R_t^d$ for deposit for different values of ρ_s and θ^d. The spread is expressed as an annualized percentage.

Figure 3.18: Stochastic steady-state for interest spreads for CBDC and deposit.

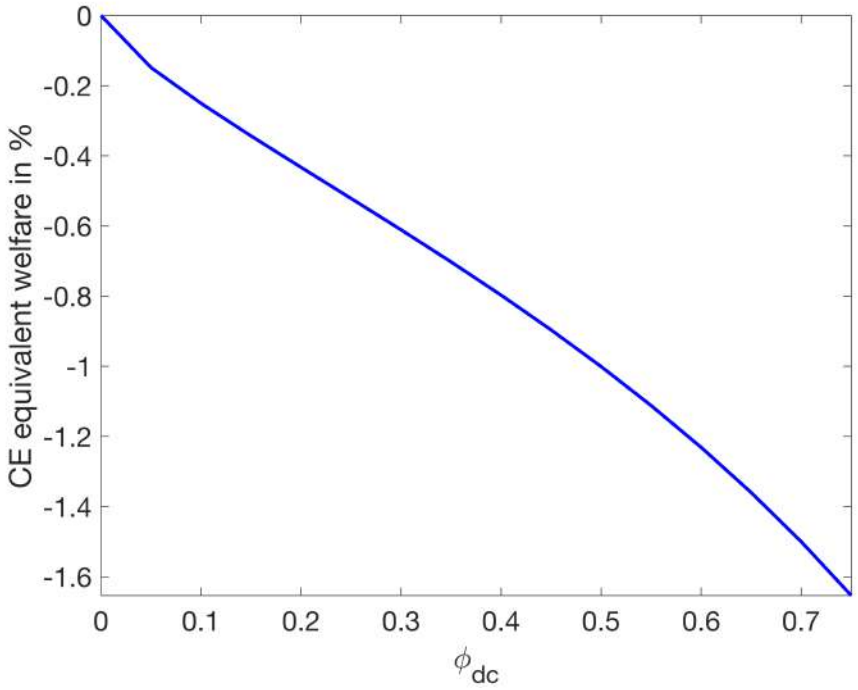

Figure 3.19: Consumption-equivalent welfare is plotted for varying degrees of CBDC issuance. The supply rule is $DC_t = \phi_{dc} Y_t$. The consumption equivalent welfare is reported in percentage.

neutral from the central bank's balance sheet perspective. The blue lines, on the other hand, correspond to non-neutral CBDC issuance. There are two fundamental differences between these models. When CBDC is non-neutral, the central bank's policy is essentially a quantity policy. In contrast, when the size of the central bank's balance sheet is fixed,

the level of CBDC is endogenously determined. To make the two models comparable, I fix the supply of CBDC in the non-neutral model at the same level as in the neutral model.

Under a monetary policy shock, the response of the real sector of the economy is similar in both models. The response of government bonds behaves as expected: in the neutral case, bond holdings remain constant, whereas in the non-neutral case, the decline in cash is reflected in a decline on the asset side of the central bank. From a policymaker's perspective, it is useful to check whether the impact of CBDC issuance is robust across different balance-sheet configurations of the central bank.

In Figure 3.20, I show the impulse responses to a CBDC supply shock for both models. Notice that the response of the real economy differs in this case. Let us first focus on liquid instruments. CBDC and cash become substitutes here, with small differences arising from the facts that cash has a storage cost and is unremunerated. Although they are not perfect substitutes, the fixed asset side of the central bank's balance sheet makes them closer substitutes.

Because the overall level of bonds in the economy differs between the two cases, declining by about 10% in the neutral case, the tax level declines. This leads to higher consumption in the neutral case, unlike in the non-neutral introduction of CBDC. Although the impact response of deposits is the same in both cases, they diverge after eight quarters: the non-neutral case appears more accommodating for deposits (reaching about -1.7%), whereas in the neutral case deposits fall to -2.7%. Banks therefore lose more funding in the neutral case, which leads to a relative contraction in capital and investment and thus to lower output.

Inflation rises to about 0.15% after 40 quarters in the neutral case, whereas under non-neutral CBDC introduction, inflation increases only to about 0.1% above the steady state. In summary, for a CBDC supply shock, keeping the central bank's balance sheet fixed is more costly for both the real economy and financial intermediaries compared with the case where the asset side of the central bank's balance sheet is flexible.

3.7 Conclusion

The comprehensive analysis presented in this paper demonstrates the intricate dynamics of the banking sector and the broader economy in response to various shocks and policy changes, with a particular focus on the implications of CBDC introduction in the banking economy with long-term depositor-banker relationships. Drawing on both theoretical modeling and empirical evidence, the study sheds light on the multifaceted considerations surrounding CBDC implementation and its potential ramifications for monetary policy

effectiveness, financial stability, and societal welfare. Notably, the response of the economy to monetary policy shocks, capital quality shocks, and shocks to the depositor-banker relationship each exhibited unique patterns, reflecting the underlying mechanisms at play within the banking sector and the broader economy.

The response to a contractionary monetary policy shock revealed significant adjustments in various financial variables. Banks faced increased funding costs, leading to a contraction in net worth and capital assets. However, the counter-cyclical nature of deposit and credit spreads underscored the market power of banks, allowing them to mitigate profit shrinkage through adjustments in asset returns and deposit rates. Additionally, the substitution of cash for CBDC highlighted potential implications for central bank balance sheets and monetary policy operations.

In contrast, a shock to capital quality resulted in a distinct response, with a decline in asset prices and capital triggering adjustments in bank behavior. The counter-cyclicality of credit spreads persisted, but the deposit spread exhibited pro-cyclical behavior, reflecting shifts in depositor behavior and bank strategies to maintain profitability. These findings emphasize the importance of capital quality in shaping financial stability and the transmission of shocks within the banking sector.

Furthermore, the analysis of shocks to the depositor-banker relationship elucidated the impact of changes in the effective monopoly power of banks. A reduction in the hold-up effect led to expansions in consumption and output, highlighting the role of depositor-banker dynamics in influencing economic activity. The subsequent adjustments in deposit levels, interest rates, and asset prices underscored the complex interplay between financial intermediaries and households in shaping macroeconomic outcomes.

The welfare implications derived from the model underscored the nuanced effects of introducing CBDC and associated costs on societal welfare. While CBDC adoption offered potential benefits, such as improved depositor-banker relationships and reduced transaction costs, the magnitude of these benefits varied depending on factors such as the strength of existing relationships and the cost of CBDC implementation. These findings provide valuable insights for policymakers grappling with decisions regarding the adoption and design of CBDC initiatives.

Overall, the findings contribute to our understanding of the transmission mechanisms of monetary policy and the dynamics of financial intermediation in the presence of shocks. By incorporating detailed modeling of banking sector behavior and depositor-banker relationships, the study offers important implications for monetary policy effectiveness, financial stability, and the design of digital currency frameworks.

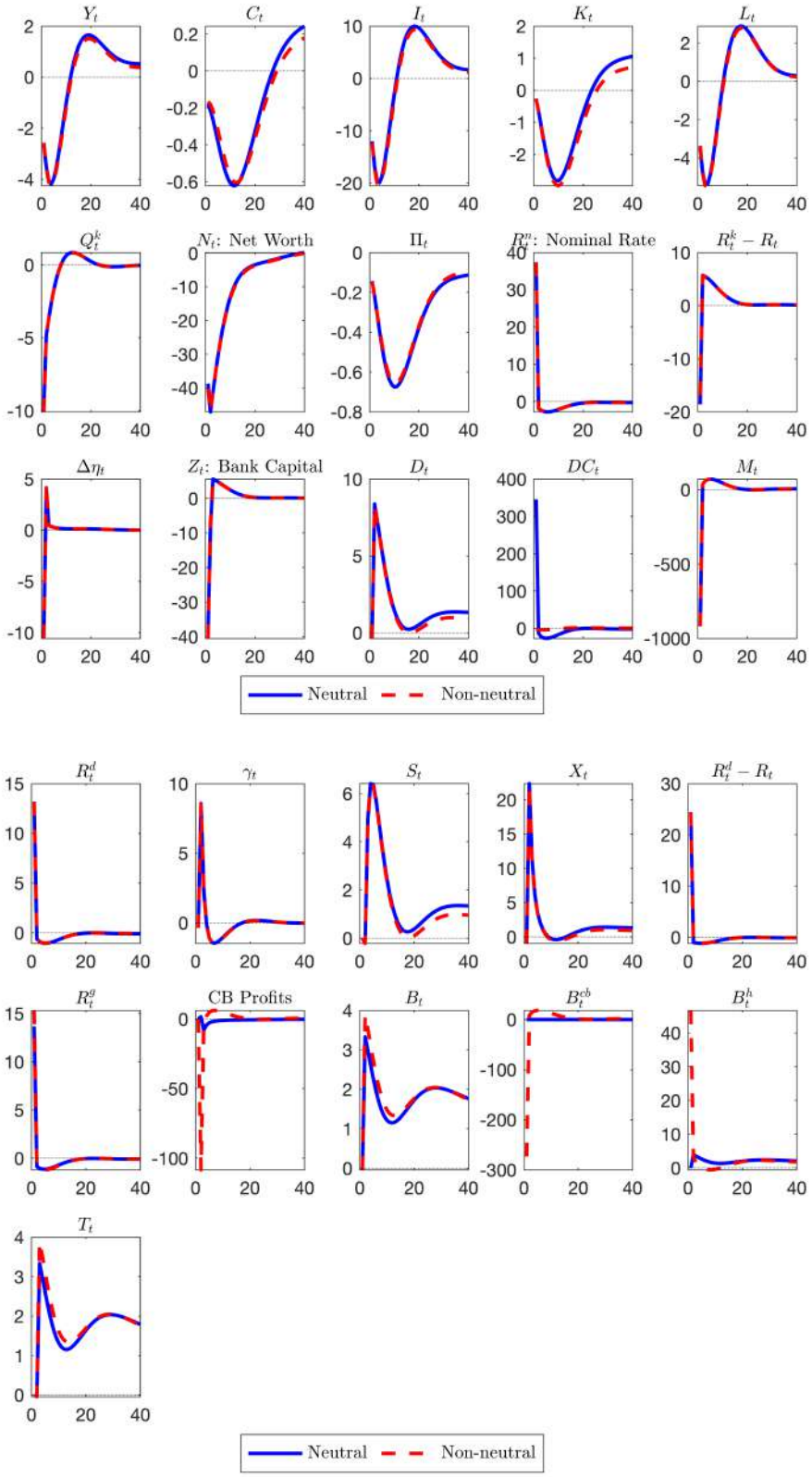

Figure 3.20: IRFs for contractionary monetary policy shock for (i) neutral CBDC policy where asset side of the central bank remains fixed (blue line) and (ii) non-neutral CBDC where asset side of the central bank is flexible (red line). Variables are percentage deviations from the respective steady-states

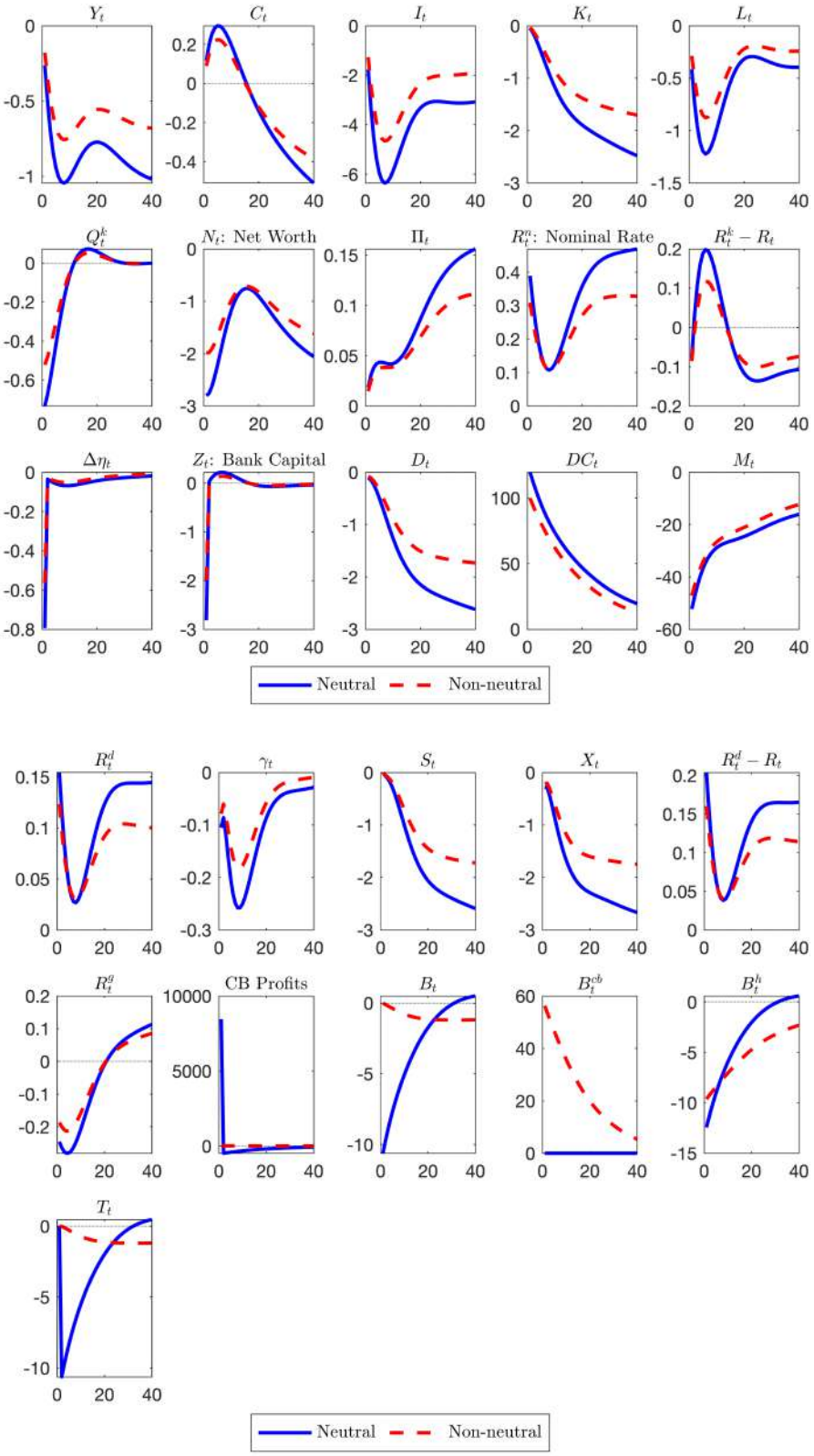

Figure 3.21: IRFs for CBDC supply shock for (i) neutral CBDC policy where the asset side of the central bank remains fixed (blue line) and (ii) non-neutral CBDC where the asset side of the central bank is flexible (red line). Variables are percentage deviations from the respective steady-states

Appendices

3.A Full model equations

Household:

$$\varrho_t = (C_t - hC_{t-1})^{-\sigma} - \beta h \mathbb{E}_t (C_{t+1} - hC_t)^{-\sigma} \tag{3.73}$$

$$\lambda_{t,t+1} = \frac{\mathbb{E}_t \varrho_{t+1}}{\varrho_t} \tag{3.74}$$

$$\chi L_t^{\varphi} = (1-\alpha)\varrho_t P_t^m \frac{Y_t}{L_t} \tag{3.75}$$

$$\varrho_t = \beta \mathbb{E}_t \frac{\varrho_{t+1} R_t^g}{\pi_{t+1}} \tag{3.76}$$

$$\varrho_t = \omega_d \frac{\chi_{z,t}}{LB_t} \left(\frac{LB_t}{D_t} \right)^{\frac{1}{\eta_{z,t}}} + \beta \mathbb{E}_t \frac{\varrho_{t+1} R_t^d}{\pi_{t+1}} \tag{3.77}$$

$$\varrho_t = \vartheta_t \frac{\chi_{z,t}}{LB_t} \left(\frac{LB_t}{X_t^d} \right)^{\frac{1}{\eta_{z,t}}} + \beta \mathbb{E}_t \frac{\varrho_{t+1} R_t^{dc}}{\pi_{t+1}} \tag{3.78}$$

$$\varrho_t (1 + f'(M_t)) = \frac{\chi_{z,t}}{LB_t} \left(\frac{LB_t}{M_t} \right)^{\frac{1}{\eta_{z,t}}} + \beta \mathbb{E}_t \frac{\varrho_{t+1}}{\pi_{t+1}} \tag{3.79}$$

$$LB_t = \left[M_t^{\frac{\eta_{z,t}-1}{\eta_{z,t}}} + \vartheta_t DC_t^{\frac{\eta_{z,t}-1}{\eta_{z,t}}} + \omega_d X_t^{d\,\frac{\eta_{z,t}-1}{\eta_{z,t}}} \right]^{\frac{\eta_{z,t}}{\eta_{z,t}-1}} \tag{3.80}$$

Retail bank:

$$R_t - R_t^d = \frac{R_t^d}{\epsilon_t^d}\left(\frac{\gamma_t}{\theta^d - \gamma_t}\right) - \theta^d(1-\rho_s)\beta\mathbb{E}_t\lambda_{t,t+1}\frac{R_{t+1}^d}{\epsilon_t^d}\left(\frac{\gamma_{t+1}}{\theta^d - \gamma_{t+1}}\right) \tag{3.81}$$

$$\gamma_t = \frac{D_t}{S_{t-1}} \tag{3.82}$$

$$S_{t-1} = \rho_s S_{t-2} + (1-\rho_s)D_{t-1} \tag{3.83}$$

$$D_t = X_t^d + \theta^d S_{t-1} \tag{3.84}$$

Wholesale bank:

$$\eta_t = \beta\mathbb{E}_t\lambda_{t,t+1}[(1-\theta)R_t + \theta Z_{t+1}\eta_{t+1}] \tag{3.85}$$

$$\nu_t = (1-\theta)\beta\mathbb{E}_t\lambda_{t,t+1}(R_{t+1}^k - R_t) + \theta\beta\mathbb{E}_t\lambda_{t,t+1}X_{t+1}\nu_{t+1} \tag{3.86}$$

$$\phi_t = \frac{\eta_t}{\lambda - \nu_t} \tag{3.87}$$

$$Z_t = (R_t^k - R_{t-1})\phi_{t-1} + R_{t-1} \tag{3.88}$$

$$X_t = \frac{\phi_t}{\phi_{t-1}}Z_t \tag{3.89}$$

$$Q_t^k K_t = \phi_t N_t \tag{3.90}$$

$$D_t = (\phi_t - 1)N_t \tag{3.91}$$

$$N_t = N_t^e + N_t^n \tag{3.92}$$

$$N_t^e = \theta Z_t N_{t-1}\epsilon_t^n \quad \text{where } \epsilon_t^n \text{ is exogenous shock to net worth} \tag{3.93}$$

$$N_t^n = \omega Q_t^k \xi_t K_{t-1} \quad \text{where } \xi_t \text{ is exogenous shock to capital quality} \tag{3.94}$$

Capital producer:

$$R_t^k = \frac{\left[\alpha P_t^m \frac{Y_t^m}{\xi_t K_{t-1}} + (Q_t^k - \delta_t)\right]\xi_t}{Q_{t-1}^k} \tag{3.95}$$

$$\begin{aligned} Q_t^k = 1 &+ \frac{\eta^i}{2}\left(\frac{I_t^n + I^n}{I_{t-1}^n + I^n} - 1\right)^2 + \eta^i\left(\frac{I_t^n + I^n}{I_{t-1}^n + I^n} - 1\right)\left(\frac{I_t^n + I^n}{I_{t-1}^n + I^n}\right) \\ &- \beta\mathbb{E}_t\lambda_{t,t+1}\eta^i\left(\frac{I_{t+1}^n + I^n}{I_t^n + I^n} - 1\right)\left(\frac{I_{t+1}^n + I^n}{I_t^n + I^n}\right)^2 \end{aligned} \tag{3.96}$$

$$\delta_t = \bar{\delta} - \frac{\tilde{\delta}}{1+\zeta} + \frac{\tilde{\delta}}{1+\zeta}U_t^{1+\zeta} \tag{3.97}$$

$$I_t^n = I_t - \delta_t \xi_t K_{t-1} \tag{3.98}$$

$$K_t = \xi_t K_{t-1} + I_t^n \tag{3.99}$$

$$\tag{3.100}$$

Production:

$$Y_t^m = A_t \Big(\xi_t U_t K_{t-1} \Big)^{\alpha} L_t^{1-\alpha} \tag{3.101}$$

$$\alpha P_t^m \frac{Y_t^m}{U_t} = \delta'(U_t) \xi_t K_{t-1} \tag{3.102}$$

$$\tag{3.103}$$

Pricing:

$$\varsigma_t = \gamma \varsigma_{t-1} P_{t-1}^{-\kappa\epsilon} P_t^{\epsilon} + (1-\gamma) \left[\frac{1}{1-\gamma} \left\{ 1 - \gamma P_{t-1}^{\kappa(1-\gamma)} P_t^{\gamma-1} \right\} \right]^{-\frac{\epsilon}{1-\gamma}} \tag{3.104}$$

$$\mu_t = \frac{1}{P_t^m} \tag{3.105}$$

$$F_t = Y_t P_t^m + \beta\gamma \mathbb{E}_t \lambda_{t,t+1} P_{t+1}^{\epsilon} P_t^{-\epsilon\kappa} F_{t+1} \tag{3.106}$$

$$H_t = Y_t + \beta\gamma \mathbb{E}_t \lambda_{t,t+1} P_{t+1}^{\epsilon-1} P_t^{(1-\epsilon)\kappa} H_{t+1} \tag{3.107}$$

$$P_t^* = \frac{\epsilon}{\epsilon - 1} \frac{F_t}{H_t} P_t \tag{3.108}$$

$$P_t^{1-\epsilon} = \gamma P_{t-1}^{(1-\epsilon)\kappa} + (1-\gamma)(P_t^*)^{(1-\epsilon)} \tag{3.109}$$

Government:

$$G_t = G\mu_t^g \quad \text{where } \mu_t^g \text{ is exogenous shock to government spending} \tag{3.110}$$

Aggregate resource:

$$Y_t = C_t + G_t + I_t + \frac{\eta^i}{2} \left(\frac{I_t^n + I^n}{I_{t-1}^n + I^n} - 1 \right)^2 (I_t^n + I^n) + f(M_t) \tag{3.111}$$

$$Y_t^m = \varsigma_t Y_t \tag{3.112}$$

$$\tag{3.113}$$

Central Bank:

$$\frac{R_t^n}{R} = \left(\frac{R_{t-1}^n}{R}\right)^{\rho_R} \left[\Pi_t^{\phi_\pi} \left(\frac{Y_t}{Y_t^f}\right)^{\phi_Y}\right]^{1-\rho_R} \exp(\varepsilon_t^R) \tag{3.114}$$

$$\frac{R_t^n}{\mathbb{E}_t \Pi_{t+1}} = R_{t+1} \tag{3.115}$$

$$DC_t = \phi_{DC} Y_t \tag{3.116}$$

3.B Derivation of total earning from deposit holding

$$\begin{aligned}
\int_0^1 R_{j,t-1}^d D_{ij,t-1} dj &= \int_0^1 R_{j,t-1}^d \left[\left(\frac{R_{j,t-1}^d}{R_{t-1}^d}\right)^{-\epsilon_t^d} X_{t-1}^d + \theta^d S_{j,t-2}\right] dj \\
&= \int_0^1 R_{j,t-1}^d \left(\frac{R_{j,t-1}^d}{R_{t-1}^d}\right)^{-\epsilon_t^d} X_{t-1}^d dj + \theta^d \int_0^1 R_{j,t-1}^d S_{j,t-2} dj \\
&= \int_0^1 (R_{j,t-1}^d)^{1-\epsilon_t^d} (R_{t-1}^d)^{\epsilon_t^d} X_{t-1}^d dj + \Delta_{t-1}^d \\
&= (R_{t-1}^d)^{\epsilon_t^d} X_{t-1}^d \int_0^1 (R_{j,t-1}^d)^{1-\epsilon_t^d} dj + \Delta_{t-1}^d \\
&= (R_{t-1}^d)^{\epsilon_t^d} X_{t-1}^d (R_{t-1}^d)^{1-\epsilon_t^d} + \Delta_{t-1}^d \\
&= R_{t-1}^d X_{t-1}^d + \Delta_{t-1}^d
\end{aligned}$$

3.C Log-linearized version of the non-linear model

Household:

$$\hat{\varrho}_t = \frac{\beta h \sigma \mathbb{E}_t(\hat{C}_{t+1} - h\hat{C}_t)}{(1-\beta h)(1-h)} - \frac{\sigma \mathbb{E}_t(\hat{C}_t - h\hat{C}_{t-1})}{(1-\beta h)(1-h)} \tag{3.117}$$

$$\hat{\lambda}_{t,t+1} = \hat{\varrho}_{t+1} - \hat{\varrho}_t \tag{3.118}$$

$$-\iota(1-\beta R^d)\hat{X^d}_t = \hat{\varrho}_t - \beta R^d(\mathbb{E}_t \hat{\varrho}_{t+1} + \hat{R}_t^d - \hat{\pi}_{t+1}) \tag{3.119}$$

$$-\iota(1-\beta R^{dc})\hat{DC}_t = \hat{\varrho}_t - \beta R^{dc}(\mathbb{E}_t \hat{\varrho}_{t+1} + \hat{R}_t^{dc} - \hat{\pi}_{t+1}) \tag{3.120}$$

$$\begin{aligned}
\iota(1-\beta)\hat{m}_t = {} & \hat{\varrho}_t + \psi_m(\hat{m}_t + \hat{\pi}_t - \hat{m}_{t-1}) \\
& - \beta \mathbb{E}_t\{\hat{\varrho}_{t+1} - \hat{\pi}_{t+1} + \psi_m(\hat{m}_{t+1} + \hat{\pi}_{t+1} - \hat{m}_t)\}
\end{aligned} \tag{3.121}$$

$$(1+\varphi)\hat{L}_t = \hat{\varrho}_t + \hat{P}_t^m + \hat{Y}_t \tag{3.122}$$

Retail bank:

$$\left(\frac{1-(1-\rho_s)\beta\theta^d}{R-R^d}\right)(R\hat{R}_t - R^d\hat{R}_t^d) = \hat{R}_t^d - \hat{\epsilon}_t^d + \left(\frac{\theta^d}{\theta^d-\gamma^d}\right)(\hat{\gamma}_t^d - \hat{\theta}_t^d) - (1-\rho_s)\beta\theta^d\left[\hat{R}_{t+1}^d + \hat{\theta}_{t+1}^d + \hat{\lambda}_{t,t+1} - \hat{\epsilon}_{t+1}^d + \left(\frac{\theta^d}{\theta^d-\gamma^d}\right)(\hat{\gamma}_{t+1}^d - \hat{\theta}_{t+1}^d)\right] \tag{3.123}$$

$$\hat{\gamma}_t^d = \hat{D}_t - \hat{S}_{t-1}^d \tag{3.124}$$

$$\hat{S}_{t-1} = \rho_s\hat{S}_{t-2} + (1-\rho_s)\hat{D}_{t-1} \tag{3.125}$$

Wholesale bank:

$$\hat{\eta}_t = \hat{\lambda}_{t,t+1} + (1-\theta\beta Z)\hat{R}_t + \theta Z\beta(\hat{Z}_{t+1} + \hat{\eta}_{t+1}) \tag{3.126}$$

$$\hat{\nu}_t = \hat{\lambda}_{t,t+1} + \frac{(1-\theta\beta X)}{R^k-R}[R^k\hat{R}_{t+1}^k - R\hat{R}_t] + \theta\beta X[\hat{X}_{t+1} + \hat{\nu}_{t+1}] \tag{3.127}$$

$$\hat{\phi}_t = \hat{\eta}_t + \left(\frac{\nu}{\lambda-\nu}\right)\hat{\nu}_t \tag{3.128}$$

$$\hat{Z}_t = \left[\frac{\phi(R^k-R)}{Z}\right]\hat{\phi}_{t-1} + \left[\frac{\phi R^k}{Z}\right]\hat{R}_t^k + \left[\frac{(1-\phi)R}{Z}\right]\hat{R}_{t-1} \tag{3.129}$$

$$\hat{X}_t = \hat{\phi}_t - \hat{\phi}_{t-1} + \hat{Z}_{t-1} \tag{3.130}$$

$$\hat{Q}_t^k + \hat{K}_t = \hat{\phi}_t + \hat{N}_t \tag{3.131}$$

$$\hat{N}_t = \frac{N^e}{N}\hat{N}_t^e + \frac{N^n}{N}\hat{N}_t^n \tag{3.132}$$

$$\hat{N}_t^e = \hat{Z}_t + \hat{N}_{t-1} + \hat{\epsilon}_t^n \tag{3.133}$$

$$\hat{N}_t^n = \hat{Q}_t^k + \hat{K}_{t-1} + \hat{\xi}_t \tag{3.134}$$

$$\tag{3.135}$$

Capital producer:

$$\hat{R}_t^k = \left(\frac{\alpha P^m Y^m}{R^k K}\right)(\hat{P}_t^m + \hat{Y}_t^m - \hat{K}_{t-1}) + \frac{\hat{Q}_t^k}{R^k} - \hat{Q}_{t-1}^k - \left(\frac{\delta}{R^k}\right)\hat{\delta}_t + \frac{(1-\delta)}{R^k}\hat{\xi}_t \tag{3.136}$$

$$\tag{3.137}$$

Production:

$$\hat{Y}_t^m = \hat{A}_t + \alpha(\hat{U}_t + \hat{K}_{t-1} + \hat{\xi}_t) + (1-\alpha)\hat{L}_t \tag{3.138}$$

$$\hat{Y}_t^m + \hat{P}_t^m = (1+\zeta)\hat{U}_t + \hat{K}_{t-1} + \hat{\xi}_t \tag{3.139}$$

Expressing the deposit spread: Define $\mu_t^d = \frac{r_t^d}{r_t}$ as the deposit markdown on the risk-free

interest rate. Then the deposit spread equation becomes

$$1-\mu_t^d=\left(\frac{\mu_t^d}{\epsilon_t^d}\right)\left(\frac{\gamma_t}{\theta_t^d-\gamma_t}\right)-\theta_{t+1}^d(1-\rho_s)\beta\mathbb{E}_t\lambda_{t,t+1}\left(\frac{r_{t+1}}{r_t}\right)\left(\frac{\mu_{t+1}^d}{\epsilon_{t+1}^d}\right)\left(\frac{\gamma_{t+1}}{\theta_{t+1}^d-\gamma_{t+1}}\right)$$

Log-linearization around the deterministic steady state obtains

$$\begin{aligned}[1-\beta\theta^d(1-\rho_s)]\left(\frac{\mu_d}{\mu_d-1}\right)\hat{\mu}_t^d=(\hat{\mu}_t^d-\hat{\epsilon}_t^d)+\frac{1}{\theta^d-\gamma}(\hat{\gamma}_t-\hat{\theta}_t^d)\\-\beta(1-\rho_s)\left(\frac{\theta^d}{\theta^d-1}\right)\Big\{\hat{\theta}_{t+1}^d+\hat{\lambda}_{t,t+1}+\hat{\mu}_{t+1}^d-\hat{\epsilon}_{t+1}^d\\+\hat{r}_{t+1}-\hat{r}_t+\theta^d(\hat{\gamma}_{t+1}-\hat{\theta}_{t+1}^d)\Big\}\end{aligned}$$

$$\begin{aligned}&[1-\beta\theta^d(1-\rho_s)]\left(\frac{\mu_d}{\mu_d-1}\right)\hat{\mu}_t^d-\hat{\mu}_t^d=(-\hat{\epsilon}_t^d)+\frac{1}{\theta^d-1}(\hat{\gamma}_t-\hat{\theta}_t^d)\\&-\beta(1-\rho_s)\left(\frac{\theta^d}{\theta^d-1}\right)\Big\{(1-\theta^d)\hat{\theta}_{t+1}^d+\hat{\lambda}_{t,t+1}+\hat{\mu}_{t+1}^d-\hat{\epsilon}_{t+1}^d+\hat{r}_{t+1}-\hat{r}_t+\theta^d(\hat{\gamma}_{t+1})\Big\}\end{aligned}$$

$$\begin{aligned}\mu^d\left[\frac{1}{(1-\theta^d)\epsilon_t^d}-1\right]\hat{\mu}_t^d=\\+\frac{\mu^d\theta^d}{\epsilon_t^d(\theta^d-1)^2}\{\hat{\gamma}_t-\beta(1-\rho_s)\theta^d\hat{\gamma}_{t+1}\}\\+\frac{\mu^d\theta^d}{\epsilon_t^d(\theta^d-1)^2}\left[(1-\rho_s)\beta\hat{\theta}_{t+1}^d-\hat{\theta}_t^d\right]\\-\beta(1-\rho_s)\left(\frac{\mu^d}{\epsilon_t^d}\right)\left(\frac{\theta^d}{\theta^d-1}\right)\hat{\lambda}_{t,t+1}\\-\beta(1-\rho_s)\left(\frac{\mu^d}{\epsilon_t^d}\right)\left(\frac{\theta^d}{\theta^d-1}\right)(\hat{r}_{t+1}-\hat{r}_t)\\-\beta(1-\rho_s)\left(\frac{\mu^d}{\epsilon_t^d}\right)\left(\frac{\theta^d}{\theta^d-1}\right)\hat{\mu}_{t+1}^d\\+\left(\frac{\mu^d}{\epsilon_t^d(\theta^d-1)}\right)\left[(1-\rho_s)\beta\hat{\theta}^d\hat{\epsilon}_{t+1}^d-\hat{\epsilon}_t^d\right]\end{aligned}$$

or,

$$
\begin{aligned}
[1-(1-\theta^d)\epsilon_t^d]\ \hat{\mu}_t^d = & \\
& + \frac{\theta^d}{1-\theta^d}\{\hat{\gamma}_t - \beta(1-\rho_s)\theta^d\ \hat{\gamma}_{t+1}\} \\
& + \frac{\theta^d}{1-\theta^d}\left[(1-\rho_s)\beta\ \hat{\theta}_{t+1}^d - \hat{\theta}_t^d\right] \\
& + \beta(1-\rho_s)\theta^d\ \hat{\lambda}_{t,t+1} \\
& + \beta(1-\rho_s)\theta^d\ (\hat{r}_{t+1} - \hat{r}_t) \\
& + \beta(1-\rho_s)\theta^d\ \hat{\mu}_{t+1}^d \\
& + \left[\hat{\epsilon}_t^d - (1-\rho_s)\beta\theta^d\ \hat{\epsilon}_{t+1}^d\right]
\end{aligned}
\tag{3.140}
$$

3.D Additional tables

Variable	ψ_{DC}**=0.02** (1)	ψ_{DC}**=0** (2)	**Difference (1)-(2)**
Y_t	0.875397	0.877053	-0.001656
Y_t^m	0.875397	0.877053	-0.001656
K_t	6.21677	6.25248	-0.03571
I_t	0.155419	0.156312	-0.000893
C_t	0.529578	0.544605	-0.015027
G_t	0.175079	0.175411	-0.000332
R_t^k	1.01032	1.01018	0.00014
R_t	1.00782	1.00768	0.00014
N_t	1.55419	1.56312	-0.00893
N_t^e	1.53689	1.54552	-0.00863
N_t^n	0.0172991	0.0176039	-0.0003048
ν_t	0.00334883	0.00332823	0.0000206
η_t	1.35	1.34152	0.00848
$\Delta\nu_t$	1.01782	1.01768	0.00014
$\Delta\eta_t$	1.01782	1.01768	0.00014
Z_t	3.77016	3.85808	-0.08792
D_t	4.66258	4.68936	-0.02678
DC_t	1.20915	1.25936	-0.05021
M_t	0.264466	0.269301	-0.004835
r_t	0.00781657	0.0076813	0.00013527
r_t^d	0.00365525	0.00359199	0.00006326
S_t	4.66258	4.68936	-0.02678
X_t	1.77178	1.78196	-0.01018
SPRD_t	0.00416132	0.0040893	0.00007202

Table 3.2: Comparison of steady-state values for $\psi_{DC} = 0.02$ and $\psi_{DC} = 0$. Highlighted rows indicate an increase in values due to the introduction cost of CBDC.

Table 3.3: Steady-state ratios and levels across CBDC policy regimes

Ratio / Variable	**Interest rate rule:** $r_{dc} = 0$	**Interest rate rule:** $r_{dc} = 0.01r$	**Interest rate rule:** $r_{dc} = 0.1r$	**No CBDC:** $\phi_{dc} = 0$	**Quantity rule:** $\phi_{dc} = 0.3443$	**Quantity rule:** $\phi_{dc} = 2 \times 0.3443$
C/Y	0.6389	0.6390	0.6404	0.6319	0.6381	0.6414
I/Y	0.1610	0.1609	0.1595	0.1679	0.1618	0.1585
G/Y	0.2000	0.2000	0.2000	0.2000	0.2000	0.2000
$Q^k K/N$	4.0000	4.0000	4.0000	4.0000	4.0000	4.0000
D/N	3.0000	3.0000	3.0000	3.0000	3.0000	3.0000
Credit spread (%)	1.0000	1.0000	1.0000	1.0000	1.0000	1.0000
Policy–deposit spread (%)	2.4371	2.4437	2.5137	2.0984	2.3947	2.5682
Policy–CBDC spread (%)	4.5778	4.5444	4.2495	334.5930	4.8178	4.0744
Cash/Y	0.3437	0.3404	0.3060	0.5381	0.3656	0.2807
CBDC/Y	0.4197	0.4321	0.5703	0.0000	0.3443	0.6886
Deposits/Y	4.8301	4.8262	4.7859	5.0357	4.8549	4.7549
Z/Y	2.7958	2.8095	2.9594	2.2140	2.7112	3.0848
Bond interest rate	1.0101	1.0101	1.0101	1.0101	1.0101	1.0101
Central bank profit	0.0064	0.0065	0.0068	0.0046	0.0062	0.0070
Total govt. bonds	4.3622	4.4118	4.9844	3.1387	4.0668	5.4960
CB bond holding	0.6369	0.6441	0.7277	0.4582	0.5937	0.8024
HH bond holding	3.7253	3.7677	4.2566	2.6804	3.4730	4.6936
Tax	0.2045	0.2049	0.2096	0.1974	0.2021	0.2140
Tax parameter	0.0469	0.0464	0.0421	0.0629	0.0497	0.0389
CB bond share	0.1460	0.1460	0.1460	0.1460	0.1460	0.1460

Notes: All spreads are annualized percentage points. All ratios are relative to steady-state output Y. Values rounded to four decimals from the model's numerical steady state.

3.E Additional figures

3.E.1 IRFs for 4 different models

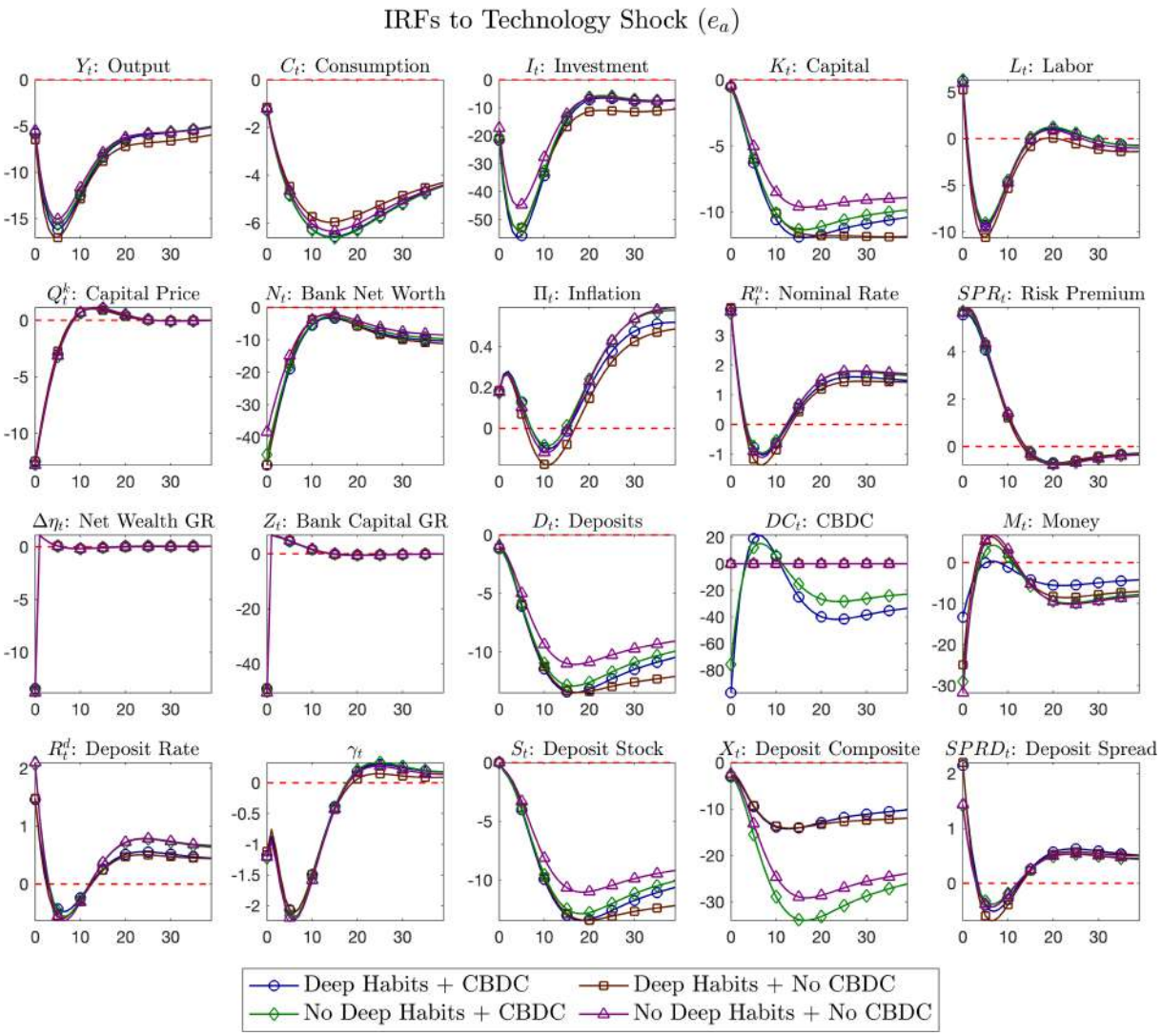

Figure 3.22: Impulse response function of some selected variables of the model to 1 s.d. negative TFP shock. Deviations are measured in percentage

3.E.2 IRFs for different values of θ^d

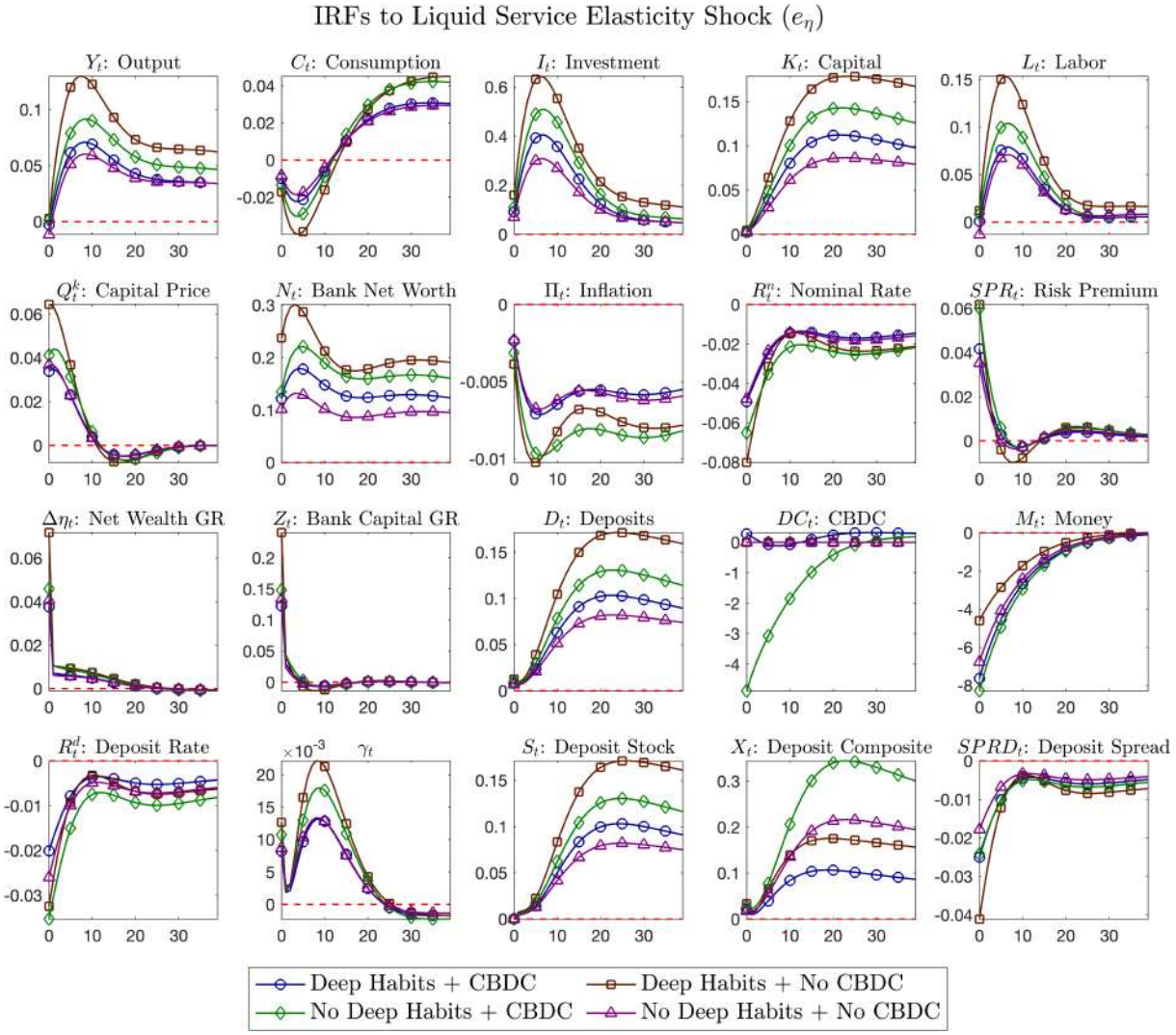

Figure 3.23: Impulse response function of some selected variables of the model to 1 s.d. positive shock to elasticity of substitution of liquidity instruments in the CES bundle. Deviations are measured in percentage

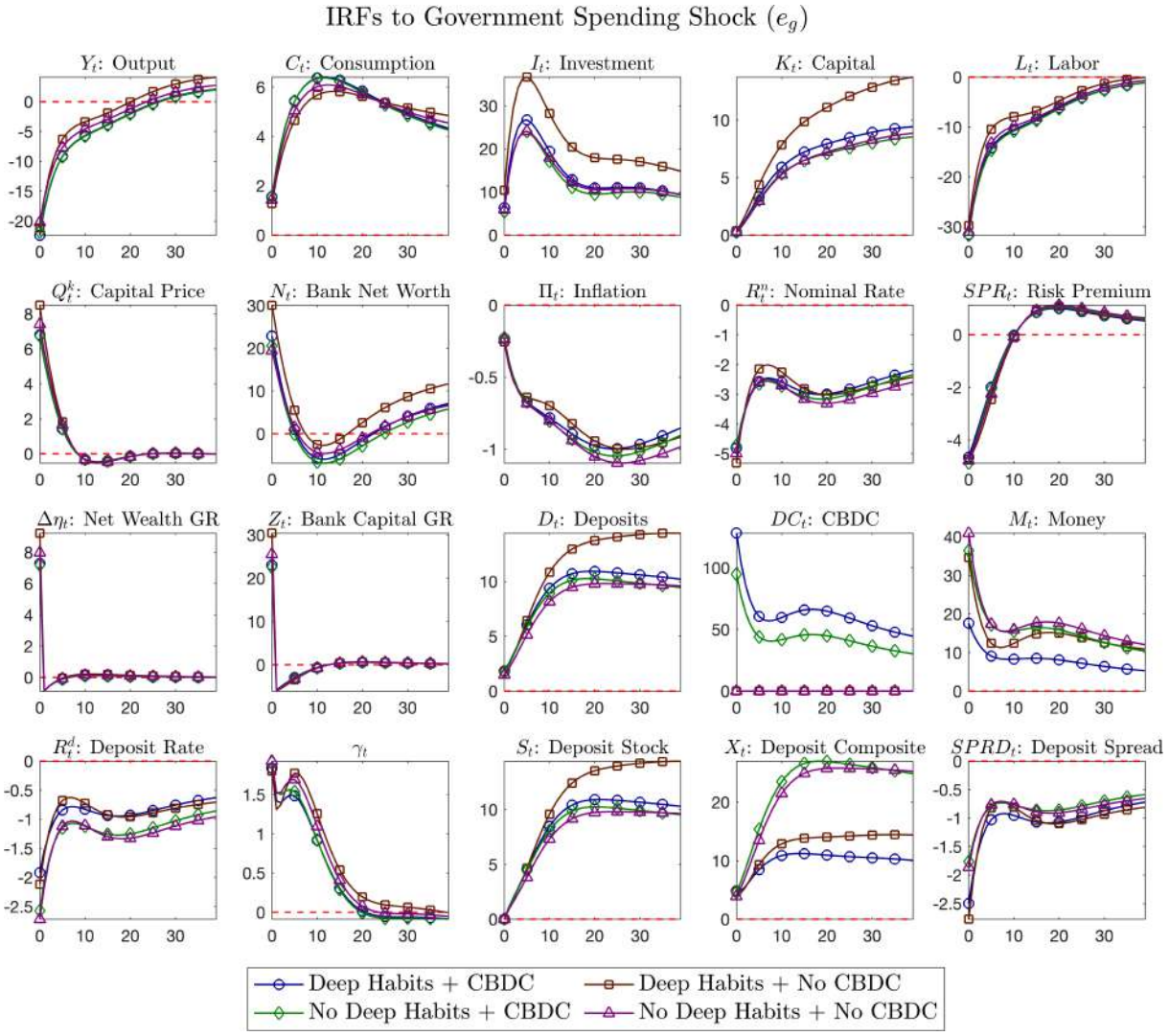

Figure 3.24: Impulse response function of some selected variables of the model to 1 s.d. negative government spending shock. Deviations are measured in percentage

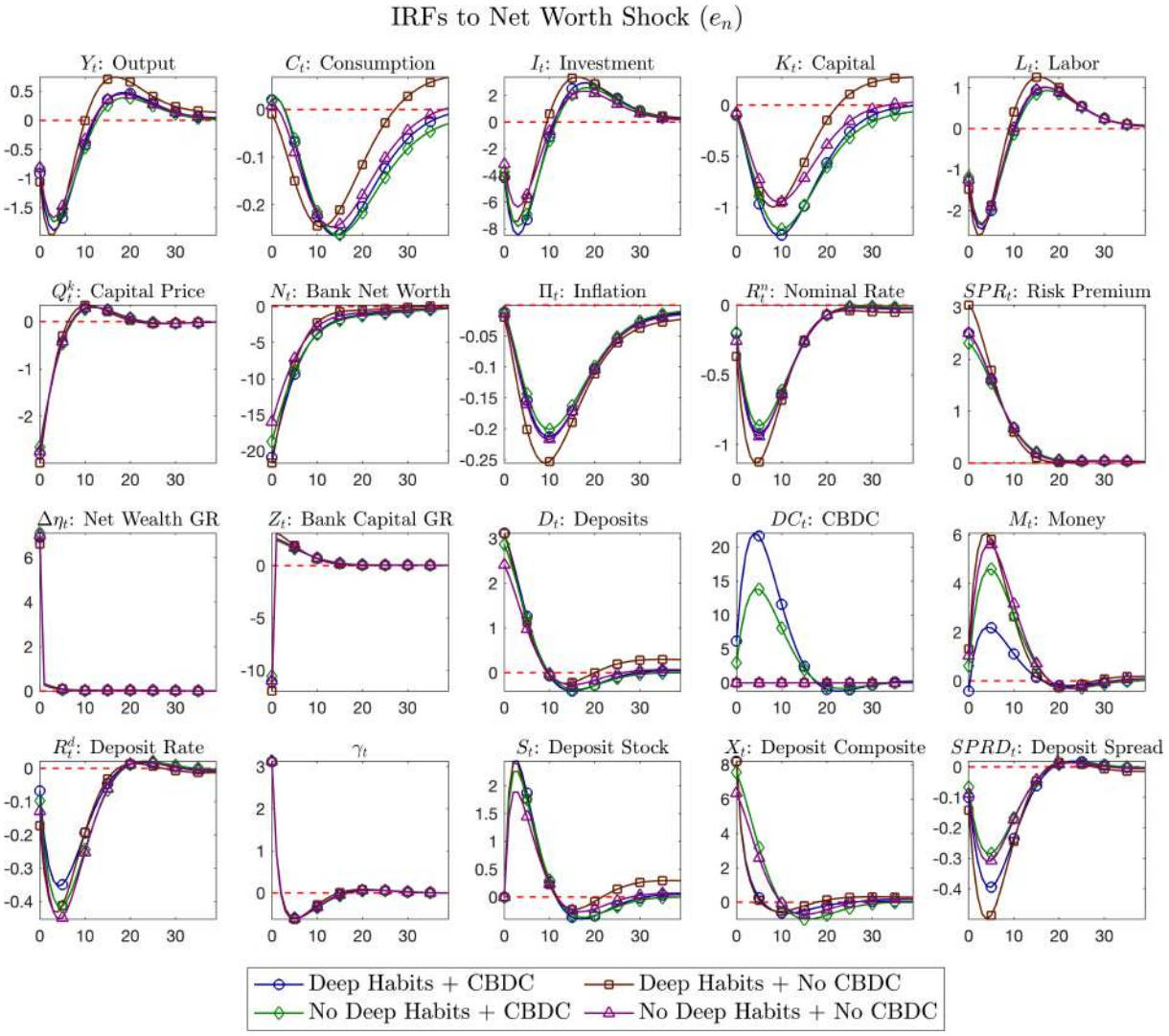

Figure 3.25: Impulse response function of some selected variables of the model to 1 s.d. negative shock to bank's net worth. Deviations are measured in percentage

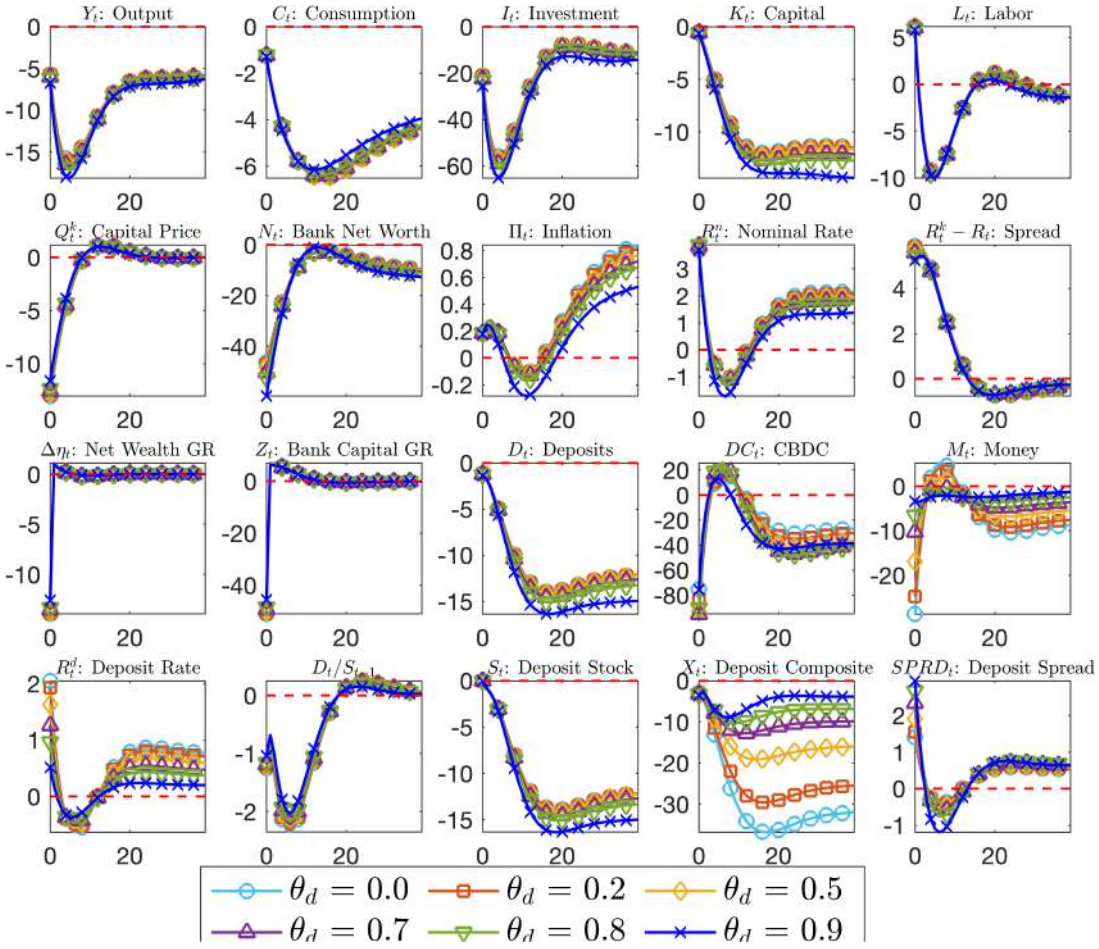

Figure 3.26: Impulse response function of some selected variables of the model to 1 s.d. negative TFP shock for different values of θ^d. Deviations are measured in percentage

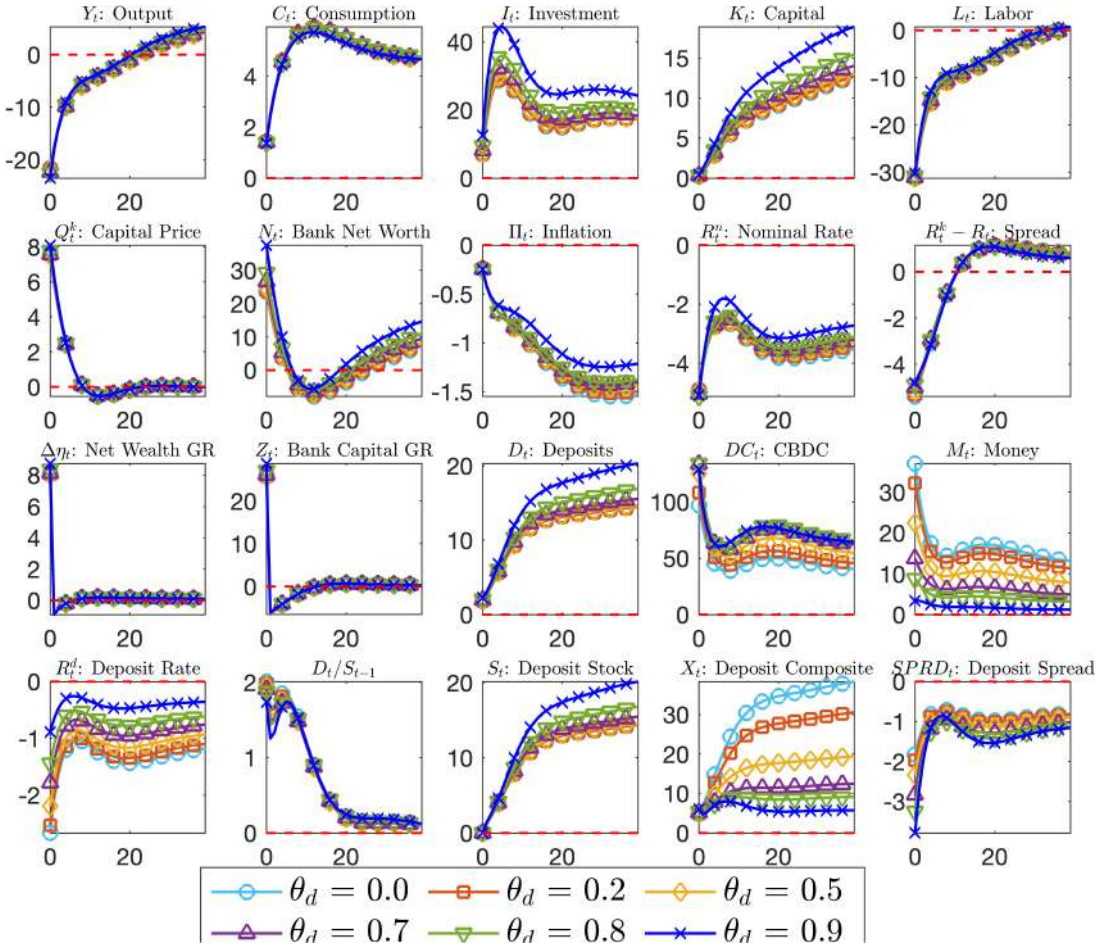

Figure 3.27: Impulse response function of some selected variables of the model to 1 s.d. negative government spending shock for different values of θ^d. Deviations are measured in percentage

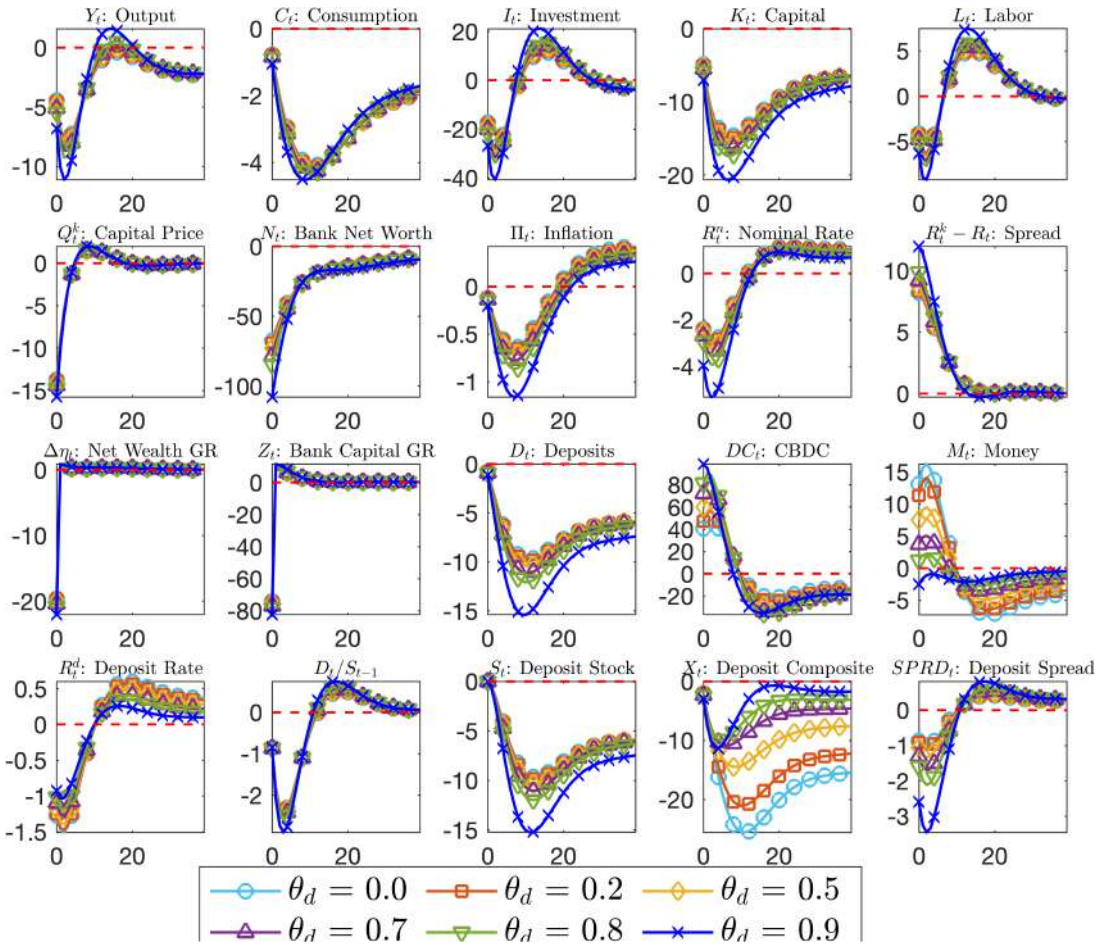

Figure 3.28: Impulse response function of some selected variables of the model to 1 s.d. negative capital quality shock for different values of θ^d. Deviations are measured in percentage

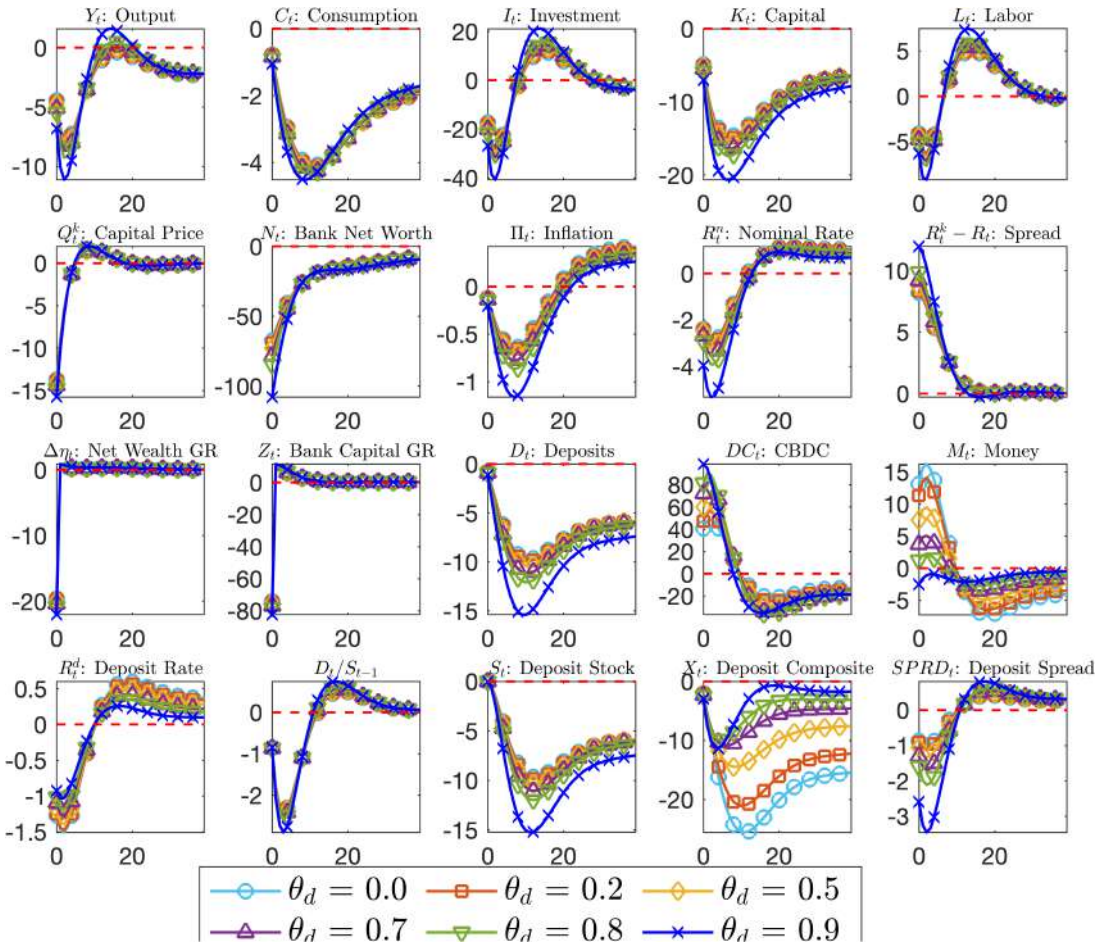

Figure 3.29: Impulse response function of some selected variables of the model to 1 s.d. negative shock to the net worth of banks for different values of θ^d. Deviations are measured in percentage

Chapter 4

Optimizing the Calibration of ABMs through Reinforcement Learning[1]

4.1 Introduction

Over the past decade, the reach and scope of agent-based models (ABMs) in macroeconomics and finance have expanded at a remarkable pace. The continuous progress in computer hardware and software is only one of the reasons. The AB approach, in fact, attracts interest essentially for its *granularity* and *flexibility*, features that allow it to investigate the consequences on macroeconomic outcomes of complex interactions among heterogeneous agents in a bounded rationality setting.

But flexibility is both a blessing and a curse. From the point of view of theory, the critics argue that there are too many *degrees of freedom* in building ABMs and therefore too many widely different models of the same phenomenon. [2] The AB approach has been criticized also for excess flexibility in empirical validation. According to this critique, ABMs are characterized by too many parameters, which are set by means of debatable calibration procedures. In this paper we focus on this critique and propose a new calibration technique that makes use of recent advances in artificial intelligence.

The calibration of ABMs has a long history (Fagiolo et al. (2007)) but interest in this issue has grown remarkably in recent times due to ever-increasing data abundance. The exploitation of large amounts of real data is a promising path to address the problem of ABM flexibility in calibration by appropriately restricting it in a data-driven and systematic manner (Axtell and Farmer (2022)).

A common challenge of all calibration frameworks is the need to efficiently search for

[1] This chapter is co-authored with Aldo Glielmo, Marco Favorito, and Domenico Delli Gatti and has been published as Glielmo et al. (2023).
[2] See Dawid and Delli Gatti (2018) for a discussion of this issue.

optimal parameter combinations in high-dimensional spaces, a problem made particularly arduous by the high computational cost of state-of-the-art ABM simulations. This is why several heuristic search methods have been proposed in the ABM literature. For instance, Lamperti et al. (2018) proposes the use of machine learning surrogates, specifically in the form of XG-boost regressors, to generate promising parameter combinations by interpolating the results of previously computed ABM simulations. Angione et al. (2022) expand on this idea and test the ability of several machine learning surrogate algorithms, such as Gaussian processes, random forests, and support vector machines, to reproduce ABM simulation data.

Taking advantage of the progress made so far, in this paper we propose a new calibration technique articulated in three stages: (i) A machine learning-based search method suggests a set of parameters to explore; (ii) we run a large number of simulations for each selected parameter; (iii) by means of a loss function, we measure the goodness of fit of the simulations with respect to the empirical time series. Iterating this procedure allows us to find numerical parameters corresponding to progressively lower loss values, and the parameter corresponding to the lowest loss value can be considered optimal.

We test our methods on a well-known macroeconomic ABM (Assenza et al. (2015)), which we will refer to as the ADG model. The main results of our computational exploration are the following:

- The macroeconomic ABM considered can be efficiently calibrated to reproduce a variety of real time series.
- Methods based on random forest machine learning surrogates are particularly effective searchers in the highly non-convex and discretely changing loss function induced by ABMs.
- Combining together different search methods almost always provides better overall performance. This mixed search method is a convenient heuristic in the calibration practice.
- Reinforcement-learning techniques can be effectively leveraged to automatically aggregate any number of search methods into a mixed method, allowing for superior performances with respect to standard aggregation strategies.

The rest of the paper is organized as follows. After a concise review of the literature (section 4.2), in section 4.3 we overview the ADG model (an extended description is provided in Appendix 4.A). Section 4.4 is devoted to a description of the calibration technique considered and the search methods that we employ individually and in combination. In Section 4.5 we describe our benchmarking experiments and the results obtained, while in section 4.6 we describe the reinforcement learning scheme we propose to automatically combine existing methods and demonstrate its performance. In Section 4.7 we verify

that the calibrated model reproduces the target real data and that our findings hold well against changes in the model and in the loss function. [3]. In Section 4.9 we conclude.

4.2 Related literature

AB macroeconomics has grown rapidly in the last two decades (see Dawid and Delli Gatti (2018) for an extensive survey), attracting interest (and skepticism) in the profession. ABMs have also become mature enough to be adopted and used within central banks and other financial institutions, albeit for specific research tasks and specific markets (Plassard et al. (2020), Turrell (2016)).[4] These successes have revived interest in the issue of empirical validation so that in the last decade a sizable number of new papers have been published that propose new estimation, forecasting, and calibration techniques.

The (arduous) problem of parameter estimation in ABMs has been approached mostly via the *method of simulated moments* (Franke (2009), Gilli and Winker (2003), Grazzini and Richiardi (2015)), which essentially consists in minimizing a measure of distance between summary statistics of real and simulated time series. More recently, Grazzini et al. (2017) and Platt (2021) have put forward and successfully tested approaches based on maximum likelihood or Bayesian statistics. In a recent paper, Platt (2020) compares and contrasts ABM estimation techniques to find that the Bayesian estimation method generally outperforms alternative procedures.

As to forecasting, Delli Gatti and Grazzini (2020) provides one of the first attempts at forecasting based on simulations of an ABM (the ADG model). In their exercise, however, a statistical VAR model outperforms simulations-based forecasting. Poledna et al. (2023a) have broken the spell. Their simulation-based technique has outperformed other structural models and statistical models in out-of-sample forecasting for the first time.

We now turn to calibration, which is the focus of the present paper. Lamperti et al. (2018), building on the work of Conti and O'Hagan (2010), propose the use of machine learning surrogates – specifically in the form of XG-boost regressors – to generate promising parameter combinations by interpolating the results of previously computed ABM simulations. Along the same lines, Angione et al. (2022) test the ability of several machine learning surrogates, such as Gaussian processes, random forests, and support vector

[3] For this work we made extensive use of *Black-it* Benedetti et al. (2022), an open source calibration kit for ABMs available at https://github.com/bancaditalia/black-it

[4] A particularly noteworthy application domain is the modelling of the housing market, pioneered by the Bank of England Baptista et al. (2016) and later studied by many other central banks Carro (2022), Catapano et al. (2021), Cokayne (2019), Méro et al. (2022). Other successful applications can be found in the modelling of financial stability Bookstaber et al. (2014), Covi et al. (2020), or of the banking sector Chan-Lau (2017).

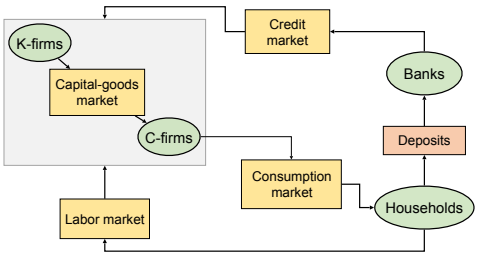

Figure 4.1: Agents and markets in the ADG model. Agent groups are represented by green ovals and markets by yellow rectangles. The grey rectangle represents the corporate sector consisting of C- and K-firms.

machines, to reproduce ABM simulation data. Platt (2020) instead proposes particle swarm samplers Kaveh (2017), Stonedahl (2011), as well as the search heuristic of Knysh and Korkolis (2016). Research efforts in this direction have often focused on the introduction of new calibration methods for certain types of ABMs (Farmer et al. (2022), Franke (2009), Grazzini et al. (2017), Knysh and Korkolis (2016), Lamperti (2018), Platt (2021), Stonedahl (2011)).

As we focus particularly on the calibration of the ADG model, our work can greatly benefit from a direct comparison with Delli Gatti and Grazzini (2020), in which the authors test a Bayesian calibration method on the same task attempted here. The present contribution is strongly related to the previous work Benedetti et al. (2022), where combinations of search methods are also proposed and tested, but it crucially extends it by focusing on a state-of-the-art ABM rather than on a set of toy-models, and by proposing a novel reinforcement learning technique to intelligently combine search methods.

4.3 The ADG model

The ADG model consists of four classes of agents: households, final-goods-producing firms (C-firms), capital-producing firms (K-firms), and banks. Figure 5.1 illustrates these classes of agents and the markets through which they interact. There are N_H households that fall into two categories: N_W workers and N_F firm owners. There are N_F firms that fall into two categories: N_F^k producers of capital goods (K-firms) and N_F^c producers of consumption goods. The number of *active* firms may change over time due to entry and exit but never exceeds N_F. The banking system is represented by a single bank, collectively owned by firm owners.

A household indexed with $h \in (1, N_W)$ is a worker. Workers can be either economically active or inactive. Each active worker supplies 1 unit of labor inelastically. If employed,

they receive a uniform wage and pay a fraction of this wage to the government. A household indexed with $h = N_W + f$ is the owner of the f-th firm, $f = 1, 2, ..., N_F$. The income of this household consists of dividends, which are equal to a fraction of the after-tax profit of the firm owned by that household. The firm pays out dividends only if profits are positive. In addition, all households receive interest income on deposits held at the bank, which represent the only financial asset owned by households.

The *consumption budget* – essentially planned expenditure – of the household is given by a weighted average of past disposable incomes and a fraction of its financial wealth (deposits). The parameters ξ and χ and the tax rate t_w show up in the equation of the consumption budget (see appendix). The household/consumer shops at a limited number of C-firms and starts to purchase goods from the firm that charges the lowest price. Shopping goes on until the budget is completely exhausted.

C-firms indexed with $f \in (1, N_F^c)$ set their price and desired scale of activity under uncertainty. Two *rules of thumb* govern price changes and quantity changes, respectively. Excess demand and the difference between the price set by the firm $P_{f,t}$ and the average price P_t dictate the *direction* of price adjustment: the firm will increase (reduce) the price next period if it has registered excess demand (supply) and has underpriced (overpriced) the good in the current period. Otherwise it will leave the price unchanged. The *magnitude* of price adjustments is stochastic and ranges between zero and $\bar{\eta}$.

Both the direction and the magnitude of quantity adjustment are determined by excess demand. The firm will reduce inventories (at the rate δ^k) or increase production next period if it has registered excess demand in the current period; it will downsize production if it has registered excess supply (i.e., involuntary inventory accumulation). The parameters ρ show up in the quantity adjustment heuristic.

Technology is represented by a Leontief production function, the arguments of which are capital and labor. Once a decision has been taken on desired output, a firm determines how much capital and labor it needs to reach that level of activity.

We assume that a fraction γ of C-firm carries out investment in any given period. The investing firm calculates average capital stock by means of an adaptive algorithm based on a memory parameter ν. The firm purchases new capital goods so as to reach a target capital stock that is somehow proportional to the average capital stock.

Firms experience a financing gap when their costs (to pay wages and capital goods) are greater than their liquidity. In this case the firm goes to the bank and asks for a loan. The credit line the bank is willing to extend depends on the bank's leverage ζ. The bank sets the interest rate on loans, adding a markupμ to the risk-free interest rate. In every period, borrowers repay a fraction θ of their outstanding loans.

In the interest of space, we do not describe the details of the model here but report

them in Appendix 4.A. We also refer the interested reader to Assenza et al. (2015) for an in-depth exposition.

4.4 Calibration

In the previous section we mentioned 11 parameters that characterize the model. The parameters are listed in table 4.1 together with the range of their admissible numerical values. The calibration procedure we propose is organized in three steps. First we use a search method (a *sampler* hereafter) to obtain a set of numerical values for the parameters (a calibration). Then we carry out a number of simulations for each calibration. Finally, we use a loss function to measure the efficiency of the calibration, i.e., the goodness of fit of the simulated time series with respect to the empirical time series. By iterating these three steps, we find sets of numerical values of the parameters corresponding to progressively lower values of the loss function. The set of numerical values corresponding to the lowest value of the loss function can be considered the optimal (most efficient) calibration.

In order to calibrate AB models, it is straightforward to adopt the Method of Simulated Moments (MSM). This method is based on the representation of the real economy and the artificial economy (the model) by means of the statistical moments of the distributions of the observed and artificial data. MSM consists in minimizing the distance between the moments of the distributions of the data generated by these two economies (McFadden, 1989; Pakes and Pollard, 1989). We write the period-t values of the macroeconomic variables generated by each simulation in compact form as follows:

$$\mathbf{y}_t = F(\mathbf{\Psi}_t; \boldsymbol{\theta})$$

where $\mathbf{y}_t$ is the $D \times 1$ vector of period-t values of D macroeconomic variables. In our case, $D = 5$ as we follow Delli Gatti and Grazzini (2020) and calibrate the model using the time series of GDP, personal consumption, gross private investment (all in real terms), the implicit GDP deflator (price level), and the civilian unemployment rate. $F(.)$ represents the model, $\mathbf{\Psi}_t$ are all the random shocks from period 0 to the current period, and $\boldsymbol{\theta}$ is the $k \times 1$ vector of numerical values of the parameters used in the simulation. In our case $k = 11$.

The total number of simulated periods (ignoring the transient period) is T. We simulate the model for 1100 periods and discard a transient of 300 periods so that $T = 800$ in our case. The simulation output of the model is represented by the $D \times T$ matrix of simulated data $\mathbf{Y} = [\mathbf{y}_1, \mathbf{y}_2, ..., \mathbf{y}_T]$. The statistical properties of the time series generated by the model depend on the parameters in $\boldsymbol{\theta}$ and on the random seed s govern-

ing the set of random shocks $\mathbf{\Psi}_t$.[5] With a slight abuse of notation, therefore, we can characterize the matrix of simulated data as $\mathbf{Y} = \mathbf{Y}(\boldsymbol{\theta}, \mathbf{s})$. We simulate the model S times with the same parameter values but S different random seeds, obtaining a matrix $\mathbf{Y}(\boldsymbol{\theta}, \mathbf{s}) = [\mathbf{Y}(\boldsymbol{\theta}, s_1), \mathbf{Y}(\boldsymbol{\theta}, s_2), ..., \mathbf{Y}(\boldsymbol{\theta}, s_S)]$ of D stacked time series each with a length of $T \times S$ periods. We will refer to $\mathbf{Y}(\boldsymbol{\theta}, \mathbf{s})$ as the *ensemble* distribution, and we will use it to describe the behavior of the model as a function of $\boldsymbol{\theta}$ in the calibration procedure.

From $\mathbf{Y}(\boldsymbol{\theta}, \mathbf{s})$ we compute the simulated moments of the distributions of the D variables. We use the following *Loss function* (often called *distance* in the AB literature) for all calibrations: [6]

$$L = \frac{1}{D} \sum_{d=1}^{D} \mathbf{g}_d^{\mathrm{T}} \mathbf{W}_d \mathbf{g}_d, \tag{4.1}$$

where $\mathbf{g}_d$ is the (column) vector of differences between the real (empirical) and the simulated moments of the one-dimensional time series d (e.g., GDP), and $\mathbf{W}_d$ is $D \times D$ the weighting matrix.

We consider the following moments and statistical measures: mean, variance, skewness, and kurtosis of each variable in levels; autocorrelations of the levels at increasing time lags; mean, variance, skewness, and kurtosis of each variable in first differences; and autocorrelations of the differentiated time series.

Different choices for the weighting matrices $\mathbf{W}_d$ have been proposed in the literature (Franke (2009), Franke and Westerhoff (2012)). In this paper, we define $\mathbf{W}_d$ as a diagonal matrix with elements $(\mathbf{W}_d)_{ii}$ inversely proportional to the square of the real i-th moment of the one-dimensional time series d. This choice guarantees that the same weight is given to all moments considered, independently of the different scales or units of measure that the different moments might have.

Therefore, the scalar $\mathbf{g}_d^{\mathrm{T}} \mathbf{W}_d \mathbf{g}_d$ is the weighted sum of squared differences between the empirical and the simulated moments of variable d. As a consequence, the loss is the mean of the weighted sums of squared differences (between the empirical and the simulated moments) computed across dimensions (number D of macroeconomic variables). The lower the loss, the more *efficient* is the calibration process.

Since we use a common loss function for all calibrations, the only difference between the calibration runs is the choice of the search method. We consider five search methods, all of which are implemented in *Black-it* Benedetti et al. (2022), an open-source library for ABM calibration: [7] Our baseline is the Halton sampler, which is close to a pure random search method. Three of the four non-baseline search methods are machine learning surrogate samplers. These samplers are "adaptive" search methods because they make

[5] We abstract for simplicity from the role of initial conditions.
[6] For similar applications of MSM, see Chen and Lux (2018), Franke (2009).
[7] `https://github.com/bancaditalia/black-it`

use of the information gathered from previous explorations of the parameter space in order to continue searching in the vicinity of the locally optimal parameters. The fourth non-baseline sampler is a genetic algorithm. In the following, we describe these methods better.

Halton sampler (H)**.** This sampler suggests points according to the Halton series (Halton (1964), Kocis and Whiten (1997)). The Halton series is a low-discrepancy series providing a quasi-random sampling that guarantees an evenly distributed coverage of the parameter space. Since this method is very close to a purely random search, we use it as the *baseline method*. **Random forest sampler** (RF)**.** This machine learning surrogate sampler interpolates the previously computed loss values using a random forest classifier (Bajer et al. (2015)), and suggests parameters in the vicinity of the lowest values of the interpolated loss surface. We use a random forest classifier with 500 independent estimators ("trees") and use 10 classes chosen as the 10 quantiles of the distribution of evaluated losses.

XG-boost sampler (XB)**.** This machine learning surrogate sampler interpolates loss values using an XG-Boost regression (Chen and Guestrin (2016)), as proposed in Lamperti et al. (2018). We use a learning rate of 0.1, a maximum tree depth of 5, and 10 estimators.

Gaussian process sampler (GP)**.** This machine learning surrogate sampler interpolates loss values using a Gaussian process regression (Conti and O'Hagan (2010), Rasmussen (2004)). We use a Matérn covariance function with $\nu = 5/2$ and with the length scale optimized at every iteration via maximum marginal likelihood.

Best batch sampler (BB)**.** This sampler is a genetic algorithm (Stonedahl (2011)) that takes the parameters corresponding to the current lowest loss values and perturbs them slightly in a purely random fashion to suggest new parameter values to explore. The random perturbation is specifically obtained by first selecting a random subset of dimensions and then changing the parameter value along those dimensions uniformly but within a short range (plus/minus 0.006 in our case).

4.5 Benchmarking experiments

Similarly to Delli Gatti and Grazzini (2020), we calibrate the model using the time series of GDP, personal consumption, gross private investment (all in real terms), the implicit GDP deflator, and the civilian unemployment rate for the USA from 1948 to 2019, downloaded from the FRED database(McCracken and Ng (2016)). To make simulated and observed data comparable, we remove the trend component from GDP, consumption, and investment using an HP filter (Ravn and Uhlig (2002)); and we use simulated and observed price levels to compute de-meaned inflation rates.

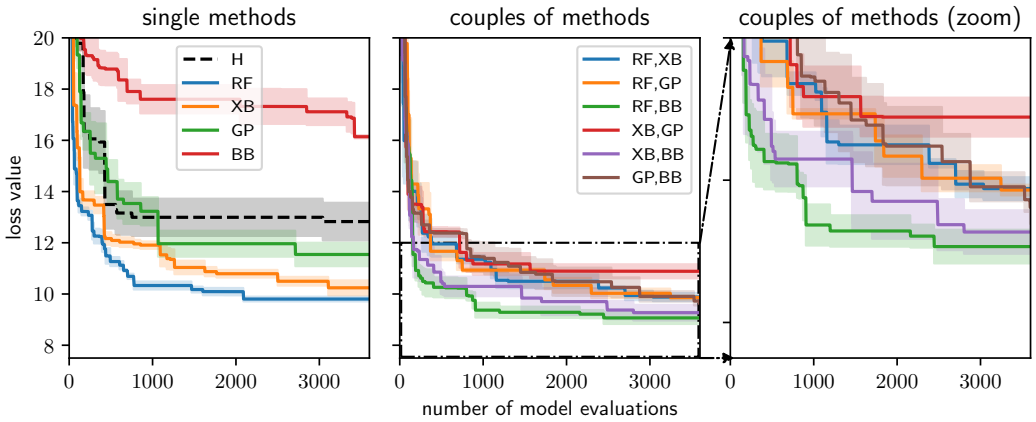

Method	H	RF	XB	GP	BB	RF,XB	RF,GP	RF,BB	XB,GP	XB,BB	GP,BB
Mean	12.83	**9.803**	10.24	11.96	16.87	9.88	9.861	**9.07**	10.89	9.27	9.83
Std. Err.	0.73	0.094	0.29	0.51	0.59	0.16	0.075	0.24	0.27	0.31	0.26

Figure 4.2: Top graphs: Loss as a function of the number of model evaluations for the single methods (left), and for couples of methods (middle and right). Bottom table: Means and standard errors of the lowest losses achieved by the different strategies. Note that these results are directly comparable with those shown in Figure 4.3 and discussed in the next section, as both x and y axes have identical ranges.

In Table 4.1 we list the parameters considered for calibration and the range of numerical values each parameter can assume. Each simulated time series consists of 800 time-steps generated by running the model for 1100 time steps and discarding the first 300.[8] For each combination of the parameters, we perform 5 simulations (with different random seeds). We label this set of 5 simulations a *model evaluation*. We consider 3600 combinations of parameter values, and for each combination we get a model evaluation. We label this set of 3600 model evaluations a *calibration run*. A calibration run then consists of $3600 \times 5 = 18000$ simulations. Using the five samplers described in the previous section and the 6 combinations of any two non-baseline samplers, we obtain 11 search methods. For each search method, we perform 3 independent calibration runs. Therefore, for each search method, we run $18000 \times 3 = 54000$ simulations. Considering the whole set of search methods, therefore, we reach the number of $54000 \times 11 = 594000$ simulations. This makes up a total of more than 50 days of CPU time, which we were able to compress in less than two days by leveraging parallel computing both within and between calibrations.

Figure 4.2 shows the cumulative minimum loss achieved by the different sampling strategies as a function of the number of model evaluations performed. The lines and the shaded areas indicate averages and standard errors over 3 calibration runs of the

[8] In 4.B we provide evidence that a transient of 300 simulation periods is sufficient to generate persistent dynamic patterns.

Param.	Description	Range
ξ	Memory parameter in consumption	0.5-1
χ	Wealth parameter in consumption	0-0.5
ρ	Quantity adjustment coefficient	0-1
$\bar{\eta}$	Price adjustment coefficient	0-1
μ	Bank's gross mark-up	1-1.5
ζ	Bank's leverage	0-0.01
δ^k	Inventories depreciation rate	0-0.5
γ	Fraction of investing C-firms	0-0.5
θ	Rate of debt reimbursement	0-0.1
ν	Memory parameter in investment	0-1
t_w	Tax rate	0-0.4

Table 4.1: Parameter descriptions and their corresponding ranges.

experiment. Single samplers are shown in the left graph, while couples of samplers are reported in the middle graph as well as –zoomed– in the right graph. The table at the bottom of the graphs reports the minimum loss achieved by the different methods.

Single samplers. When samplers are taken in isolation, the random forest sampler (RF) clearly outperforms all other methods, the XG-boost sampler (XB) is the second best, and the Gaussian process sampler (GP) is substantially worse than the other two machine learning surrogate samplers. The low performance of the GP sampler can be ascribed to the smoothness and regularity assumptions inherent in Gaussian process regression models, assumptions that are not present in random-forest or XG-boost models and not suited to describe the roughed and complex loss landscape of ABM calibrations. The best batch sampler (BB) performs very poorly in isolation and underperforms even in comparison with the baseline H sampler. This is not surprising, since the BB sampler can only propose small perturbations around current loss minima and can thus easily remain stuck in one of the many local minima of the highly non-convex landscape typical of ABMs loss functions.

Coupled samplers. All the samplers listed above are characterized by intrinsic sampling biases that can hinder their performance in the long run and make them converge to suboptimal solutions. We therefore explore the effects on the efficiency of the calibration process of fixed *scheduling strategies,* i.e., combinations of two different samplers employed in naive alternation (also known as *round robin combinations*). We find that these strategies can strongly mitigate the above-mentioned biases. The efficiency-enhancing effect of mixed methods can be observed in the second and third panels of Figure 4.2: combinations of methods perform on par or better than the best single samplers (RF and XB) with the only exception of the (XB, GP) pair. Interestingly, the best overall performances are achieved by coupling one machine learning surrogate sampler with the genetic BB sampler. The (RF, BB) and (XB, BB) combinations are particularly effective and achieve

the lowest loss values.

We summarize the output of simulations so far in the following result.

Result 1 *Among the search methods taken in isolation, two machine learning surrogate samplers,* RF *and* XB*, stand out as particularly well suited to efficiently search in the parameter space of the considered ABM.*

The performance of the RF *or* XB *samplers can be significantly improved if each one is used in round-robin combination with the* BB *sampler, i.e., with the genetic sampler.*

The success of the RF and XB samplers can be ascribed to the capability of the machine learning surrogates to correctly approximate high-dimensional and possibly discontinuous functions in the absence of regularities. [9]

The improvement in efficiency recorded when a machine learning surrogate is coupled with the genetic algorithm may be due to the fact that the combined use of these (very different) search methods can offset the sampling biases of each of the individual search methods. In fact, combinations of two machine learning surrogates do not yield comparable improvements since they both follow similar procedures.

The results presented so far can already offer useful guidance for researchers interested in calibrating medium- and large-scale ABMs, as they provide an easy recipe to boost calibration efficiency by simple alternation of existing search methods. In the next section, we move a step forward and consider the combination of multiple methods in a more general setting, going beyond the simple scenario of a "round-robin" selection.

4.6 Reinforcement learning

Result 1 shows that the combination of different types of sampling methods can increase the efficiency of the calibration process even if the samplers are naively alternated during the searching process. It is reasonable to conjecture that a more sophisticated – and more flexible – scheduling strategy in the employment of combined search methods could lead to even more efficient calibrations.

The desirable scheduling strategy should be characterized by *adaptivity*, i.e., it should be able to choose the sampling method that has more chances to pick in t an efficient set of parameter values, taking into account the progress of the calibration process until t-1. To devise a desirable scheduling strategy, therefore, we must conceive the calibration of the ABM – i.e., the choice of the set of numerical values for the parameters – as a *Reinforcement Learning (RL)* problem: the AB model builder, in its role of decision-maker who wants to optimize the calibration process, must devise a *flexible scheduling strategy*

[9] This result is in line with the claim in Lamperti et al. (2018).

that chooses at each time step the action (search method) that is most "promising" – i.e.,that is likely to sample a set of parameter values associated to a lower loss. Key in the application of RL to the calibration of ABMs is the *feedback* that the decision-maker receives and exploits concerning the effects of the search method in the form of a *reward signal* computed from the sampled loss function values. This is what makes the scheduling strategy adaptive: search methods that provide loss reductions more often are more rewarding in the eyes of the decision-maker, and they have more chances of being chosen in the next calibration step. On the other hand, whenever a search method does not show to be rewarding anymore, the decision-maker may switch to another search method. Adopting the terminology of control theory (Dorf and Bishop (2008)), fixed scheduling strategies, such as the round robin combinations of two samplers explored in the previous section, are *open-loop*, i.e., they do not change regardless of their performance. On the contrary, RL-based scheduling strategies are *closed-loop*, because the preferred sampling methods can change on the basis of the feedback received by the decision maker.

To be specific, we frame the calibration process as a *multi-armed bandit (MAB)* problem (Auer et al. (2002a), Berry and Fristedt (1985), Gittins et al. (2011), Katehakis and Veinott Jr (1987), Lattimore and Szepesvári (2020), Weber (1992)), a classic problem in the field of reinforcement learning and sequential decision-making. In a MAB, the decision maker has to choose one action in a set of possible actions with the goal of maximizing the cumulative reward of these actions over a series of trials (a sequence of time steps). At each time step, the decision maker must choose which action to adopt and observe the resulting reward. Crucially, the decision maker does not know the true reward probability of each action. This setting exemplifies the *exploration–exploitation trade-off* (Sutton and Barto (2018)). The challenge for the decision maker is to balance the *exploration* of potentially more rewarding actions (i.e., gathering information about their payoffs) and the exploitation of actions that have shown promising rewards so far. The goal is to find the optimal strategy that maximizes the long-term reward by effectively trading off exploration and exploitation.

There are different specifications of the multi-armed bandit problem, such as the stochastic bandit problem (where the rewards of each action are randomly generated from a distribution) and the contextual bandit problem (where additional contextual information is available to inform the action selection). We will use a contextual MAB algorithm momentarily.

In our setting the decision maker is the AB model builder, the actions are the sampling methods, and the reward signals are loss improvements. To be specific, we define the

reward at time t as the percent improvement achieved over the previous best loss,

$$R_t = \max\{0, \frac{L^*_{t-1} - L_t}{L^*_{t-1}}\} \tag{4.2}$$

where L_t is the loss obtained for the simulations sampled at time t, and L^*_{t-1} is the best loss sampled up to time $t-1$. Note that it R_t is a random variable because it L_t depends on the simulated time series generated by the ABM and the chosen parameter vector. As in most of the MAB problems, the goal for the decision maker is to maximize the cumulative sum of rewards,

$$S_N = \sum_{t=1}^{N} R_t, \tag{4.3}$$

where N is the number of calibration steps.

Differently from the usual MAB setting, the reward probability distribution associated with each sampler is *non-stationary*. Non-stationarity is the most general assumption one can make concerning the behavior of reward probability distributions in MABs (Auer et al. (2002b)). In our case, the non-stationarity assumption is due to the lack of knowledge on both the ABM and the samplers' behaviors. Stationarity for our MAB can be written as follows: $\forall t: \ p_t(R|sampler) = p(R|sampler)$ where $p_t(R|sampler)$ is the conditional probability of getting reward R when the decision-maker chooses a given sampler. This condition is never satisfied because, for any sampler, the probability of reducing the loss decreases over time time (it is increasingly difficult to decrease the loss as the calibration progresses). At the end of a calibration, all the methods – even the best ones – stop providing any improvement in the loss, and hence the reward distributions become progressively more peaked around zero.

In the following, we test our MAB framework in two experiments. First, in the *offline-learning* experiments, we let the decision maker learn from the previously executed calibrations of Section 4.5. Then, in the *online-learning* experiments, we let the decision maker interact with the environment and optimize its policy on-the-fly during each calibration.

4.6.1 Offline experiments.

In this section, we train a MAB decision maker over past calibration histories (those considered in Figure 4.2). More precisely, we identify the actions with the search methods considered in Section 4.5 and process them as if they were observed by a MAB algorithm. This approach allows to estimate the expected gain of each method, and therefore provides information on the effectiveness of the method in the specific calibration task.

In the context of MAB problems, the procedures to estimate the values of (previous)

Sampler	Single samplers only	All data	High L_t^*	Low L_t^*
RF	**0.25**	**0.27**	**1.3**	0.052
XB	0.23	0.23	0.61	0.033
GP	0.21	0.17	0.26	0.068
BB	0.11	0.23	0.28	**0.18**
H	0.20	0.20	0.24	N.A.

Table 4.2: Estimated Q functions for the different search methods under different scenarios. The column entitled *Single samplers only* uses only the calibrations obtained by means of single search methods (those of the panel on single search methods of figure 4.2). The column entitled *All data* uses all calibrations (both the panel on single search methods and that of coupled methods in figure 4.2). The column *high* L_t^* uses all calibration but only actions taken when the loss is *above* the median loss. The column *low* L_t^* uses all calibration but only actions taken when the loss is *below* the median loss. Results are reported on a scale of 10^{-3}.

actions and to select the (current) action on the basis of these estimates go under the name of *action-value methods* (Sutton and Barto (2018)). Let $Q_t(a)$ be the value of action be, a i.e., in our context, the value of using a specific search method in period t during a calibration. One natural way to estimate such value is by averaging the rewards actually received while using a:

$$Q_t(a) = \frac{\sum_{t=1}^{N} R_t \cdot \mathbb{1}_{A_t=a}}{\sum_{t=1}^{N} \mathbb{1}_{A_t=a}}, \tag{4.4}$$

where A_t is the type of action chosen at step t and $\mathbb{1}_{A_t=a}$ is an indicator function that takes value 1 if the the chosen action is a, zero otherwise. The numerator of the fraction above is the sum of rewards when action a is taken prior to t while the denominator is the number of times action a is taken. This approach is often called the *sample-average* method (Sutton and Barto (2018)).

The first two columns of Table 4.2 show the estimates Q when only the single sampler calibrations are considered ("Single samplers only" column) and when all calibrations are considered ("All data" column). Not surprisingly, the RF sampler reaches the highest Q value in both columns, and the results of the "Single samplers" column replicate the ranking of samplers of the first panel of Figure 4.2. Interestingly, the value of the BB sampler dramatically increases when all data are considered, confirming the analysis carried out in the previous section on the efficiency-enhancing effect of using the BB sampler in combination with a machine learning surrogate sampler.

The third and fourth columns of Table 4.2 offer additional insights. In these columns, we restrict the estimation of the Q-value to actions performed in one of two different

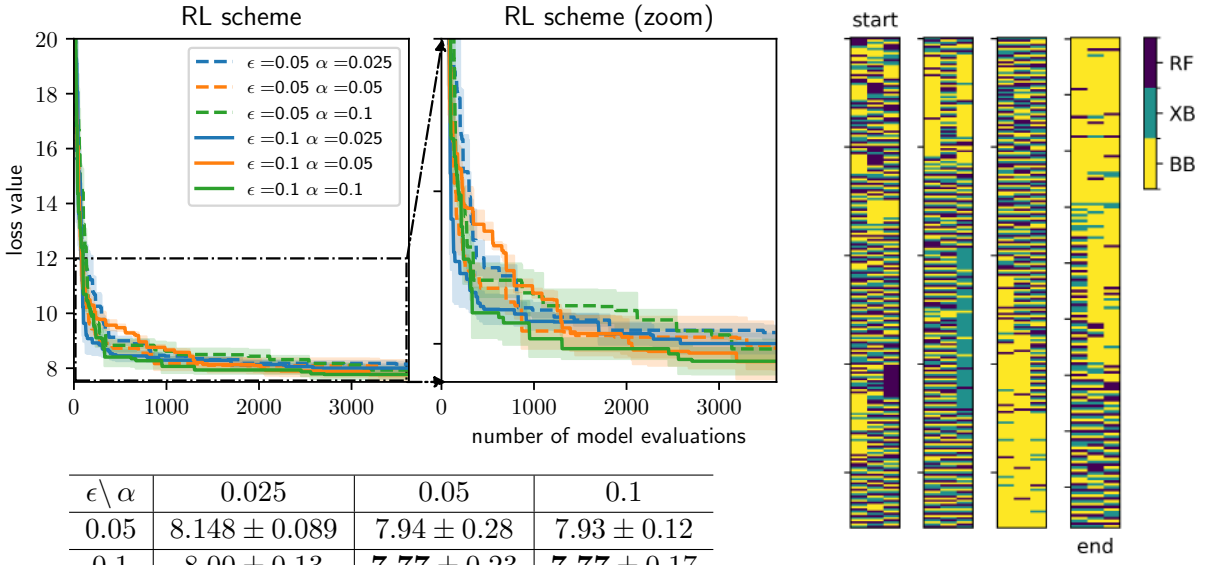

$\epsilon \backslash \alpha$	0.025	0.05	0.1
0.05	8.148 ± 0.089	7.94 ± 0.28	7.93 ± 0.12
0.1	8.00 ± 0.13	$\mathbf{7.77} \pm 0.23$	$\mathbf{7.77} \pm 0.17$

Figure 4.3: Top graphs: (left and middle) Loss as a function of the number of model evaluations for the RL scheme with different choices of parameters and for a naive alternation of the samplers, (right) the specific samplers ('actions') selected by the RL scheme with parameters $\epsilon = 0.1$ and $\alpha = 0.1$ during the 900 periods of a calibration for each of the 3 independent runs, to be read from left to right, from top to bottom, note that each epoch provides 4 model evaluations. Bottom table: Means and standard errors of the lowest losses achieved by the RL scheme. These results can be compared directly with those of Figure 4.2 as they have identical ranges on both x and the y axes.

'states', characterized by the best loss L_t^* being either above the median (High L_t^* column) or below the median (Low L_t^* column). Models of this kind, where the actions of a MAB decision maker depend on one or more states (in this case high/low L-value) are known as *contextual* MABs Langford and Zhang (2007), Li et al. (2010).

The results clearly indicate that when the loss is high (a situation that typically occurs at the beginning of the calibration) the optimal (value-maximizing) action is the RF sampler, but when the loss is low (typically at the end of the calibration) the optimal action becomes, by far, the BB sampler. The analysis performed so far can be summarized in the following.

Result 2 *The ranking of single search methods emerging from the selection process pursued in the previous section is confirmed in the MAB model. The* RF *sampler reaches the highest Q value while the* BB *sampler is associated with the lowest Q value. The value of the* BB *sampler, however, doubles when the combined dataset is used. This suggests that the combination of a* BB *sampler and a machine learning surrogate sampler will boost the efficiency of the sampling method.*

The explanation of this result emerges from the analysis of the *contextual* MAB. It turns

out that when the loss is high (typically at the beginning of the calibration), the optimal action is the RF sampler, while when the loss is low (typically at the end of the calibration), the optimal action becomes, by far, the BB sampler. The BB sampler, in fact, proposes small perturbations around low-loss parameter combinations, and hence it can be expected to be particularly effective when the calibration has already reached a *good* minimum, which can be further explored with this method. The best method consists of a mixed search scheme that exploits a machine learning surrogate sampler (say RF or XB) at the beginning of the calibration, when the loss is sufficiently high, and switches to the BB sampler towards the end of the calibration, when the loss is low.

However, this specific strategy is not generally applicable, as, on a new calibration task, the decision maker does not know in advance the size of the loss that can be achieved, and hence cannot set any loss threshold on the choice of sampler. In the following section, we show how a MAB decision maker trained on-the-fly can solve this problem by learning this behavior, without any prior information, during the course of a single calibration run.

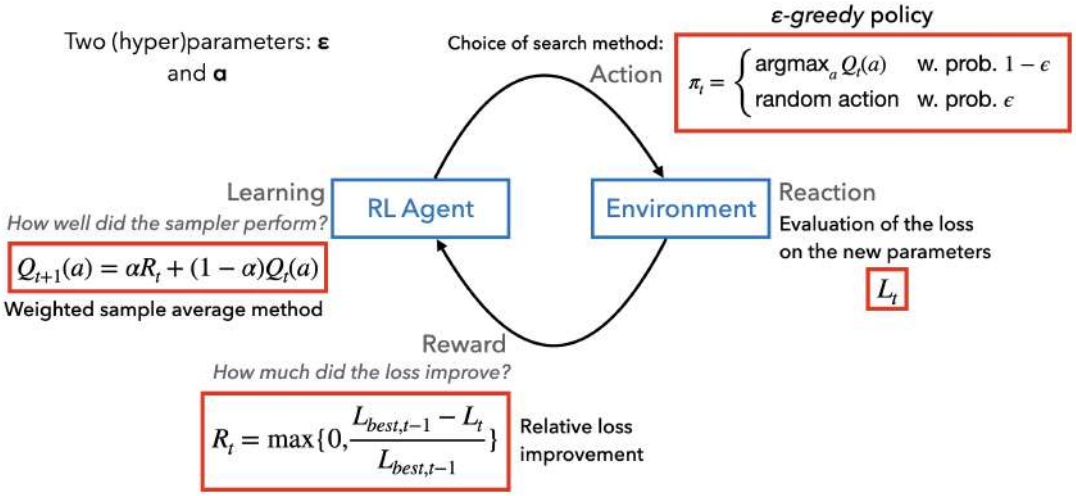

Figure 4.4: An illustration of the online reinforcement learning scheme designed to choose efficient search methods during each calibration run. With high probability (1 - ε) the RL agent selects the search method a with the highest Q value, and with small probability ε it selects a completely random method. Then, the chosen search method is called to suggest parameter combinations, leading to a corresponding loss evaluation L_t. If L_t is lower than the previously found lowest loss $L_{best,t-1}$, the reward R_t is computed as the fractional loss improvement, otherwise is set to zero. Finally, the Q value of the chosen search method is updated, taking the latest reward into account through a moving average with parameter α. The entire scheme depends on two hyper-parameters: ε and α.

4.6.2 Online experiments.

In online learning schemes, the decision maker interacts with the environment through a specific *policy* π. We propose the ϵ-greedy policy with a fixed learning rate (Sutton and

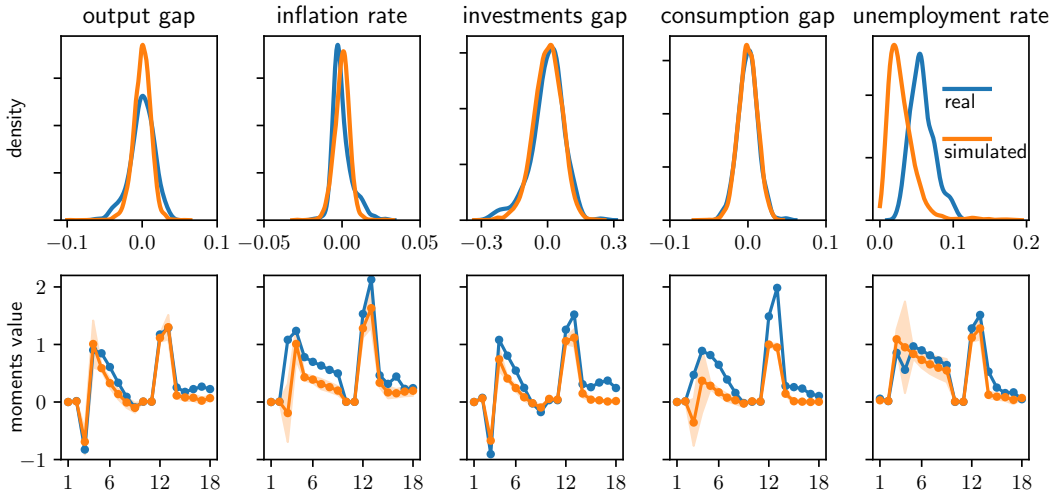

Figure 4.5: A comparison between distributions and moments of the real series (blue) and the simulated series of lowest loss (orange). The first row reports density estimates obtained via a kernel density estimator. The second row reports the value of the moments. In the second row, the indices from 1 to 18 on the x-axis represent the following statistics. 1-4): mean, variance, skewness and kurtosis, 5-9): autocorrelations of increasing time lags. 10-13): mean, variance, skewness, and kurtosis of the differentiated time series; 14-18): autocorrelations of the differentiated time series.

Barto (2018)). This is one of the most well-known algorithms for online learning of MAB decision-makers in non-stationary environments. In this framework, at each step$t$, the decision-maker chooses a 'greedy' action – i.e., they select the action a with the highest value $Q(a)$ – with a high probability $1-\epsilon$ and select a purely random action with a small probability ϵ. We can hence write the ϵ-greedy MAB policy as follows

$$\pi_t = \begin{cases} \text{argmax}_a \; Q_t(a) & \text{with probability } 1-\epsilon \\ \text{random action} & \text{with probability } \epsilon \end{cases} \tag{4.5}$$

After the selected action a is performed, the agent receives a reward R_t, and updates the value $Q_t(a)$ as

$$Q_{t+1}(a) = \alpha R_t + (1-\alpha) Q_t(a), \tag{4.6}$$

where α is the *learning rate*. Note that using the above updating rule $Q_t(a)$ turns out to be an exponentially weighted moving average of past rewards obtained through action a. Exponential weighting guarantees that the current value of the Q function is not substantially affected by rewards received many steps earlier and, in turn, this allows the algorithm to adapt to changes of the environment on-the-fly during a calibration.

Figure 4.3 shows the results obtained when using the described scheme with a set of possible actions given by the tree samplers RF, XB and BB. The left and middle panels of

the figure can be directly compared with the graphs in Figure 4.2, as they have identical ranges on both the x and y axes. For comparison, the figure also reports –in a black dotted curve– the loss achieved by combining the three samplers RF, XB and BB in a simple ('naive') alternation.

Result 3 *The proposed RL scheme (ϵ-greedy policy with fixed learning rate) strongly outperforms any other method, or combination of methods, tested in the previous section. This is true for all values considered for the parameters ϵ and α, with the best results –by a very narrow margin– obtained with $\epsilon = \alpha = 0.1$.*

The simple alternation method, that does not use RL, provides a lower-bound to the performance of the RL scheme. It clearly leads to a significantly slower convergence.

The right panel of Figure 4.3 helps us build intuition around the excellent performance of the RL scheme proposed. It depicts with different colours the different actions (samplers) selected during the 3 RL calibration runs performed with the best parameters $\epsilon = \alpha = 0.1$. At the beginning of the calibration (say, the first two columns), the agent explores the different strategies by alternating between the 3 samplers and sometimes exploits a specific sampler with long streaks of identical sampler choices. Towards the end of the calibration (say, the last two columns), when the loss is low, the agent instead more decisively exploits the BB sampler, in agreement with the offline experiments described earlier and summarised in Table 4.2.

Designing the calibration process as an online learning MAB problem, with actions being given by different search methods, allows us to detect the most promising search methods during the course of a single calibration. This gives rise to a very efficient sampling scheme, and represents a practical tool to intelligently combine different search methods in the calibration of economic ABMs.

The ϵ-greedy –fixed learning rate– scheme we use here is a particularly simple and intuitive algorithm for MAB learning, but other options have been suggested in the literature. In Appendix 4.C we explore some of them for a simplified calibration setting, and find no substantial improvements in the calibration efficiency. Furthermore, it is important to note here that the simplicity of the RL scheme proposed –merely involving the running average and argmax operations of Eqs. 4.6 and 4.5– also entails great computational efficiency, which, in turn, implies the absence of any overhead in using the RL scheme over naive method combinations.

4.7 Validation

Calibrated model. It is straightforward to verify that the calibrated model is capable of approximately replicating the behavior of the five variables in the real dataset. Figure

4.5 shows the distribution and the moments of the simulated series with the lowest loss, compared with those computed for the real time series. In agreement with Delli Gatti and Grazzini (2020), output, consumption, and investment are very well captured by the ADG model, while stronger deviations can be observed in inflation and unemployment rates. Also in agreement with Delli Gatti and Grazzini (2020) we find that, in general, the ADG model can only partially account for the persistence of the real time series. This is clear from the fact that the simulated series have systematically lower values of virtually all autocorrelations considered (indices 5-9 and 14-18 in the second-row graphs).

Different models and loss functions. This study aims to address the challenge of calibrating a standard macroeconomic ABM using a method of moments loss function. While the focus is on the ADG model, we believe our findings to be relevant for other ABMs and loss functions. In Appendix 4.D we present further numerical results supporting this claim. Specifically, we performed calibration experiments in two different settings: the paradigmatic 'Brock and Hommes' asset pricing model Brock and Hommes (1998) with a method of moments loss, and a SIR model on a small-world network topology Simoes et al. (2008) with a Euclidean loss. In agreement with the rest of this work, we find that the RF sampler is the best-performing sampler when methods are used in isolation, that coupling different samplers generally provides better performances, and that our RL-scheme can be successfully used to intelligently combine search methods. However, the alternative calibration tasks presented in the appendix are much simpler than the calibration of the CATS model considered in the rest of this work. For this reason, we do not see a significant performance improvement in using RL combinations over simple combinations, but, importantly, we consistently find the performance of the RL-scheme to be as good as the best samplers or sampler-combinations tested, without requiring any trial and error.

4.8 Calibration and shocks

In Table 4.3, we show the numerical values of the parameters in the original model (ADG), in DG and with RL. The calibration of ADG is based on simple output validation (comparison between stylized facts). The calibration in DG is based on Bayesian estimation. The numerical values are not dramatically different with the exception of δ^k and ν that are much higher under RL. We carry out experiments by subjecting the model to aggregate shocks using these calibrations.

For the sake of comparison, we follow DG in building Impulse-Response functions to explore in a clear way the trajectory of a macroeconomic variable after a shock to an aggregate variable. In a macro ABM it is impossible to completely shut off after-shock randomness. The same aggregate shock may trigger different dynamic paths of prices

Param.	Description	ADG	DG	RL
ξ	Memory parameter in consumption	0.96	0.738	0.881
χ	Wealth parameter in consumption	0.05	0.017	0.069
ρ	Quantity adjustment coefficient	0.9	0.730	0.816
$\bar{\eta}$	Price adjustment coefficient	0.1	0.165	0.089
μ	Bank's gross mark-up	1.2	1.007	1.377
ζ	Bank's leverage	0.02	0.02	0.016
δ^k	Inventories depreciation rate	0.3	0.078	0.764
γ	Fraction of investing C-firms	0.25	0.326	0.36
θ	Rate of debt reimbursement	0.05	0.033	0.044
ν	Memory parameter in investment	0.5	0.159	0.956
t_w	Tax rate	0.4	0.059	0.02

Table 4.3: Parameter values in three types of calibration.

and quantities in the presence of different random seeds. We follow Delli Gatti and Grazzini in analyzing to tackle this problem. Let y_t represent the level of an aggregate variable (e.g., GDP at constant prices) in period-t generated by the benchmark simulation ($t = 1, 2, ..., 1100$) and $\tilde{y}_t$ period-t GDP generated by the shocked simulation, characterized by the same random seed but an exogenous increase of an exogenous variable or parameter in period $\tau = 1000$. To analyze the macroeconomic effects of the shock, we compute the percent deviation of the shocked GDP from the benchmark GDP:

$$\hat{y}_t = \log \tilde{y}_t - \log y_t$$

Of course, $\hat{y}_t$ is exactly equal to zero for any $t \leq \tau$. After the shock $\hat{y}_t$ is generally different from zero. $\hat{y}_t$ after the shock is the Impulse-Response function associated with a specific random seed. Hence we will refer to $\hat{y}_t$ as a *Seed-specific IR (SIR) function.* The dynamics of $\hat{y}_t$ however does not behave nicely as in standard DSGE models, with a smooth monotonic departure from and return to the steady state. This is due at least in part to the specific random seed. To form a *robust evaluation* of the response of a macroeconomic variable to an aggregate shock in an ABM, we must carry out a number of simulations with different random seeds and compute the average response of the variable in question to the aggregate shock. To build *robust Impulse-Response (IR) functions* we use the following method.

1. We simulate the ABM (over T=1100 periods) with a given set of parameters and exogenous variables with $S = 500$ different random seeds. These are the S benchmark simulations. We denote the benchmark time series of variable y^d (where $d = 1, 2, ..., D$) in simulation s ($s = 1, 2, ..., S$) with $y^d_{s,t}$ where $t = 1, 2, ..., T$.

2. Then, we simulate the ABM with the same seeds as above but with an aggregate

shock in period $\tau < T$. These are the S shocked simulations. We denote the shocked time series of variable y^d in simulation s with $\tilde{y}^d_{s,t}$.

3. We compute S Single-seed Impulse-Response functions, i.e., log differences of the shocked and benchmark time series, for each variable. We denote the SIR of variable y^d in simulation s with $\hat{y}^d_{s,t} = \log \tilde{y}^d_{s,t} - \log y^d_{s,t}$.

4. Finally, we compute the robust Impulse-Response function for each variable as the mean of the single seed impulse response functions across seeds:

$$\bar{y}^d_t = \frac{\sum_{s=1}^{S} \hat{y}^d_{s,t}}{S} \quad t = 1, 2, ..., T$$

In this section we apply the methodology proposed above to our ABM in order to build IRs for $D = 9$ variables: GDP, GDP deflator, gross capital formation, consumption, the unemployment rate, total debt of the corporate sector, the bankruptcy rate (fraction of firms that go bankrupt), total capital stock and bank net worth. We will consider $\Sigma = 3$ aggregate shocks: 2 real shocks (exogenous change of consumption and investment), and 1 nominal shocks (exogenous change of the risk-free interest rate).

To build IRs we simulate the ABM over $T = 1100$ periods $S = 500$ times with different seeds. We generate $S = 500$ benchmark time series for each of the $D = 500$ variables.

Then, we simulate the ABM S times with the same seeds but hitting the economy with an aggregate shock in period $\tau = ...$ We repeat the procedure for each of the Σ shocks. We get $S = ...$ shocked time series for each variable and each shock. Therefore we compute $S = ...$ Seed specific IR functions for each variable and each shock.

Finally, we compute the Robust IR functions (IRs). We take the average of SIRs across random seeds for each variable and each shock. Overall therefore we have $D \times \Sigma = ...$ IRs. Figures show the IRs for 100 periods starting from the period of the shock, together with the 20th and 80th percentiles to account for the variability of the response to the shock.

The dynamic pattern of IRs is generally similar to those of IRs in DSGE models. The shock generates a departure of the variable from the benchmark statistical equilibrium and a return to it with the passing of time. In some cases the return to equilibrium may occur by means of long dampening swings.

The first set of IRs in Figure 4.6 captures the response of 8 variables to a (positive) consumption shock generated by a uniform exogenous increase of permanent income.[10] A shock to permanent income therefore can be interpreted as a sudden change of the

[10] We assume that the permanent income of all workers goes up by 30% in period $\tau = ...$ Permanent income can be interpreted as the expectation the agent holds of her "human capital" in the future (in our setting, this expectations is formed by means of an adaptive rule).

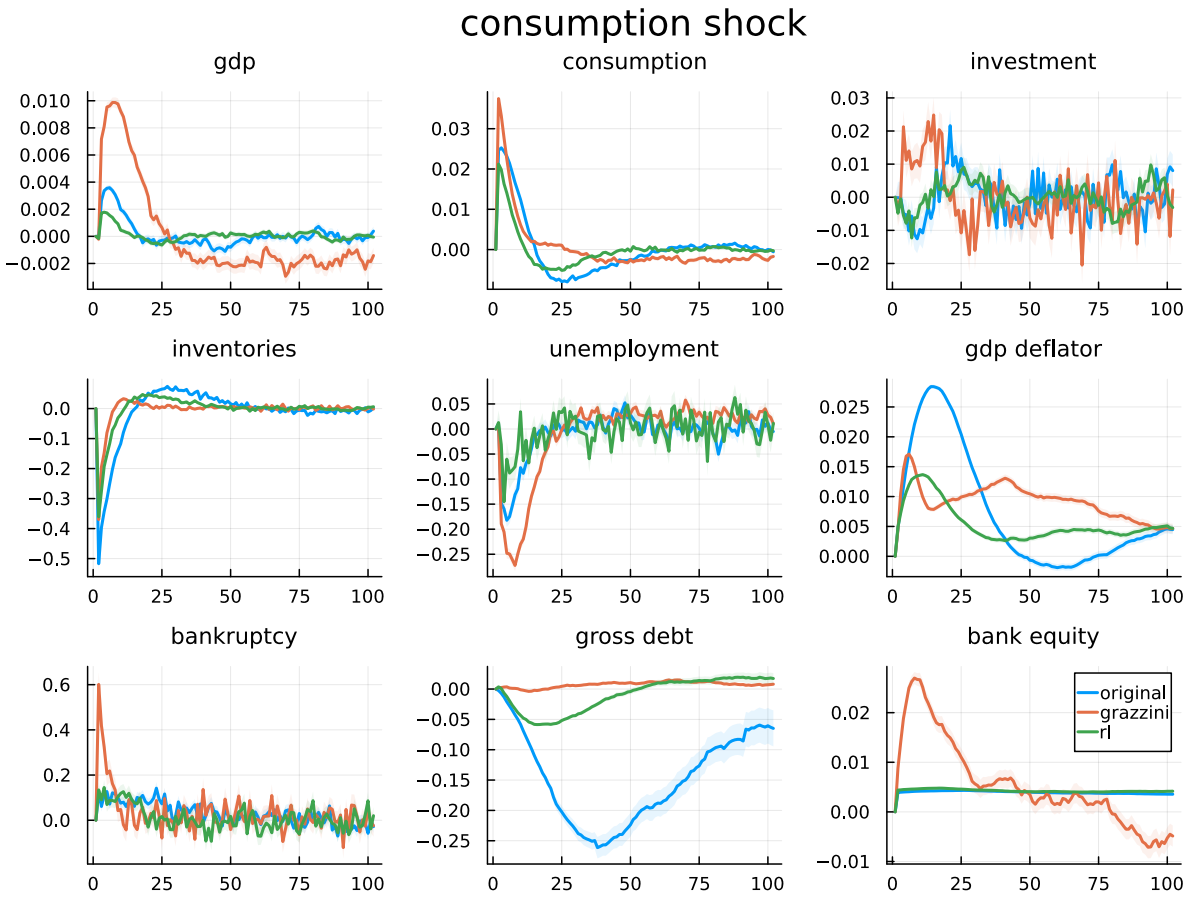

Figure 4.6: Shock to permanent income

agents' expectations of human capital. Consumption increases on impact, since households feel richer and allocate a bigger budget to consumption, and then goes back to the benchmark statistical equilibrium.[11] The increase in consumption has three effects on firms. First, higher demand for consumption goods implies that firms charging higher prices will sell more. This leads to an increase of inflation on impact. Second, higher demand translates into higher revenues, leading to higher profits and a decrease in the bankruptcy rate. Third, firms react to higher consumption by increasing production and employment, so that production increases and the unemployment rate decreases. The effects of the consumption shock on investment and the capital stock are negligible.

The upper-right panel of Figure 4.7 shows the IRs following a (negative) investment shock, i.e., a reduction of the probability to investγ.[12] Thanks to the law of large numbers, it γ can be conceived as the fraction of firms able to adjust their capital stock in each

[11] In the comments that follow we will focus on the short run effects of the shock. To avoid repetitions we will not reiterate that RIRs go back to zero over the long run.

[12] We assume that the probability to invest goes down by 80%. To make the effect of the shock more interesting, we assume that after the shock γ converges back gradually to its benchmark value. In other words, we assume that there is a persistent, rather than temporary, shock to the probability to invest.

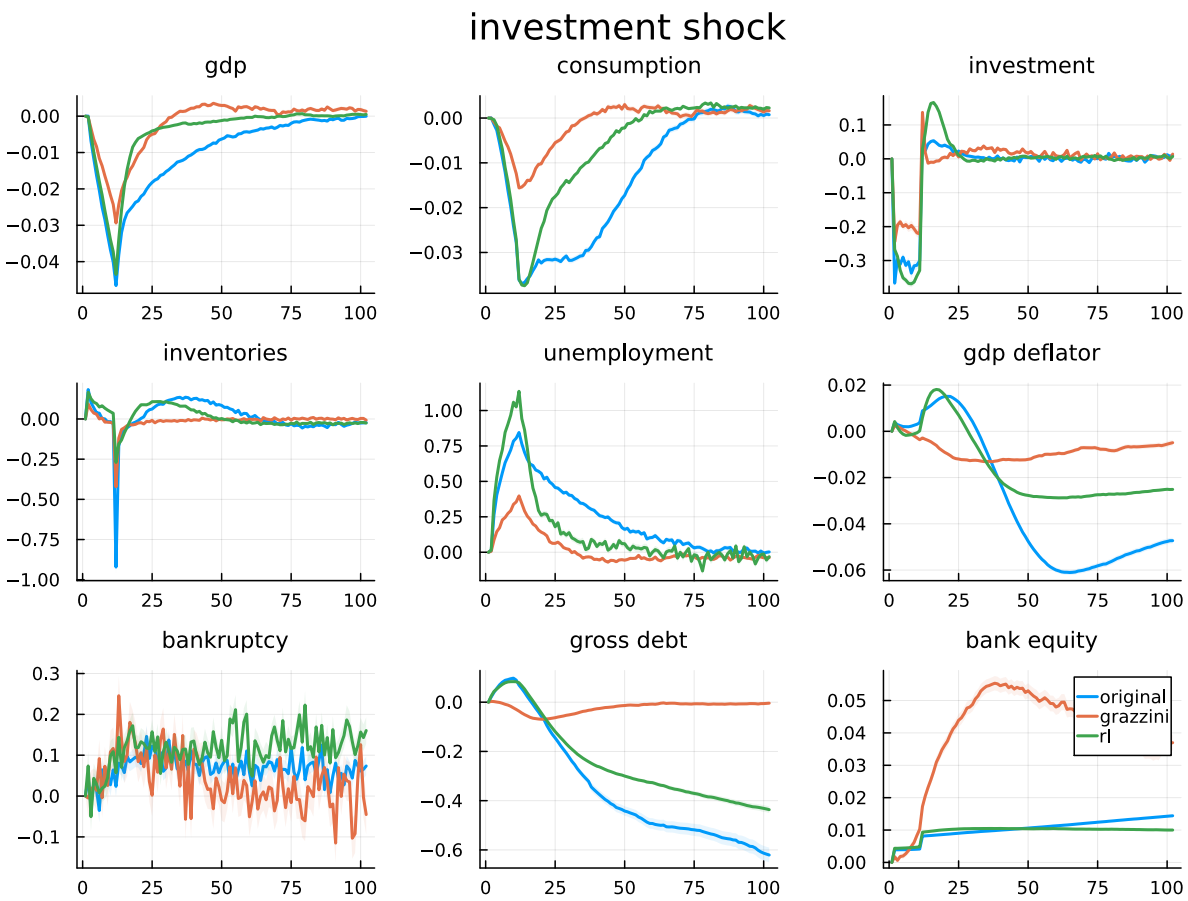

Figure 4.7: Shock to investment parameter gamma

period. It is worth noticing that, given the investment decision described above, when it γ goes down, firms that can adjust their capital stock will invest more, anticipating that it will be less likely for them to be able to invest in the future. Therefore, a reduction of γ makes the number of investing firms shrink but boosts the investment of those firms that are able to invest. The first effect prevails so that the shock will lead to a reduction of gross fixed capital formation and of the capital stock. Production goes down, and the unemployment rate increases. Moreover, the reduction of investment leads to a decrease in corporate debt.

4.9 Conclusions

In this work, we systematically compare the performance of 5 search strategies, taken in isolation and in combination, on a method-of-moments calibration of a standard macroeconomic ABM. Our results show that calibration based on machine learning surrogate samplers of the kind proposed in Lamperti et al. (2018) but using a random forest algorithm for interpolation provides superior performance with respect to the other search

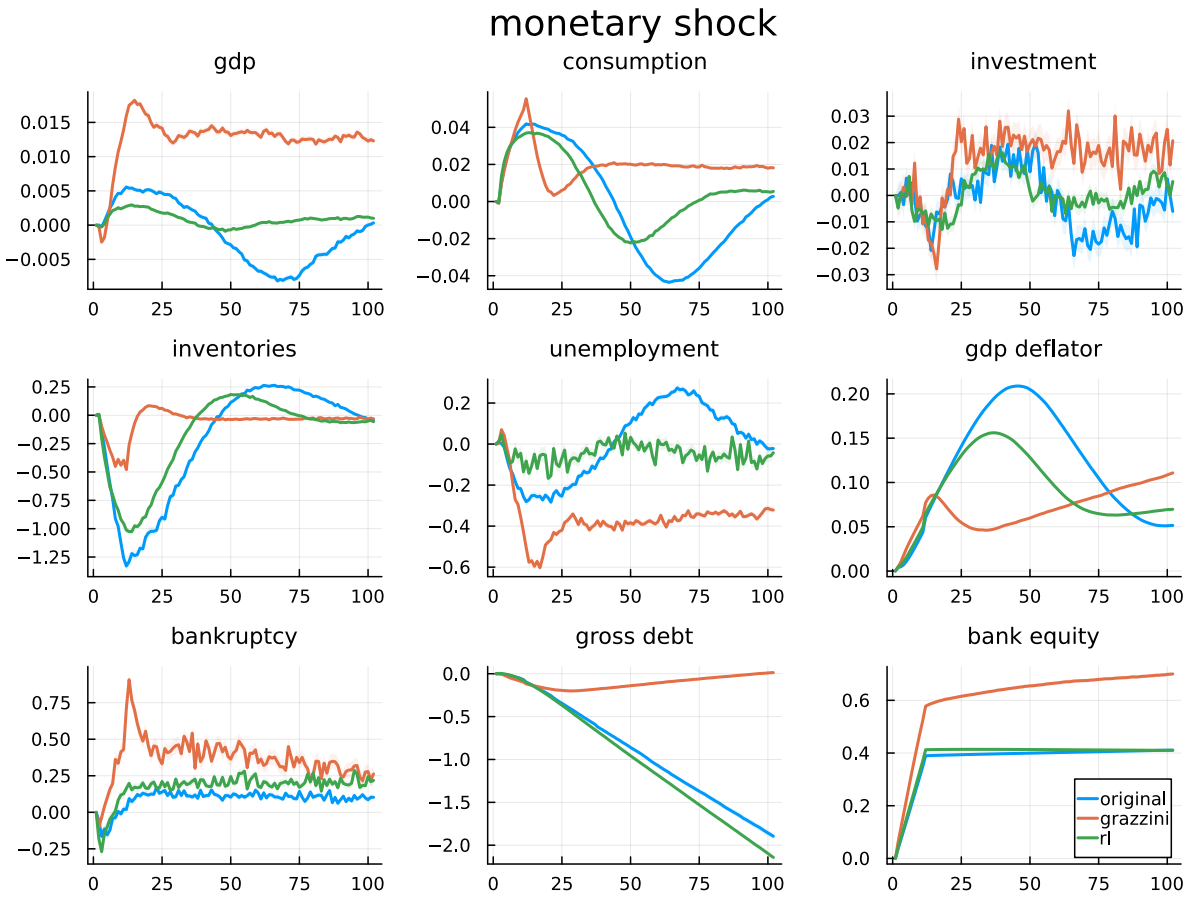

Figure 4.8: Shock to interest rate

methods. Our results further show that coupling different search methods together gives rise to search strategies that typically improve over their constituents. The empirical efficacy of random forest search methods and of combining different search methods can be of practical help to researchers interested in calibrating and using medium and large-scale economic ABMs. However, when combining different search methods a natural issue arises about which methods should be combined, and in which way.

We provide a solution to this issue by framing the choice of search methods as a multi-armed bandit problem, and leveraging a well-known reinforcement learning scheme to select the best method on-the-fly during the course of a single calibration. The RL scheme proposed outperforms any other method or method combination tested, and thus provides a practical tool for researchers interested in efficiently calibrating ABMs.

In the future, it would be interesting to deepen the analyses of the present study in two possible lines of research, based on either extensions of the banchmarking experiments of Section 4.5 or on further investigations into the RL scheme of Section 4.6.

The benchmarking framework could be extended in several dimensions. The first is the testing of other standard search methods, such as particle swarm samplers or machine

learning samplers based on neural networks. The second is the inclusion in the analysis of other measures of goodness of fit, in addition to the method of moments, such as likelihood measures, Bayesian measures Grazzini et al. (2017), or information theoretic measures Lamperti (2018). The third is the addition of other widely known macroeconomic ABMs Dawid and Delli Gatti (2018) to the analysis, such as the so-called "K+S" model Dosi et al. (2010), or the recent large-scale model of Poledna et al. (2023b). This would allow quantitative benchmarking not only of the calibration strategies, but also of the different models when calibrated on the same data. The final direction would involve appropriately increasing the data on which the ABMs are calibrated and tested, potentially with more variables and with more national economies. In essence, while the present work is an important step towards a systematic assessment calibration methods for medium and large-scale economic ABMs, all of the above mentioned directions would surely represent equally important steps towards an increasingly more data-driven ABM development.

Given the excellent results achieved, the RL scheme proposed also deserves further specific investigation. For example, one could verify whether the RL search method developed here maintains its high performance also in the more general setting of black-box function optimisation, perhaps in other specific application domains that might have peculiarities similar to the ABM calibration problem. One might also try to extend the simple (yet effective) MAB framework introduced here, by providing more 'contextual' information to the agent and hence attempting to represent the ABM calibration problem either as an online contextual-MAB problem, or directly as a partially-observable MDP Kaelbling et al. (1998). Potentially, the problem could even be made suited for a pure MDP formulation by feeding the entire history of the past sampled point to the agent that needs to decide on the next search method, or directly decide the specific points to sample as proposed in Chen et al. (2017).

Acknowledgments

D.C. acknowledges funding from the European Union's Horizon 2020 research and innovation programme under the Marie Skłodowska-Curie grant agreement No 956107, "Economic Policy in Complex Environments" (EPOC). We would like to thank Marco Pangallo (CENTAI institute), Herbert Dawid (Bielefeld University), Bence Méro (Bank of Hungary) and the anonymous reviewers of AI4ABM workshop, for early feedback on the manuscript. The views and opinions expressed in this paper are those of the authors and do not necessarily reflect the official policy or position of Banca d'Italia.

Appendices

4.A Extended model description

The model used for our experiments was originally proposed in Assenza et al. (2015), and consists of four classes of interacting agents: households, final-goods producing firms (C-firms), capital producing firms (K-firms) and banks. Figure 5.1a of the main text illustrates these classes of agents and the main mechanisms of interactions among them.

4.A.1 Household

The household sector consists of workers and capitalists. Each worker supplies one unit of labour in-elastically. An unemployed worker randomly selects Z_e firms and takes the job at the firm with a vacant position on a first come first serve basis. Each worker receives wage w until laid off. Firms are owned by capitalists and they receive dividends and hold equity at those firms but do not work. When a firm becomes bankrupt, it is replaced by a new entrant firm and a capitalist provides equity. All of the households consume final goods and therefore participate in search and matching in the consumption market. They determine their consumption budget according to

$$C_{c,t} = \overline{Y}_{c,t} + \chi D_{c,t}, \tag{4.7}$$

where $\overline{Y}_{c,t}$ is the *permanent income* of the consumer c at time t, $D_{c,t}$ is the financial wealth deposited at a bank and $\chi \in (0, 1)$ is the fraction of the bank deposit used for consumption. Unlike the standard macroeconomic models, *permanent income* is the weighted average of current and past incomes with exponentially decaying weights and follows

$$\overline{Y}_{c,t} = \xi \overline{Y}_{c,t-1} + (1 - \xi) Y_{c,t} \tag{4.8}$$

where $Y_{c,t}$ is the actual income of period t and $\xi \in (0, 1)$ is the *memory parameter* of the consumer.

Each consumer visits a set of randomly selected firms and sorts their prices from lowest

to highest (this gives rise to implicit negative relative price elasticity of demand). If the consumption budget is not exhausted on the first firm, the consumer goes to the second firm in the order. If consumption budget is not exhausted after all buying opportunities, the consumer involuntarily saves the rest.

4.A.2 Price and quantity setting

One of the distinctive features of the CATS model is its expectation formation of the future demand and price setting of the firms, summarised in Figure 5.1b of the main text, and detailed in this section. C-firms and K-firms decide the quantity and price in a similar fashion. The only difference between these two is that C-goods are non-storable, unlike K-goods. Firms start off with the pair $(P_{i,t}, Y_{i,t})$ and notice the actual sale $Q_{i,t} = \min(Y_{i,t}, Y^d_{i,t})$ as demanded quantity can differ from produced quantity. Therefore, firms base their decision on two signals: their relative price and actual sale. Now any decision can be mapped to one of the quadrants of the $(P_{i,t}, Y_{i,t})$ space depending on the signal. Hence firm $i \in \{\text{C-firms}, \text{K-firms}\}$ update their next period desired output as

$$Y^*_{i,t+1} = \begin{cases} Y_{i,t} + \rho(-\Delta_{i,t}) - \mathbb{1}_{i\in K} Y^k_{i,t+1} & \text{if } \Delta_{i,t} \leq 0 \;\; P_{i,t} \geq P_t \text{ ('c')} \\ Y_{i,t} - \rho\Delta_{i,t}\mathbb{1}_{i\in K} Y^k_{i,t+1} & \text{if } \Delta_{i,t} > 0 \;\; P_{i,t} < P_t \text{ ('d')} \end{cases} \tag{4.9}$$

where $\Delta_{i,t} = Y_{i,t} - Y^d_{i,t}$, $\rho \in (0,1)$ and $Y^k_{i,t+1} = (1-\delta^k)(Y^k_{i,t} + \Delta_{i,t})$ i.e., the inventory dynamics of capital firms. Here $\delta^k \in (0,1)$ is the depreciation parameter of the inventories.

In short, when demand is higher than the current period's production, increase the next period's production and vice-versa. Notice that in the four possible signal scenarios, depicted in the four quadrants of Figure 5.1b of the main text, firms can only change either prices or adjust their quantities. Equation (5.11) describes quadrants 'c' and 'd' of the figure, for the price setting in the other two scenarios (quadrants 'a' and 'b' of the figure) firms follow the updating rule

$$P_{i,t+1} = \begin{cases} P_{i,t}(1+\eta_{i,t+1}) & \text{if } \Delta_{i,t} \leq 0 \;\; P_{i,t} < P_t \text{ ('a')} \\ P_{i,t}(1-\eta_{i,t+1}) & \text{if } \Delta_{i,t} > 0 \;\; P_{i,t} \geq P_t \text{ ('b')} \end{cases} \tag{4.10}$$

where $\eta_{i,t+1} \sim \mathcal{U}(0, \bar{\eta})$. So when there is excess demand, firms increase their price if it is lower than average, since consumers will be willing to pay a higher price and vice-versa. Firms also have average costs (AC) and can not set the price below the level of AC. C-firms produce taking the output of the K-firms as input and therefore participate in the K-goods market using search and match exactly like in consumption goods market.

4.A.3 Production, investment and employment

Means of production in the C-firms are capital $K_{i,t}$ and labour $N_{i,t}$. The production function follows Leontief technology i.e., $\hat{Y}_{i,t} = \min(\alpha N_{i,t}, \kappa K_{i,t})$ where α and κ are labor and capital productivity respectively. If the labour is abundant and capital is not fully utilized then the output becomes $Y_{i,t} = \omega_{i,t}\hat{Y}_{i,t} = \omega_{i,t}\kappa K_{i,t}$ where $\omega_{i,t} \in (0,1)$ is the *capacity utilization rate*. Therefore the required labor for the production is $N_{i,t} = (\kappa/\alpha)\omega_{i,t}K_{i,t}$. Capital is accumulated by the firms and follows

$$K_{i,t+1} = (1 - \delta\omega_{i,t})K_{i,t} + I_{i,t} \tag{4.11}$$

where only utilized capital depreciates and $I_{i,t}$ is the investment.
Investment opportunities of the firms are infrequent (one in every $1/\gamma$ periods where γ is the fraction of firms adjusting capital) and capital is fixed in the short run. This gives rise to sticky and durable capital, as firms take investment decisions in an uncertain environment before the consumption market opens and this anchors decisions on average lifetime capital stock. The average lifetime capital stock evolves as

$$\overline{K}_{i,t-1} = \nu\overline{K}_{i,t-2} + (1 - \nu)\omega_{i,t-1}K_{i,t-1} \tag{4.12}$$

where $\nu \in (0,1)$.
Firms decide on investment in two parts. Firstly, they make up for the worn-out capital keeping in the mind the future opportunities of capital adjustment i.e $I^r_{i,t} = \frac{\delta}{\gamma}\overline{K}_{i,t-1}$. Secondly, they target the *desired long-term rate of capital utilization* $\overline{\omega}$. Therefore, the total investment of the firm becomes

$$I_{i,t} = \left(\frac{1}{\overline{\omega}} + \frac{\delta}{\gamma}\right)\overline{K}_{i,t-1} - K_{i,t} \tag{4.13}$$

and the capital stock evolves as:

$$K_{i,t+1} = \left(\frac{1}{\overline{\omega}} + \frac{\delta}{\gamma}\right)\overline{K}_{i,t-1} - \delta\omega_{i,t}K_{i,t} \tag{4.14}$$

If the required capital for the desired level of production is lower than the available capital stock, the firm uses a fraction of the stock. If the required capital is higher than the available capital stock, the firm fully utilizes the stock but the level of production is not reached. Following these rules, we get the required number of workers as

$$N^*_{i,t+1} = \min\left(\frac{\kappa}{\alpha}K^*_{i,t+1}, \frac{\kappa}{\alpha}K_{i,t+1}\right), \tag{4.15}$$

where $K^*_{i,t+1}$ is the required capital for desired production level and $K_{i,t+1}$ is the available capital stock.
After deciding on the required number of workers to match the desired level of production, firms post vacancies as follows

$$\nu_{i,t+1} = \max\left(N^*_{i,t+1} - N_{i,t}, 0\right). \tag{4.16}$$

K-firms produce only using labour input from the workers and use linear technology $Y_{j,t} = \alpha N_{j,t}$. Hence labour requirement of the firm is $N_{j,t}/\alpha$. To make up for the required workers, firms post vacancies and compete with C-firms in the labour market for hiring.

4.A.4 Credits and banks

Each firm takes loans from the bank to fund its production when internal funding is in short supply. For C-firms there are typically two costs, the wage of the workers and the funding for investment whereas K-firms only acquire the cost of wage. Hence the required loans by the firms are

$$F_{i,t} = \max\ (wN_{i,t} - \mathbb{1}_{i\in C-firms} P_{k,t-1} I_{i,t} D_{i,t-1}, 0) \tag{4.17}$$

There is only one bank in the economy. It accepts all deposits from agents and does not provide deposit interests. Bank evaluates the financial soundness of the firms using the entire past data of the firm's balance sheet. For each firm f, it computes the following leverage ratio

$$\lambda_{f,t} = \frac{L_{f,t-1} + F_{f,t}}{E_{f,t-1} + L_{f,t-1} + F_{f,t}}. \tag{4.18}$$

The bank then estimates a logistic regression of the individual bankruptcy probability ϕ_f for each firm as $\phi_f = f(\lambda_f)$. Considering that the firms are paying θ fraction of their loan back each period, the bank sets the interest rates of loan for each bank as

$$r_{f,t} = \mu \left\{ \frac{1 + \frac{r}{\theta}}{\Phi(\theta, T_{f,t})} - \theta \right\}, \tag{4.19}$$

where $T_{f,t} = 1/\phi_{f,t}$ i.e., number of periods after which firm defaults. Optimization of the lending is done by considering a maximum admissible loss for the bank as a fraction of the bank's equity. If $\Delta L_{f,t}$ is the new extended loan to the firm then it follows that

$$\phi_f(\Delta L_{f,t} + L_{f,t-1}) \leq \zeta E^b_t, \tag{4.20}$$

and the maximum admissible loan for a firm f becomes

$$\overline{F}_{f,t} = \frac{\zeta E_t^b - \phi_f L_{f,t-1}}{\phi_f}. \tag{4.21}$$

In summary, if the loan requirement of the firm is less than the maximum admissible loan for that firm, the firm gets the full funding. On the other hand, if the loan requirement is higher than the maximum admissible loan, the bank lends only up to the limit and the firm has to cut down its hiring, production etc.

4.B A visual evaluation of length of transient effects

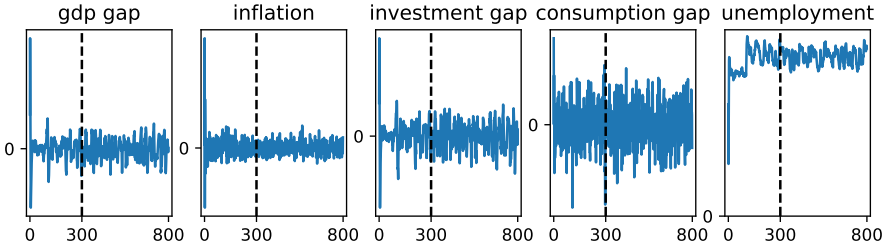

Figure 4.9: A typical simulation trace from the CATS model. The dashed vertical lines mark 300 simulation periods.

Figure 4.9 we report the results of an ABM run for a typical model evaluation with arbitrary initial conditions. We use 300 periods as the initial burn-in period to equilibrate the model. This differs from choice made in the original paper Assenza et al. (2015), where 1000 periods are used to this aim, but we believe our choice to be fully justified considering that 300 periods appeared more than sufficient for a complete equilibration of the model. As a practical illustration of this claim, Figure 4.9 well illustrates that transient effects are substantial only within the first 100 periods, and are typically absent already after 200 periods.

4.C A comparison of multiple MAB learning algorithms

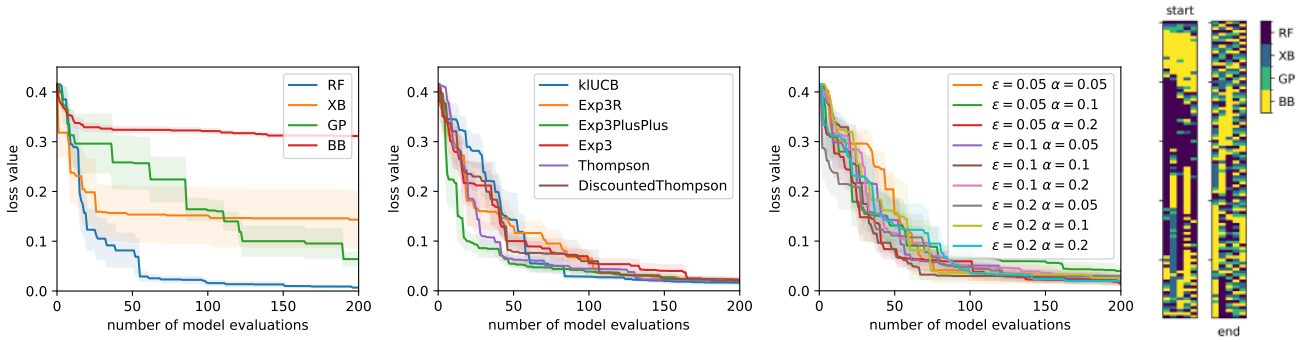

(a) (b) (c) (d)

Figure 4.10: Tests of the RL calibration framework with different MAB learning algorithms. (a)-(c) Loss values as a function of the number of model evaluations for different sampling strategies. Lines and shaded areas represent means and standard errors over 5 repetitions of each calibration run. (a) Baseline calibrations using the 4 different samplers individually. (b) RL calibrations using 6 different MAB learning algorithms. (c) RL calibrations using the fixed-α, ϵ-greedy learning algorithm proposed in the main text. (d) The specific 'actions' selected by the fixed-α, ϵ-greedy RL scheme with $\alpha = \epsilon = 0.1$ in the 5 calibration repetitions.

In this appendix, we test the performance of a number of variations of the RL framework introduced in the main text obtained by coupling it with different learning algorithms for multi-armed bandits (MABs). For reasons of computational cost, the comparison is performed in a simplified setting, and not on the calibration of the economic ABM analysed in the rest of this work. The experimental setting consists of a method of moments calibration of a 5-state Markov process defined by a diagonal transition matrix, with 5 free parameters to calibrate. The target time series is generated by simulating the model for 5000 steps with diagonal transition parameters $(0.1, 0.2, 0.3, 0.4, 0.5)$. We define the action space of the MAB as the set of the 4 samplers (RF,XB,GP,BB).

Figure 4.10a shows the baseline calibrations obtained using the 4 samplers individually, and we see that also for this model the RF sampler outperforms all other search methods. Figure 4.10b shows several RL calibrations obtained by couopling the RL framework described in the main text with the following MAB learning algorithms, all available through the *SMPyBandits* package Besson (2018): 'kl-UCB' Garivier and Cappé (2011), 'Exp3' Bubeck et al. (2012), 'Exp3.R' Allesiardo and Féraud (2015) and 'Exp3++' Seldin and Slivkins (2014), 'Thompson' and 'Discounted Thompson' sampling Raj and Kalyani (2017). All of the learning schemes achieve satisfactory results by outperforming all suboptimal samplers, and performing on par with the RF sampler, but without any prior

information about the best sampler at the agent's disposal. Figure 4.10c shows the RL calibration obtained using the ϵ-greedy scheme proposed and tested also in the main text, for different choices of ϵ and α. The ϵ-greedy scheme is also seen to outperform all single samplers of Figure 4.10a except the optimal one, and its performance is found to be very similar to those of the other algorithms tested in Figure 4.10c.

Figure 4.10d depicts the actions selected during the 5 runs pertaining to the ϵ-greedy calibration with $\epsilon = \alpha = 0.1$. Some patterns are clearly visible, such as the preferential choice of the BB sampler and the RF sampler, particularly in the first half of the calibration where the loss decreases rapidly before reaching a plateau.

4.D A check of robustness to changes in the model and in the loss function

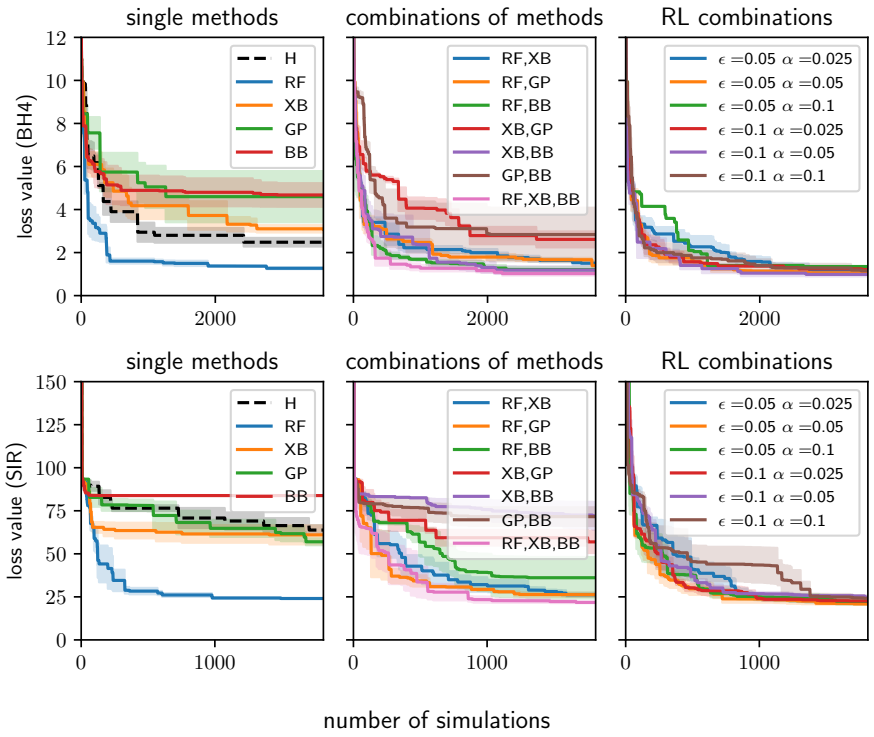

Figure 4.11: Loss as a function of the number of model evaluations for single methods, simple method combinations, and RL method combinations, for the BH4 model Brock and Hommes (1998) with a method of moments loss (1st row) and for the SIR model with a Euclidean loss (2nd row).

Here, we check the robustness of our results by performing further numerical experiments on two different models, and in one case using a different loss function. As a first model, we chose the asset pricing model of Brock and Hommes (1998), a paradigmatic model within the ABM community often used to test novel calibration or estimation algorithms Platt (2020). The calibration was performed on synthetic data generated with the following set of parameters: $r = 0.1$, $\beta = 1.0$, $\sigma = 1.0$, $[g_1, g_2, g_3, g_4] = [0.0, 0.9, 0.9, 1.01]$, and $[b_1, b_2, b_3, b_4] = [0.0, 0.2, -0.2, 0.0]$. The loss function was the same used for the calibration of the CATS model i.e., a method-of-moments loss. As a second model, we chose a SIR model on a Watts-Strogatz network Simoes et al. (2008), Watts and Strogatz (1998), fitted on weakly Italian Covid-19 epidemiological data. For the second model, we used a different loss function: a simple squared difference between the two series.

The first and second rows of plots in Figure 4.11 report the results of these new numerical experiments for the 'Brock and Hommes' model with 4 agent types (BH4) and for the SIR model, respectively. We observe that similar considerations can be drawn

for such models to the ones already expressed for the CATS model. Specifically, we see that when methods are used in isolation, the best-performing ones are the RFand the XBwhile GPand BBstrongly underperform for the reasons discussed in the main text. We also notice a similar general improvement when coupling search methods, with the best-performing method combinations being RFand BBcombined with the BBsampler. Both models are, however, much simpler to calibrate than the CATS model. For such simple calibration tasks, we do not see large improvements in using RL combinations over simple combinations, but, importantly, the RL performance is as good as the best combinations without requiring trial and error.

4.E Data and code availability

In the interest of reproducibility, the code, the data, and the scripts used to generate the key results and the main graphs of this work are available to download as supplementary material of the paper. Furthermore, an easy-to-use implementation of the reinforcement learning scheduler proposed in this work has been released in open source within the *Black-it* package Benedetti et al. (2022), a Jupyter notebook to experiment with it is available at `https://github.com/bancaditalia/black-it/blob/main/examples/RL_to_combine_search_methods.ipynb`.

Chapter 5

An Agent-Based Model of Central Bank Digital Currency[1]

5.1 Introduction

The history of payment methods stretches back approximately 12,000 years, encompassing a vast array of diverse systems that have evolved and dissipated over time. While thousands of payment methods have existed throughout human history, the majority have faded into obscurity, reflecting the dynamic nature of economic systems and societal needs. Despite the passage of millennia, the fundamental purpose of these payment methods remains consistent: facilitating the exchange of goods and services among buyers and sellers. Remarkably, among the ancient and modern payment methods, cash retains a remarkable resilience and widespread popularity. Khiaonarong and Humphrey (2023) note its enduring significance and substantial circulation worldwide. The tangible nature of cash and its universal acceptance in transactions highlight its enduring relevance in contemporary commerce. In an era characterized by rapid digital transformation, understanding the factors influencing the adoption and usage of various payment methods becomes increasingly crucial. The coexistence of traditional cash transactions alongside emerging digital payment systems underscores the complexity of consumer preferences and institutional dynamics in the modern financial landscape. The success of a payment method hinges on a multitude of factors that contribute to its utility for users. Among these factors, ease of usage, cost-effectiveness, and security stand out as paramount considerations. Adrian and Mancini-Griffoli (2021) offer a comprehensive examination of these factors within the context of the modern era of digitization, shedding light on the evolving landscape of payment methods and their implications for users and financial systems. As the global financial landscape evolves, major central banks are actively engaged in the development,

[1] This chapter is co-authored with Aldo Glielmo and Domenico Delli Gatti

discussion, and planning of Central Bank Digital Currencies (CBDCs), as reported by Auer et al. (2022). This heightened focus on CBDCs amplifies the significance of understanding the dynamics of payment method adoption and usage in the contemporary context. The potential integration of CBDCs into mainstream financial systems introduces novel considerations regarding financial inclusion, technological infrastructure, and regulatory frameworks. In light of these developments, exploring the factors driving the adoption and diffusion of payment methods remains essential for policymakers, financial institutions, and individuals navigating the evolving terrain of modern finance.

In this paper, we mainly focus on several policy questions contributing to the ongoing research on CBDC that several central banks deem important, such as (a) under what design features of the CBDC is it widely adopted across the economy? (b) How are profit margins of banks affected by the introduction of CBDC? (c) What are the transmission channels of the new payment method to the real economy? (d) How does speed of adoption affect the economy? In order to shed light on the aforementioned questions, we constitute a macroeconomic agent-based model (ABM) of payment method adoption built up on Assenza et al. (2015). Agent-based macroeconomic models are becoming workhorse models for studying monetary policy, fiscal policy, and energy economics from a *bottom-up* approach, as noted by Gatti et al. (2011). These models are often accompanied by a characteristic property widely known as *emergent behavior,* which is a result of the interaction of agents. Granularity of the interactions provides a great framework to study the markets of methods of payments and their effect on the economy as a result of interactions between agents participating in those markets. For example, Alexandre et al. (2023) studied a bank-firm credit network, producing stylized facts about how shocks to the policy interest rate impact key topological measures of those networks. In Reale (2024) she analyzed an interbank market using a stock-flow consistent agent-based model following Lengnick (2013). Her results showed that divergent maturity mismatches between surplus and deficit banks could lead to uneven funding tensions, potentially preceding explanations related to credit and sovereign risk in interbank dynamics. Application of ABMs has been well established in the studies of climate change and energy market-related topics and their implications on the macroeconomy. Balint et al. (2017) provides a great overview of the literature on applications of ABMs and has produced valuable insights for climate-change-related topics. Ciola et al. (2023) built an ABM model in line with Assenza et al. (2015) to study transmission of energy shocks in the US and find the contractionary effect of the shocks.

5.2 Literature overview

Our paper contributes to the expanding body of literature on CBDC, with emphasis on their adoption and their impact on existing payment infrastructure. For instance, Brunnermeier et al. (2022) construct a framework in which digital platforms distribute tokens as a form of payment while deriving rents, such as fees or seigniorage. Customers embrace these tokens due to network effects: the acceptability of trading tokens presently stems from their future purchasing potential. CBDC, as a universally recognized payment medium, vies with private tokens and curtails the market dominance of platforms. Williamson (2022) shows using a banking and payment model that the interest-bearing nature of CBDC does not confer an advantage, as its substitution for physical currency fails to broaden the feasible range of equilibrium allocations. However, CBDC holds the potential to enhance societal well-being by contesting private payment methods and reallocating secure assets from the private banking realm to a quasi-narrow banking facility. Goldstein et al. (2023) studied the implication of CBDC introduction and the tension between its role as a medium of exchange and store of value. Their theory explains why payments often experience delays and disruptions, even as technology advances, due to the scarcity of valuable reserve assets beyond transactional use. Thus, the central bank might need to reconsider the reserve system that it operates in and the potential effects of a new payment method where agents have access to their balance sheet. Using a two-sided market model of payments, Tan (2023) established that adoption of CBDC for firms and households is complementary. Lower cost and efficiency are important factors for households when considering the adoption, while for the firms, they care more about low fees, tax exemptions, etc. They report that CBDC adoption can attain low adoption equilibrium if the attributes of CBDC not contingent upon merchant acceptance, such as remuneration and the efficacy of cross-border and government payments, are not compelling enough. This scenario may also arise if the subset of households benefiting from these attributes represents a small fraction of the merchant's clientele. Huynh et al. (2022) explored another factor involved in the two-sided market for payment methods where *informed* and *uninformed* transactions matter for the equilibrium effects. While transaction costs have a negative effect on adoption in their estimated model, higher acceptance of a payment method by firms has a positive effect on adoption of it by consumers. Welfare analysis in their model shows that when the issuer has a monopoly, optimal and full pass-through of interchange fees produces different welfare-maximizing levels of fee reduction. In a different approach to understanding the adoption of CBDC, Arifovic et al. (2023) built an experimental setup with consumers and merchants. Their results show that a minimal fixed cost encourages swift adoption of the novel payment method across all participants. Conversely, with sufficiently high fixed costs, merchants progressively opt to

decline the new payment method. Furthermore, compelling evidence of network effects emerges, highlighting the significance of fixed costs in driving robust adjustments in seller acceptance decisions in response to buyer adoption decisions. In a similar approach of experimental setup with remunerated *sophisticated tokens* and unremunerated *plain tokens*, Camera (2022) showed that sophisticated tokens reduce coordination and decrease payoff. Interest-bearing sophisticated tokens incentivize hoarding, causing a shift towards myopic behavior, illiquidity, and hampered circulation, while penalties for holding sophisticated tokens reduce their acceptance as a payment method. Ryu and Webb (2023) uses a two-period overlapping generation model to analyze consequences of payment choices and asset allocation. They find that changes in the CBDC rate have no impact on commercial banks' profitability in the loan sector, whereas fluctuations in the Interest on Reserves (IOR) rate affect profitability in both deposit and loan sectors. Appropriate CBDC interest rates can foster a balance among cash, CBDC, and deposit utilization, while the crowding-out effect intensifies when the CBDC rate surpasses a certain threshold.

Our paper is closely aligned with a handful of studies employing ABM frameworks to explore the multifaceted impacts of introducing CBDC on the economy. For example, Ramadiah et al. (2021) considers an *online* and *offline* market of payments and finds that if CBDC is properly designed, bank balance sheets would be impervious to it. On the other hand, payment intermediaries will see a fall in transactional revenues. León et al. (2025) provides a more detailed contribution to the adoption narrative. Calibrating their ABM of payment transactions to the Spanish market, they find that attractive design features and targeted stimulus policies are key drivers of CBDC uptake, reinforcing the claims made by Tan (2023). The main difference between their adoption mechanism and ours is that they assume a random allocation of CBDC to consumers, whereas in our framework consumers adopt CBDC through an optimized decision based on the perceived properties of payment instruments—such as security, privacy, and ease of use. While positive spread of remuneration encourages adoption, balance limits are functional for thwarting full-scale crowding-out effect of CBDC. Gross and Letizia (2023) uses reinforcement learning for banks learning Nash equilibria in the deposit market in an ABM framework. Their results show that central banks income could increase due to a drop in excess reserves and increasing lending to banks, while banks will be negatively affected due to deposit losses. While all these existing studies in the ABM framework have primarily focused on adoption and payment markets, they have not extensively explored the analysis of macroeconomic effects. Consequently, our paper distinguishes itself by addressing this critical gap. By integrating the microfoundation of payments and adoption with the macroeconomic ramifications of merchant and consumer interactions, our research endeavors to provide a comprehensive understanding of the broader economic

implications. In doing so, we aim to contribute to a more holistic comprehension of the dynamics between individual adoption decisions and their aggregate impact on the macroeconomy.

5.3 Model description

We introduce CBDC in our baseline model, which closely follows Assenza et al. (2015). The entire duration of the simulation is thus divided into two sub-periods, i.e., before and after the introduction of CBDC. Consumers can now be labeled as *users* and *non-users* subject to the adoption of CBDC. The adoption mechanism is described in one of the following sections. When CBDC is introduced, it becomes an additional payment instrument in the already existing set of payment instruments consisting of cash and deposit. [2] Thus, in our model, agents perform portfolio allocation based on 2 instruments, i.e., cash and deposit. Post-CBDC introduction, agents perform portfolio allocation based on 3 instruments, i.e., cash, deposit, and CBDC.

5.3.1 Household

The household sector consists of workers and capitalists. Each worker supplies one unit of labor inelastically. An unemployed worker randomly selects Z_e firms (where Z_e is a subset of the total firms i.e. sum of capital and consumer firms in the model) and takes the job at the firm with a vacant position on a first-come, first-served basis. Each worker receives a wage w_t until laid off. Firms are owned by capitalists, and they receive dividends and hold equity at those firms but do not work. When a firm becomes bankrupt, it is replaced by a new entrant firm, and a capitalist provides equity. A household h has the following nominal income depending on its type:

$$Y_{h,t} = \begin{cases} w_t & \text{if worker} \\ \tau DIV_{f,t-1} & \text{if firm owner} \end{cases} \tag{5.1}$$

All of the households consume final goods and therefore participate in search and matching in the consumption market. They determine their consumption budget according to

$$C_{h,t} = \overline{Y}_{h,t} + \chi(D_{h,t} + W_{h,t}^{CBDC} + W_{h,t}^{Cash}) \tag{5.2}$$

[2] Kevin et al. (2022) reports 8 available payment instruments for the USA. These are cash, check, money order, debit card, credit card, prepaid card, bank account number payment, and online banking bill payment. Among these, cash, check, and money order are considered paper instruments, and we refer to all of these as cash payment methods for simplicity. We consider rest of the payment instruments as deposit payment instruments for simplicity since they require direct interaction with bank account while issuing the payment.

where $\overline{Y}_{h,t}$ is the *permanent income* of the consumer c at time t, $D_{h,t}$ is the financial wealth is deposited at a bank, $\chi \in (0,1)$ the fraction of the bank deposit used for consumption, and $W_{h,t}^{CBDC}, W_{h,t}^{Cash}$ the wallets of CBDC and cash. Therefore, households take into account bank deposits and balances in the wallets of CBDC and cash while deciding on a consumption budget. Here we use "consumer" and "household" interchangeably since all types of households consume and participate in the consumption goods market. Unlike the standard macroeconomic models, *permanent income* is the weighted average of current and past incomes with exponentially decaying weights and follows

$$\overline{Y}_{h,t} = \xi \overline{Y}_{h,t-1} + (1-\xi) Y_{h,t} \tag{5.3}$$

where $Y_{h,t}$ the actual income of the period is t and $\xi \in (0,1)$ is the *memory parameter* of the consumer.

Consumers may not spend the entire consumption budget due to existing frictions in the consumption goods market. Every consumer randomly selects a group of firms to visit and arranges their prices in ascending order, creating an implicit negative relative price elasticity of demand. If the consumer doesn't spend their entire budget at the first firm, they proceed to the next in line. If there's still budget left after exploring all buying options, the consumer involuntarily saves the remainder. We provide much detailed analysis of the matching protocol in 5.3.3

Household's decision of payment instrument and CBDC adoption

The model combines optimizing behavior with simple behavioral rules, and it is therefore important to clarify the underlying notion of rationality we adopt. Consumers are assumed to behave with procedural rationality in the sense of Simon: they optimize over choices that are routine, frequent, and supported by well-defined preferences, namely the allocation of payment features and instruments in the CES framework, while relying on heuristics when facing decisions that are novel, infrequent, or subject to significant uncertainty (Simon (1976, 1978)). The optimization of payment features captures stable transactional preferences for security, privacy, and convenience, for which consumers are assumed to have sufficient experience to form consistent evaluations. By contrast, CBDC adoption is modeled through a threshold rule with gradual updating, reflecting that adoption of a new technology is characterized by limited information, habit formation, and social diffusion rather than fully informed maximization. This mixed approach is consistent with the broader literature on bounded and procedural rationality in macro-behavioral and agent-based models, where agents often solve local optimization problems but follow simple rules for expectations or adoption dynamics (e.g., Visco and Zevi (2020); Borsos

et al. (2025); Tsiatsios et al. (2023)). In this sense, the heterogeneity in behavioral rules is not accidental but corresponds to differences in the cognitive demands and information environments of the underlying decisions.

Choice of payment instrument There are 4 payment features in our model that the consumers consider while deciding which payment instrument to use. These are namely security, privacy, convenience, and peer effect. Each consumer solves a nested Constant-Elasticity of Substitution (CES) utility function before going to the final-goods market. In the first step they maximize each element of the $\boldsymbol{P}$ which is a $K \times 1$ vector of features. They are optimizing the following problem,

$$\begin{aligned} &\max_{\boldsymbol{P}} \left(\alpha_1 p_1^{-\gamma} + \alpha_2 p_2^{-\gamma} + \cdots + \alpha_K p_K^{-\gamma}\right)^{-\frac{1}{\gamma}} \\ &\text{subject to } \; p_1 + p_2 + \cdots + p_K = P \end{aligned} \tag{5.4}$$

where P is the total value of the payment in dollars to be made. This optimization problem of the consumers can be thought of as if they are choosing what fraction of their entire requirement of payment in terms of value they need to be secure, what fraction of payment is needed to remain private, etc. The solution of the above problem is

$$p_i^* = \frac{P}{\sum_{j=1}^{K} \left(\frac{\alpha_i}{\alpha_j}\right)^{-\frac{1}{\gamma+1}}} \tag{5.5}$$

Now consider $\boldsymbol{P}$ a linear combination of N payment instruments $m_i, \; i = 1, \cdots, N$ i.e. $\boldsymbol{P} = \boldsymbol{\Theta M}$ where $\boldsymbol{\Theta}$ is a $K \times N$ matrix of coefficients and $\boldsymbol{M}$ is a $N \times 1$ vector of instruments. This $\boldsymbol{\Theta}$ matrix is a combination of design features of the payment instruments and consumers' perception of features attributed to each instrument. In our model, $K = 4$ and $N = 3$. Since we are considering payment features that are constructed through the survey of the consumers, the ranking of these should be understood in relative terms. Take, for example, security and privacy. These two are subjective features that are perceived differently across consumers, but they consider privacy to be an advantageous feature of cash (ECB). The second stage of the optimization involves choosing the optimal level of instrument given the choices of the features. Thus, K allocations that are a function of policy choices $\Theta_{i,n}$ and the previously optimized allocation of features p_i^* are obtained by solving the following problem:

$$\begin{aligned} &\max \left(\Theta_{i1} m_{i1}^{-\gamma_2} + \Theta_{i2} m_{i2}^{-\gamma_2} + \cdots + \Theta_{iN} m_{iN}^{-\gamma_2}\right)^{-\frac{1}{\gamma_2}} \\ &\text{subject to } \; m_{i1} + m_{i2} + \cdots + m_{iN} = p_i^* \end{aligned} \tag{5.6}$$

The solution to the above problem is

$$m_{in}^{*} = \frac{p_i^{*}}{\sum_{m=1}^{N} \left(\frac{\Theta_{in}}{\Theta_{im}}\right)^{-\frac{1}{\gamma_2+1}}} \tag{5.7}$$

Hence the final allocation to a means of payment n is the sum of all allocations of that instrument across all features, i.e.,

$$m_n^{*} = \sum_{i=1}^{K} m_{in} \tag{5.8}$$

The objective of the optimization problem can be interpreted in the following way. Imagine one has to spend a certain amount of money in order to buy consumption goods. Ideally it would not matter which payment instrument to use unless different instruments follow different units of account. Nonetheless, many different methods of payment coexist for various reasons. Those reasons are what we are mentioning as *features* . Now these *features* are certain attributes independent of methods of payment, but each method of payment shares each of these *features* to different degrees. A consumer derives utility from these *features,* as they provide some transactional services.

Adoption of CBDC After the introduction of CBDC by the central bank, it will become widely available in that concerning economy. Thus, adoption of CBDC would typically depend on how a consumer sees its worth in terms of making transactions. Our framework for *feature optimization* provides a suitable tool to understand the adoption. For each time period t consumers have a set of optimal allocations of payment instruments, i.e., $\{m_{t,cash}^{*}, m_{t,deposit}^{*}, m_{t,cbdc}^{*}\}$ which denotes the fraction of consumption budget they would like to spend using the respective method of payment. If the allocation is in CBDC $m_{t,cbdc}^{*} > 0.1 = \overline{m}_{cbdc}$ in the long run, consumers will adopt CBDC and start using it for transactional purposes. We do not consider the possibility of riddance of CBDC. Therefore, once onboarding of the consumer has happened, he keeps using it even if it is $m_{t,cbdc}^{*} < 0.1$ for him in a certain period in the future. At the initialization, we keep this threshold very high (~ 1) but gradually decrease it to our desired level of threshold for 0.1 following an AR (1) process.

$$\overline{m}_{t,cbdc} = 0.1(1-\rho_m) + \rho_m \overline{m}_{t-1,cbdc} + \epsilon_t \tag{5.9}$$

The parameter ρ_m captures the speed with which the threshold converges to the desired threshold value $\overline{m}_{cbdc}$. Higher ρ_m would translate into slower convergence, causing slower adoption of CBDC.

Updating Cash and CBDC wallet

Once a consumer h has decided upon its consumption budget $C_{h,t}$ and optimal allocation of payment instruments$\{m^*_{t,cash}, m^*_{t,deposit}, m^*_{t,cbdc}\}$, it needs to replenish the cash and CBDC wallets if the balances in these wallets are not sufficient to perform the required transactions. Therefore, consumers need to make sure it has at least $m^*_{t,cbdc}C_{h,t}$ as much balance in the CBDC wallet $m^*_{t,cash}C_{h,t}$ as in the cash wallet. The required funds are taken from the bank account of the concerned household. The updating can be expressed as follows:

$$W^j_{h,t+1} = W^j_{h,t} + \max\left(m^*_{t,j}C_{h,t} - W^j_{h,t}, 0\right) \qquad \text{where } j = \{Cash, CBDC\} \tag{5.10}$$

Notice that the household will always have sufficient funds for spending using the deposit $m^*_{t,deposit}C_{h,t} < C_{h,t} < D_{h,t}$ as long as *permanent income* is low. We do not allow for consumer credit in our model. Therefore, the desired level of consumption cannot exceed the available wealth and income of the household.

5.3.2 Price and quantity setting

A distinguishing characteristic of the CATS model lies in its unique approach to forecasting future demand and establishing prices for firms. Both C-firms and K-firms follow analogous procedures in determining quantity and pricing. The primary distinction between these two lies in the nature of their goods, as C-goods are non-storable, unlike K-goods, and C-firms consider the pass-through of the cost of new payment instruments. Before the introduction of the CBDC, firms set prices and quantities in the following manner: they start off with the pair $(P_{i,t}, Y_{i,t})$ and notice the actual sale, $Q_{i,t} = \min(Y_{i,t}, Y^d_{i,t})$ as demanded quantity can differ from produced quantity. Therefore, the relative price of the consumption goods and the actual sale are the basis for the firm's decision-making. Now any decision can be mapped to one of the quadrants of the $(P_{i,t}, Y_{i,t})$ space depending on the signal from the competing firms. Firms $i \in \{\text{C-firms}, \text{K-firms}\}$ update their next period's desired output as

$$Y^*_{i,t+1} = \begin{cases} Y_{i,t} + \rho(-\Delta_{i,t}) - \mathbb{1}_{i\in K}Y^k_{i,t+1} & \text{if } \Delta_{i,t} \leq 0 \;\; P_{i,t} \geq P_t(\text{`c'}) \\ Y_{i,t} - \rho\Delta_{i,t}\mathbb{1}_{i\in K}Y^k_{i,t+1} & \text{if } \Delta_{i,t} > 0 \;\; P_{i,t} < P_t(\text{`d'}) \end{cases} \tag{5.11}$$

where$\Delta_{i,t} = Y_{i,t} - Y^d_{i,t}$, $\rho \in (0,1)$ $Y^k_{i,t+1} = (1-\delta^k)(Y^k_{i,t} + \Delta_{i,t})$ i.e., the inventory dynamics of capital firms. Here $\delta^k \in (0,1)$ is the depreciation parameter of the inventories. The parameter ρ controls the effect of the output forecasting error of that firm. The expected

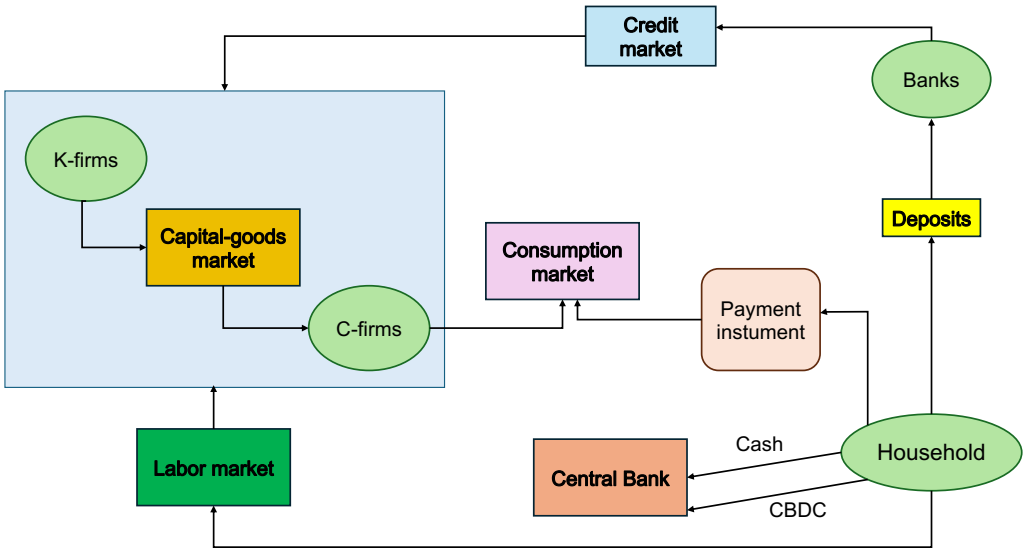

(a)

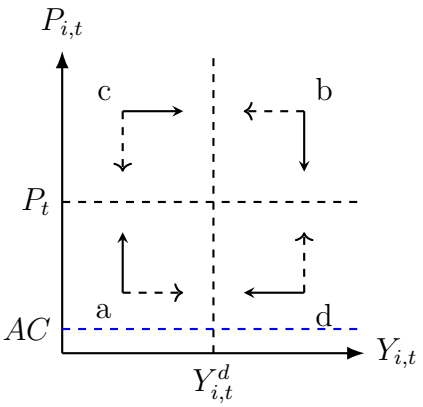

(b)

Figure 5.1: The CATS-CBDC model. (a) An illustration of the agent classes of the model and their interactions. Agent classes are represented in green ovals, interaction types are specified in rectangles, and markets are specified in yellow rectangles. The directions of the arrows indicate the flow of the specific good, e.g., consumption goods are acquired by households from C-firms, while labor is acquired by firms from households. The payment instrument block represents the transactions in between households and C-firms in the consumption market. A household holds CBDC, cash, and deposit as payment instruments. The arrows with cash, CBDC and deposits are directed from households to the bank and central bank because households hold deposits at the bank and holds cash and CBDC at the central bank (meaning these are the liabilities of the central bank). (b) An illustration of the firms' decisions on the price-quantity space. Prices $P_{i,t}$ and quantities $Y_{i,t}$ of goods are updated following the 4 solid black arrows (representing Equations (5.15) and (5.11)), and not the dashed black arrows. The dashed blue line is the minimum price they can charge, corresponding to the average cost for production.

future demand of the firm follows an adaptive rule:

$$Y^e_{i,t+1} = Y^e_{i,t} + \rho(Y^d_{i,t} - Y^e_{i,t}) \tag{5.12}$$

Therefore, the expected demand of the firm is the weighted average of the current and past quantities with exponentially decaying weights.

In short, when demand is higher than the current period's production, increase the next period's production and vice versa. Notice that in the four possible signal scenarios, depicted in the four quadrants of Figure 5.1b of the main text, firms can only change either prices or adjust their quantities. Equation (5.11) describes quadrants 'c' and 'd' of the figure; for the price setting in the other two scenarios (quadrants 'a' and 'b' of the figure), firms follow the updating rule

$$P_{i,t+1} = \begin{cases} P_{i,t}(1+\eta_{i,t+1}) & \text{if } \Delta_{i,t} \leq 0 \;\; P_{i,t} < P_t \text{ ('a')} \\ P_{i,t}(1-\eta_{i,t+1}) & \text{if } \Delta_{i,t} > 0 \;\; P_{i,t} \geq P_t \text{ ('b')} \end{cases} \tag{5.13}$$

where $\eta_{i,t+1} \sim \mathcal{U}(0, \bar{\eta})$. So when there is excess demand, firms increase their price if it is lower than average, since consumers will be willing to pay a higher price, and vice versa. Firms also have average costs (AC) and cannot set the price below the level of AC. C-firms produce, taking the output of the K-firms as input, and therefore participate in the K-goods market using search and match exactly like in the consumption goods market.

The introduction of CBDC as a new payment instrument brings adoption and adjustment costs for merchants. These costs are not meant to represent a permanent pecuniary fee but the short-run frictions associated with integrating an unfamiliar technology, upgrading infrastructure, training staff, and adapting internal processes. As noted by Hall (2004), such transitional burdens are typical in the diffusion of new technologies, and Désiré Kanga and Murinde (2022) delivers evidence that fintech adoption across countries proceeds slowly and unevenly, with measurable effects on long-run economic outcomes.

In this context, firms in our model perceive CBDC adoption as a potentially disruptive process and adjust their pricing strategies to compensate for temporary setbacks. This assumption is consistent with empirical evidence of merchant pass-through of payment-related costs in North America (Stavins et al., 2023). Accordingly, after CBDC is introduced, the pricing mechanism of C-firms changes to incorporate the expected short-run costs of transitioning to the new payment system—such as forecast errors regarding CBDC usage or short-lived mismatches between consumer payment preferences and firm readiness.

While CBDC may reduce long-run operational costs at the system level, these benefits do not eliminate the transitional phase. Under the intermediated design assumed here, the

introduction of CBDC can even increase balance-sheet interactions, as firms must convert CBDC into deposits and consumers must top up CBDC wallets from the banking system. Our modeling of a temporary payment cost therefore reflects short-run adoption frictions rather than a structural claim about the long-run costliness of CBDC.

Let's imagine that out of total trade, σ_t a fraction comes from existing methods of payment (cash and deposit) and $1 - \sigma_t$ is carried out using CBDC. CBDC transactions are costly, and they cost τ_t a fraction of the transaction volume, whereas transactions made using deposits are costless. Therefore, net revenue after subtracting the costs becomes

$$\text{Revenue}_t = \Big[\sigma_t + (1 - \sigma_t)(1 - \tau_t)\Big] P_t Y_t \tag{5.14}$$

C-firms anticipate these costs and take that into account while setting prices to make up for the losses due to additional transaction costs incurred for CBDC. Consequently, the new price-setting mechanism becomes

$$P_{i,t+1} = \begin{cases} \frac{P_{i,t}}{X_{i,t+1}}(1 + \eta_{i,t+1}) & \text{if} \Delta_{i,t} \leq 0 \text{ and } P_{i,t} < P_t \\ \\ \frac{P_{i,t}}{X_{i,t+1}}(1 - \eta_{i,t+1}) & \text{if} \Delta_{i,t} > 0 \text{ and } P_{i,t} \geq P_t \end{cases} \tag{5.15}$$

where $X^e_{i,t+1} = \sigma^e_{i,t+1} + (1 - \sigma^e_{i,t+1})(1 - \tau_{t+1})$. Notice that if C-firms anticipate that all trades will be in deposit, then $\sigma^e_{t+1} = 1$ and $X^e_{t+1} = 1$. Hence, C-firms get back to the original pricing mechanism used in the absence of CBDC. On the other hand, if the C-firms anticipate that all future trades will be in CBDC, then $\sigma^e_{t+1} = 0$ and $X^e_{t+1} = 1 - \tau_{t+1}$. Setting prices in this way, C-firms make sure that their expected revenue in the next period is the same as it would have been in the absence of CBDC and any transaction costs.

The expected share of deposit transactions evolves as,

$$\sigma^e_{i,t+1} = \kappa \sigma_{i,t} + (1 - \kappa)(1 - n_t) \tag{5.16}$$

where n_t is the fraction of CBDC users in the economy in period t.

When $\kappa = 0$, the C-firms is taking only a fraction of CBDC users in the whole economy into consideration but not its past experience with the number of CBDC users visiting it. Therefore, $\sigma^e_{i,t+1} = 1 - n_t$ in that case. In the long run when $n_t \to 1$, the pricing update factor i.e $X^e_{i,t+1} = 1 - \tau_{t+1}$. So if C-firms neglect their firm-specific experience and only consider the aggregate economy, in the long run these two decisions are equivalent.

5.3.3 Production, investment, and employment

Means of production in the C-firms are capital $K_{i,t}$ and labour $N_{i,t}$. The production function follows Leontief technology, i.e., $\hat{Y}_{i,t} = \min(\alpha N_{i,t}, \kappa K_{i,t})$ where α and κ are labor and capital productivity, respectively. If the labor is abundant and capital is not fully utilized, then the output becomes $Y_{i,t} = \omega_{i,t}\hat{Y}_{i,t} = \omega_{i,t}\kappa K_{i,t}$ where $\omega_{i,t} \in (0,1)$ is the *capacity utilization rate*. Therefore, the required labor for the production is $N_{i,t} = (\kappa/\alpha)\omega_{i,t}K_{i,t}$. Capital is accumulated by the firms and follows

$$K_{i,t+1} = (1 - \delta\omega_{i,t})K_{i,t} + I_{i,t} \tag{5.17}$$

where only utilized capital depreciates and $I_{i,t}$ is the investment.
Investment opportunities of the firms are infrequent (one in every $1/\gamma$ period, where γ is the fraction of firms adjusting capital), and capital is fixed in the short run. This gives rise to sticky and durable capital, as firms take investment decisions in an uncertain environment before the consumption market opens, and this anchors decisions on average lifetime capital stock. The average lifetime capital stock evolves as

$$\overline{K}_{i,t-1} = \nu\overline{K}_{i,t-2} + (1 - \nu)\omega_{i,t-1}K_{i,t-1} \tag{5.18}$$

where $\nu \in (0,1)$.
Firms decide on investment in two parts. Firstly, they make up for the worn-out capital, keeping in mind the future opportunities of capital adjustment i.e $I^r_{i,t} = \frac{\delta}{\gamma}\overline{K}_{i,t-1}$. Secondly, they target the *desired long-term rate of capital utilization* $\overline{\omega}$. Therefore, the total investment of the firm becomes

$$I_{i,t} = \left(\frac{1}{\overline{\omega}} + \frac{\delta}{\gamma}\right)\overline{K}_{i,t-1} - K_{i,t} \tag{5.19}$$

and the capital stock evolves as follows:

$$K_{i,t+1} = \left(\frac{1}{\overline{\omega}} + \frac{\delta}{\gamma}\right)\overline{K}_{i,t-1} - \delta\omega_{i,t}K_{i,t} \tag{5.20}$$

if the required capital for the desired level of production is lower than the available capital stock, the firm uses a fraction of the stock. If the required capital is higher than the available capital stock, the firm fully utilizes the stock, but the level of production is not reached. Following these rules, we get the required number of workers as

$$N^*_{i,t+1} = \min\left(\frac{\kappa}{\alpha}K^*_{i,t+1}, \frac{\kappa}{\alpha}K_{i,t+1}\right), \tag{5.21}$$

where $K^*_{i,t+1}$ is the required capital for the desired production level, and $K_{i,t+1}$ is the available capital stock.
After deciding on the required number of workers to match the desired level of production, firms post vacancies as follows:

$$\nu_{i,t+1} = \max\left(N^*_{i,t+1} - N_{i,t}, 0\right). \tag{5.22}$$

K-firms produce only using labor input from the workers and use linear technology $Y_{j,t} = \alpha N_{j,t}$. Hence, the labor requirement of the firm is $N_{j,t}/\alpha$. To make up for the required workers, firms post vacancies and compete with C-firms in the labor market for hiring.

Consumer matching protocol

Prior to the introduction of the CBDC in the economy, our model follows the matching protocol of the consumption goods market present in Assenza et al. (2015). The general framework of matching works in the following way: consumers randomly choose Z_c (here Z_c is a subset of total consumption firms in the model) firms among F consumption firms and sort them according to the ascending order of their prices. If the first firm has a sufficient stock of goods, the consumer will spend all his budget. Otherwise, he will buy as much as he can buy from that firm and will go to the next firm in line. He will keep doing this either until he consumes his entire consumption budget or the total production of Z_c firms is lower than his consumption budget. In the latter case, the consumer saves the rest as an involuntary savings. Matching occurs in a slightly different way once we consider the possibility of using different payment methods. Let's start with the simple case prior to CBDC. Please note that all the following steps are preceded by the sorting of Z_c firms.

- *With cash and deposits only:* If the first firm has sufficient goods to sell, the consumer spends all the consumption budget i.e. he spends $m^*_{t,deposit}C_{h,t}$ from bank deposit, $m^*_{t,cash}C_{h,t}$ form cash wallet. In case the firm does not have enough goods, the consumer buys as much as he can and randomly chooses either cash or deposit to pay with. If he chooses cash to pay for the entire purchase from that firm, he might face a lack of sufficient balance in his wallet. In that case, he pays the rest using the deposit. Contrarily, if he chooses deposit, he pays from his bank account, and the balance in the wallet is left untouched. Notice that in these events, consumers may end up accumulating cash that they originally intended to use or might spend more than what they intended from the deposit.
- *With cash, deposits, and CBDC:* The consumer base gets divided into two groups

in this case: we have *users*, who have adopted CBDC and *non-users* who have not adopted CBDC. There are 4 possibilities that arise depending on the consumer's adoption/firm's acceptance status.

- Consumer *user* vs. firm *accepts*: we can think of this occurrence as perfect matching. This is similar to the transaction algorithm with cash and deposits only. The major difference is that consumers now spend $m^*_{t,deposit}C_{h,t}$ from bank deposits, $m^*_{t,cash}C_{h,t}$ from cash wallets, and $m^*_{t,cbdc}C_{h,t}$ from CBDC wallets. When the current firm does not have enough goods, the consumer buys as much as he can and randomly chooses from cash, CBDC, and deposit to pay with. If he chooses CBDC (cash) to pay for the entire purchase from that firm, he might face a lack of sufficient balance in his CBDC wallet (cash wallet). In that case he pays the rest using the deposit. Contrarily, if he chooses deposit, he pays from his bank account, and the balance in the CBDC wallet and cash wallet is left untouched. Contrarily, if he chooses to deposit, he pays from his bank account, and the balance in the wallet is left untouched.
- Consumer *user* vs. firm *non-acceptance*: This case causes a major friction in the consumption market. Since the consumer cannot spend its allocated budget on CBDC, it saves the $m^*_{t,cbdc}C_{h,t}$. Thus, the consumer spends the non-CBDC fractions of the allocated budget, and we have the same transaction algorithm as the one without the CBDC case. Notice that the firm faces a reduction in sales as it did not accept CBDC. This creates a short-term contractionary transmission channel for affecting the real economy due to the introduction of a new payment method.
- Consumer *non-user* vs. firm *non-accept*: this case can also be considered a perfect match, and the transaction algorithm is just like the one before the introduction of CBDC. Here, the firm's decision of acceptance of CBDC does not matter.
- Consumer *non-user* vs. firm *acceptance*: This case is similar to the one before, as the firm's decision of acceptance of CBDC also does not matter. The transaction algorithm follows the one before the introduction of CBDC.

Empirically, frictions in payment acceptance can indeed lead consumers to postpone or abandon intended purchases, generating patterns similar to the involuntary saving mechanism in our model. Evidence from the online retail sector shows that when consumers reach the checkout stage but cannot complete a transaction, often due to missing payment options, technical obstacles, or lack of compatibility with the merchant's preferred

payment channel, they frequently exit without purchasing, despite having a positive consumption intention. Recent research documents that "hesitation at checkout" and the absence of suitable payment methods are among the strongest predictors of shopping cart abandonment, a phenomenon with rates exceeding 70% globally and exceeding 80% in certain environments (see Ong et al. (2022)). These findings illustrate that consumers regularly curtail planned consumption when payment frictions arise, even temporarily, which in practice produces unplanned or involuntary saving.

5.3.4 Credits and banks

Each firm takes loans from the bank to fund its production when internal funding is in short supply. For C-firms there are typically two costs, the wage of the workers and the funding for investment, whereas K-firms only acquire the cost of wages. Hence the required loans by the firms are

$$F_{i,t} = \max\ (wN_{i,t} - \mathbb{1}_{i \in C-firms} P_{k,t-1} I_{i,t} D_{i,t-1}, 0) \tag{5.23}$$

There is only one bank in the economy. It accepts all deposits from agents and does not provide deposit interest. The bank evaluates the financial soundness of the firms using the entire past data of the firm's balance sheet. For each firm$f$, it computes the following leverage ratio:

$$\lambda_{f,t} = \frac{L_{f,t-1} + F_{f,t}}{E_{f,t-1} + L_{f,t-1} + F_{f,t}}. \tag{5.24}$$

The bank then estimates a logistic regression of the individual bankruptcy probability ϕ_f for each firm as $\phi_f = f(\lambda_f)$. Considering that the firms are paying θ a fraction of their loan back each period, the bank sets the interest rates of the loan for each bank as

$$r_{f,t} = \mu \left\{ \frac{1 + \frac{r}{\theta}}{\Phi(\theta, T_{f,t})} - \theta \right\}, \tag{5.25}$$

where $T_{f,t} = 1/\phi_{f,t}$ i.e., the number of periods after which the firm defaults. Optimization of the lending is done by considering a maximum admissible loss for the bank as a fraction of the bank's equity. If $\Delta L_{f,t}$ is the new extended loan to the firm, then it follows that

$$\phi_f(\Delta L_{f,t} + L_{f,t-1}) \leq \zeta E_t^b, \tag{5.26}$$

the maximum admissible loan for a firm f becomes

$$\overline{F}_{f,t} = \frac{\zeta E_t^b - \phi_f L_{f,t-1}}{\phi_f}. \tag{5.27}$$

In summary, if the loan requirement of the firm is less than the maximum admissible loan for that firm, the firm gets the full funding. On the other hand, if the loan requirement is higher than the maximum admissible loan, the bank lends only up to the limit, and the firm has to cut down its hiring, production, etc.
The bank remunerates the deposits/savings at a variable interest rate r_t^d. We assume that the ex-ante bank remunerates the 1 quarter of the central bank's policy rate. This is in line with much empirical literature that explored the limited pass-through of policy rate to deposit rate (for example, see Drechsler et al. (2017)). Since the equity of the bank may default on paying the interest rate on deposits. Therefore, we define an effective deposit interest rate as follows:

$$\tilde{r}_t^d = \max(0, \min(0.2\text{Equity}, r_t^d D_t)) \tag{5.28}$$

Thus, the bank only pays the ex-ante deposit interest rate if the total interest payable is lower than 20% of the equity of the bank.

Government bailout of banks: We introduce government bailout in terms of equity of the banks. Whenever the book value of the equity of the bank (i.e., the difference between the asset and liability columns of the balance sheet of the bank) is negative, the bank cannot continue to operate. This becomes a hurdle for the loan process and deposit remuneration process. Since we have a single bank in the economy, a representative bank should always be operative in order to sustain the primary model dynamics for our research purposes. During the bailout process, the government replenishes the bank's equity to the initialized value (3000 in our example). The bailout cost goes into the balance sheet of the government as an expenditure.

5.3.5 Central Bank

The central bank in our model is the sole issuer of cash, CBDC and bank reserves. These monetary assets enter the economy in a demand driven manner: whenever households or banks choose to hold more of a particular instrument, the central bank supplies it by expanding its balance sheet and adjusting its holdings of government bonds. In this sense the supplies of cash, CBDC and reserves are perfectly elastic, and there is no quantity constraint imposed by the central bank.
Monetary policy operates through the policy rate, which follows a Taylor type rule,

$$r_t = \rho_{CB} r_{t-1} + (1 - \rho_{CB})\{\lambda_u(u_t - \bar{u}) + \lambda_\pi(\pi_t - \bar{\pi})\}, \tag{5.29}$$

where $\bar{u}$ and $\bar{\pi}$ denote the central bank's unemployment and inflation targets. The policy rate also determines the interest rate on government bonds. CBDC and cash carry no interest, consistent with recent ECB discussions (see ECB (2024a)), while reserves earn a fixed spread of 0.8 percent per year above the policy rate.

On the liability side of the balance sheet, the central bank records cash, CBDC and reserves, and on the asset side, it holds government bonds. Because it accommodates all desired holdings of monetary assets, the central bank effectively acts as a lender of last resort within the model.

5.4 Calibration and Validation

Table 5.1: Model Parameters

Parameter	**Value**	**Description**
z_c	2	Number of applications in consumption–good market
z_k	2	Number of applications in capital–good market
z_e	5	Number of job applications per worker
ξ	0.73817	Household wealth memory parameter
χ	0.017175	Consumption wealth share
q_{adj}	0.73011	Quantity adjustment parameter
p_{adj}	0.16485	Price adjustment parameter
μ	1.007	Bank gross markup
η	0.03	Capital depreciation rate
I_{prob}	0.32595	Investment probability
ϕ	0.0023828	Bank leverage parameter
θ	0.032792	Debt–reimbursement rate
δ	0.15908	Memory parameter in capital–utilization dynamics
α	0.66667	Labour productivity
k	0.33333	Capital productivity
div	0.2	Dividend share
$\bar{X}$	0.85	Desired capital utilization
δ_{inv}	0.078131	Inventory depreciation rate
b_1	-15	Risk–evaluation parameter (general)
b_2	13	Risk–evaluation parameter (general)
b_{k1}	-5	Risk–evaluation parameter (capital goods)
b_{k2}	5	Risk–evaluation parameter (capital goods)
tax_rate	0.0	Tax rate on profits

Table 5.1 – Continued

Parameter	Value	Description
w_{up}	0.1	Wage upward adjustment parameter
w_{down}	0.01	Wage downward adjustment parameter
u_{target}	0.1	Unemployment target
w_b	1.0	Base wage
τ_d	0.00	Tax rate on dividends
r_f	0.01	Refinancing rate
r	0.01	Baseline interest rate
τ	0.01	CBDC transaction cost for firms
κ	0.8	Revenue–share parameter
b_3	-10	Firm CBDC-acceptance parameter
γ	-2	Elasticity of payment preferences

For calibrating the parameters related to the adoption of payment methods, we follow both existing empirical literature and ad hoc values. The parameters α_i in the CES aggregator represent the relative importance that consumers assign to each payment feature: security, privacy, convenience, and peer influence, when choosing how to allocate the value of a payment across these characteristics. Rather than fixing these weights exogenously, we calibrate them using a procedure that captures heterogeneity in perceived feature importance. Specifically, we draw the vector α from a Dirichlet distribution whose shape parameters $\mu = (10,\ 1.5,\ 1.0,\ 1.5)$ encode the empirical ranking of features observed in survey data. In practice, this is implemented by sampling independent Gamma$(\mu_i, 1)$ random variables and normalizing the result so that the elements of α sum to one. The relatively large value of μ_1 reflects that consumers systematically place greater weight on security, while the smaller parameters for privacy, convenience, and peer effects allow for more dispersion in perceived importance. This calibration approach permits each consumer to draw a personalized set of feature weights, thereby introducing realistic cross-sectional variation in payment preferences. In our baseline model, initialize the model by θ taking the following value:

$$\theta = \begin{bmatrix} 1 & 0 & 0.01 \\ 0.2 & 0.8 & 0.01 \\ 1 & 1 & 0 \\ 1 & 1 & 0 \end{bmatrix}$$

In this matrix, each column signifies cash, deposits, and CBDC, while each row represents aspects such as privacy, security, convenience, and peer pressure. Throughout a simulation run, parameters corresponding to cash and deposit remain constant, while the security and privacy parameters for CBDC are updated in each epoch. The rationale behind this approach is to introduce uncertainty regarding the design of CBDC, particularly in terms of security and privacy, to users. Consequently, agents receive distorted signals about these design parameters. However, over time, the noise diminishes, leading these parameters to converge towards the actual design parameters established by the central bank. The remaining parameters governing behavior in the real side of the economy follow

Balance sheet items	Households	C-firms	K-firms	Bank	Central bank	Total
Capital		K				K
Inventories		Δ^C	Δ^K			Δ
Deposits	D^H	D^C	D^K	$-D$		0
Reserves				R^b	$-R^b$	0
Loans		$-L^C$	$-L^K$	L		0
Govt. Bonds					B	B
Equity	$-E^H$	$-E^C$	$-E^K$	$-E^B$		$-(K+\Delta+B)$
CBDC	DC^H	DC^C	DC^K		$-DC$	0
Cash	$Cash^H$	$Cash^C$	$Cash^K$		$-Cash$	0

Table 5.2: The balance sheets of different blocks of the model.

closely the ranges and interpretations used in Assenza et al. (2015).[3] In the consumption-good sector, the capital–productivity parameter κ and the labor–productivity parameter α jointly determine the Leontief technology used by C-firms. In the benchmark calibration, we set $\alpha = 0.6667$ and $\kappa = 0.3333$, which implies a capital–labor ratio consistent with the numerical examples in Assenza et al. (2015). These values ensure that firms face meaningful capacity constraints whenever demand expands, reproducing the bottleneck dynamics that are essential in generating realistic business-cycle fluctuations. The depreciation rate of effective capital, $\delta = 0.159$, is calibrated to match the stylized fact that only the utilized portion of the capital stock wears out.

Turning to behavioral parameters, the price- and quantity-adjustment coefficients $(p_{\text{adj}}, q_{\text{adj}})$ regulate how aggressively firms respond to forecasting errors in demand. Following Assenza et al. (2015), we choose $p_{\text{adj}} = 0.1649$ and $q_{\text{adj}} = 0.7301$, values that generate granular but persistent dispersion in individual prices and production plans. Inventory depreci-

[3] See Assenza et al. (2015) for a detailed discussion of the behavioural rules of C-firms and K-firms, their adjustment frictions, and the capital–credit feedback mechanisms that shape the dynamics of the model.

ation for K-firms is set at $\delta_{\text{inv}} = 0.0781$, capturing the fact that capital-goods inventories deteriorate faster than installed capital. The desired utilization rate of capital,$\bar{X} = 0.85$, reflects the long-run level around which firms stabilize their production plans once short-term shocks dissipate.

On the labor-market side, the wage-adjustment parameters w_{up} and w_{down} translate the asymmetric Phillips curve mechanism embedded in the model. Increasing wages at a faster rate ($w_{\text{up}} = 0.1$) than they decrease ($w_{\text{down}} = 0.01$) is consistent with the empirical observation that nominal wages are more flexible downward only in recessions, a feature built into the original model through region-dependent adjustment rules. The target unemployment rate $u_{\text{target}} = 0.1$ anchors wage dynamics around a meaningful labor-market tightness threshold.

Financial parameters are set in accordance with the credit block described in Assenza et al. (2015). The leverage-sensitivity coefficients $(b_1, b_2, b_{k1}, b_{k2})$ govern how the bank maps firm leverage into default probabilities via logistic regressions updated over time. Their values, $b_1 = -15$, $b_2 = 13$, $b_{k1} = -5$, and $b_{k2} = 5$, produce a convex response of bankruptcy risk to rising leverage, consistent with the empirical patterns recovered by the bank in the model's learning window. The refinancing rate is fixed at $r_f = 0.01$, while the parameter governing the repayment schedule, $\theta = 0.0328$, is chosen to reproduce realistic maturities of firms' debt contracts as described in Eq. (8.2). Finally, the dividend share div $= 0.2$ and the consumption-wealth share $\chi = 0.017$ ensure that households' spending remains sensitive to income fluctuations, thereby propagating shocks through the demand side of the economy. Overall, these parameters jointly replicate the key mechanisms identified in Assenza et al. (2015), adaptive price and quantity adjustment, sticky capital accumulation, credit-sensitive financial fragility, and endogenous fluctuations in aggregate demand, while allowing the extended model to accommodate the additional payment-instrument block described in the present paper.

To evaluate the empirical performance of the model, we compare simulated macroeconomic series with U.S. quarterly data from 1948Q1 to 2019Q4 using kernel density estimates, as shown in Figure 5.2. This distributional comparison provides a transparent measure of goodness of fit by assessing whether the model replicates the shape, dispersion, and skewness of the empirical data rather than only matching selected moments. The simulated consumption and investment gaps reproduce several qualitative features of the historical distributions, including their right-skewed shape and moderate dispersion, reflecting the asymmetric adjustment of firms under capacity constraints and financial frictions. Inflation dynamics also display a realistic concentration around moderate inflation rates with a visible right tail, echoing patterns in the data. At the same time, the model systematically underestimates volatility in unemployment and the output gap,

generating distributions that are substantially more compressed than those observed in the U.S. economy; this suggests that the current specification of labor-market frictions and demand propagation may not produce sufficient amplification of shocks. Overall, the kernel densities highlight that while the model captures the broad qualitative distributional features of several business-cycle variables, it remains conservative in generating macroeconomic volatility, providing a clear benchmark against which the introduction of CBDC-related mechanisms can be subsequently evaluated.

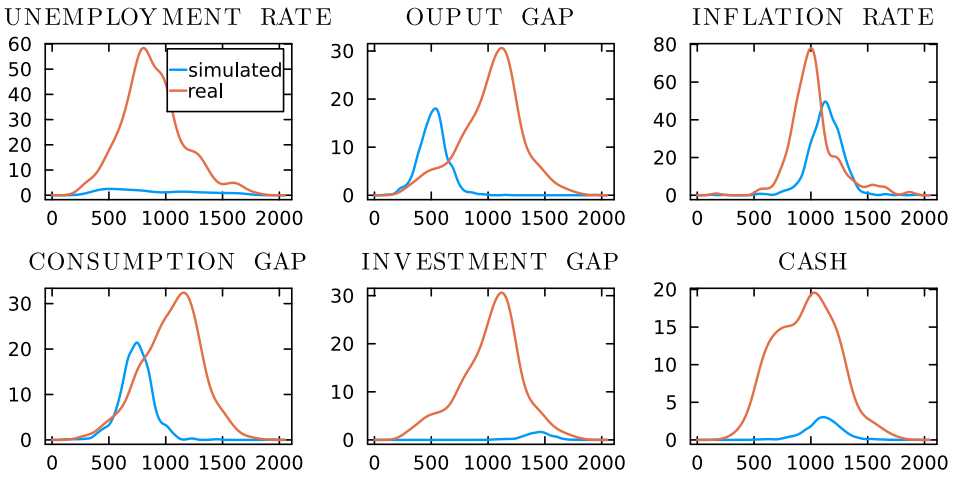

Figure 5.2: Kernel density estimate of real and simulated data from MABM without CBDC

5.5 Results

5.5.1 Model without CBDC

Our baseline model for the analysis is an economy where CBDC has not yet been introduced. Therefore, agents have access to only two payment instruments: cash and deposits. The features of these payment instruments remain consistent across both the baseline and the CBDC-augmented models. Agents optimally adapt and allocate their use of payment instruments based on these shared features, though the parameter values may differ across instruments.

It is important to note that we do not distinguish between wealth and deposits in this model—agents save exclusively through bank deposits. Moreover, these are not term deposits; agents can withdraw them overnight while still receiving remuneration. This

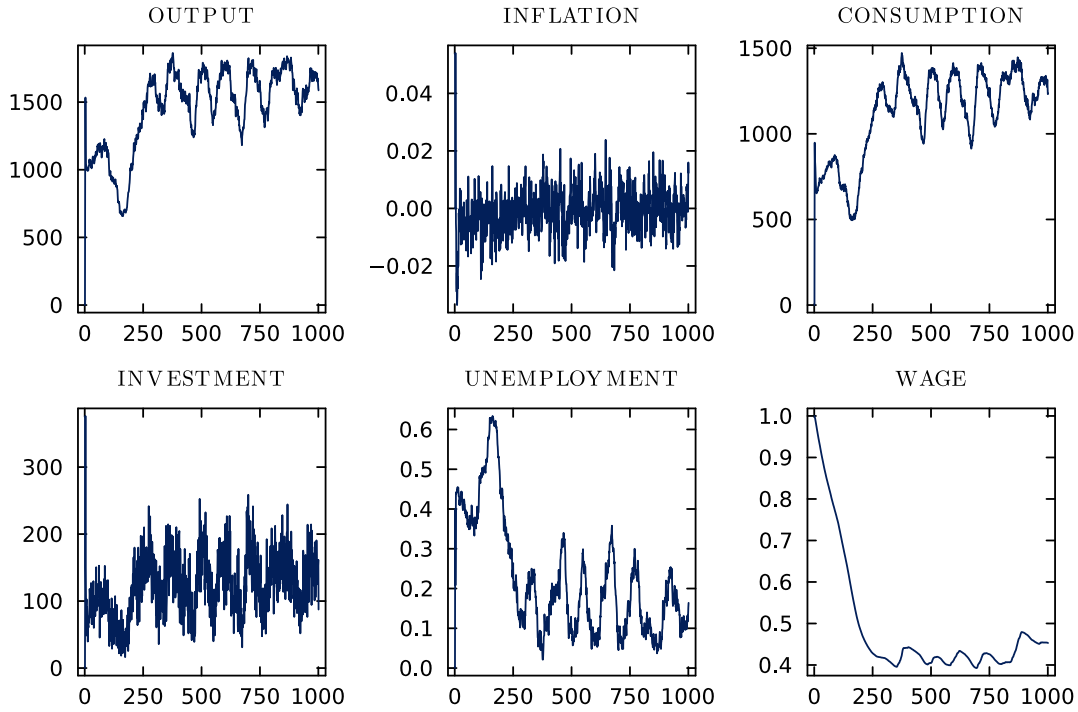

Figure 5.3: This figure several simulated macroeconomic variables obtained from our MABM model without CBDC. The model is able to produce standard results of the macroeconomic variables as in Assenza et al. (2015). The endogenous business cycle of the economy is produced without any exogenous shocks, a niche of the ABM model.

assumption results in a very large outstanding deposit amount.

In the baseline model, we simulate the economy for 1,000 periods, and the results are shown in Figure 5.3. Aggregate variables such as output, consumption, investment, and unemployment behave as in a standard macroeconomic agent-based model (ABM) with credit (see Assenza et al. (2015)). Fluctuations in these variables are not driven by exogenous shocks but rather emerge endogenously as an *emergent property* of the model. The system is never in a true equilibrium but fluctuates around a steady-state value.

This setup achieves two things: first, endogenous fluctuations arise without any external disturbance; second, the fluctuations remain within a bounded range, producing a 'no-growth' economy. This latter point is important, as we do not include any growth factors in the model.

Simulations show that during normal times, liquidity circulates among economic agents, maintaining macroeconomic stability. However, as firms expand and capital goods prices rise, liquidity imbalances increase, leading to higher debt burdens and heightened risk perceptions. This causes credit rationing, which reduces investment and production, ultimately triggering a recession. During downturns, capital goods prices fall, debt levels decline, and firms rebuild liquidity. Recovery begins when firms regain access to credit,

boosting production and employment.
On the banking side, high debt accumulation typically precedes recessions, as banks tighten lending in response to rising firm risk. Conversely, recoveries are facilitated by easing credit conditions, which enable economic expansion. The correlation between debt and unemployment in this artificial economy mirrors real-world patterns, underscoring the critical role of financial constraints in shaping business cycles.
Figure 5.4 shows the response of variables related to payment instruments. We refer to M1 variables as those that comprise the M1 measure of money in an economy. In the baseline economy, these are deposits and cash. Since there is only a single deposit measure, the total level of deposits is much higher than that of cash. However, the usage of cash and deposits, as reflected in the total number of transactions, is similar. The same holds for the total transaction volume.
This indicates that deposits are used as frequently as cash in transactions, despite their larger storage value. The volume of cash used per transaction is slightly higher than that of deposits, as agents value deposits more highly. This is because deposits earn interest, unlike cash, which makes them more attractive for storing value. Notice that the peak difference between the volume of cash transactions and the volume of deposit transactions is larger than the difference at the troughs. This implies that during times when banks are unable to maintain deposit interest rates due to equity losses, the storage value of deposits depreciates relative to cash.

5.5.2 Model with CBDC

We study the introduction of CBDC in the baseline economy as a sudden regime change whereby CBDC becomes available to consumers as a new method of payment alongside cash and deposits. This experiment replicates a structural shift in the economy. Since the model is backward-looking, there are no anticipation effects. Thus, the introduction of CBDC functions like an MIT (mechanical, immediate, and temporary) shock. We introduce CBDC at $t = 400$ during a simulation that runs for 1,000 periods, providing sufficient time for the model to stabilize.From Figure 5.5, we observe that introducing CBDC in the baseline model has a clear contractionary effect on the economy. The key driver of this contraction is the adoption of the new payment technology. The adoption of CBDC affects the economy through a two-sided market mechanism. On the demand side of the economy, agents adopt the new payment technology gradually. This slow adoption is due to noisy dissemination of information about the technical design of CBDC. We assume that when the central bank first launches CBDC, its features are not fully trusted by agents due to initial skepticism. As a result, agents assign lower values to the features in the θ matrix when optimally allocating across payment instruments. Over

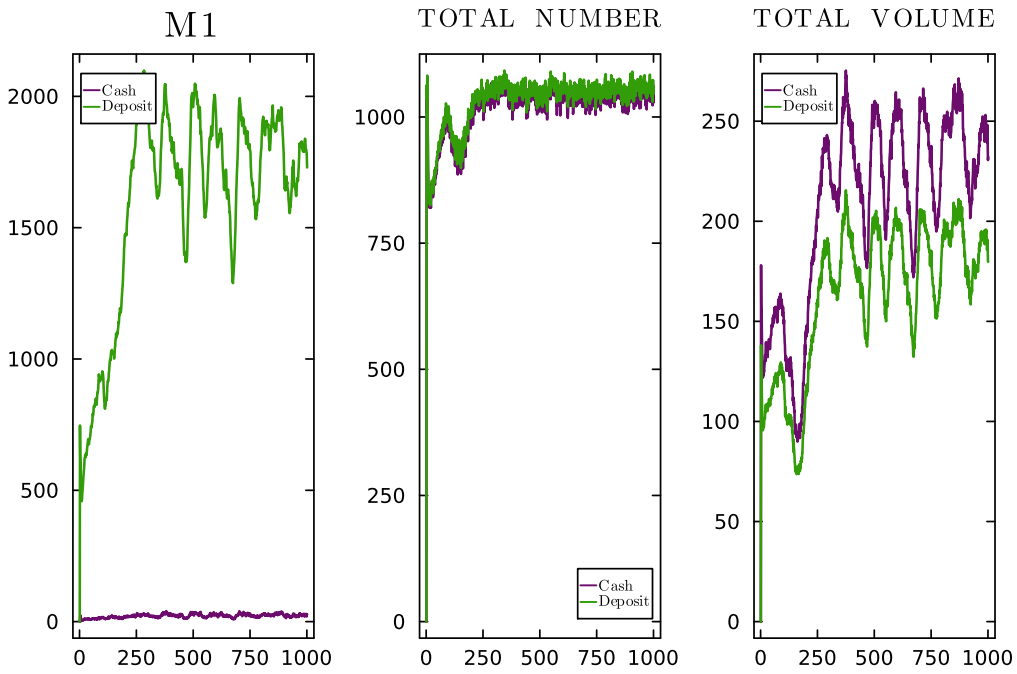

Figure 5.4: Some relevant simulated time series of payment instruments in our MABM model without CBDC. Deposit remains the largest share in the M1 as we do not make distinction between checking deposit and time deposits this reflecting entire wealth of the agents.

time, through increased usage and exposure, the features become more credible, resulting in higher adoption. In Figure 5.6, we plot the variables related to payment instruments. The total number and volume of CBDC transactions grow gradually as more consumers begin using the new payment method. It is noteworthy that the levels of cash and deposit usage remain substantially higher than that of CBDC. This is due to the initially lower perceived values of CBDC in terms of security and privacy compared to the existing payment instruments. Now turning to the supply side of the economy: consumer goods-producing firms begin accepting CBDC as a payment method while still considering the expected number of transactions made via traditional means, i.e., cash and deposits. The probability of acceptance of CBDC is given by the following function:

$$\mathbb{P}(accept) = \frac{\exp(4 + b_3\sigma_t)}{1 + \exp(4 + b_3\sigma_t)} \tag{5.30}$$

The parameter b_3 takes a negative value in our model. Therefore, the probability of accepting CBDC decreases if firms expect that consumers will use traditional means of payment in the next period. During the initial phase of the CBDC launch, fewer consumers use CBDC, leading firms to anticipate more payments in cash and deposits. As a result, consumers who are willing to pay in CBDC often do not find firms that accept

it. This leads to involuntary savings, as consumers retain the unspent portion of their intended expenditures, resulting in a buildup of CBDC wallet and deposit balances (see Figure 5.7). This has a twofold effect on firms: (1) they expect lower payments in CBDC in the subsequent period, reinforcing their reluctance to accept it, and (2) they reduce production in response to lower effective demand caused by the mismatch in payment instruments. Consequently, firms downsize their operations by laying off workers and distributing lower dividends to households.

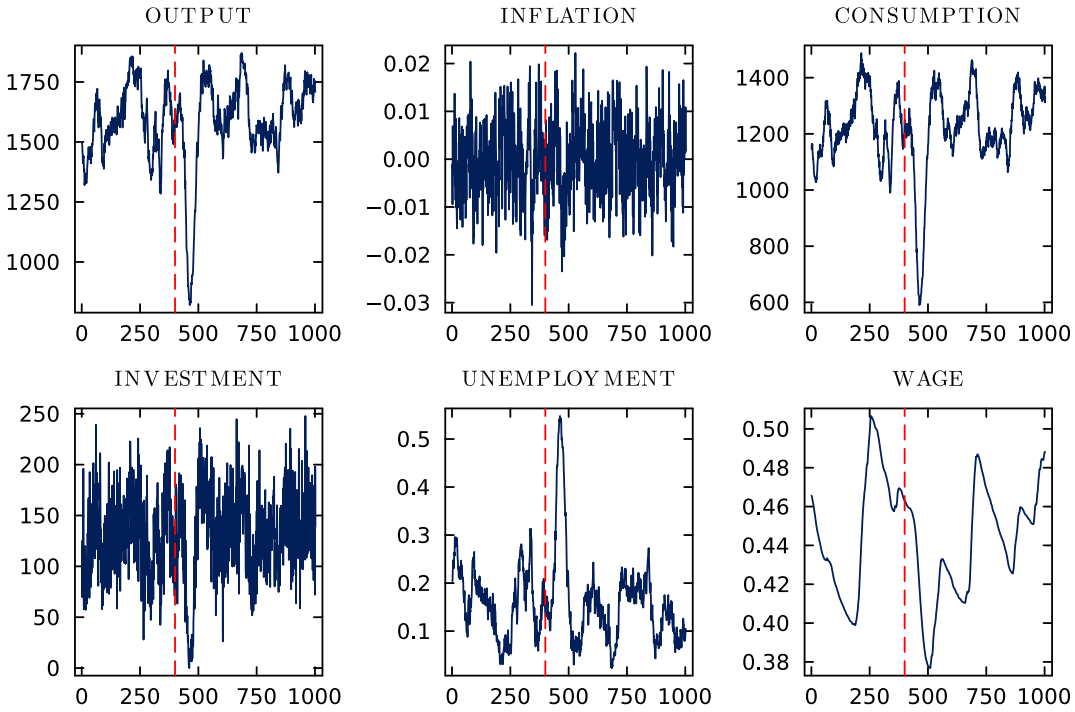

Figure 5.5: This figure several simulated macroeconomic variables obtained from our MABM model when CBDC is introduced at $t = 400$ in our baseline parameter setting

5.5.3 Sensitivity analysis

In this exercise, we examine the effects of strong complementarity between the features of payment instruments that consumers consider in their decision-making. In the baseline model, we set $\gamma = -2$ and then increase the absolute value to $\gamma = -10$. A higher absolute value of γ implies stronger complementarity among payment features.

From Figure 5.8, we observe that a higher degree of complementarity introduces a lag in the response of major macroeconomic variables. Both output and consumption display this lag, which can be attributed to the initial drag in CBDC usage. With stronger complementarity, consumers assign similar importance to other payment instruments like cash and deposits. Consequently, when CBDC adoption is low, due to factors such as

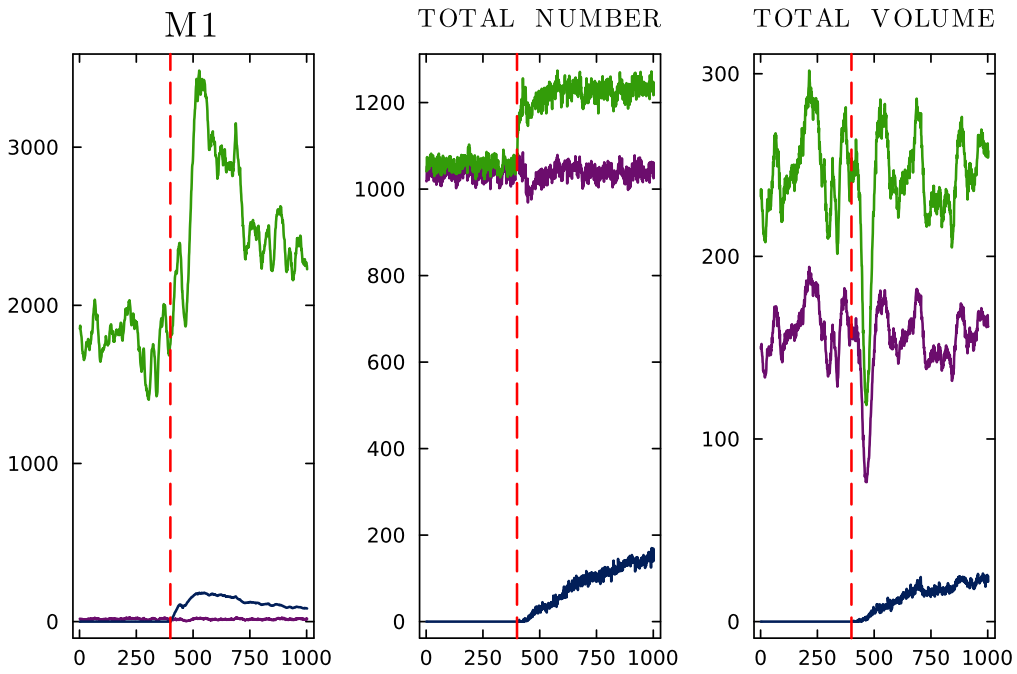

Figure 5.6: Some relevant simulated time series of payment instruments in our MABM model when CBDC is introduced at $t = 400$ in our baseline parameter setting. The green line is for deposits, the blue line is CBDC and the purple line is for cash. As CBDC was introduced at $t = 400$, the level of CBDC usage starts gradually increasing after $t = 400$

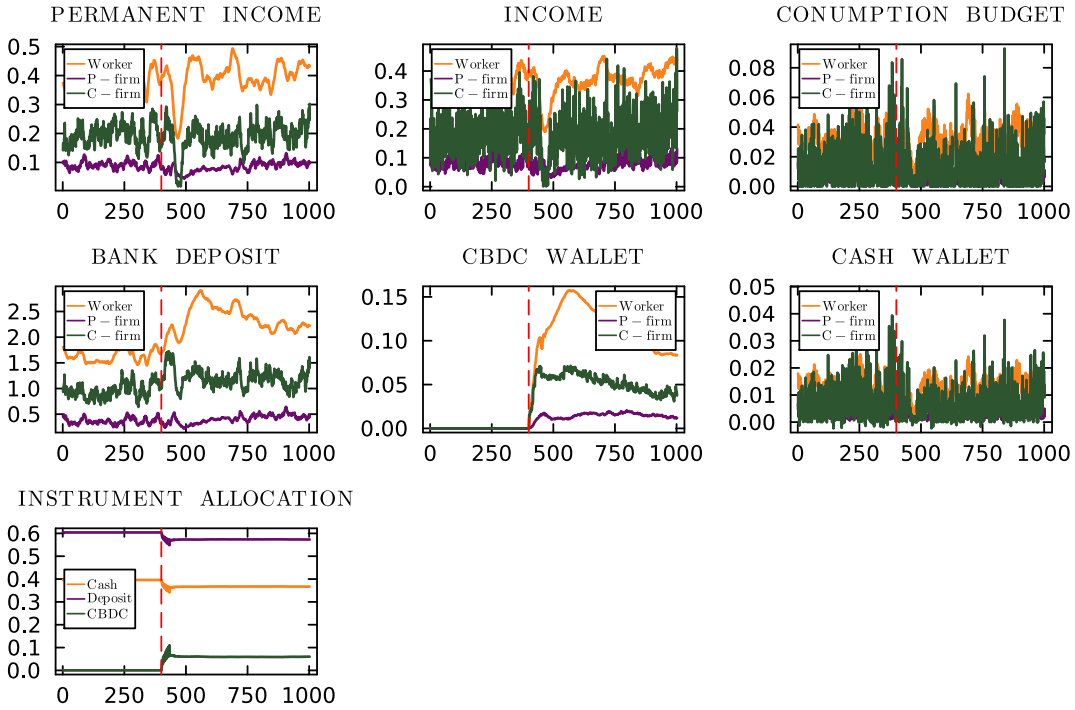

Figure 5.7: Some relevant simulated time series of consumer behaviour in our MABM model when CBDC is introduced at $t = 400$ in our baseline parameter setting

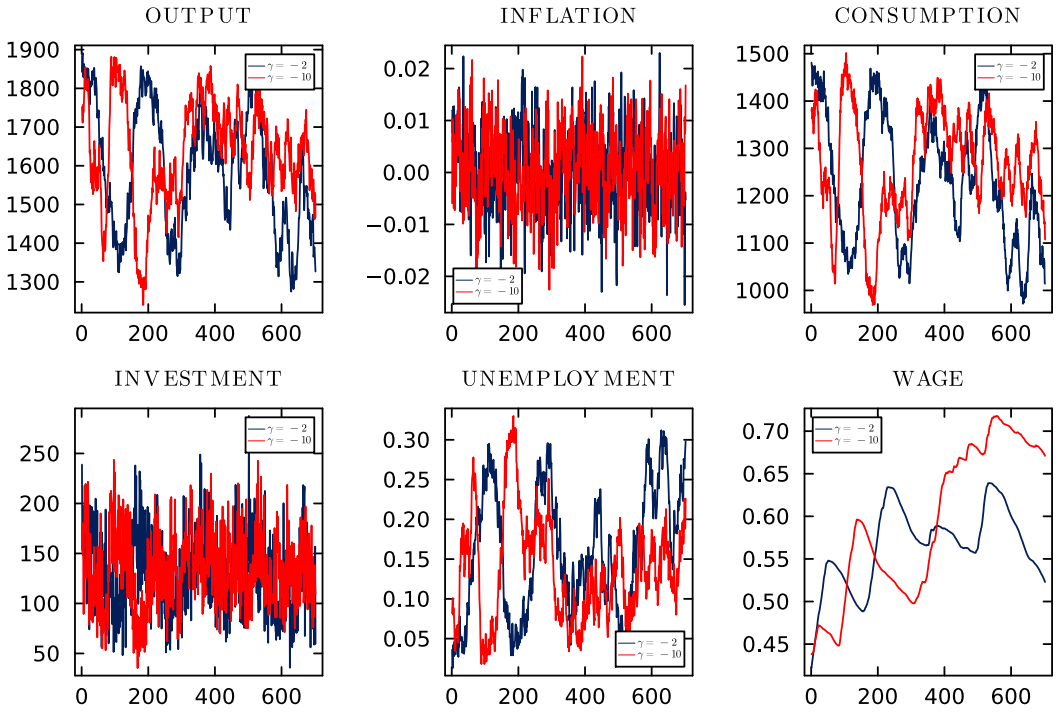

Figure 5.8: The red line plots the behavior of macroeconomic variables, $\gamma = -10$ and blue line plots our baseline parameter setting (i.e.,$\gamma = -2$) in our MABM with CBDC

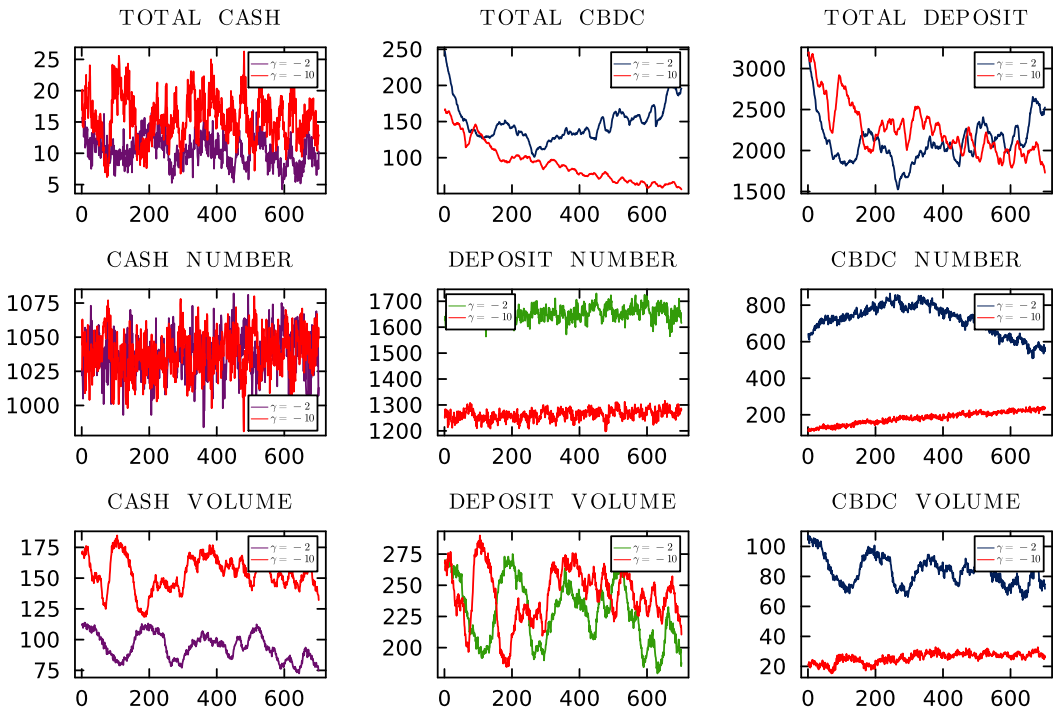

Figure 5.9: The red line plots behavior of some payment instrument variables with $\gamma = -10$ and blue line plots our baseline parameter setting (i.e. $\gamma = -2$) in our MABM with CBDC

lack of usage or vendor acceptance, consumers also reduce their usage of the other instruments. As a result, final goods producers experience lower sales compared to the high-substitution case.

In response, C-firms reduce production due to inventory buildup and downsize their workforce. Unemployment rises accordingly and follows the same lagged pattern seen in output and consumption. Figure 5.9 plots variables related to payment instruments. The total CBDC level is noticeably lower in the high-complementarity scenario compared to the high-substitution scenario. CBDC usage is significantly reduced when γ is more negative. Furthermore, the volatility of CBDC payment volume is higher in the high-substitution case than in the high-complementarity case. Since stronger complementarity reduces overall payment instrument usage, it also dampens volatility. As CBDC adoption increases, the lag in output, consumption, and other macroeconomic variables diminishes, and these variables begin to move in sync with the economic cycle. Interestingly, once adoption reaches a critical level, output and consumption become higher in the complementarity scenario than in the substitution scenario, resulting in lower unemployment.

5.6 Conclusions

This paper set out to explore how the introduction of a CBDC might affect a modern economy, using an agent-based macroeconomic model grounded in micro-level behavior. Our simulations show that the introduction of CBDC is far from a neutral change; it creates a period of adjustment that significantly impacts macroeconomic variables such as output, consumption, and employment.

In the short run, we find that the economy contracts following the introduction of CBDC. This is primarily due to mismatches in adoption between consumers and firms: while consumers are slow to adopt the new payment method—particularly when uncertain about its privacy and security—firms are reluctant to accept CBDC unless a sufficient number of customers are already using it. This creates a feedback loop: limited acceptance discourages usage, and limited usage discourages acceptance. As a result, some consumers are unable to spend their full consumption budgets, reducing effective demand, prompting firms to scale back production, and causing unemployment to rise.

Importantly, we also find that the design of the CBDC and the perceived value of its features play a major role in how this transition unfolds. When consumers view features such as privacy, convenience, and security as complementary rather than substitutable, CBDC adoption is even slower. In such scenarios, the initial economic contraction is deeper and more persistent. However, once adoption catches up, the economy rebounds and can achieve higher output and lower unemployment compared to the baseline.

Overall, the results suggest that while CBDC has the potential to improve payment efficiency and long-term welfare, the path to that outcome is shaped by behavioral frictions and coordination problems. Policymakers should take these transitional dynamics seriously. Early communication about CBDC design, efforts to build trust, and temporary adoption incentives could help smooth the adjustment and mitigate the short-run economic costs observed in our model.

Appendices

5.A Optimization on features and instruments

Say we are optimizing the following problem:

$$\max_{\boldsymbol{P}} \left(\alpha_1 p_1^{-\gamma} + \alpha_2 p_2^{-\gamma} + \cdots + \alpha_K p_K^{-\gamma}\right)^{-\frac{1}{\gamma}} \tag{5.31}$$

$$\text{subject to } \; p_1 + p_2 + \cdots + p_K = P \tag{5.32}$$

Where $\boldsymbol{P}$ is a $K \times 1$ vector with elements $p_i = 1, \cdots, K$. Taking the first-order condition with respect to a generic element p_j we get,

$$-\frac{1}{\gamma}(\alpha_1 p_1^{-\gamma} + \alpha_2 p_2^{-\gamma} + \cdots + \alpha_K p_K^{-\gamma})^{-\frac{1}{\gamma}-1}(-\gamma)p_j^{-\gamma-1}\alpha_j = \lambda$$

$$(\alpha_1 p_1^{-\gamma} + \alpha_2 p_2^{-\gamma} + \cdots + \alpha_K p_K^{-\gamma})^{-\frac{1}{\gamma}-1}\alpha_j p_j^{-\gamma-1} = \lambda$$

Where λ is the Lagrangian multiplier.
Therefore, taking ratio of the FOCs of the two generic elements $\boldsymbol{P}$, we get

$$\frac{\alpha_j}{\alpha_i}\left(\frac{p_j}{p_i}\right)^{-\gamma-1} = 1 \qquad \text{for } j \neq i$$

$$\frac{p_j}{p_i} = \left(\frac{\alpha_i}{\alpha_j}\right)^{-\frac{1}{\gamma+1}}$$

Dividing Eq 5.32 by p_i we get,

$$\frac{p_1}{p_i} + \frac{p_2}{p_i} + \cdots + \frac{p_j}{p_i} + \cdots + \frac{p_K}{p_i} = \frac{P}{p_i}$$

$$p_i^* = \frac{P}{\frac{p_1}{p_i} + \frac{p_2}{p_i} + \cdots + \frac{p_j}{p_i} + \cdots + \frac{p_K}{p_i}}$$

$$p_i^* = \frac{P}{\left(\frac{\alpha_i}{\alpha_1}\right)^{-\frac{1}{\gamma+1}} + \left(\frac{\alpha_i}{\alpha_2}\right)^{-\frac{1}{\gamma+1}} + \cdots + \left(\frac{\alpha_i}{\alpha_K}\right)^{-\frac{1}{\gamma+1}}}$$

$$p_i^* = \frac{P}{\sum_{j=1}^{K} \left(\frac{\alpha_i}{\alpha_j}\right)^{-\frac{1}{\gamma+1}}}$$

Notice that, we can repeat the same process for all other elements of $\boldsymbol{P}$ and obtain their optimal values.

Now consider $\boldsymbol{P}$ is a linear combination of N payment instruments $m_i,\ i = 1, \cdots, N$ i.e. $\boldsymbol{P} = \boldsymbol{\Theta}\boldsymbol{M}$ where $\boldsymbol{\Theta}$ is a $K \times N$ matrix of coefficients and $\boldsymbol{M}$ is a $N \times 1$ vector of instruments. Therefore the optimal level of features takes the form,

$$\boldsymbol{P}^* = \boldsymbol{\Theta}\boldsymbol{M}^*$$

from which we can retrieve the optimal level of instruments as

$$\boldsymbol{M}^* = \boldsymbol{\Theta}^{-1}\boldsymbol{P}^* \tag{5.33}$$

5.B Optimization with constraints on the instruments

Say we are optimizing the same problem:

$$\max_{\boldsymbol{P}} \left(\alpha_1 p_1^{-\gamma} + \alpha_2 p_2^{-\gamma} + \cdots + \alpha_K p_K^{-\gamma}\right)^{-\frac{1}{\gamma}} \tag{5.34}$$

but with a constraint that the total allocation on different instruments should sum to the available liquidity. Therefore the constraint takes the form of

$$m_1 + m_2 + \cdots + m_N = P \tag{5.35}$$

Notice that we can write the constraint 5.35 in terms of payment features using the relationship of features and instruments i.e. $\boldsymbol{M} = \boldsymbol{\Theta}^{-1}\boldsymbol{P}$. Now if the matrix has the following form

$$\boldsymbol{\Theta}^{-1} = \begin{bmatrix} \tilde{\theta}_{11} & \dots & \tilde{\theta}_{1K} \\ \vdots & \ddots & \vdots \\ \tilde{\theta}_{N1} & \dots & \tilde{\theta}_{NK} \end{bmatrix}$$

Therefore, the constraint 5.35, takes the following form:

$$(\tilde{\theta}_{11} + \cdots + \tilde{\theta}_{N1})p_1 + (\tilde{\theta}_{12} + \cdots + \tilde{\theta}_{N2})p_2 + \cdots + (\tilde{\theta}_{1K} + \cdots + \tilde{\theta}_{NK})p_K = P \tag{5.36}$$

In short, the coefficientp_j in the constraint is the sum of the elements of jth column of $\boldsymbol{\Theta}^{-1}$. Hence the first-order condition of the optimization problem is,

$$\left(\alpha_1 p_1^{-\gamma} + \alpha_2 p_2^{-\gamma} + \cdots + \alpha_K p_K^{-\gamma}\right)^{-\frac{1}{\gamma}-1} \alpha_j p_j^{-\gamma-1} = \lambda(\tilde{\theta}_{1j} + \cdots + \tilde{\theta}_{Nj})$$

Therefore, taking ratio of the FOCs of the two generic elements$\boldsymbol{P}$, we get

$$\frac{\alpha_j}{\alpha_i}\left(\frac{p_j}{p_i}\right)^{-\gamma-1} = \frac{(\tilde{\theta}_{1j} + \cdots + \tilde{\theta}_{Nj})}{(\tilde{\theta}_{1i} + \cdots + \tilde{\theta}_{Ni})} \qquad \text{for } j \neq i$$

$$\frac{p_j}{p_i} = \left(\frac{(\tilde{\theta}_{1j} + \cdots + \tilde{\theta}_{Nj})}{(\tilde{\theta}_{1i} + \cdots + \tilde{\theta}_{Ni})}\frac{\alpha_i}{\alpha_j}\right)^{-\frac{1}{\gamma+1}}$$

Dividing Eq 5.36 by p_i we get,

$$(\tilde{\theta}_{11}+\cdots+\tilde{\theta}_{N1})\frac{p_1}{p_i}+(\tilde{\theta}_{12}+\cdots+\tilde{\theta}_{N2})\frac{p_2}{p_i}+\cdots+(\tilde{\theta}_{1j}+\cdots+\tilde{\theta}_{Nj})\frac{p_j}{p_i}+\cdots+(\tilde{\theta}_{1K}+\cdots+\tilde{\theta}_{NK})\frac{p_K}{p_i}=\frac{P}{p_i}$$

$$p_i^*=\frac{P}{(\tilde{\theta}_{11}+\cdots+\tilde{\theta}_{N1})\frac{p_1}{p_i}+(\tilde{\theta}_{12}+\cdots+\tilde{\theta}_{N2})\frac{p_2}{p_i}+\cdots+(\tilde{\theta}_{1j}+\cdots+\tilde{\theta}_{Nj})\frac{p_j}{p_i}+\cdots+(\tilde{\theta}_{1K}+\cdots+\tilde{\theta}_{NK})\frac{p_K}{p_i}}$$

$$p_i^*=\frac{P}{(\tilde{\theta}_{11}+\cdots+\tilde{\theta}_{N1})\left(\frac{(\tilde{\theta}_{11}+\cdots+\tilde{\theta}_{N1})}{(\tilde{\theta}_{1i}+\cdots+\tilde{\theta}_{Ni})}\frac{\alpha_i}{\alpha_1}\right)^{-\frac{1}{\gamma+1}}+(\tilde{\theta}_{12}+\cdots+\tilde{\theta}_{N2})\left(\frac{(\tilde{\theta}_{12}+\cdots+\tilde{\theta}_{N2})}{(\tilde{\theta}_{1i}+\cdots+\tilde{\theta}_{Ni})}\frac{\alpha_i}{\alpha_2}\right)^{-\frac{1}{\gamma+1}}}$$

$$+\cdots+(\tilde{\theta}_{1j}+\cdots+\tilde{\theta}_{Nj})\left(\frac{(\tilde{\theta}_{1j}+\cdots+\tilde{\theta}_{Nj})}{(\tilde{\theta}_{1i}+\cdots+\tilde{\theta}_{Ni})}\frac{\alpha_i}{\alpha_j}\right)^{-\frac{1}{\gamma+1}}$$

$$+\cdots+(\tilde{\theta}_{1K}+\cdots+\tilde{\theta}_{NK})\left(\frac{(\tilde{\theta}_{1K}+\cdots+\tilde{\theta}_{NK})}{(\tilde{\theta}_{1i}+\cdots+\tilde{\theta}_{Ni})}\frac{\alpha_i}{\alpha_K}\right)^{-\frac{1}{\gamma+1}}$$

$$p_i^*=\frac{P}{\sum_{j=1}^{K}(\tilde{\theta}_{1j}+\cdots+\tilde{\theta}_{Nj})\left(\frac{(\tilde{\theta}_{1j}+\cdots+\tilde{\theta}_{Nj})}{(\tilde{\theta}_{1i}+\cdots+\tilde{\theta}_{Ni})}\frac{\alpha_i}{\alpha_j}\right)^{-\frac{1}{\gamma+1}}}$$

Bibliography

Ramón Adalid, Álvaro Álvarez-Blázquez, Katrin Assenmacher, Lorenzo Burlon, Maria Dimou, Carolina López-Quiles, Natalia Martín Fuentes, Barbara Meller, Manuel Muñoz, Petya Radulova, et al. Central bank digital currency and bank intermediation. *ECB Occasional Paper*, (2022/293), 2022. URL https://www.ecb.europa.eu/pub/pdf/scpops/ecb.op293~652cf2b1aa.en.pdf?985167870ac2551e31097f06382d01d9.

Tobias Adrian and Tommaso Mancini-Griffoli. The rise of digital money. *Annual Review of Financial Economics*, 13(1):57–77, 2021. doi: 10.1146/annurev-financial-101620-063859. URL https://doi.org/10.1146/annurev-financial-101620-063859.

Itai Agur, Anil Ari, and Giovanni Dell'Ariccia. Designing central bank digital currencies. *IMF Working Papers*, 2019, 2019. ISSN 1018-5941. doi: 10.5089/9781513519883.001.

Marco Airaudo and María Pía Olivero. Optimal monetary policy with countercyclical credit spreads. *Journal of Money, Credit and Banking*, 51(4):787–829, 2019. doi: https://doi.org/10.1111/jmcb.12598. URL https://onlinelibrary.wiley.com/doi/abs/10.1111/jmcb.12598.

Michel Alexandre, Gilberto Tadeu Lima, Luca Riccetti, and Alberto Russo. The financial network channel of monetary policy transmission: an agent-based model. *Journal of Economic Interaction and Coordination*, 18(3):533–571, July 2023. ISSN 1860-7128. doi: 10.1007/s11403-023-00377-w. URL https://doi.org/10.1007/s11403-023-00377-w.

Roger Aliaga-Díaz and María Pía Olivero. Macroeconomic implications of "deep habits" in banking. *Journal of Money, Credit and Banking*, 42(8):1495–1521, 2010. URL https://onlinelibrary.wiley.com/doi/abs/10.1111/j.1538-4616.2010.00351.x.

Robin Allesiardo and Raphaël Féraud. Exp3 with drift detection for the switching bandit problem. In *2015 IEEE International Conference on Data Science and Advanced Analytics (DSAA)*, pages 1–7. IEEE, 2015.

David Andolfatto. Assessing the Impact of Central Bank Digital Currency on Private Banks. *The Economic Journal*, 131(634):525–540, 09 2020. ISSN 0013-0133. doi: 10.1093/ej/ueaa073. URL https://doi.org/10.1093/ej/ueaa073.

Claudio Angione, Eric Silverman, and Elisabeth Yaneske. Using machine learning as a surrogate model for agent-based simulations. *Plos one*, 17(2):e0263150, 2022.

Jasmina Arifovic, John Duffy, and Janet Hua Jiang. Adoption of a new payment method: Experimental evidence. *European Economic Review*, 154:104410, 2023. ISSN 0014-2921. doi: https://doi.org/10.1016/j.euroecorev.2023.104410. URL https://www.sciencedirect.com/science/article/pii/S0014292123000399.

Tiziana Assenza, Domenico Delli Gatti, and Jakob Grazzini. Emergent dynamics of a macroeconomic agent based model with capital and credit. *Journal of Economic Dynamics and Control*, 50:5–28, 2015. ISSN 0165-1889. doi: https://doi.org/10.1016/j.jedc.2014.07.001. URL https://www.sciencedirect.com/science/article/pii/S0165188914001572. Crises and Complexity.

Peter Auer, Nicolo Cesa-Bianchi, and Paul Fischer. Finite-time analysis of the multiarmed bandit problem. *Machine learning*, 47(2):235–256, 2002a.

Peter Auer, Nicolò Cesa-Bianchi, Yoav Freund, and Robert E. Schapire. The nonstochastic multiarmed bandit problem. *SIAM J. Comput.*, 32(1):48–77, 2002b.

Raphael A Auer, Holti Banka, Nana Yaa Boakye-Adjei, Ahmed Faragallah, Jon Frost, Harish Natarajan, and Jermy Prenio. *Central bank digital currencies: a new tool in the financial inclusion toolkit?* Bank for International Settlements, Financial Stability Institute, 2022. URL https://www.bis.org/fsi/publ/insights41.pdf.

Robert L Axtell and J Doyne Farmer. Agent-based modeling in economics and finance: Past, present, and future. *Journal of Economic Literature*, 2022.

Lukáš Bajer, Zbyněk Pitra, and Martin Holeňa. Benchmarking gaussian processes and random forests surrogate models on the bbob noiseless testbed. In *Proceedings of the Companion Publication of the 2015 Annual Conference on Genetic and Evolutionary Computation*, pages 1143–1150, 2015.

T. Balint, F. Lamperti, A. Mandel, M. Napoletano, A. Roventini, and A. Sapio. Complexity and the economics of climate change: A survey and a look forward. *Ecological Economics*, 138:252–265, 2017. ISSN 0921-8009. doi: https://doi.org/10.1016/j.ecolecon.2017.03.032. URL https://www.sciencedirect.com/science/article/pii/S092180091630828X.

Rafa Baptista, J Doyne Farmer, Marc Hinterschweiger, Katie Low, Daniel Tang, and Arzu Uluc. Macroprudential policy in an agent-based model of the uk housing market. *Bank of England Working Paper*, 2016.

Marco Benedetti, Gennaro Catapano, Francesco De Sclavis, Marco Favorito, Aldo Glielmo, Davide Magnanimi, and Antonio Muci. Black-it: A ready-to-use and easy-to-extend calibration kit for agent-based models. *Journal of Open Source Software*, 7(79): 4622, 2022. doi: 10.21105/joss.04622. URL https://doi.org/10.21105/joss.04622.

Allen N. Berger, Asli Demirgüç-Kunt, Ross Levine, and Joseph G. Haubrich. Bank concentration and competition: An evolution in the making. *Journal of Money, Credit and Banking*, 36(3):433–451, 2004. ISSN 00222879, 15384616. URL http://www.jstor.org/stable/3838945.

Donald A Berry and Bert Fristedt. Bandit problems: sequential allocation of experiments (monographs on statistics and applied probability). *London: Chapman and Hall*, 5 (71-87):7–7, 1985.

Lilian Besson. SMPyBandits: an Open-Source Research Framework for Single and Multi-Players Multi-Arms Bandits (MAB) Algorithms in Python. Online at: github.com/SMPyBandits/SMPyBandits, 2018. URL https://github.com/SMPyBandits/SMPyBandits/. Code at https://github.com/SMPyBandits/SMPyBandits/, documentation at https://smpybandits.github.io/.

Ulrich Bindseil. Tiered cbdc and the financial system. *Available at SSRN 3513422*, 2020. URL http://dx.doi.org/10.2139/ssrn.3513422.

Ulrich Bindseil and Richard Senner. Macroeconomic modelling of cbdc: a critical review. 2024. URL https://ssrn.com/abstract=4941163.

Richard Bookstaber, Mark Paddrik, and Brian Tivnan. An agent-based model for financial vulnerability. Technical report, Office of Financial Research Working Paper Series, 2014.

Michael D Bordo. Central bank digital currency in historical perspective: Another crossroad in monetary history. Technical report, National Bureau of Economic Research, 2021. URL https://www.nber.org/papers/w29171.

Michael D Bordo and Andrew T Levin. Central bank digital currency and the future of monetary policy. 2017. URL https://www.nber.org/papers/w23711.

Andras Borsos, Adrian Carro, Aldo Glielmo, Marc Hinterschweiger, Jagoda Kaszowska-Mojsa, and Arzu Uluc. Agent-based modelling at central banks: Recent developments

and new challenges. *Bank of England Working Paper*, 2025. URL https://ssrn.com/abstract=5227617.

William A. Brock and Cars H. Hommes. Heterogeneous beliefs and routes to chaos in a simple asset pricing model. *Journal of Economic Dynamics and Control*, 22(8):1235–1274, 1998. ISSN 0165-1889. doi: https://doi.org/10.1016/S0165-1889(98)00011-6. URL https://www.sciencedirect.com/science/article/pii/S0165188998000116.

M. Brunetti, R. Ciciretti, and Lj. Djordjevic. The determinants of household's bank switching. *Journal of Financial Stability*, 26:175–189, 2016. ISSN 1572-3089. doi: https://doi.org/10.1016/j.jfs.2016.08.004. URL https://www.sciencedirect.com/science/article/pii/S1572308916300894.

Markus Brunnermeier, Jonathan Payne, et al. Platforms, tokens and interoperability. *Princeton University Working Paper*, 2022. URL https://economics.princeton.edu/working-papers/platforms-tokens-and-interoperability/.

Markus K. Brunnermeier and Dirk Niepelt. On the equivalence of private and public money. *Journal of Monetary Economics*, 106:27–41, 2019. ISSN 0304-3932. doi: https://doi.org/10.1016/j.jmoneco.2019.07.004.

Markus K Brunnermeier, Harold James, and Jean-Pierre Landau. The digitalization of money. Technical report, National Bureau of Economic Research, 2019.

Sébastien Bubeck, Nicolo Cesa-Bianchi, et al. Regret analysis of stochastic and nonstochastic multi-armed bandit problems. *Foundations and Trends® in Machine Learning*, 5(1):1–122, 2012.

Lorenzo Burlon, Manuel A. Muñoz, and Frank Smets. The optimal quantity of cbdc in a bank-based economy. *American Economic Journal: Macroeconomics*, 16(4):172–217, October 2024a. doi: 10.1257/mac.20220152. URL https://www.aeaweb.org/articles?id=10.1257/mac.20220152.

Lorenzo Burlon, Manuel A. Muñoz, and Frank Smets. The optimal quantity of cbdc in a bank-based economy. *American Economic Journal: Macroeconomics*, 16(4):172–217, October 2024b. doi: 10.1257/mac.20220152. URL https://www.aeaweb.org/articles?id=10.1257/mac.20220152.

Guillermo A. Calvo. Staggered prices in a utility-maximizing framework. *Journal of Monetary Economics*, 12(3):383–398, 1983. ISSN 0304-3932. doi: https://doi.org/10.1016/

0304-3932(83)90060-0. URL https://www.sciencedirect.com/science/article/pii/0304393283900600.

Gabriele Camera. Introducing new forms of digital money: Evidence from the laboratory. *ESI Working Paper 22-11*, 2022. URL https://digitalcommons.chapman.edu/esi_working_papers/372/.

Francesca Carapella and Jean Flemming. Central bank digital currency: A literature review. *FEDS Notes. Washington: Board of Governors of the Federal Reserve System*, 2020. doi: https://doi.org/10.17016/2380-7172.2790.

Santiago Carbo-Valverde, Timothy H. Hannan, and Francisco Rodriguez-Fernandez. Exploiting old customers and attracting new ones: The case of bank deposit pricing. *European Economic Review*, 55(7):903–915, 2011. ISSN 0014-2921. doi: https://doi.org/10.1016/j.euroecorev.2011.02.001. URL https://www.sciencedirect.com/science/article/pii/S0014292111000250.

Adrian Carro. Could spain be less different? exploring the effects of macroprudential policy on the house price cycle. *Banco de Espana Working Paper*, 2022.

Gennaro Catapano, Francesco Franceschi, Michele Loberto, and Valentina Michelangeli. Macroprudential policy analysis via an agent based model of the real estate sector. *Bank of Italy Temi di Discussione (Working Paper) No*, 1338, 2021.

Mr Jorge A Chan-Lau. *ABBA: An agent-based model of the banking system*. International Monetary Fund, 2017.

Hanfeng Chen, Matthias Hänsel, and Hiep Nguyen. Monetary policy transmission, central bank digital currency, and bank market power. 2024. URL https://hanfengchen.com/assets/papers/mp_cbdc_bankpower.pdf.

Tianqi Chen and Carlos Guestrin. Xgboost: A scalable tree boosting system. In *Proceedings of the 22nd acm sigkdd international conference on knowledge discovery and data mining*, pages 785–794, 2016.

Yutian Chen, Matthew W Hoffman, Sergio Gómez Colmenarejo, Misha Denil, Timothy P Lillicrap, Matt Botvinick, and Nando Freitas. Learning to learn without gradient descent by gradient descent. In *International Conference on Machine Learning*, pages 748–756. PMLR, 2017.

Zhenxi Chen and Thomas Lux. Estimation of sentiment effects in financial markets: A simulated method of moments approach. *Computational Economics*, 52(3):711–744, 2018.

Jonathan Chiu, Seyed Mohammadreza Davoodalhosseini, Janet Jiang, and Yu Zhu. Bank market power and central bank digital currency: Theory and quantitative assessment. *Journal of Political Economy*, 2023. doi: 10.1086/722517. URL https://doi.org/10.1086/722517.

Dimitris Christelisa, Dimitris Georgarakos, Tullio Jappelli, and Maarten van Rooij. Trust in the central bank and inflation expectations. *International Journal of Central Banking*, 16:1–37, 2020. URL https://www.ijcb.org/journal/ijcb20q5a1.htm.

Emanuele Ciola, Enrico Turco, Andrea Gurgone, Davide Bazzana, Sergio Vergalli, and Francesco Menoncin. Enter the matrix model:a multi-agent model for transition risks with application to energy shocks. *Journal of Economic Dynamics and Control*, 146: 104589, 2023. ISSN 0165-1889. doi: https://doi.org/10.1016/j.jedc.2022.104589. URL https://www.sciencedirect.com/science/article/pii/S0165188922002925.

Fernando Cirelli and Remo Nyffenegger. Cbdc and bank lending: The role of financial frictions. *Available at SSRN 4678281*, 2023. URL https://ssrn.com/abstract=4678281.

Graeme Cokayne. The effects of macroprudential policies on house price cycles in an agent-based model of the danish housing market. Technical report, Danmarks Nationalbank Working Papers, 2019.

Stefano Conti and Anthony O'Hagan. Bayesian emulation of complex multi-output and dynamic computer models. *Journal of statistical planning and inference*, 140(3):640–651, 2010.

G Covi, M Montagna, and G Torri. On the origins of systemic risk. Technical report, European Central Bank Working Papers, 2020.

Herbert Dawid and Domenico Delli Gatti. Agent-based macroeconomics. *Handbook of computational economics*, 4:63–156, 2018.

Hans Degryse and Steven Ongena. Competition and regulation in the banking sector: A review of the empirical evidence on the sources of bank rents. *Handbook of financial intermediation and banking*, 2008:483–554, 2008.

Domenico Delli Gatti and Jakob Grazzini. Rising to the challenge: Bayesian estimation and forecasting techniques for macroeconomic agent based models. *Journal of Economic Behavior & Organization*, 178:875–902, 2020.

Douglas W. Diamond. Financial Intermediation and Delegated Monitoring. *The Review of Economic Studies*, 51(3):393–414, 07 1984. ISSN 0034-6527. doi: 10.2307/2297430. URL https://doi.org/10.2307/2297430.

Richard C.. Dorf and Robert H Bishop. *Modern control systems*. Pearson Prentice Hall, 2008.

Giovanni Dosi, Giorgio Fagiolo, and Andrea Roventini. Schumpeter meeting keynes: A policy-friendly model of endogenous growth and business cycles. *Journal of Economic Dynamics and Control*, 34(9):1748–1767, 2010.

Itamar Drechsler, Alexi Savov, and Philipp Schnabl. The Deposits Channel of Monetary Policy*. *The Quarterly Journal of Economics*, 132(4):1819–1876, 05 2017. ISSN 0033-5533. doi: 10.1093/qje/qjx019. URL https://doi.org/10.1093/qje/qjx019.

Itamar Drechsler, Alexi Savov, and Philipp Schnabl. Banking on deposits: Maturity transformation without interest rate risk. *The Journal of Finance*, 76(3):1091–1143, 2021. doi: https://doi.org/10.1111/jofi.13013. URL https://onlinelibrary.wiley.com/doi/abs/10.1111/jofi.13013.

Laurence Harris Désiré Kanga, Christine Oughton and Victor Murinde. The diffusion of fintech, financial inclusion and income per capita. *The European Journal of Finance*, 28(1):108–136, 2022. doi: 10.1080/1351847X.2021.1945646. URL https://doi.org/10.1080/1351847X.2021.1945646.

ECB. Progress on the preparation phase of a digital euro: Second progress report. Technical report, European Central Bank, 2024a. URL https://www.ecb.europa.eu/euro/digital_euro/progress/shared/pdf/ecb.deprp202412.en.pdf.

ECB. Study on the payment attitudes of consumers in the euro area (SPACE), 2024b. URL https://www.ecb.europa.eu/stats/ecb_surveys/space/shared/pdf/ecb.space2024~19d46f0f17.en.pdf.

European Central Bank (ECB). Study on the payment attitudes of consumers in the euro area (space). 2020. URL https://www.ecb.europa.eu/stats/ecb_surveys/space/html/ecb.spacereport202212~783ffdf46e.en.html#toc9.

Giorgio Fagiolo, Alessio Moneta, and Paul Windrum. A critical guide to empirical validation of agent-based models in economics: Methodologies, procedures, and open problems. *Computational Economics*, 30(3):195–226, 2007.

Ester Faia and Tommaso Monacelli. Optimal interest rate rules, asset prices, and credit frictions. *Journal of Economic Dynamics and Control*, 31(10):3228–3254, 2007. ISSN 0165-1889. doi: https://doi.org/10.1016/j.jedc.2006.11.006.

J Doyne Farmer, Joel Dyer, Patrick Cannon, Sebastian Schmon, et al. Black-box bayesian inference for economic agent-based models. Technical report, Institute for New Economic Thinking at the Oxford Martin School, University ..., 2022.

Massimo Ferrari Minesso, Arnaud Mehl, and Livio Stracca. Central bank digital currency in an open economy. *Journal of Monetary Economics*, 127:54–68, 2022. ISSN 0304-3932. doi: https://doi.org/10.1016/j.jmoneco.2022.02.001. URL https://www.sciencedirect.com/science/article/pii/S0304393222000186.

Reiner Franke. Applying the method of simulated moments to estimate a small agent-based asset pricing model. *Journal of Empirical Finance*, 16(5):804–815, 2009.

Reiner Franke and Frank Westerhoff. Structural stochastic volatility in asset pricing dynamics: Estimation and model contest. *Journal of Economic Dynamics and Control*, 36(8):1193–1211, 2012.

Milton Friedman and Anna J. Schwartz. Has government any role in money? *Journal of Monetary Economics*, 17(1):37–62, 1986. ISSN 0304-3932. doi: https://doi.org/10.1016/0304-3932(86)90005-X. URL https://www.sciencedirect.com/science/article/pii/030439328690005X.

Jordi Galí. *Monetary policy, inflation, and the business cycle: an introduction to the new Keynesian framework and its applications*. Princeton University Press, 2015. URL https://press.princeton.edu/books/hardcover/9780691164786/monetary-policy-inflation-and-the-business-cycle?srsltid=AfmBOoqI62w6sLI5LpdFspknFWpW_V6IXRbmUY3rLlFc-egwWp8v5bqC.

Aurélien Garivier and Olivier Cappé. The kl-ucb algorithm for bounded stochastic bandits and beyond. In *Proceedings of the 24th annual conference on learning theory*, pages 359–376. JMLR Workshop and Conference Proceedings, 2011.

Rodney Garratt, Jiaheng Yu, and Haoxiang Zhu. How central bank digital currency design choices impact monetary policy pass-through and market composition. *Available at SSRN 4004341*, 2022.

Domenico Delli Gatti, Saul Desiderio, Edoardo Gaffeo, Pasquale Cirillo, and Mauro Gallegati. *Macroeconomics from the Bottom-up*, volume 1. Springer Science & Business Media, 2011. URL https://link.springer.com/book/10.1007/978-88-470-1971-3.

Dimitris Georgarakos, Geoff Kenny, Luc Laeven, and Justus Meyer. Consumer attitudes towards a central bank digital currency. 2025. URL https://papers.ssrn.com/sol3/papers.cfm?abstract_id=5176496.

Andrea Gerali, Stefano Neri, Luca Sessa, and Federico M. signoretti. Credit and banking in a dsge model of the euro area. *Journal of Money, Credit and Banking*, 42(s1): 107–141, 2010. doi: https://doi.org/10.1111/j.1538-4616.2010.00331.x. URL https://onlinelibrary.wiley.com/doi/abs/10.1111/j.1538-4616.2010.00331.x.

Mark Gertler and Peter Karadi. A model of unconventional monetary policy. *Journal of Monetary Economics*, 58(1):17–34, 2011. ISSN 0304-3932. doi: https://doi.org/10.1016/j.jmoneco.2010.10.004. URL https://www.sciencedirect.com/science/article/pii/S0304393210001261. Carnegie-Rochester Conference Series on Public Policy: The Future of Central Banking April 16-17, 2010.

Mark Gertler and Peter Karadi. Monetary policy surprises, credit costs, and economic activity. *American Economic Journal: Macroeconomics*, 7(1):44–76, January 2015. doi: 10.1257/mac.20130329. URL https://www.aeaweb.org/articles?id=10.1257/mac.20130329.

Manfred Gilli and Peter Winker. A global optimization heuristic for estimating agent based models. *Computational Statistics & Data Analysis*, 42(3):299–312, 2003.

John Gittins, Kevin Glazebrook, and Richard Weber. *Multi-armed bandit allocation indices*. John Wiley & Sons, 2011.

Aldo Glielmo, Marco Favorito, Debmallya Chanda, and Domenico Delli Gatti. Reinforcement learning for combining search methods in the calibration of economic abms. In *Proceedings of the Fourth ACM International Conference on AI in Finance*, ICAIF '23, page 305–313, New York, NY, USA, 2023. Association for Computing Machinery. ISBN 9798400702402. doi: 10.1145/3604237.3626889. URL https://doi.org/10.1145/3604237.3626889.

Itay Goldstein, Ming Yang, and Yao Zeng. Payments, Reserves, and Financial Fragility. November 2023. URL https://ssrn.com/abstract=4547329.

Gary B Gorton and Jeffery Zhang. Protecting the sovereign's money monopoly. *U of Michigan Law & Econ Research Paper*, (22-031), 2022. URL https://ssrn.com/abstract=4162884.

Jakob Grazzini and Matteo Richiardi. Estimation of ergodic agent-based models by simulated minimum distance. *Journal of Economic Dynamics and Control*, 51:148–165, 2015.

Jakob Grazzini, Matteo G Richiardi, and Mike Tsionas. Bayesian estimation of agent-based models. *Journal of Economic Dynamics and Control*, 77:26–47, 2017.

Mr Marco Gross and Elisa Letizia. To demand or not to demand: On quantifying the future appetite for cbdc. *Working Paper No. 2023/009*, 2023. URL https://www.imf.org/en/Publications/WP/Issues/2023/01/20/To-Demand-or-Not-to-Demand-On-Quantifying-the-Future-Appetite-for-CBDC-528060.

Bronwyn H Hall. Innovation and diffusion. (10212), January 2004. doi: 10.3386/w10212. URL http://www.nber.org/papers/w10212.

John H Halton. Algorithm 247: Radical-inverse quasi-random point sequence. *Communications of the ACM*, 7(12):701–702, 1964.

Timothy H. Hannan and Robert M. Adams. Consumer switching costs and firm pricing: Evidence from bank pricing of deposit accounts. *The Journal of Industrial Economics*, 59(2):296–320, 2011. doi: https://doi.org/10.1111/j.1467-6451.2011.00456.x. URL https://onlinelibrary.wiley.com/doi/abs/10.1111/j.1467-6451.2011.00456.x.

Friedrich August Hayek. *Denationalism of Money: An Analysis of the Theory and Practice of Concurrent Currencies*. Institute of Economic Affairs (Great Britain), 1976.

Kim P Huynh, Gradon Nicholls, and Oleksandr Shcherbakov. Equilibrium in two-sided markets for payments: Consumer awareness and the welfare cost of the interchange fee. Technical report, Bank of Canada Staff Working Paper, 2022. URL https://www.bankofcanada.ca/2022/03/staff-working-paper-2022-15/.

Matteo Iacoviello. House prices, borrowing constraints, and monetary policy in the business cycle. *American Economic Journal: Macroeconomics*, 2005.

Matteo Iacoviello and Stefano Neri. Housing market spillovers: Evidence from an estimated dsge model. *American Economic Journal: Macroeconomics*, 2:125–164, 4 2010. ISSN 19457715. doi: 10.1257/mac.2.2.125.

IMF. *Digital Money Across Borders: Macro-Financial Implications*. International Monetary Fund, 2020. URL https://www.imf.org/-/media/Files/Publications/PP/2020/English/PPEA2020050.ashx.

Rustam Jamilov and Tommaso Monacelli. Bewley banks. *Available at SSRN 3732172*, 2023. URL http://dx.doi.org/10.2139/ssrn.3732172.

Erica Jiang, Gregor Matvos, Tomasz Piskorski, and Amit Seru. Banking without deposits: Evidence from shadow bank call reports. (26903), March 2020. doi: 10.3386/w26903. URL http://www.nber.org/papers/w26903.

Leslie Pack Kaelbling, Michael L Littman, and Anthony R Cassandra. Planning and acting in partially observable stochastic domains. *Artificial intelligence*, 101(1-2):99–134, 1998.

Michael N Katehakis and Arthur F Veinott Jr. The multi-armed bandit problem: decomposition and computation. *Mathematics of Operations Research*, 12(2):262–268, 1987.

Ali Kaveh. Particle swarm optimization. In *Advances in Metaheuristic Algorithms for Optimal Design of Structures*, pages 11–43. Springer, 2017.

Todd Keister and Daniel Sanches. Should Central Banks Issue Digital Currency? *The Review of Economic Studies*, 90(1):404–431, 03 2022. ISSN 0034-6527. doi: 10.1093/restud/rdac017. URL https://doi.org/10.1093/restud/rdac017.

Foster Kevin, Greene D Clair, and Joanna Stavins. The 2022 survey of consumer payment choice: summary results. *Research Data Reports Paper*, (23-3), 2022.

Tanai Khiaonarong and David Humphrey. Measurement and use of cash by half the world's population. 2023. URL https://ssrn.com/abstract=4403782.

Jinill Kim, Sunghyun Kim, Ernst Schaumburg, and Christopher A. Sims. Calculating and using second-order accurate solutions of discrete time dynamic equilibrium models. *Journal of Economic Dynamics and Control*, 32(11):3397–3414, 2008. ISSN 0165-1889. doi: https://doi.org/10.1016/j.jedc.2008.02.003. URL https://www.sciencedirect.com/science/article/pii/S0165188908000316.

Nobuhiro Kiyotaki and John Moore. Credit cycles. *Journal of Political Economy*, 105(2):211–248, 1997. doi: 10.1086/262072. URL https://doi.org/10.1086/262072.

Paul Knysh and Yannis Korkolis. Blackbox: A procedure for parallel optimization of expensive black-box functions. *arXiv preprint arXiv:1605.00998*, 2016.

Ladislav Kocis and William J Whiten. Computational investigations of low-discrepancy sequences. *ACM Transactions on Mathematical Software (TOMS)*, 23(2):266–294, 1997.

Ricardo Lagos and Randall Wright. A unified framework for monetary theory and policy analysis. *Journal of Political Economy*, 113(3):463–484, 2005. ISSN 00223808, 1537534X. URL http://www.jstor.org/stable/10.1086/429804.

Matías Lamas and David Martinez Miera. Sectorial holdings and stock prices: the household-bank nexus. *Working Paper 2130*, 2021. URL http://dx.doi.org/10.2139/ssrn.3920902.

Francesco Lamperti. An information theoretic criterion for empirical validation of simulation models. *Econometrics and Statistics*, 5:83–106, 2018.

Francesco Lamperti, Andrea Roventini, and Amir Sani. Agent-based model calibration using machine learning surrogates. *Journal of Economic Dynamics and Control*, 90: 366–389, 2018.

John Langford and Tong Zhang. The epoch-greedy algorithm for contextual multi-armed bandits. *Advances in neural information processing systems*, 20(1):96–1, 2007.

Tor Lattimore and Csaba Szepesvári. *Bandit algorithms*. Cambridge University Press, 2020.

Matthias Lengnick. Agent-based macroeconomics: A baseline model. *Journal of Economic Behavior & Organization*, 86:102–120, 2013. ISSN 0167-2681. doi: https://doi.org/10.1016/j.jebo.2012.12.021. URL https://www.sciencedirect.com/science/article/pii/S0167268112002806.

Carlos León, Jose F. Moreno, and Kimmo Soramäki. Simulating the adoption of a retail cbdc. *Jahrbücher für Nationalökonomie und Statistik*, 245(4-5):401–433, 2025. doi: doi:10.1515/jbnst-2024-0002. URL https://doi.org/10.1515/jbnst-2024-0002.

Jiaqi Li. Predicting the demand for central bank digital currency: A structural analysis with survey data. *Journal of Monetary Economics*, 134:73–85, 2023. ISSN 0304-3932. doi: https://doi.org/10.1016/j.jmoneco.2022.11.007. URL https://www.sciencedirect.com/science/article/pii/S0304393222001398.

Jiaqi Li, Andrew Usher, and Yu Zhu. Central bank digital currency and banking choices. *Available at SSRN 4705512*, 2024. URL https://ssrn.com/abstract=4705512.

Lihong Li, Wei Chu, John Langford, and Robert E. Schapire. A Contextual-Bandit Approach to Personalized News Article Recommendation. In *Proceedings of the 19th international conference on World wide web - WWW '10*, page 661, 2010. doi: 10.1145/1772690.1772758. URL http://arxiv.org/abs/1003.0146. arXiv:1003.0146 [cs].

Michael W McCracken and Serena Ng. Fred-md: A monthly database for macroeconomic research. *Journal of Business & Economic Statistics*, 34(4):574–589, 2016.

MW McCracken and S Ng. Fred-md and fred-qd: monthly and quarterly databases for macroeconomic research, 2021. URL https://research.stlouisfed.org/econ/mccracken/fred-databases/.

Bence Méro, András Borsos, Zsuzsanna Hosszú, Zsolt Oláh, and Nikolett Vágó. A high resolution agent-based model of the hungarian housing market. *MNB Working Papers*, 7, 2022.

Alan Moreira and Alexi Savov. The macroeconomics of shadow banking. *The Journal of Finance*, 72(6):2381–2431, 2017. ISSN 00221082, 15406261. URL http://www.jstor.org/stable/26653288.

Dirk Niepelt. Money and banking with reserves and cbdc. *CEPR Discussion Paper No. 18444*, 2022. URL https://cepr.org/publications/dp18444.

OMFIF. Digital currencies: A question of trust. *OMFIF report on global public confidence in monetary, financial and payment institutions*, 2020. URL https://www.omfif.org/wp-content/uploads/2020/02/Digital-currencies-A-question-of-trust-1.pdf.

Ardvin Kester S. Ong, Marjorie Joy R. Dejucos, Mary Anne F. Rivera, John Vincent D.J. Muñoz, Miguel S. Obed, and Kirstien Paola E. Robas. Utilizing semrfc to predict factors affecting online shopping cart abandonment during the covid-19 pandemic. *Heliyon*, 8(11):e11293, 2022. ISSN 2405-8440. doi: https://doi.org/10.1016/j.heliyon.2022.e11293. URL https://www.sciencedirect.com/science/article/pii/S2405844022025816.

Monika Piazzesi and Martin Schneider. Credit lines, bank deposits or cbdc? competition and efficiency in modern payment systems. *Unpublished, Stanford University*, 2020. URL https://web.stanford.edu/~piazzesi/CBDC.pdf.

Monika Piazzesi, Ciaran Rogers, and Martin Schneider. Money and banking in a New Keynesian model. *Working Paper*, 2022. URL https://www.ecb.europa.eu/press/conferences/ecbforum/shared/pdf/2019/rogers_paper.el.pdf.

Romain Plassard et al. Making a breach: The incorporation of agent-based models into the bank of england's toolkit. Technical report, Groupe de REcherche en Droit, Economie, Gestion (GREDEG CNRS), Université . . . , 2020.

Donovan Platt. A comparison of economic agent-based model calibration methods. *Journal of Economic Dynamics and Control*, 113:103859, 2020.

Donovan Platt. Bayesian estimation of economic simulation models using neural networks. *Computational Economics*, pages 1–52, 2021.

S. Poledna, M. Miess, C. Hommes, and K. Rabitsch. Economic forecasting with an agent-based model. *European Economic Review*, 2023a.

Sebastian Poledna, Michael Gregor Miess, Cars Hommes, and Katrin Rabitsch. Economic forecasting with an agent-based model. *European Economic Review*, 151:104306, 2023b.

Vishnu Raj and Sheetal Kalyani. Taming non-stationary bandits: A bayesian approach. *arXiv preprint arXiv:1707.09727*, 2017.

Amanah Ramadiah, Marco Galbiati, and Kimmo Soramäki. Agent-based simulation of central bank digital currencies. *Available at SSRN 3959759*, 2021. URL `https://papers.ssrn.com/sol3/papers.cfm?abstract_id=3959759`.

Carl Edward Rasmussen. *Gaussian processes in machine learning*. Springer, 2004.

Morten Ravn, Stephanie Schmitt-Grohé, and Martín Uribe. Deep habits. *The Review of Economic Studies*, 73(1):195–218, 2006. ISSN 00346527, 1467937X. URL `http://www.jstor.org/stable/3700622`.

Morten O Ravn and Harald Uhlig. On adjusting the hodrick-prescott filter for the frequency of observations. *Review of economics and statistics*, 84(2):371–376, 2002.

Jessica Reale. Interbank decisions and margins of stability: an agent-based stock-flow consistent approach. *Journal of Economic Dynamics and Control*, 160:104822, 2024. ISSN 0165-1889. doi: https://doi.org/10.1016/j.jedc.2024.104822. URL `https://www.sciencedirect.com/science/article/pii/S0165188924000149`.

Julio J. Rotemberg. Monopolistic price adjustment and aggregate output. *The Review of Economic Studies*, 49(4):517–531, 1982. ISSN 00346527, 1467937X. URL `http://www.jstor.org/stable/2297284`.

Doojin Ryu and Robert I Webb. Central bank digital currency: Payment choices and commercial bank profitability. *Available at SSRN 4333510*, 2023. URL `https://papers.ssrn.com/sol3/papers.cfm?abstract_id=4333510`.

Jonathan Schiller and Jonas Gross. A model for central bank digital currencies: Implications for bank funding and monetary policy. 2021. URL `http://hdl.handle.net/10419/242350`.

Heiko Schmiedel, Gergana L Kostova, and Wiebe Ruttenberg. The social and private costs of retail payment instruments: a european perspective. *ECB Occasional paper*, (137), 2012. URL `http://dx.doi.org/10.2139/ssrn.2145439`.

Yevgeny Seldin and Aleksandrs Slivkins. One practical algorithm for both stochastic and adversarial bandits. In *International Conference on Machine Learning*, pages 1287–1295. PMLR, 2014.

Steven A. Sharpe. Asymmetric information, bank lending, and implicit contracts: A stylized model of customer relationships. *The Journal of Finance*, 45(4):1069–1087, 1990. doi: https://doi.org/10.1111/j.1540-6261.1990.tb02427.x. URL https://onlinelibrary.wiley.com/doi/abs/10.1111/j.1540-6261.1990.tb02427.x.

Steven A. Sharpe. The effect of consumer switching costs on prices: A theory and its application to the bank deposit market. *Review of Industrial Organization*, 12(1):79–94, 1997. ISSN 0889938X, 15737160. URL http://www.jstor.org/stable/41798685.

Marcos Simoes, MM Telo da Gama, and André Nunes. Stochastic fluctuations in epidemics on networks. *Journal of the Royal Society Interface*, 5(22):555–566, 2008.

Herbert A. Simon. From substantive to procedural rationality. pages 65–86, 1976. URL https://doi.org/10.1007/978-1-4613-4367-7_6.

Herbert A. Simon. Rationality as process and as product of thought. *The American Economic Review*, 68(2):1–16, 1978. ISSN 00028282. URL http://www.jstor.org/stable/1816653.

Joanna Stavins, Marie-Hélène Felt, Fumiko Hayashi, and Dr Angelika Welte. Regressive effects of payment card pricing and merchant cost pass-through in the united states and canada. *Available at SSRN 4342018*, 2023. URL https://papers.ssrn.com/sol3/papers.cfm?abstract_id=4342018.

Rune Stenbacka and Tuomas Takalo. Switching costs and financial stability. *Journal of Financial Stability*, 41:14–24, 2019. ISSN 1572-3089. doi: https://doi.org/10.1016/j.jfs.2018.12.001. URL https://www.sciencedirect.com/science/article/pii/S1572308917306514.

Forrest J Stonedahl. *Genetic algorithms for the exploration of parameter spaces in agent-based models*. PhD thesis, Northwestern University, 2011.

Richard S Sutton and Andrew G Barto. *Reinforcement learning: An introduction*. MIT press, 2018.

Brandon Joel Tan. Central Bank Digital Currency Adoption: A Two-Sided Model. *IMF Working Paper No. 2023/127*, 2023. ISSN 9798400244858/1018-5941. URL https://www.imf.org/en/Publications/WP/Issues/2023/06/16/Central-Bank-Digital-Currency-Adoption-A-Two-Sided-Model-534325.

Georgios Alkis Tsiatsios, I Leventides, Evangelos Melas, and Costas Poulios. A bounded rational agent-based model of consumer choice. *Data Science in Finance and Economics*, 3(3):305–323, 2023. URL https://www.aimspress.com/aimspress-data/dsfe/2023/3/PDF/DSFE-03-03-018.pdf.

Arthur Turrell. Agent-based models: understanding the economy from the bottom up. *Bank of England Quarterly Bulletin*, page Q4, 2016.

Ignazio Visco and Giordano Zevi. Bounded rationality and expectations in economics. pages 459–470, 2020. URL https://www.taylorfrancis.com/chapters/edit/10.4324/9781315658353-35/bounded-rationality-expectations-economics-ignazio-visco-giordano-zevi.

Duncan J Watts and Steven H Strogatz. Collective dynamics of 'small-world'networks. *Nature*, 393(6684):440–442, 1998.

Richard Weber. On the gittins index for multiarmed bandits. *The Annals of Applied Probability*, pages 1024–1033, 1992.

Toni M Whited, Yufeng Wu, and Kairong Xiao. Will central bank digital currency disintermediate banks? *Available at SSRN 4112644*, 2022. URL https://ssrn.com/abstract=4112644.

Stephen Williamson. Central bank digital currency: Welfare and policy implications. *Journal of Political Economy*, 130(11):2829–2861, 2022. doi: 10.1086/720457. URL https://doi.org/10.1086/720457.